A neutronic study to reduce the costs of pebble bed reactors by varying fuel compositions

WA Boyes

orcid.org/0000-0002-5268-2627

Mini-dissertation submitted in partial fulfilment of the requirements for the degree *Master of Engineering in Nuclear Engineering* at the North-West University

Supervisor: Prof DE Serfontein

Graduation May 2018

Student number: 28193865

ABSTRACT

Pebble Bed Reactor (PBR) fuel is expensive at around 17% of the total cost of electrical power produced. This if for the Steenkampskraal Thorium Limited (STL) financial model for a single 100 MW_{th} reactor with a cylindrical core, Once Through Then Out (OTTO) fuelling cycle with a thermal efficiency of 40%, due to a steam temperature and pressure of (540˚C, 15MPa), with 33 MW_{el} being sent to the grid. The fuel costs are modelled based on a capacity of 250 000 fuel spheres per annum fuel cost model courtesy of STL. A larger fuel plant would reduce the fuel sphere costs but would require a larger fleet of PBRs. If the fuel costs per unit of electrical energy produced ($/kWh) can be reduced it would make the pebble bed reactor a more feasible option and could make them comparable in terms of costs to other types of nuclear technologies.

The two major components of the cost of producing the fuel spheres are broken down into the manufacturing costs (kernel casting costs, kernel coating costs, graphite matrix costs and the fuel sphere production costs) and the nuclear material costs (SWU's, enrichment, HM loading amount and raw material costs). The cost of the manufacturing dominates over the cost of the nuclear materials. Apart from reducing fuel sphere manufacturing costs, the other important way to reduce the total fuel cost is to increase the total amount of heat energy generated from each fuel sphere, i.e. increasing the cumulative energy per fuel sphere. This can be done by increasing the burn-up of the nuclear fuel and by increasing the heavy metal (HM) loading per fuel sphere.

This was attempted by varying the enrichment and HM loading for LEU and for a mixture of thorium (Th) and LEU (ThLEU), as well as a mixture of Th and Highly Enriched Uranium (HEU). The neutron physics and thermo-hydraulic performance of this core were simulated using the VSOP 99/11 suite of codes. The aim with the addition of Th was to improve the neutron economy as the U-233 which is bred from the Th-232 is the fissile nuclear fuel with the best neutron economy in thermal nuclear reactors. The HEU-based fuels showed the best performance. However, since the use of HEU is contentious in most countries, due to its high nuclear weapons proliferation risk, the performance of the HEU fuels will be excluded from this summary.

As was expected, the results showed that the burn-up of the nuclear fuel increased sharply and monotonously with increasing enrichment. Therefore, the LEU with the

highest allowable enrichment, namely 20 wt%, produced the highest burn-up and therefore the highest cumulative energy per fuel sphere and therefore the lowest total fuel cost per unit of electrical energy produced.

Adding Th to LEU fuel spheres in order to obtain a ThLEU fuel sphere by definition reduces the enrichment of the mixture and increases the HM loading. This decrease in enrichment decreased the burn-up to such an extent that the ThLEU fuel spheres always produced lower cumulative energies per fuel sphere than the pure 20 wt% LEU fuel spheres from which they were derived.

From the very low HM loading of 5 g HM per fuel sphere, the burnup first increased with increasing HM loading until it peaked at 7 g HM for LEU and at 10 g HM for ThLEU, where after it decreased with increasing HM loading. The reason for the poor burn-up at very low HM loadings was excessive neutron leakage from the core. The reason for decreasing burnups at very high HM loadings was that the decreasing distance between fuel kernels resulted in under moderation, which decreases the neutron economy and is thus known to reduce burn-up.

Since, for a given burn-up, cumulative energy per fuel sphere is directly proportional to HM loading, increasing the HM loading above the values of maximum burn-up initially resulted in increased cumulative energies, where after it peaked and declined as increasing HM loading sharply reduced the burn-up by increasing the problem of under moderation. The maximum cumulative energy was achieved at 16 g HM loading for LEU and at 16 g HM loading for ThLEU, however the lowest Levilised Unit Energy Costs (LUEC) were achieved at 12 g HM for LEU and 12 g HM for ThLEU for all the enrichments. The general trend which is observed is that as the enrichment and HM content increases, the cumulative amount of heat energy per fuel sphere increases and the LUEC decreases. However, there is a point at where increasing the HM loading to an even greater extent actually increases the LUEC and there is an optimum for each fuel type. Generally, 12 g HM actually provided a lower LUEC than 16 g HM for each fuel type.

The lowest total fuel costs were achieved for the following fuel compositions for a single First of a Kind (FOAK) reactor per site, as opposed to a multi-pack (many reactors on one site). This explains why the resulting costs were high.

LEU at 20 wt% for 12 g HM would provide the lowest Levilised Unit Energy Cost (LUEC) of 117 US$/MWh, closely followed by LEU at 10 g HM (LUEC = 117 US$/MWh) and LEU at 16 g HM (LUEC = 118 US$/MWh).

Lower enrichments such as 15 wt% ThLEU have the lowest LUEC at 12 g HM (LUEC = 119 US$/MWh), followed by ThLEU at 16 g HM (LUEC = 120 US$/MWh) and ThLEU at 10 g HM (LUEC = 120 US$/MWh). LEU at 15 wt% would have a minimum at 12 g HM (LUEC = 121 US$/MWh).

At 10 wt% enrichment it can be seen that at higher enrichments ThLEU has a lower LUEC compare to LEU at the same enrichment. ThLEU being lowest at 16 g HM (LUEC = 125 US$/MWh) followed by 12 g HM (LUEC = 126 US$/MWh) while LEU at 12 g HM is lowest (LUEC = 131 US$/MWh).

Increasing the enrichment unfortunately substantially increased the maximum fuel temperature during Depressurised Loss of Forced Coolant (DLOFC) accidents. The reason was that by increasing the enrichment, the sharpness in the peaks of the axial power density profiles, which were observed near the top of the fuel core, increased. This increased power hotspot near the top of the core also resulted in a hotspot in the decay heat and thus in the maximum temperature profiles during DLOFC accidents. This increase in DLOFC temperatures with increasing enrichment means that there is a limit to the extent that increasing enrichments can be used to reduce fuel costs.

On the other hand, increasing the HM loading slightly reduced the maximum DLOFC temperatures. The reason was that increasing HM loading reduced the sharpness of the axial power density peaks and thus, by the logic explained above, reduced the maximum DLOFC temperatures slightly.

Although it was not investigated in this study, it is well-known that increasing HM loading increases the risk of the reactivity increases and, therefore, power increases during water ingress accidents. This means that although increasing HM loading in many cases decreased the total fuel cost and decreased the maximum DLOFC temperature slightly, there is again a limit to which this technique can be utilized safely. Near the optimum point, a large increase in HM loading also often produced only a small decrease in fuel cost and DLOFC temperature. In such cases it is recommended

that the lower HM loading be selected, as this will probably produce a relatively large reduction in the safety risk regarding water ingress, at the cost of only a small increase in fuel cost. The addition of thorium did in fact increase the maximum DLOFC fuel temperature. However, the ThLEU fuels at lower enrichments did not exceed the maximum DLOFC temperature limit.

The fuel plant cost model that was used assumed a production rate of 250 000 fuel spheres/annum (147.26 $/FS, 10 wt% 10 g HM LEU). However, increasing this to to 800 000 fuel spheres/annum would reduce the fuel costs drastically to 91.05 $/FS. However, a large enough pebble bed fleet would be needed to warrant such a large fuel plant. An example of a fuels that would be suitable for this reactor is LEU at 10wt% at 12 g HM (LUEC = 131 US$/MWh), which would provide a low LUEC and would adhere to the maximum DLOFC temperature limit. However, lower HM loadings are advisable, such as 7 g HM loading, due to problems associated with water-ingress at high HM loadings. This fuel configuration would produce a LUEC of 138.49 US$/MWh. Correspondingly, an advisable fuel configuration for ThLEU would be 10wt% and 12 g HM. The reason for advising a higher HM loading for ThLEU is that ThLEU can be inherently safe at a higher HM loading in a water ingress scenario. The resulting LUEC being 126 US$/MWh.

This study was a multi-criteria decision/optimization analysis which kept the geometry, control rod positions (situated in the top reflector) and the amount of fuel passes (OTTO) constant. The fuel types were varied (LEU, ThLEU & ThHEU) as well as the HM loadings, enrichments and mixtures of the various material fractions within the fuel spheres. The fuel plant cost models were adapted for the various fuel and enrichments. A comparison was done to see how the various fuels behaved and how much cumulative energy each fuel type could provide while carefully observing how the fuel costs changed in the fuel plant cost model. The safety case for each fuel type in terms of maximum fuel temperature during a DLOFC and the reactivity spike due to water-ingress was discussed. However, it was not calculated.

Safety is the number one priority in nuclear engineering and cost comes second. Therefore, the final fuel choices which are suggested to a utility are the safest fuels in the study and secondly the most cost effective.

The study is suited to reactor cores of various geometries and loading schemes (OTTO & MODUL) due to the fact that the general trends are the same, that is the more heavy metal and enrichment, the higher the cumulative amount of heat energy etc. The HTR cost figures are generic and not specific to a certain country.

Keywords:

Fuel Spheres (Fuel Sphere), Highly Enriched Uranium (HEU), High Temperature Reactor (HTR), Low Enriched Uranium (LEU), Levilised Unit Energy Cost (LUEC), Pebble Bed Reactor (PBR), VSOP (Very Superior Old Program).

ACKNOWLEDGEMENTS

I would like to thank my supervisor, Professor Dawid Serfontein, and my co-supervisor, Mr Marius Tchonang-Pokaha, as well as Professor Eben Mulder who is an extraordinary Professor at the North West University and Mr Frederik Reitsma, who is the Team Leader of Gas-Cooled Reactors Technology at the IAEA, for their invaluable guidance, patience and mentorship in the field of neutronics, which helped me to complete my thesis.

I would also like to thank the Steenkampskraal Thorium Limited (STL) team for their valuable knowledge and expertise regarding the fuel & reactor cost models especially David Boyes on the fuel cost models and Yvotte Brits on the reactor cost models.

Table of Contents

List of figures

List of tables

ABBREVIATIONS

Acronym/ Abbreviation	Definition
dpa	displacement per atom
EJ	Exajoule ($1x10^{18}$ Joules)
ESP	Especially
ETA (η)	Number of neutrons released in fission per neutron absorbed by a fissile nucleus
HEU	Highly Enriched Uranium
HM	Heavy Metal
HTR	High Temperature Reactor
k_{eff}	Neutron multiplication factor of a finite reactor core
LEU	Low enriched Uranium (U-235 <20 wt%)
LUEC	Levilised Unit Energy Costs
LWR	Light Water Reactor
PBMR	Pebble Bed Modular Reactor
SG	Steam Generator
STL	Steenkampskraal Thorium Limited
Th	Thorium
ThHEU	Thorium mixed with High Enriched Uranium (U-235 93 wt%)
ThLEU	Thorium mixed with Low Enriched Uranium (U-235 20 wt%)
TRISO	Tri-structural Isotropic
U	Uranium
VSOP	Very Superior Old Program

1 INTRODUCTION

1.1 Background

Well-designed HTRs feature good neutron economies and fuel utilization allowing them to exploit various fuel cycles and achieve high burn-ups (Lung & Gremm, 1997). In order to obtain a good neutron economy, a large fuel core, with a large diameter, is required. This is because neutrons leak largely at the outer surface of the fuel core. Fore as cylindrical core, the ratio of the outer surface area to fuel volume decreases as the diameter increases. Therefore, larger diameters produce lower neutron leakage fractions, which result in improved neutron economies. Unfortunately, the rate of heat leakage out of the fuel core also happens at the outer surface of the core and therefore larger diameters similarly reduces the core's ability to leak heat during a Depressurised Loss of Forced Coolant flow (DLOFC) accident. Since the ability to quickly evacuate decay heat during a DLOFC accident, and thus to keep the maximum fuel temperature below the allowable safety limit, is key to the claim of good inherent safety features for HTRs. Therefore, as one increases the diameter in order to improve the neutron economy, the inherent passive safety is reduced. On the other hand, increasing the length of the fuel core improves the ability to evacuate decay heat. However, there are practical limits for the length of the core. If the core is made too long, the fuel spheres substantially burn out during their long journey from top to bottom. Therefore, the fuel quality at the bottom is so low that the fuel there burns at a much lower power than at the top. This leads to an overconcentration of power at the top, which leads to an undesirable temperature hotspot near the top, which reduces the inherent safety of the core. There is thus a trade-off between the diameter and the length of the core, which results in a trade of between good neutron economy and good inherent passive safety features. The designer must thus choose an optimum core geometry, aligned with the purpose for which the core is designed.

The pebble bed HTR has an advantage over conventional prismatic HTRs and that is has the ability to be fuelled online, which is due to is spherical ceramic fuel elements know as Fuel Spheres (FS) or pebbles.

1.2 Problem statement

Pebble Bed Reactor (PBR) fuel is expensive and if the fuel costs can be reduced by any means it would make the pebble bed reactor a more economic option. Fuel costs are around 17% (STL 2013) of the total costs of a PBR for a single First of a Kind (FOAK) reactor on site, not a multi-pack (many reactors on one site).

1.3 Purpose of the investigation

The fuel consumption rate needs to be reduced by varying the fuelling schemes that would increase the burn-up, conversion ratio and neutron economy for the OTTO cycle 100MW_{th} reactor. One such method to reduce the fuel consumption is by prolonging the residence time that the fuel spends in the reactor, thus allowing it to achieve higher burn-ups and extract more energy from each fuel sphere. This is done by varying fuel type, HM loading and enrichment. The main driving factor in the reduction of costs is the cumulative amount of heat energy which is obtained from the burn-up multiplied by the amount of heavy metal per fuel sphere. Therefore, due to the high cost of fuel spheres, the lowest fuel cost per kWh electricity produced, is more related to the cumulative amount of heat energy produced during the life of each fuel sphere, than to the burn-up. Therefore, increasing the heavy metal loading and enrichment will likely result in higher cumulative energy per fuel sphere and thus lower fuel cost per kWh electrical energy produced. The problem to be solved in this study is to reduce the fuel cost by improving the fuel design, within the required safety limits.

A key intrinsic safety characteristic of typical HTR design is keeping the fuel temperatures during a DLOFC accident low enough that the leakage of radioactive fission products through the coating layers around the fuel kernels will be limited to acceptable levels. A rule of thumb from the PBMR design philosophy was that the maximum fuel temperature during a DLOFC accident should remain below 1600°C. However, a detailed design for reducing the said leakage of radioactive fission products during a DLOFC is much more complicated than that: The amount of leakage increases with the number of fuel spheres that reach these elevated temperatures and increases with the time during which these fuel spheres remain at such elevated temperatures. Furthermore, some fuel compositions are less prone to leakage, for instance UCO fuel kernels can safely sustain higher temperatures than UO_2 kernels. The diameter of the fuel kernel and the thickness of the different coating layers, as well as the quality of manufacturing all play crucial roles in determining the leakage rate.

Another crucial safety issue is the risk of steam ingress accidents into the fuel core: The ^{1}H nuclei in light water are much more effective moderators that the ^{12}C nuclei in the graphite matrix of the fuel spheres. Therefore, water ingress will sharply increase neutron moderation. As HTR cores are normally under moderated, this increase in neutron moderation will increase the neutron economy of the fuel core, which will lead to an increase in the reactivity of the fuel and thus to an increase in power output. If appropriate safety features are not put in place, such an incident could lead to a serious nuclear accident. The risk of steam ingress is especially high when the core is coupled to a Rankine steam cycle for power conversion.

However, all these detailed safety design issues fall outside the scope of this study. Therefore, this study simply stuck to the said rule of thumb that the maximum DLOFC temperature during a DLOFC accident must remain below 1600°C.

1.4 Method

The proposed dissertation compares various fuels, raw material costs, enrichment and manufacturing costs of pebble bed reactor fuel to obtain the various optimal pebble bed fuelling schemes by ultimately comparing burn-ups, cumulative heat energies, conversion ratios, neutron economy and fuel production costs, with the aim to try reduce the fuel cost per unit electrical energy produced by increasing the cumulative heat energy while reducing the cost of a fuel sphere. Three fuel cycles (LEU, ThLEU and ThHEU) were simulated and compared using the VSOP 99/11 suite of codes together with the STL fuel cost models (Steenkampskraal Thorium Limited, 2017).

1.5 Structure of the report

This report consists of the following chapters:

1. **Introduction**: The introduction includes the background, problem statement, purpose and method to conduct the study.
2. **Literature survey**: The literature survey begins with the worlds energy consumption, it discusses fossil fuels, renewables and nuclear energy and then goes on to discuss various types of nuclear reactors preferably HTRs, specifically pebble bed HTRs, their fuel schemes and fuel cycles as well as thorium as a nuclear fuel ending with discussions about burn-up and the costs associated with nuclear fuels.
3. **Neutronic model development:** This discusses the HTMR100 OTTO core model
4. **Analysis and discussion of results**: Discussion of the equilibrium core results, DLOFC fuel temperatures and cost calculations
5. **Summary, conclusions and recommendations**
6. **References**
7. **Appendices**

2 LITERATURE SURVEY

2.1 Worlds energy consumption

Energy has become a vital part of our everyday lives and our technologically advanced society. Energy provides technological and economic development as well as a higher standard of living to the general populous. The energy demand is increasing at an alarming rate which is related to the worlds increasing population and economic growth. The worlds energy requirements both electricity and liquid fuels had reached 473EJ in 2008 and is expected to increase to 570EJ by the year 2050 based on the population being 9.3 billion by that time (Lior, 2009).

Most of the worlds energy generation comes from coal, oil and natural gas which amounts to 85% of the worlds energy, nuclear being 5% and renewables 10% (BP, 2015). Nuclear energy hydro-power and combustion of fossil fuels are the only forms of energy that can supply base load power and are dependable for a constant energy supply. Most developing countries as well as developed countries will still rely on fossil fuels to satisfy their energy needs for many years to come, however fossil fuels are associated with a lot of problems and environmental hazards.

2.2 Fossil fuels, renewables and nuclear energy

Fossil fuel power plants produce large amounts of pollutants that contaminate the soil, air and water. These pollutants are hazardous to human, animal and plant life. Combustion of these fossil fuels produce large amounts of greenhouse gasses such as carbon dioxide (CO_2), carbon monoxide (CO), nitrogen oxides (NO, NO_2) and sulphur oxides (SO_2, SO_3). Fossil fuels also deposit tons of ash and soot into the environment which contain biologically toxic elements, such as lead, mercury, nickel, tin, cadmium, antimony, and arsenic, as well as radio isotopes of thorium, uranium and strontium. Greenhouse gasses produced from the combustion of fossil fuels amount to 90% of the total world's production the other 10% is produced from agriculture and other industrial processes (International Energy Agency, 2015). The greenhouse gasses, such as carbon dioxide (CO_2), are leading to global warming and a long-term temperature increase of 3.5˚C (International Energy Agency, 2011). Coal produces

800-1000 gCO_{2eq}/kWh_e, oil 500-1200 gCO_{2eq}/kWh_e and natural gas produces 360-575 gCO_{2eq}/kWh_e (Weisser, 2006).

To reduce our greenhouse gas emissions other alternatives should be taken into account such as renewables and nuclear energy which will reduce the worlds carbon footprint.

Nuclear energy can supply constant base load power with a 90% availability and minimal greenhouse gas emissions of 0.74 – 1.3 gCO_{2eq}/kWh_e (Weisser, 2006), a reduction of approximately 799 gCO_{2eq}/kWh_e would be achieved by switching from coal to nuclear energy. If, however, bas-load nuclear plants are used, gas turbine peaking plants will have to be run to supply the power demand peaks, which will add a small, but substantial carbon footprint. Fossil fuels are consumed faster than they are produced, in the near future these resources will diminish and prices will increase. An advantage of nuclear energy is the required amount of fuel, less fuel offers more energy, 30-70kg of uranium ore produces 230g U_3O_8 and 30g of enriched uranium which produces 8000 KWh_{el}. Coal on the other hand requires 3000kg of black coal or 9000kg of brown coal to produce 8000KWh_{el}, there is around 300-900kg of fly ash released as well as many tons of CO_2 and SO_2 emissions (Kruger, 2014).The problems associated with nuclear are nuclear waste, political and public opposition, possible accidents as well as uranium supply. All these aspects are to be addressed when nuclear energy is chosen as an energy source.

Interest in thorium as a nuclear fuel continues to increase which could be used as an alternative nuclear fuel to prolong fissile reserves. In October 2014, the Colorado School of Mines published a report entitled “Thorium: Does Crystal Abundance Lead to Economic Availability?” (Jordan, et al., 2014). This report considers the possibility that thorium could be used as a nuclear fuel and that the demand for thorium could eventually give rise to nearly 4,000 tons per year. The report studies where this thorium would be obtained. The report states that the Steenkampskraal mine in South Africa will be the lowest cost producer of thorium in the world, with an estimated production cost of $ 3.56 per kg of thorium. The company therefore expects to play an important part in the development and introduction of Thorium as a nuclear fuel (Jordan, et al., 2014).

2.3 Types of nuclear reactors

Nuclear energy has come a long way since the first artificial nuclear reactor, the Chicago-pile became critical in 1942. Generation II (Gen II) reactors were developed in the 1960s (Goldberg & Rosner, 2011). They consist out of Boiling Water Reactors (BWRs) and Pressurized Water Reactors (PWRs), CANada Deuterium Uranium reactors (CANDUs), MAGNOX and Advanced Gas-cooled Reactors (AGRs). These Gen II reactors comprise the majority of the world's 400+ commercial PWRs and BWRs. These reactors, typically referred to as light water reactors (LWRs), use traditional active safety features involving electrical or mechanical operations that are initiated automatically. These reactors were designed for a lifetime of 40 years, although life extensions have been given to most of them. Some even last 60-80 years due to design margins.

Gen III nuclear reactors are essentially Gen II reactors with evolutionary, state-of-the-art design improvements. These improvements are in the areas of fuel technology, thermal efficiency, modularized construction, safety systems (especially the use of passive rather than active systems), and standardized design. Improvements in Gen III reactor technology have aimed at a longer operational life, typically 60 years of operation and more. The typical types of reactors include Advanced Boiling Water Reactors (ABWRs) and Advanced Pressurized Water Reactors (APWRs) as well as Advanced Heavy Water Reactors (AHWRs) (Goldberg & Rosner, 2011).

Gen III+ reactor designs are an evolutionary development of Gen III reactors, offering significant improvements in safety over Gen III reactor designs. These designs offer both passive and active safety systems. Passive safety systems utilise natural forces and phenomenon to cool reactor cores down in an accident situation such as (gravity, natural convection, condensation and evaporation), e.g. Economic Simplified Boiling Water Reactors (ESBWRs), Advanced CANDU reactors (ACR-1000) and APWRs the (AP-1000). Active safety systems consist of multiple trains of safety systems that are electrically or mechanically initiated automatically; such as the European Pressurized Reactor (EPR). The Water-Water Energetic Reactor (WWER-1000) is designed to consist of both active and passive safety systems (Goldberg & Rosner, 2011).

Gen IV reactors have all of the features of Gen III+ units, as well as the ability when operating at high temperature, to support economical hydrogen production, thermal energy off-taking, and water desalination. In addition, these designs include advanced actinide management and should be inherently safe with no possible chance of a core melt (Goldberg & Rosner, 2011).

There are many new Gen IV reactor concepts such as Molten Salt Fast Reactors (MSRs), Gas-cooled Fast Reactors (GFRs), Sodium-cooled fast Reactors (SFRs), Lead-cooled Fast Reactors (LFRs), Super-Critical Water Reactors (SCWRs), Very High Temperature Reactors (VHTRs), and High Temperature Gas-cooled Reactors (HTGRs). HTGRs can either one of two types, prismatic type and the pebble bed type. HTGRS are the most significant and can be realised as they have been built and operated previously.

Generation IV reactors are the future and are meant to be inherently safe. Inherent safety means that by natural effects the safety function of reactivity control, heat removal and confinement will be performed without any active or passive safety systems. This occurs by design which will be discussed in the following section. The only reactors to have proved inherent safety on an experimental scale are the HTR reactors.

2.4 High temperature reactors & inherent safety

The new Gen IV nuclear reactors are focused on safety. The nuclear reactors of interest are the High Temperature Reactors (HTRs) which were developed in the 1960s. These reactors use graphite as a moderator and helium as a coolant and can reach high temperatures of the outlet gas ranging from 700-950˚C which is perfectly suited for process heat applications such as sea water desalination, liquid fuel and hydrogen production (Kugeler, et al., 1989). These types of process heat applications could be used domestically in South Africa or abroad. South Africa may find desalination a more feasible option due to water shortages in the country, while European and American markets may be better suited to use high temperature heat for process heat applications.

The fuel compacts and pebbles contain TRISO (TRI-ISOtropic) coated particles. TRISO particles are fuel kernels uranium/thorium/plutonium oxides/carbides that contain a variety of coating layers, the various layers perform various functions, the most important being the SiC layer which is the main diffusion barrier to retain metallic fission products. The maximum fuel temperature of the fuel should remain below 1600˚C in the case of oxide fuels and 1800 ˚C in the case of UCO fuel which has a lower internal gas pressure. This ensures that most of the gaseous fission products remain within the SiC layer. Above these temperature limits the SiC layer becomes increasingly permeable to fission products (Kugeler, et al., 1989). The reason is that the fission products in all cases diffuse through the SiC layers. At low temperatures the diffusion rate is insignificant. However, as the temperature increases towards and above these limits, the diffusion rate increases exponentially and therefore reach unacceptable levels.

There are two types of High Temperature Reactors, Prismatic Block Reactors and Pebble Bed Reactors. Prismatic fuel elements are fuel compacts containing TRISO coated particles which make up a fuel rod, these rods are inserted into hexagonal graphite blocks. The cores are, in most cases, of an annular type, with a central graphite zone and an annular fuel arrangement where the fuel blocks, coolant channels and control rods are situated, this fuel region is surrounded by a graphite reflector. The fuel rods are approximately 3.4 cm in diameter but do vary in size and are situated within the graphite blocks. Helium is used to cool the core (Tanaka, et al., 1991).

In the pebble bed type, the core consists of thousands of pebbles forming a randomly packed bed inside a cylindrical graphite reflector. Each pebble has a diameter of 6cm, it has a fuel region of 5cm in diameter and a fuel free region of 0.5cm in diameter. The Fuel region contains thousands of TRISO coated particles in a graphite matrix. A PBR core is cooled by helium flowing through the pebble bed. There are several advantages of pebble fuel when compared with the prismatic block type the advantage of online fuelling, high tolerance with respect to the size and shape of the pebbles and uniform heat distribution (Kugeler, et al., 1989). The fundamental principle of an HTR is that it should be inherently safe, non-melting and be able reach high gas outlet temperatures.

The PBR is based on six principles: (Kugeler, et al., 1989):

1. The reactor core should contain only fissile & fertile material together with a very weak absorbing moderator – no unproductive capture of neutrons
2. A gaseous inert coolant should be used to avoid chemical reactions with core materials
3. An all-ceramic core which is operated at very high temperatures is to be used so that no melt-down is possible
4. Achieve coolant outlet temperatures suitable for closed cycle gas turbine plants for high efficiencies
5. Distribute fuel uniformly in the core to provide a high-power density in the fuel and give more heat transfer surface area
6. Have a good neutron economy to exploit, U-235, Th-232 & U-233 fuel cycles

2.4.1 Safety of HTRs

The three safety aspects of a nuclear reactor are to:

1. Control Reactivity
2. Keep core integrity under normal operations and in an accident scenario
3. Ensure insignificant radioactive material exposure to the public

In the Gen III+ reactors the most advanced systems use active or passive means to control the reactivity, cool the core and ensure that there is no radioactive release to the public. Gen IV HTRs ensure that these three criteria are met inherently which means that no active or passive systems are needed to ensure that the safety requirements are met. A safe design (large surface area for heat dissipation), a good selection in terms of materials of construction (all ceramic core and fuel) and natural phenomenon such as the negative temperature reactivity coefficient which will ensure that an HTR core will never melt as the reactor becomes less reactive as the temperature rises. These criteria will never lead to another nuclear accident such as (Three Mile Island, Chernobyl and Fukushima). The systems that these reactors had in place to prevent a core melt were not sufficient and this is why inherently safe reactors are the way forward.

2.4.2 Safety design features

The reactor design consists of a number of reactivity control and shutdown systems, these systems are independent, diverse and redundant and any of these systems are capable of a full shut-down of the core. These systems include control and shutdown rods which are situated in channels next to the core, Small Absorber Spheres (SAS) or KLAK (Klein Absorber Kugel System) which are small borated spheres which fall into channels alongside the core. Another option is borated pebbles which drop directly into the reactor core. Forced helium flow removes heat generated by the reactor core and additional heat is removed by the residual heat removal system (shutdown cooling system) which provides cooldown when the reactor is under maintenance or if the main cooling loop has failed. These systems are put in place to ensure that if the reactors need to be shut down and the heat removed, there are multiple systems in place to do so. These systems can deal with severe accidents such as a loss of coolant accident or a control rod ejection as they will shut down the nuclear chain reaction and remove decay heat from the core. These systems however do not provide inherent safety. Inherent safety is that if all the systems were to fail the reactor can still come to a safe shutdown state without any active or passive safety systems in place and the decay heat can be removed with no core melt and insignificant release of radioactivity to the public. This inherent safety is achieved through the following characteristics, safety by design, materials of construction and natural phenomenon, the properties associated with this inherent safety will now be discussed. HTRs are not safe unless the designers follow the strict rules to design a safe HTR. This is when inherent safety can be claimed. The good neutron economy and safety by design/inherent safety (which requires a large heat transfer area, large length to diameter ratio L=3D, a low power

density and adequate materials of construction) oppose one another so the core designer is required to find the optimum to ensure that the fuel remains below its limitations in a Depressurised Loss Of Coolant (DLOFC) accident so that the Core Damage Frequency (CDF) is kept to a minimum, as well as obtaining a low neutron leakage and good controllability with the core design.

2.4.2.1 Helium as a coolant

Helium is used as a coolant and is chemically inert thus no chemical reactions will take place within the core. Helium does not interact with neutrons and does not lead to unproductive captures of neutrons. Helium is inert after irradiation and remains in a gaseous phase over the entire temperature range in which the reactors operate (Kugeler, et al., 1989).

2.4.2.2 Graphite core and fuel

The core and fuel are fully ceramic (graphite), this material maintains its structural integrity at very high temperatures. The graphite has a high heat capacity and due to the low power density of an HTR the thermal responses are slow and gradual, thus allowing more time to initiate counter-measures to prevent transients from becoming accidents (Kugeler, et al., 1989).

The coated fuel particles specifically the SiC layer largely retains fission products up to 1600˚C for oxide fuels before the layer becomes increasingly permeable to the fission products due to high internal pressures produced in the coated particle. The reactors design, length to diameter ratio ensures that the heat will dissipate naturally as the area for heat dissipation is large and thus ensures that the fuel remains under the 1600˚C limit for oxide-based fuels such as UO_2 and UO_2/ThO_2. UCO which is developed in the United States of America (USA) can handle higher fuel temperature limits (1800 ˚C) due to the lower internal gas pressures encountered in these kernels due to one less oxygen molecule. The purpose of this study was to analyse oxide-based fuels so UCO will not be mentioned further. It is important to discuss that the amount of fuel which is subjected to these extreme temperatures would be a fraction of the total volume (this is discussed below). A volume temperature analysis is

preformed and shows that in a DLOFC only 2% to 5% is the maximum amount of fuel that would be subjected to this for the oxide based fuels used in this reactor design.

2.4.2.3 Passive cooling

If all active cooling systems were to fail and the reactor core heats up, the heat would naturally dissipate due to the core being designed with a large length to diameter ratio, thus a large surface area for heat to naturally dissipate through. This together with the materials of construction prevents a core melt (Kugeler, et al., 1989).The large volume leads to a low power density and large heat transfer surface for the dissipation of heat in an accident scenario; however, this large surface area is counterproductive when it comes to neutron economy as the large length to diameter ratio would leak more neutrons. The best design in terms of neutron economy would be a sphere or a cylinder with a large diameter. But the best design with regards to heat loss in an accident scenario would be a cylinder with a much smaller diameter and a much larger length, compared to its diameter. There is an optimum which is normally found based on the maximum fuel temperature in an accident scenario. If the fuel temperature is to hot the length to diameter ratio can be increased to lower the power density and increase the heat transfer area.

2.4.2.4 Reactivity coefficients

There are three temperature reactivity coefficients, the fuel temperature reactivity coefficient, moderator temperature reactivity coefficient and reflector temperature reactivity coefficient. For LEU fuels, the fuel and moderator coefficients are negative by nature. The cause of the negative fuel temperature reactivity coefficient is the Doppler effect. The reflector coefficient is positive but to a much lower degree, so the overall coefficient of all three is negative. This sum of effects is called the negative temperature coefficient which is most influenced by the negative fuel coefficient. Furthermore, the thick reflectors take a long time to heat up and therefore their positive reactivity effects take a long time to kick in, which provides sufficient time to take countermeasures, such as inserting control rods to reduce the reactivity of the core. By contrast, the negative fuel temperature reactivity effect kicks in almost instantaneously as the fission heat is produced in the fuel and therefore lifts the fuel temperature almost instantaneously. This is therefore called a prompt negative

reactivity effect. Due to its prompt nature, it will shut the fission reaction down before the heat can reach the reflectors to activate its positive reactivity effect. This fact contributes greatly to the safety of the core.

When the reactor heats up due to a loss of cooling accident or a control rod withdrawal the nuclear fuel heats up and both the resonance and fission absorption cross sections enlarge upon heating, however the absorption cross sections enlarge at a larger rate compared to the fission cross sections. The result is that the chain reaction is shut down. If all reactivity control and shutdown systems were to fail the negative temperature coefficient would take the reactor to a hot safe shutdown state in a loss of coolant accident and will prevent a run away. This would be the case in a loss of coolant accident as well (Kugeler, et al., 1989).

After the fission chain reaction has shut down, the substantial heat decay heat production will cause the fuel temperatures to increase towards the upper limit of 1600˚C for oxide based fuels. However, only a small fraction of the fuel sees temperatures of about 1600˚C for the oxide fuels. In the temperature/volume analysis of the fuel observed in the VSOP accident scenarios for LEU fuel at 20wt% and 10 g HM which has the highest fuel temperature of the usable fuels the percentage of fuel that sees around 1600˚C is only 2.9% for most cases and the fuel seeing above 1650˚C is 1.8% for most cases. This means that even when these temperature limits are exceeded and substantial releases of radioactive fission products do happen, only a small fraction of the available radioactivity will leak out. that the temperature limit is thus not set in stone.

Gas cooled reactors do not have a coolant which changes phase so void coefficients are not applicable. The large increase in reactivity would come from water/steam ingress into the reactor core from a steam generator tube break called water-ingress.

2.4.2.5 Water ingress

In general, water ingress into the primary circuit of a high temperature reactor poses a considerable hazard. One of these hazards is that the penetration of neutron moderating steam into the core may cause an increase in reactivity and thus an

intolerable power excursion for certain core layouts. The second hazard is the possibility that steam may be converted by a chemical reaction with the hot graphite structures and the hot graphitic fuel elements into a mixture of H_2 and CO gasses, which might become flammable when mixed with air (Lohnert G.H., 1992).

When steam ingress occurs, the influx of steam as an additional moderator gives rise to two effects. Firstly, the reactor increases its reactivity since the neutron spectrum softens, which in turn increases the average microscopic fission cross section in the thermal energy region. Due to improved neutron moderation, the number of neutrons captured in the radiative capture resonances of U-238 in the fuel kernels decreases and thus the resonance escape probability increases. Secondly, due to improved neutron moderation the overall neutron diffusion coefficient decreases, which in turn decreases the overall neutron leakage (Lohnert G.H., 1992). A decrease in neutron leakage however decreases the rod worth of the absorbers in the side reflector, so that in a shutdown or partially shut down core the overall effect of water ingress is the sum of reactivity increase and rod worth decrease.

Limiting the mass of heavy metal per fuel sphere (inherent safety) will limit the reactivity increase when water ingresses into the reactor core. A lower HM loading reduces the volume fraction of the coated fuel particles and thus increases the average distance between fuel kernels. Neutrons thus, on average, traverse longer path lengths of graphite between collisions with fuel kernels. The probability of getting moderated before being captured in the resonances of U-238, i.e. the resonance escape probability, thus increases. Since less neutrons are captured in the fuel in such a fuel sphere with improved moderation, reducing these captures even further, by increasing the moderation by means of water ingress, will thus cause a smaller increase in k_{eff}.

Newer literature sources are available on water ingress. However, since water ingress will not be modelled in this study and is only mentioned here in passing, no further attention will be given to the matter.

2.4.3 OTTO vs MEDUL

Pebble Bed Reactors can be refuelled during operation by loading fresh pebbles at the top while removing depleted/burnt pebbles at the bottom. A Once Through Then Out (OTTO) fuel cycle is where the pebbles pass through the core slowly and once

removed are stored for final storage. A MEDUL fuel cycle recirculates partially burnt pebbles back into the top of the reactor and only once the pebbles reach a specific burn-up they are removed and sent to final storage. An OTTO cycle has a higher power peaking factor and would have a higher fuel temperature in an accident scenario, however it does away with the complex fuel handling system needed for a MEDUL fuelling scheme. A MEDUL fuelling scheme has a flatter power distribution within the core, however the complex fuelling scheme is costly and it creates a lot of graphite dust which is generated by the recirculation of pebbles. The fuel pebble can be tracked easier in an OTTO cycle, meaning the relative position of where the pebble is in its lifetime. However, in a MEDUL the pebbles cannot be tracked and due to the recirculation, some pebbles may be burnt to higher values than what was designed for. An OTTO cycle was chosen for this reactor due to the simplicity of the fuel handling system and significant cost reductions associated with this simple system. The OTTO cycle has a higher power peaking factor and would have a higher fuel temperature in a loss of cooling accident known as a Depressurized Loss Of Forced Cooling (DLOFC) accident. Therefore, the nominal power of the core will have to be reduced by about 50% when one switches from a MEDUL to an OTTO cycle. This will obviously sharply reduce the revenue from power sales. However, even so, the benefits of a simpler and cheaper core might outweigh the disadvantage of the reduced revenue and therefore the OTTO fuel cycle was chosen for the reactor design and the neutronic modelling in this study.

2.5 Previous and current HTRs

2.5.1 Previous HTRs

2.5.1.1 DRAGON

The DRAGON was an Organization for Economic Co-Operation and Development (OECD) project that was based at Winfrith in Dorset, England, and was operated by the United Kingdom Atomic Energy Authority. It was a High Temperature Reactor. In 1964 the 20MW_{th} graphite moderated, helium cooled fuel and material test DRAGON reactor came online. It used coated particle (Th/U)O_2 and (Th/U)C_2 fuel. It was a hexagonal array and prismatic in nature, it ran at 1000˚C and provided high burn-ups of around 100000MWd/THM it was operated until 1975 (Mcdowell, et al., 2011).

2.5.1.2 Peach Bottom

The Peach Bottom Reactor was an 115MW_{th} experimental prismatic block design. It operated from 1966-1974. It was also a graphite moderated, helium cooled reactor which used (Th/U)O_2 and (Th/U)C_2 coated particle fuel, it operated at around 700-750˚C (Mcdowell, et al., 2011).

2.5.1.3 AVR

The AVR (Arbeitsgemeinschaft VersuchReaktor) was the first pebble bed, graphite moderated, helium cooled reactor with 46MW_{th}. The reactor ran from 1967-1988 providing a lot of data for pebble bed reactors specifically pebble beds. This reactor had a low power density of 2.6MW/m^3 and operated at 950˚C. It reached burn-ups of 100000MWd/THM (Mcdowell, et al., 2011). The AVR proved inherent safety by shutting off the helium coolant to simulate a Loss Of Coolant Accident (LOCA). The main LOCA test lasted for 5 d. After the test began, core temperatures increased for approximately 13 h and then gradually and continually decreased as the rate of heat dissipation from the core exceeded accident levels of decay power. Throughout the test, temperatures remained below limiting values for the core and other reactor components. The main factor here which was shown was that the fuel temperatures remained below the theoretical fuel temperature limit of 1600 ˚C.

2.5.1.4 THTR

The THTR (Thorium High Temperature Reactor) was the first commercial pebble bed reactor that was graphite moderated, helium cooled and produced 750MW_{th}. It ran from 1985-1991 before it was shut down due to political reasons and problems with pebble breakage and consequent release of measurable amounts of radioactivity into the atmosphere. This pebble breakage was caused by multiple control rods being inserted simultaneously into the pebble bed. The reactor had a power density of 6MW/m^3 and provided outlet temperatures of 750˚C. The fuel elements consisted of 0.96g of U-235 and 10.2g of Th-232 and provided burn-ups of 100000MWd/THM. This proved that thorium fuel was a viable option for HTR reactors (Mcdowell, et al., 2011).

2.5.2 Current HTRs

2.5.2.1 HTTR

The HTTR (High Temperature Test Reactor) in Japan is a prismatic block reactor, graphite moderated, helium cooled. This reactor was developed to further prove HTR technology and H_2 production. The HTTR delivers 30MW_{th}. It is fuelled with UO_2 and has a maximum helium outlet temperature of 950˚C. The reactor started up in 1998 and is currently on halt due to the Fukushima accident. A restart is planned, pending regulatory approval. (Mcdowell, et al., 2011).

2.5.2.2 HTR-10

The HTR-10 is the only pebble bed currently in operation. It was commissioned in 2000. It is a High Temperature Pebble Bed Reactor, graphite moderated and helium cooled. It has a thermal power of 10MW_{th}, a power density of 2MW/m^3 and produces outlet temperatures of 700˚C, the fuel used is UO_2 TRISO particle fuel. This reactor has demonstrated inherent safety for low powered reactors by stopping the helium blowers, where after the coolant flow ceased and the reactor temperature rose until the negative temperature coefficient shut the chain reaction down with all control rods withdrawn. The reactor was able to cool down naturally and the heat was dissipated to the environment with no core melt, the fuel temperature remained below the1600 ˚C limit (Wu & Zhong, 2002). The HTR-10 also demonstrated inherent safety by performing two simulated Anticipated Transients Without Scram (ATWS) tests, loss of

heat sink by tripping the helium blower without scram and reactivity abnormal increase by means of withdraw a control rod without scram were selected as first phase safety demonstration experimental items. The test of tripping the helium circulator ATWS was conducted on October 15,2003. The helium blower was switched off during normal operation with 3MW, which means the primary coolant system was disconnected. Although none of the 10 control rods were moved, the reactor power immediately decreased due to the negative temperature coefficient. After 50 minutes, the reactor becomes critical again. The output power went to a stable level of about 200kw after around 2 hours.

Unfortunately, these experiments do not prove the safety of higher powered reactors: Due to the very low decay heat production, caused by the very low normal operating core power of $10MW_{th}$, the decay heat was easily removed passively and therefore there was practically no increase in fuel temperature after the coolant flow was stopped and the fission chain reaction was shut down. However, in much higher-powered reactors, such as the 400 MW_{th} PBMR-400, the decay heat production power would be about 40 times larger than for the HTR-10. Therefore, the increase in fuel temperature during a DLOFC accident would also be much higher, which could possibly result in the maximum fuel temperature limit being breached. Therefore, in order to prove passive safety, the experiments of the HTR-10 will have to be repeated for much higher-powered reactors.

2.5.2.3 HTR-PM

The HTR-PM is being constructed in China and will have two modules of $250MW_{th}$ coupled to a conventional $210MW_{el}$ steam turbine. The fuel pebbles will contain 7g of heavy metal loading of UO_2 with an enrichment of 8.8%. The active core will contain 520 000 fuel pebbles that are expected to reach burn-ups up to 80 000 MWd/THM (Zhang, et al., 2004). A larger reactor design is currently underway, an HTR that could work as heat source for the petrochemical industry. The preliminary feasibility study of a 600 MW modular HTR (HTR-PM600) working as heat source for a typical hypothetical Chinese petrochemical factory is being designed and it is believed that this marriage of an HTR-PM600 and the petrochemical industry is achievable.

2.5.2.4 Pebble Bed Modular Reactor (PBMR)

The PBMR-400 is a 400 MW_{th} pebble bed high temperature gas cooled reactor design which achieves (165MW_e). The core is an annular arrangement with a fixed central graphite reflector It is designed such that the maximum temperature will not exceed 1600˚C under accident scenarios due to the shortened heat flow path from the inner layers of the core to the external reflector. TRISO coated UO_2 (9.6wt% enrichment and a 9 g HM loading) encased within a graphite sphere is used and this reactor uses a MEDUL fuel cycle which achieves a burn-up of 80000 MWd/THM. The primary coolant is Helium and is heated up from 560 ˚C - 900 ˚C as it is forced downwards through the pebble bed. The Helium at normal operating conditions was heated to 900 ˚C. Helium then exits the pebble bed at 900˚C and passes through turbines which are connected to compressors on single shafts. The turbines spin compressors to blow the working fluid back to the reactor. The initial PBMR design used a 3-shaft system with two turbo-compressors and a turbo-generator which creates electricity. The pre-cooler, intercooler and recuperator are used to increase the thermal efficiency of the cycle. There is no secondary steam cycle or steam generator as the primary loop turns the turbines directly. This Brayton cycle increases the thermal efficiency tremendously allowing an efficiency of 41%.

Graphite fuel spheres are loaded into the core by fuel loading machines in the central position. Fuel spheres containing Uranium are loaded at three different points in the annulus of the reactor. Fuel unloading machines are located in the centre and in the off-set positions at the bottom of the reactor. The outer reflector that houses the gas risers and control rods, is made out of graphite and the exterior reflector is made out of carbon. The control rods and shutdown rods (48 rods) are made from boron carbide and the additional reserve shutdown system is small absorber spheres called KLAK (18 places) also made of neutron absorbing material.

These reactors have not been built after the German program was closed due to an accident at the THTR where some pebbles were broken when all the control rods were inserted simultaneously into the pebble bed. This happened at the same time as the Chernobyl accident. Measurable amounts of radioactivity were released into the air and the German nuclear regulator picked it up. On top of this, the management of the THTR tried to cover the accident up. This, together with green political anti-nuclear

sentiment in Germany led to the cancellation of the German HTR program. South Africa and China were the only two countries to take the pebble bed technology further, however the pebble bed project in South Africa (PBMR) was also stopped due to huge budget and schedule overruns. Political reasons probably contributed to the decision. Now the Chinese are the only country to have built a new pebble bed reactor.

2.5.3 Conceptual HTR designs

Japan Atomic Energy Agency (JAEA) has several conceptual designs based on the experience and development work related to the HTTR test reactor. One of these designs is the **GTHTR300** (Gas Turbine High Temperature Reactor 300 MW_e), a multipurpose, inherently-safe and site-flexible small modular reactor. This reactor is under development for commercialization in the 2020s. The development of HTGR technologies in Russia includes the project to develop the 285 MW(e) Gas Turbine-Modular Helium Reactor (**GT-MHR**) for electricity production but recently also the diversification of the nuclear power applications for industrial purposes, such as the **MHR-T** reactor/hydrogen production complex that use 4x600 MW_{th} modules. Finally, the **MHR-100** prismatic modular helium reactor design of 215 MW_{th} is used in multiple configurations for electricity and cogeneration. The GT-MHR is a Russian Federation – USA jointly funded project, originally aimed at solving one of the most important tasks in the area of non-proliferation; the disposition of weapons-grade plutonium.

The South African developed Pebble Bed Modular Reactor (**PBMR-400**) design can produce electricity of 165 MW(e) at high efficiency via a direct Brayton cycle employing a helium gas turbine. The unique fixed central column design allows the larger thermal power in a pebble bed design while retaining its inherent safety characteristics for decay heat removal with passive only means even under the most severe conditions. The project was stopped in 2010 (as mentioned above) but the design information is secured and maintained. Also, in South Africa the Steenkampskraal Thorium Limited (STL) company is aiming to finish the conceptual design of the **HTMR-100** pebble bed design by 2020 and plans to be able to use a range of uranium and uranium-thorium coated particle pebble fuels in a once through-then-out (single pass) cycle. The HTMR-100 is designed to generate 35 MW_e.

In the USA, the NGNP Industry alliance has selected the AREVA 272 MW(e) **SC–HTGR** a prismatic block design for commercialization and the preparation for pre-licensing application have started. The design is based on the AREVA's ANTARES concept but coupled to two steam generators and allows for cogeneration. A privately owned and funded initiative in the USA, called X-energy, is pursuing the **Xe-100 (200MW$_{th}$)** pebble bed MEDUL reactor producing 67 MWe. A major aim of the design is to improve the economics through system simplification, component modularization, reduction of construction time and high plant availability brought about by continuous fuelling.

2.6 Pebble fuel & fuel manufacture

2.6.1 Pebble fuel

In **Figure 1** the fuel elements (graphite spheres) called pebbles/fuel spheres are shown and are designed to flow through the reactors core, they are spherical in nature, these pebbles house thousands of coated particles called kernels which contain various coating layers for the retention of fission products. These fuel spheres are made from ceramic materials (graphite) and able to withstand extreme temperatures and maintain structural integrity at these elevated temperatures.

The fuel spheres contain fissile as well as fertile material in the form of TRISO coated particles/kernels usually in a uranium/thorium/plutonium oxide or carbide form embedded in matrix graphite. Fuel spheres are 60 mm in diameter and contain about 12 000~17000 coated particles. The fuel sphere consists of an inner fuel zone of approximately 50 mm in diameter in which the TRISO coated particles are randomly embedded. A fuel-free zone of about 5 mm in thickness is surrounding the fuel zone. The coated particle consists of an inner fuel kernel (0.5 mm in diameter) containing the fissile/fertile material and is surrounded by four coating layers (International Atomic Energy Agency, 2010). Each coating has its own function - together they to a large degree retain fission products in normal and accident conditions. The layers absorb and seal in radioactive elements that are released from the fuel when it undergoes fission to produce power. The heat that is generated in the coated particles during fission is conducted by the graphite matrix to the surface of the fuel spheres and into the helium gas. The following performance requirements have led to the choice of fuel sphere materials, and the fuel sphere manufacturing process. Fuel spheres must be capable of operating at high temperatures and must be mechanically strong, and must resist abrasion, corrosion and radiation.

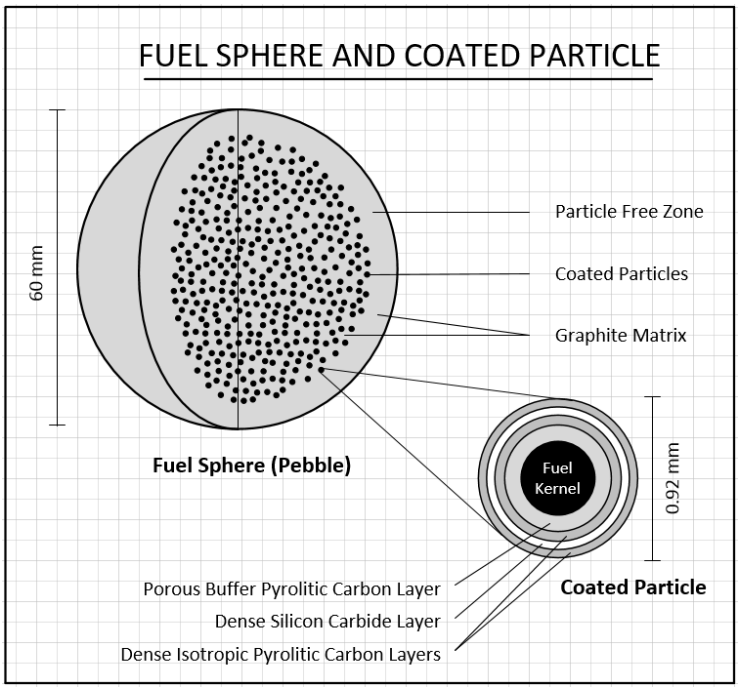

Figure 1: Fuel sphere depicting coated particle with barriers

2.6.2 Fuel manufacture

The fuel manufacturing process will now be discussed. The general process flow diagram is shown in **Figure 2**.

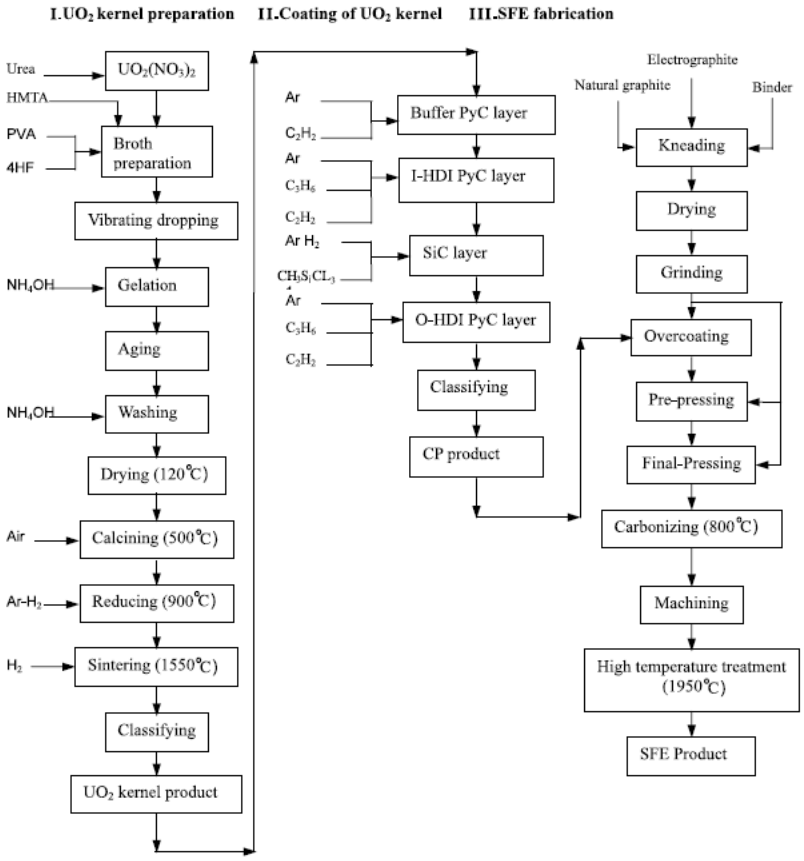

Figure 2: Fuel manufacturing scheme (International Atomic Energy Agency, 2010)

2.6.2.1 Kernels

Figure 3 shows how UO_2/ ThO_2/PuO_2 kernels (sintered microspheres) 0,5 mm in diameter are produced from a casting solution prepared from a mixture of uranyl nitrate, thorium nitrate as well as plutonium nitrate solutions ($UO_2(NO_3)_2$,$Th(NO_3)_2$ and $Pu(NO_3)_4$), THFA (tetrahydrofurfuryl alcohol) and polyvinyl alcohol (PVA) solution. The casting solution is fed through vibrating nozzles with an approximately 1 mm diameter, where the liquid stream is broken up into spherical droplets. As the spherical droplets pass through an ammonia gas curtain they solidify enough to withstand the impact on entering the liquid precipitation medium called gelation. The gelled spheres are then aged, washed, dried. The micro spheres are then calcined and sintered. Defective kernels are removed by sieving and sorting. The product is then sampled and after analyses and release, batches are combined into a lot and then portioned into

representative batches for the Coated Particle Facility (International Atomic Energy Agency, 2010).

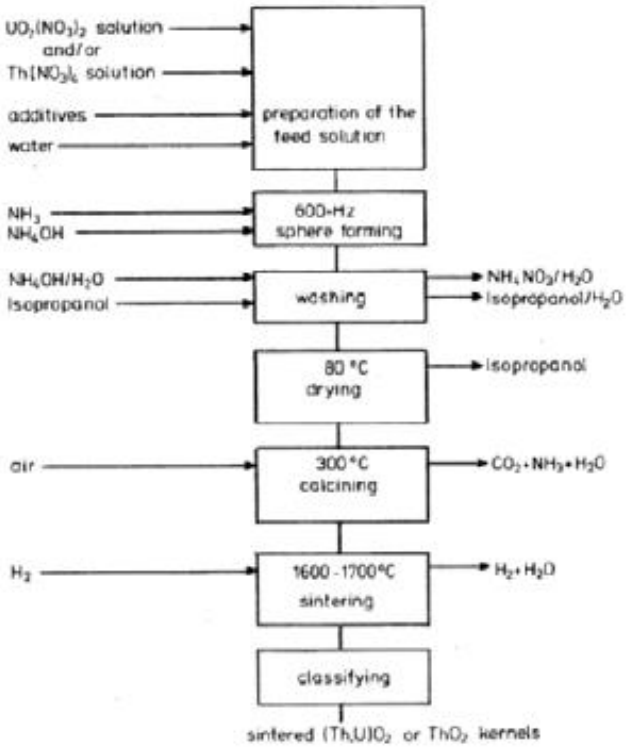

Figure 3: Kernel casting (International Atomic Energy Agency, 2010)

2.6.2.2 Coated particles

Uranium/Thorium/Plutonium dioxide kernels conforming to the product specification are coated by the decomposition of gasses in a chemical vapour fluidized-bed coating furnace called a spouted bed Chemical Vapour Deposition (CVD) shown in **Figure 4**. The flowing gases forced into the furnace suspend the kernels so that they form a fluidized-bed. Coating gases are selected which decompose and deposit on the surface of kernels at temperatures up to 1600˚C. The materials of the layers formed by this process are described as pyrolytic because they are formed by pyrolysis (thermochemical decomposition) of an organic material brought about by heat (International Atomic Energy Agency, 2010). The TRISO coated particle shall be coated with four successive layers in one furnace: The first layer, the buffer layer, a low-density carbon deposited from acetylene. The second layer, Inner Low Temperature Isotropic layer (ILTI layer), a high-density isotropic carbon, deposited

from a mixture of acetylene and propylene. The third layer, Silicon Carbide (SiC layer), deposited from methyltrichlorosilane (MTS). The fourth layer, Outer Low Temperature Isotropic layer (OLTI layer), a high-density isotropic carbon, deposited from a mixture off acetylene and propylene. The coated particles are then sieved to remove the under and over size particles before being sorted using vibrating tabling machines to remove odd-shaped and out of round particles. The coated particles are then sampled by using a percentage sampler before being combined and portioned to make up a homogeneous lot.

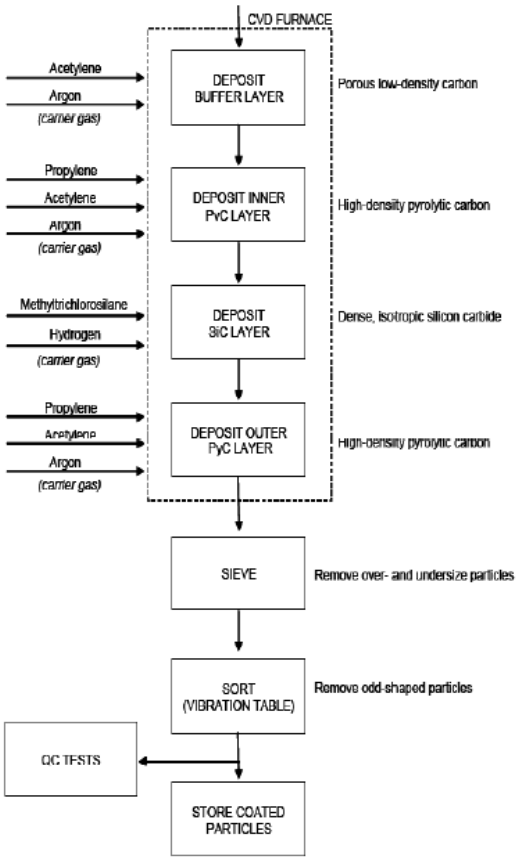

Figure 4: Chemical Vapour Deposition (CVD) process (International Atomic Energy Agency, 2010)

2.6.2.3 Fuel spheres

The fuel sphere manufacturing process is shown in **Figure 5** where the coated particles are over-coated with fine-milled matrix graphite powder. Over-coated particles are mixed with standard matrix graphite powder and pressed to form the fuel zone (core) of the fuel sphere. The fuel zone is encased in a shell of standard matrix graphite powder and is isostatically pressed to form so called green fuel spheres.

These are then machined so that the diameter of finished fuel spheres after heat treatment and are within the required tolerances. The machined fuel spheres are carbonised in an inert gas atmosphere. The carbonised fuel spheres are annealed under vacuum. Argon is used in purging the furnace for cooling down and removing the fuel spheres. The manufacturing function shall demonstrate that different manufacturing lines produce the same product during qualification.

2.6.2.4 Matrix graphite powder

The function of the graphite matrix is to contain the coated particles in a fuel sphere, protect them from mechanical damage, and provide a heat conduction path between the coated particles and the reactor coolant, helium. The carbon in the graphite matrix also acts as the moderator for neutrons in the core. Highly graphitized (i.e., aligned crystalline structure) materials are used for the graphite matrix for the following reasons:

1. Highly graphitized graphite ensures dimensional stability during irradiation with fast neutrons, as partially graphitized graphite will undergo further graphitization under fast neutron irradiation, with accompanying dimensional changes.

2. Once a fuel sphere has been pressed, it is no longer possible to change the degree of graphitization of the graphite contained in the fuel sphere. The reason is that temperatures required for graphitization (2,700°C to 3,000°C) would also damage the effectiveness of the SiC layer and Uranium will diffuse through the SiC layer contaminating the graphite matrix.

3. Highly graphitized material has the desirable property that it can be relatively easily pressed to the required density.

2.6.2.5 Over-coating

In preparation for fuel sphere manufacturing, a coating of finely milled matrix graphite powder is applied to the outer surface of each coated particle in a rotating drum. This coating is known as the ‘over-coat.’ Its primary purpose is to prevent coated particles from coming into contact with each other during final pressing, thereby damaging the coated particle coatings. Because of the lower average density (reduced segregation) and bigger diameter (increase of distance between coated particles) of the over-coated particle, a higher level of homogenisation of the fuel-containing region is achieved.

2.6.2.6 Pressing

A fuel sphere is formed by pressing over-coated particles along with additional matrix graphite powder, into an inner fuel-containing region, that will contain the coated particles. The inner fuel-containing region is then placed within a protective 5 mm thick layer of matrix graphite formed by an isostatic pressing process, machined to dimension and heat treated. Fuel spheres are pressed at high pressure, without application of external heat, to obtain the required density that ensures adequate structural stability and heat conduction. This also provides the correct amount of carbon in the reactor core to determine heat capacity, thermal conductivity and moderation.

Fuel spheres are pressed in two steps:

1. In the first step, over-coated particles and matrix graphite powder are mixed and pressed (low pressure, low matrix graphite density) to form a fuel-containing region. Coated particles are distributed evenly in this inner fuel-containing region to prevent the development of hot spots in the fuel sphere.
2. In the second step, matrix graphite powder is added to the final mould and pressed to form a fuel-free region around the fuel-containing region. The purpose of this fuel-free region is to protect the coated particle contained in the inner zone from mechanical and chemical damage during handling and operation.

Final heat treatment steps remove organic components and impurities and make the spherical fuel strong and corrosion resistant. The Graphite Matrix then consists of carbonized and purified organic binder and nuclear-grade graphite material that should exhibit high density, high thermal conductivity, high mechanical strength, low thermal expansion, low anisotropy, low Young's modulus, good corrosion resistance and good dimensional stability under neutron irradiation (International Atomic Energy Agency, 2010).

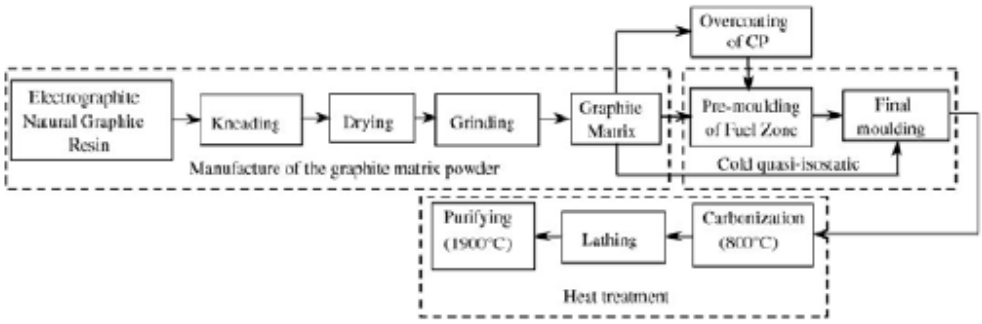

Figure 5: Fuel sphere manufacturing process (International Atomic Energy Agency, 2010)

2.6.3 Fuel Limitations

HTR fuel can withstand extremely high temperatures, without melting, due to the fact that the fuel is entirely ceramic (graphite). However, the maximum fuel temperature that can be reached for oxide-based fuels without allowing substantial diffusion of gaseous fission products through the SiC layer is 1600˚C. This diffusion happens due to the pressure build-up of gaseous radioactive fission products within the kernel. This diffusion also happens at low temperatures. However, according to the laws of diffusion, the diffusion rate increases continuously and exponentially with increasing temperature. Therefore, the diffusion rates at low temperatures are insignificant and difficult to observe. This leads to the frequently repeated false statement that no leakage happens below the given temperature limit, such as 1600˚C, and that it then suddenly happens above this temperature limit. In reality, low levels of leakage are present at all temperatures. This explains while normal operation with a maximum fuel temperature of e.g. < 1200˚C can also lead to significant leakage: the leakage rate at such low temperatures are very low. However it continuous for many years and in this process significant levels of radioactivity can slowly accumulate and contaminate the primary coolant system, as happened in the AVR. In contrast to this, the high temperatures during a DLOFC accident lasts only a few days. However, as the leakage rate would be many orders of magnitude higher, for the case where the maximum temperature limit of e.g. 1600˚C were to be exceeded, large quantities of radioactive contaminants can then accumulate in this short time span.

UCO fuel can withstand 1800˚C due to the lower internal pressures that are produced within fuel kernels due to the different chemical structure. This allows it to operate at higher temperatures in an accident condition as the internal pressure will be lower and

there will be no substantial diffusion of gaseous fission products through the SiC layer up to 1800˚C. The maximum fuel temperature in an accident case where coolant is lost should remain below these values for each specific fuel.

The statement above regarding increased diffusion through the SiC layer at 1600˚C for oxide-based fuels is an interpreted value. During the experiments, it is reported that up to 1600˚C no substantial additional fission product release (beyond the assumed failure fraction in manufacturing) has been observed in UO_2, TRISO-based fuel. At 1700˚C the Germans reported that evidence is inconclusive, since the statistical sampling have not been valid, yet at 1800˚C it was found that 2 TRISO particle failures out of 3 pebbles have been observed.

Another important limitation the pebble bed fuel has is the maximum particle packing that can be achieved. With thorium-based fuels higher heavy metal loadings are required per pebble in order to obtain a good neutron economy and effective breeding. The loadings on the THTR went up to around 12 g HM per fuel sphere (19250 kernels/sphere) using HEU as a driver. The LEU/Th fuel cycle would require more kernels/heavy metal per sphere to obtain sufficient breeding of U-233. The maximum kernels per sphere in theory is 34000 kernels/sphere which amounts to around 21 g HM per fuel element which equates to a distance of 1150 µm between particles. (International Atomic Energy Agency, 2015). The general trend for LEU fuel is around 12000 – 17000 kernels per sphere which amounts to (7 – 10.5 g HM per fuel element), this equates to a distance of 1225 µm (12000 particles) and 1175 µm (17000 particles). These values are kept lower due to problems associated with particle to particle interaction and cracking of particles. Generally, HTRs have steam cycles and associated water ingress problems therefore the HM loading is kept on the lower side of the spectrum (International Atomic Energy Agency, 2015).

However, it should be noted that cracking of particle coatings is not the only mode of leakage for radioactive fission products. As has been explained in the introduction of this section, diffusion through normal SiC coatings, which have not cracked, is the other major mode of leakage. Therefore, the data given above on cracking of coatings cannot be used as the sole measure to define the maximum temperature limit.

The general trend is that as the enrichment increases, the maximum observed fuel temperature will increase, i.e. it will start to approach the maximum temperature limit.

This explains why explains while most LEU fuel designs use enrichments much lower than the maximum limit of 20 a/o% for LEU.

2.6.4 UCO Fuel Achievements in the USA

As part of the Office of Nuclear Energy's Next Generation Nuclear Plant (NGNP) Program, the Advanced Gas Reactor (AGR) Fuel Development Program has achieved a new international record for irradiation testing of next-generation particle fuel for use in HTRs.

The AGR Fuel Development Program was initiated by the Department of Energy in 2002 to develop the advanced fabrication and characterization technologies and provide irradiation and safety performance data required to license TRISO particle fuel for the NGNP and future HTRs. The AGR Fuel team used the Idaho National Laboratory's (INL) unique Advanced Test Reactor (ATR) in a nearly three-year pivotal irradiation test to subject more than 300,000 nuclear fuel particles to an intense neutron field and temperatures around 1,250 degrees Celsius.

INL researchers say the particle fuel experiment set the world record for particle fuel performance by consuming a maximum of 19 % burn-up of the initial low-enriched uranium content, with an average burn-up of 16 % for all of the fuel tested. The maximum 19 % burn-up achieved is more than double the previous record set by similar particle fuel experiments run by German scientists in the 1980s, and more than three times that achieved by current light water reactor fuel. Additionally, none of the fuel particles experienced failure since entering the extreme neutron irradiation test environment of the ATR in December 2006.

The purpose of the fuel program is to develop this particle fuel, produce experimental data that demonstrates to the Nuclear Regulatory Commission (NRC) that the fuel is robust and safe, and re-establish a U.S. fuel manufacturing capability for high temperature gas reactors. INL has been working with Babcock and Wilcox Inc., General Atomics and Oak Ridge National Laboratory (ORNL) to establish standards and procedures for the manufacture of commercial-scale HTGR fuel. The overarching goal of the AGR Fuel Program is to qualify coated nuclear fuel particles for use in HTGRs such as the NGNP. Developing particle fuel capable of achieving very high burn-up levels will also reduce the amount of used fuel that is generated by HTRs.

2.7 HTR fuel cycles

It is well known that nuclear fission produces good neutron economies in fast reactors and well thermalised reactors, but not in reactors where a large fraction of the fissions occur in the epithermal energy range: very high energy neutrons produce fast fissions that produce substantially more neutrons per fission than thermal fissions. The radiative capture to fission ratio in the fissile isotopes is also much lower for high neutron energies. The microscopic radiative capture cross-sections for most fertile isotopes, especially ^{238}U, are also very low at high neutron energies. This increases the infinite neutron multiplication factor, k_∞, by reducing captures, thereby leaving more neutrons available to perform fissions. More importantly very fast neutrons (> 100 keV) also fission substantial numbers of fertile isotopes, especially U-238 and Pu-240, while these fissions are almost completely absent at lower neutron energies. While all the major fissile fuel isotopes perform very well at very high neutron energies, Pu-239 and Pu-241 stands out. Therefore U/Pu fuel cycles are normally the top performers in fast reactors.

Once the neutrons are moderated down to epithermal energies (roughly 4 eV to 4 keV) this situation reverses sharply: The radiative capture microscopic cross-sections of both fertile and fissile isotopes increase greatly, especially in the capture resonances, while fast fissions of fertile isotopes disappear almost completely. While substantial numbers of fission of fissile isotopes does occur in the epithermal resonances, they are now accompanied by increased numbers of radiative captures in these same isotopes. The result is that the capture to fission ratio for the fissile isotopes increases sharply, especially for Pu-239 and Pu-241, while for the fertile isotopes captures dominate completely. This results in a very poor neutron economy, especially for U/Pu fuel cycles. U-233 is the only fissile fuel that can maintain a reasonably low capture-to-fission ratio in the epithermal neutron energy range. The microscopic capture cross-sections for Th-232 are also much lower than for U-238. Therefore Th/U-233 fuel cycles are the only ones that perform reasonably well in the epithermal range.

Once neutrons have been moderated down to thermal energies the microscopic fission cross-sections of the fissile isotopes, such as U-235, Pu-239, Pu-241 and U-233 increases dramatically. While their microscopic radiative capture cross-sections also increases, they typically remains about ten times lower than the corresponding fission cross-sections. So, while the capture-to-fission ratios for thermal reactors are substantially higher than for fast reactors, they remain much lower than for epithermal reactors. The microscopic cross-sections for the fertile isotopes, especially U-238, also

drops off to insignificant values in the thermal energy range. Less captures leave more neutrons to produce fissions, which boost the infinite neutron multiplication factor (Serfontein, 2014).

This analysis explains why fast reactors generally have the best neutron economies, than thermal reactors and lastly epithermal reactors. Therefore, except for a few Th/U-233 fuel cycles, almost all breeder reactor designs are fast reactors. Since the world currently has an overproduction of uranium, breeder reactors are currently not economically important and therefore almost all commercial power reactors are burner reactors. Since thermal reactors generally have better safety features than fast reactors, almost all commercial reactors are thermal reactors.

The three dominant moderators in thermal reactor designs are the ^{1}H in light water, the ^{2}H (also called Deuterium (D)) in heavy water and the ^{12}C in graphite:

- The one proton in the nucleus of the ^{1}H has approximately the same mass as a neutron and therefore the neutron loses on average about 50% of its energy per collision with this proton. This means that light water is the most effective moderator as fast neutrons can be slowed down to thermal energies in a small number of collisions and thus also a small distance from the point where they were emitted as fission neutrons. Light water is thus the preferred moderator where the fuel core has to be small, for instance in the PWRs used in submarines, or where the fuel rods have to be close together, as is the case in most commercial PWRs or BWRs.

  Unfortunately, the microscopic radiative capture cross-sections for ^{1}H, especially at the lower end of the thermal energy range, is much higher than for ^{2}H and ^{12}C. This means that while light water is a very effective moderator, it is not a very efficient moderator as it wastes a substantial fraction of the available neutrons by capturing them in the ^{1}H to produce ^{2}H. This reduces the neutron economy substantially. Therefore, light water is normally not considered as a moderator for breeder reactors or for reactors that burn very low enriched fuels, e.g. natural uranium.

- Heavy water: The fraction of its energy that a neutron loses per average collision with a nucleus reduces sharply as the mass of the nucleus increases. So, even though the mass of the ^{2}H nucleus is only twice that of an ^{1}H nucleus, the average energy loss is much lower for ^{2}H. Therefore ^{2}H is a much less effective moderator than ^{1}H and therefore it is normally not considered as a moderator for small fuel cores. However, due to the laws of nuclear physics,

the microscopic radiative capture cross-section of ^{2}H is dramatically lower than that of ^{1}H and therefore ^{2}H is an extremely efficient moderator, as neutron losses in the moderator is almost non-existent. Therefore, heavy water is very suitable for very low enriched fuels such as the natural uranium that was used in the first CANDU reactors. It can also be used for breeder reactors, especially where Th/U-233 forms a substantial part of the fuel. This strategy is currently pursued by India.

- Graphite: As the ^{12}C nucleus has about 12 times the mass of a neutron, graphite is a somewhat ineffective moderator. Therefore, graphite moderated cores are typically much larger that light-water-moderated cores. However, even though the thermal microscopic radiative capture cross-sections of ^{12}C is substantially larger than that of ^{2}H, is still much smaller than that of ^{1}H and therefore graphite is quite an efficient moderator, as neutron losses in it are quite low. Therefore, graphite has been used as moderator for the natural uranium fuelled Magnox reactors in the UK. It has also been used as moderator for the breeder reactor designs for the Th/U-233 fuel cycle of the THTR reactor in Germany. Once again, breeding can only be achieved if the core is very large, so that the fractional neutron leakage out of the core is low. Unfortunately, the inherent safety features of such large cores are much worse than for small cores.

  Graphite has additional safety features that make it, for some applications, preferable to light water or heavy water as a moderator: at the temperatures that are plausible during nuclear reactor accidents, Graphite will not melt or evaporate. Furthermore, its excellent heat conduction abilities and its high heat capacity make it ideal for absorbing heat from the accident and for conducting it safely out of the core to the environment. These properties led to the selection of graphite as the preferred moderator for thermal High Temperature Gas-Cooled reactors.

  One of the coating layers around the uranium dioxide fuel kernels that forms the coated fuel particles in the graphite fuel spheres for most Pebble Bed Reactors consist of silicone carbide (SiC). The Si obviously also acts as a moderator. However, as its nucleus is even much heavier than that of ^{12}C, it is an even less effective moderator. Furthermore, its microscopic radiative capture cross-section is much higher than that of ^{12}C and therefore it is also a less efficient moderator. The Si is thus not included for its moderator properties, but rather for the ability of SiC to contain the radioactive fission products. It is

only once the fuel temperature increases to about 1600°C for oxide fuels and 1800°C for carbide fuels do the radioactive fission products start to substantially diffuse through these coating layers and thus start to pose a threat to the environment (Serfontein, 2014).

In an HTR, the fuel kernels are embedded in a near homogeneous mixture of moderator and fuel kernels. (Kugeler, et al., 1989). The HTR has the flexibility to accommodate many types of fuel cycles and permit full cost-effective optimisation. An HTR can meet the requirements of enhanced safety and high thermal efficiency by a clever design, flexible fuel cycle, waste management and competitiveness in an environmentally and sustainable way (International Atomic Energy Agency, 2000).

2.7.1 HTR fuel cycle flexibility

The advantages of HTRs which distinguish them from other reactor types is their fuel. Due to the unique arrangement of fuel, moderator and coolant these reactors can accommodate a variety of mixtures of fertile and fissile material without any changes to the core. The flexibility is largely due to the cooling, geometry and the moderation ratio, the heterogeneous arrangement of moderator and fuel. It is possible to modify the packing factor of the coated particles with the graphite matrix up to a theoretical value of 60% as well as change the diameters of kernels themselves as well as enrichment changes etc. (International Atomic Energy Agency, 2015).

The fuel cycle adaptability of HTRs compared to Light Water Reactors (LWR) is made possible by the following physical characteristics. The requirement of a negative moderator void reactivity coefficient limits the plutonium content of PWRs Mixed Oxide fuel (MOX) fuels to less than 10%. However in an HTR the Pu only fuel cycle can be achieved and poses a distinct advantage in this regard compared to other reactor types. However, (Serfontein, 2014) showed that such pure plutonium fuel mixtures in the PBMR-400 tended to produce positive temperature reactivity coefficients. This was due to their strong positive moderator coefficients, which dominated their week negative fuel temperature reactivity (Doppler) coefficients. These positive temperature reactivity coefficients produced power density hotspots, especially directly adjacent to the internal reflector. The result was that many of the safety limits, including the

maximum power per fuel sphere and maximum fuel temperature during normal operation, were breached.

In the event of a void being produced in the water moderator reactor by means of boiling of the water which forms stream bubbles, during a Loss Of Coolant Accident (LOCA), in a PWR the neutrons are no longer sufficiently slowed down by the moderator and the neutron spectrum becomes faster as they have a very high average speeds, this leads to an considerable increase in the neutron multiplication factor due to the presence of Plutonium (the reproduction factor increases significantly for fast neutrons). However, this problem does not occur in graphite moderated reactors when coolant is lost, since there is no liquid coolant than can boil off to a void.

HTR cores have significantly better neutron economies compared to PWR cores, this is due to the fact that there is much less parasitic/unproductive capture of neutrons in the moderator (graphite's capture cross section is 100 times smaller than water), internal structures (no metallic components in the core which capture neutrons) and by fission products (the HTR spectrum is harder and fission products have a tendency to capture more neutrons as they are thermalized) (International Atomic Energy Agency, 2015).

The performance of the TRISO coated particles to obtain extremely high burn-ups (up to about 220000 of MWD/THM) for both the uranium and plutonium-based fuels has been confirmed by various irradiation tests since the birth of the coated particle (International Atomic Energy Agency, 2015). The various fuel cycles consider various combinations of fissile material (U-235, U-233, Pu-239) and fertile material (U-238, Th-232) for nuclear fuel, U-238 can be seen as fissionable as well (fission due to a fast neutron). The fuel cycles are classified into four groups namely:

- Low Enriched Uranium (LEU) fuel cycle
- Mixed Oxide (MOX) fuel cycle
- Plutonium only fuel cycle
- Thorium based fuel cycles

2.7.1.1 Low Enriched Uranium (LEU) fuel cycle

The LEU fuel cycle utilises uranium from enrichments of 5 up to 20%, the enrichments are reactor specific. This enrichment is high for HTRs compared to other thermal reactors and is due to the diluted homogeneous uranium distribution within the HTR fuel which favours resonance capture by fertile/fissionable material (U-238). The LEU cycle was studied in the USA, UK, Germany and France from 1960-1970 and is the most viable option for commercial application. This fuel has already been employed in HTRs around the world in the past and present reactors (specifically UO_2), the advantage is that the world has good commercial experience with LEU fuel. The LEU fuel cycle has been selected as a reference fuel in all ongoing HTR projects (International Atomic Energy Agency, 2015). UCO fuel is being developed and qualified in the USA.

2.7.1.2 Mixed Oxide (MOX) fuel cycle

LWRs utilize a mixed plutonium/depleted uranium fuel which could be realised for a HTR. The mixture is in the form of a Mixed Oxide (MOX) form but could also be developed as a carbide etc. The MOX fuels have never been used in an HTR however neutronic analysis was done on this. The HTR would offer better utilisation of Plutonium, however this would not provide a significant advantage over Plutonium only fuel (International Atomic Energy Agency, 2015).

2.7.1.3 Plutonium only fuel cycle

Efforts have been made in the field of waste reduction (specifically plutonium) in the medium term by plutonium incineration in HTRs. Studies were conducted to determine the feasibility and performance of plutonium only cores containing no fertile material. This plutonium only core is unique to HTRs with the GT-MHR project which examines plutonium incineration. Extensive research and development would be needed to qualify plutonium only fuels which can reach extremely high burn-ups that are required. Experimental fuels were tested in the Peach Bottom and Dragon reactors. There may be problems in reactivity control (poisons may need to be added), moderator temperature coefficient (possible positive coefficient, a low fraction of delayed neutrons and increased residual heat) (International Atomic Energy Agency, 2015).

The problem is that the safety features of reactor-grade Pu are much worse than those of LEU and the safety features of weapons-grade Pu are even worse. The main problem is that Pu-239 and Pu-241 have positive moderator temperature coefficients, as opposed to U-235 that has a substantial negative moderator temperature reactor coefficient. If such a problem were to occur in LEU, it would be countered by the extremely strong negative fuel temperature reactor coefficient, which is provided by the Doppler effect in the massive capture resonances of U-238 and by the fact that 90% of the LEU consist of this U-238.

Reactor grade Pu, on the other hand, has a fissile enrichment in the order of 60%, which means that the fertile isotopes (mainly Pu-240 and pu-242) are in the minority. The result is that their negative Doppler effect is weaker than the positive moderator temperature coefficient of the said fissile Pu-239 and Pu-241. Therefore, the combined moderator and fuel reactor. coefficient. is positive, which is unacceptable. This causes all kinds of problems such as power and temperature hotspots, so that the limit of 4.5 kW/fuel sphere, as well as the maximum fuel temp. during normal operation and the maximum DLOFC temperatures are all exceeded. In order to make pure Pu safe, we will have to dilute it with Th or LEU (Serfontein, 2014).

2.7.1.4 Thorium based fuel cycles

1. HEU/Thorium fuel cycle

A large advantage of HEU/Th fuel cycle is the significant reduction in the consumption of natural uranium when operating in a closed loop cycle (reprocessing and recycling of uranium). The HEU/Th fuel cycle is suited to this due to the fact that very high conversion factors can be achieved with U-233 recycling, decreasing uranium requirements by a factor of two or more (International Atomic Energy Agency, 2015). The HEU/Th fuel cycle was studied in depth by the USA and Germany with the Peach Bottom and Fort Saint Vrain and the AVR and THTR reactors that used this fuel cycle. The future use of HEU/Th will require development and would only be of particular interest when uranium is in short supply. HEU is only able to be used by a few countries that already possess the right to build nuclear weapons and other alternatives will thus have to be explored (International Atomic Energy Agency, 2015). The affordability of the HEU/Th fuel cycle is unclear as Thorium does not have a market value. The main technical difficulty for U-233 recycling is the significant gamma energy emitted by the daughter product namely U-232. Recycled fuel would have to be fabricated remotely in shielded cells. This fuel cycle offers challenges namely the problem to do with proliferation of HEU and U-233 (International Atomic Energy Agency, 2015). The advantages of the ThHEU fuel cycle is the performance in the neutron spectrum of an HTR, less long-lived minor actinides (discussed in other sections as well as can be seen in the VSOP output files for the cases simulated, this is discussed) and the lower levels of radioactivity. When you use a pure Th/HEU fuel cycle there is almost no U-238 in the fuel and therefore very little Pu and its associated radioactive Minor Actinides, such as Americium and Curium, will be formed. Therefore, the waste will be much less radioactive over the long term, i.e. after most of the shorter-lived radioactive fission products have decayed. However, the driver fuel, namely HEU is excellent nuclear weapons fuel and therefore the existence of such a fuel cycle presents an excellent opportunity for terrorists to steal the fresh HEU and use it to build a nuclear bomb. Therefore, most countries will not allow such a fuel cycle.

2. (LEU)/Thorium fuel cycle

Studies of this cycle were conducted in the USA in the late 1970s as the result of the non-proliferation policy. The idea was to investigate fuel cycles capable of diminishing proliferation risks associated with the use of fissile materials suitable for the manufacture of nuclear weapons. The HEU fuel cycle was considered to be extremely proliferating, thus using cycles with limited enrichment levels of uranium (20% U-235

or 12% U-233) with a certain quantity of thorium were investigated. This cycle complicated the management of heavy nuclei from both the uranium and thorium (Pu-239, 232U, U-233) (International Atomic Energy Agency, 2015), U-233 produced from thorium has a high neutron reproduction factor compared to Pu-239 formed from U-238. Th-232 has an epithermal capture cross section which is 4 times smaller than U-238, which leads to less captures, which leaves more neutrons available to fission the fissile fuel, which will then produce more fission neutrons, which will increase K_{eff}. This thorium is converted into U-233 which is the best thermal fuel in an HTR (Lung & Gremm, 1997). U-233 has a much better neutron economy and thus also a much better conversion ratio than for Pu-239, which is bred from U-238. This explains why replacing U-238 with Th-232 results in fewer neutron captures in the Th-232 than in the U-238 and more fission neutrons produced in the U-233 than in the Pu-239. Neutron absorption by Th-232 produces Th-233 which beta-decays (with a half-life of about 22 minutes) to protactinium-233 (Pa-233) – and this decays to U-233 by further beta decay (with a half-life of 27 days). Some of the bred U-233 is converted to U-234 by further neutron capture. U-234 is an unwanted parasitic neutron absorber. It transmutates to fissile U-235 (the naturally occurring fissile isotope of uranium) through neutron capture and this somewhat compensates for this neutronic penalty. In fuel cycles involving the multi-recycle of thorium-U-233 fuels, the build-up of U-234 can be appreciable.

3. Thorium-Plutonium (Th/Pu) fuel cycle

Using Plutonium as the fissile driver material in the place of HEU with Thorium being the fertile material was considered in the early stages of HTR development with studies being performed in the UK as part of the DRAGON project in the 1960s. The USA continued studies with General Atomics and Edison Electric Institute that manufactured (Th, Pu)O_2 test specimens and successfully irradiated them in the Peach Bottom HTR. Th/Pu is of interest as an intermediate step to incinerate plutonium from LWR stockpiles. Pu can be used as the fissile driver in Thorium based fuels to produce U-233 to initiate a closed thorium fuel cycle. This fuel cycle will only be realised in countries that are allowed to deal with Plutonium. HTRs can utilise the Th/Pu fuel cycle which has many attractive features such as a more uniform power distribution, higher outlet temperature due to this, an increase in average power density and a reduction of reactivity control actions (International Atomic Energy Agency, 2015).

4. Reprocessing of spent Th/U-233 fuels

The world developed two fuel cycles: the Uranium/Plutonium and the Thorium/Uranium fuel cycles. If fissile isotopes are not bred, the world's U-235 reserves will be depleted in the future. There are two forms of breeding; Pu-239 from U-238 with fast neutrons and breeding U-233 from Th-232 with thermal neutrons. In LWRs Pu-239 is bred to some extent from U-238 using slightly enriched U-235 (3 to 5%). In some countries Pu-239 is extracted from the spent fuel and refabricated into MOX fuels. These MOX fuels are reintroduced into LWRs or fast breeder reactors.

Thorium generates U-233 which is the best fissile isotope for thermal spectrum reactors due to its nuclear characteristics. In the thermal spectrum of HTRs and LWRs the neutron reproduction factor η (average number of neutrons produced for each neutron absorbed in the fissile isotope) is high for U-233. U-233 has a reproduction factor of 2.29 compared to 2.05 for U-235 and 1.8 for Pu-239. This high reproduction factor for U-233 makes breeding theoretically possible. This concept was experimentally demonstrated in the Shipping Port reactor in the 1970s (Shippingport Atomic Power Station, n.d.).

The use of the Th-232/U-233 fuel cycle in thermal reactors is advantageous specifically in HTRs due to the fact that the neutrons are thermalized more efficiently. This fuel cycle should be used in an HTR. The only large hurdle is that the Th/U-233 has to be reprocessed and recycled. U-233 that is bred must be extracted and refabricated into new fresh fuel elements containing thorium, the unburnt thorium can also be reprocessed and reused, however thorium is very stable and has a high melting temperature which complicate the chemical treatment for the separation of Th compounds and the dissolution of reprocessing. In the USA and Germany efforts were focused on Th/U fuel cycle and reprocessing of U-233. The wet chemical solvent exchange process the THOREX process was developed similar to the PUREX process for Pu/U reprocessing. These processes were developed at the ORNL and at the Forchungszentrum Jülich in Germany. Jülich also developed a process for deconsolidating the graphite fuel sphere to expose the fuel kernels called JUPITER (International Atomic Energy Agency, 2015). This process is an expensive mechanical method to separate the fuel kernels from the graphite shell. Many other methods have also been developed to do this which are much more cost effective such as chemical

methods, volatilization through oxidation and halogenation reactions and potential methods (McWilliams, 2015).

There are two types of fuel cycles within the Th/U-233 cycle:

1. Open Fuel Cycle: Irradiation of Th and fission of U to avoid chemical reprocessing. This fuel cycle demands optimizing the use of U in the reactor to minimise the amount of wasted fissile material.
2. Closed fuel cycle. Chemical reprocessing of irradiated Thorium for recovery and reprocessing of U.

2.8 Thorium as a nuclear fuel

2.8.1 Thorium resources

Thorium reserves within the earth's crust are around 10ppm in phosphates, carbonates and oxide materials and are much more abundant than Uranium, these reserves have to still be commercially exploited (Lung & Gremm, 1997). Thorium occurs together with rare earth metals and uranium in diverse rock types. It occurs as veins in thorite/uranothorite and monazite granites, syenites and pegmatities. Monazite occurs in quartz-pebble conglomerates and sandstones. Thorium also occurs with rare earth metals in bastnaesite and carbonatites (International Atomic Energy Agency, 2000). Unlike natural uranium, thorium contains no fissile isotope and is fertile in nature and a fissile driver needs to be added to the thorium to create U-233 and eventually U-233 can be the fissile driver that is reused in a closed cycle. Th-232 is three to four times more abundant in the earth's crust than uranium (International Atomic Energy Agency, 2000).

2.8.2 Thorium

Uranium specifically U-235 is the only naturally occurring fissile driver material for nuclear power generation, non-natural sources include Pu-239, Pu-241 and U-233. Natural Uranium contains 99.3% U-238 and 0.7% U-235, therefore most reactors use enriched uranium.

Uranium fuels produce fissile Pu-239 from U-238 during irradiation with 65% fission and 35% capture of incoming neutrons, see equation 1. Neutron capture leads to Pu-239 as an additional isotope (International Atomic Energy Agency, 2015).

$$^{238}_{92}\mathrm{U} + \mathrm{n} \rightarrow {}^{239}_{92}\mathrm{U} \rightarrow {}^{239}_{93}\mathrm{Np} \rightarrow {}^{239}_{94}\mathrm{Pu} \qquad (1)$$

Thorium containing nuclear fuel produces fissile U-233 during irradiation with 90% fission and 10% capture cross section for incoming neutrons, see equation 2 .

$$^{232}_{90}\mathrm{Th} + \mathrm{n} \rightarrow {}^{233}_{90}\mathrm{Th} \rightarrow {}^{233}_{91}\mathrm{Pa} \rightarrow {}^{233}_{92}\mathrm{U} \qquad (2)$$

Uranium resources will be reduced in the years to come so alternatives fuelling options need to be studied in depth such as the thorium cycles mentioned above. Early HTRs used Thorium and HEU as fuels. Using the same fuel today would lead to the problem of handling highly enriched fissile material which is required for the start of the thorium based fuel utilisation.

2.8.3 Properties of thorium

Thorium oxide is very stable as it has a melting point of 3390˚C (Uranium oxide 2865 ˚C) which is one of the highest known refractories. This allows for a high burn-up and high temperatures however this complicates the chemical treatment for the separation of Th compounds and the dissolution for reprocessing (International Atomic Energy Agency, 2015). Thorium oxide (ThO_2) has excellent material properties for serving as a nuclear fuel. ThO_2 has a higher thermal conductivity and a lower coefficient for thermal expansion; it retains fission products better within its crystalline lattice (Lung & Gremm, 1997). Thorium oxide fuels produce less fission gas release than uranium fuels (including MOX). It is therefore recognized that thorium oxide fuels can operate safely to high burn-ups (Anantharaman, et al., 2008). ThO_2 has excellent properties from a waste point of view, even after irradiation. It is highly insoluble, thus it cannot be oxidized and it retains both fission products and actinides extremely well within its lattice.

2.8.4 Nuclear characteristics

In the thermal energy region the conversion of Th-232 into U-233 as shown in equation 2 above is more effective than the conversion of U-238 into Pu-239 due to the larger thermal neutron absorption cross section of Th-232. However, most neutron interactions occur in the epithermal region; however when U-238 is replaced with Th-232 there are benefits. Th-232 has a capture cross section which is 4 times smaller than U-238 this leads to less captures and a higher K_{eff}. Th-232 that is replacing U-238 leads to less captures in the Th-232 and thus leaves more neutrons available for causing fissions in the fissile fuel. This thorium is converted into U-233 which is the best thermal fuel in a HTR (Lung & Gremm, 1997). U-233 has a much better neutron economy and thus also a much better conversion ratio than for Pu-239, which is bread from U-238. This explains why replacing U-238 with Th-232 results in less neutron captures in the Th-232 than in the U-238 and more fission neutrons produced in the U-233 than in the Pu-239.

The bred U-233 is a better nuclear fuel compared to U-235 and Pu-239 as it has the highest fission yield per neutron absorbed in both the thermal and epithermal neutron energy ranges compared to any other fissile isotopes namely U-235, Pu-239 and Pu-241. Therefore U-233 will be a superior fuel in any thermal reactor as seen in **Figure 6**.

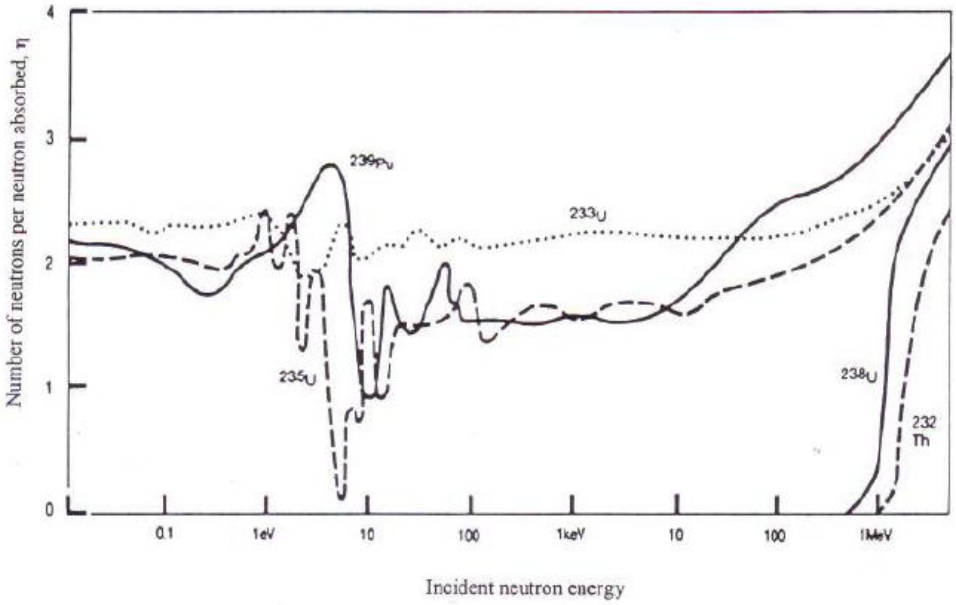

Figure 6: Fission neutron yield for fissile isotopes in the thermal and epithermal neutron energy ranges (Lung & Gremm, 1997).

Th-232 has a much lower fast fission cross section than both U-238 and Pu-240 thus replacing the U-238 with Th-232 reduces the neutron economy and the conversion ratio in reactors that require large fractions of fast fissions such as the PWRs and fast breeder reactors. Fast fissions are almost absent in HTRs, thus replacing U-238 with Th-232 would have a favourable effect on the neutron ratio because more Th-232 is available to capture neutrons and produce U-233; there is no detrimental effect on the neutron population.

The fission products produced from U-233 are less poisonous when it comes to capturing neutrons compared to U-235, thus benefiting the neutron economy (Lung & Gremm, 1997). The conversion ratio defined as the number of fissile isotopes produced per fissile isotope consumed is usually higher in thorium based fuel cycles in long term irradiation due to higher fission neutron yield and a larger absorption cross

section for Th-232 compared to U-238 as shown in **Table 1**.Thus the fissile generation capability of Th-232 is higher over longer periods and makes it a better fertile fuel in breeding fissile fuel when compared to U-238. The fuel ore requirement and enrichment per unit energy of thorium based fuel cycle is reduced (Kazimi, et al., 1999).

Table 1 – Fertile neutronic properties (Kazimi, et al., 1999)**.**

Parameter	Th-232	U-238	U-234	Pu-240
Thermal† Absorption Cross Section σ_a [barns]	4.62	1.73	63	203
Epithermal Absorption Resonance Integral RI_a [barns]	85.6	278	660	8500

†Average over Maxwellian spectrum at 300°C (0.05 eV).

U-233 retains its favourable nuclear properties over the other fissile isotopes U-235 and Pu-239 at higher temperatures (Lung & Gremm, 1997); this is of extreme importance to HTRs operating at high temperatures as shown in **Table 2**.

Table 2 – Values of η_{th}, the average number of fission neutrons emitted per neutron absorbed in a thermal flux at varying temperatures (Lamarsh & Baratta, 2001)**.**

T [°C]	U-233	U-235	Pu-239
20	2.284	2.065	2.035
100	2.288	2.063	1.998
200	2.291	2.06	1.947
400	2.292	2.05	1.86
600	2.292	2.042	1.811
800	2.292	2.037	1.785
1000	2.292	2.033	1.77

The capture cross section of U-233 in the thermal energy range is the lowest value of (54 barns) compared to U-235 (100 barns) and Pu-239 (267 barns), thus making U-233 a superior fissile fuel (Sokolov, et al., 2005).

The neutronic advantages of using thorium-based fuel cycles are the higher fission neutron yield per neutron absorbed at thermal energies and at the lower epithermal resonance capture fission ratio can be seen in **Table 3**. Pu-241 is the only isotope that performs slightly better when the fission neutron yield per neutron absorbed at epithermal energies is considered.

Table 3 – Fissile neutronic properties (Kazimi, et al., 1999)**.**

Parameter		U-233	U-235	Pu-239	Pu-241
Thermal† Absorption and Fission Cross Section [barn]	σ_a	364	405	1045	1121
	σ_f	332	346	695	842
	$\alpha=\sigma_c/\sigma_f$	0.096	0.171	0.504	0.331
Neutron Yield per Neutron Absorbed in Thermal Range	η_{th}	2.26	2.08	1.91	2.23
Epithermal Absorption and Fission Resonance Integral [barn]	RI_a	882	405	474	740
	RI_f	746	272	293	571
	$\alpha=RI_c/RI_f$	0.182	0.489	0.618	0.296
Neutron Yield per Neutron Absorbed in Epithermal Range	$\eta_{epithermal}$	2.1	1.63	1.77	2.29
Neutron Yield	ν	2.48	2.43	2.87	2.97
Delayed Neutron Yield	β	0.0031	0.0069	0.0026	0.005

†Average over Maxwellian spectrum at 300°C (0.05 eV).

Thorium based fuels can be seen to be substantially proliferation resistant, U-233 has superior nuclear properties compared to U-235 and Pu-239 which may be used for weapons production, however the decay products from Th-232 and U-232 contain 1-2.6 MeV hard gamma emitters. This demands remote processing but can be considered as a substantial safeguard against malicious use. It is thus more proliferation resistant due to the presence of U-233 and its daughters due to associated handling difficulties and easy tracing (International Atomic Energy Agency, 2015).

Thorium fuels generate at least one order of magnitude less long lived minor actinides compared to the plutonium fuel cycles (International Atomic Energy Agency, 2000). The burning of thorium fuel generates smaller amounts of plutonium and minor actinides compared to uranium fuel. Thus, thorium based fuels will achieve much greater net plutonium consumption than conventional uranium based fuels, which produce plutonium as they burn.

There are a few disadvantages of thorium being that it contains no natural fissile isotopes to drive the chain reaction, thus a driver fuel such as natural U-235 or artificial Pu-239 and U-233 produced from the uranium fuel cycle have to be used to initiate the nuclear chain reaction. The ultimate thorium fuel cycle would be the U-233/Th-232 fuel cycle; however this would require reprocessing of the unburnt fissile U-233. The chemical reprocessing is very expensive and is not economically viable at this stage until uranium reserves diminish drastically or if uranium prices increase (Lung & Gremm, 1997).

The important aspect to note is the production of Pa-233 as an intermediate isotope during breeding of U-233.Pa-233 has a half-life of 27 days and when it transmutates into U-233 there will be a reactivity surge due to the delayed neutron production (Lung & Gremm, 1997). In comparison to uranium decay to Np-239 with a half-life of 2.3 days which means the reactivity surge will end shortly after reactor shutdown. This is a safety issue and should be analysed. The fraction of delayed neutrons is much smaller than compared to the uranium cycle, this is important safety issue for reactor controllability. The control systems need to respond more rapidly to transients (Kazimi, et al., 1999).

2.9 Burn-up of nuclear fuel

The burn-up is the heat energy produced from fission per unit mass of heavy metal loaded into the fresh fuel. The mathematical formula is shown in equation 3 :

$$B = \frac{1}{\rho} \int_0^{\tau} E_f \, \Sigma_f(t) \, \Phi(t) \, dt \, (\frac{MWd}{tHM}) \quad (3)$$

$$\rho = \text{Density of } UO_2$$

$$E_f = \text{Average energy of fission process (200 Mev)}$$

$$\Sigma_f = \text{Macroscopic fission cross section}$$

$$\Phi = \text{Neutron flux}$$

$$\tau = \text{Time of insertion of fuel}$$

Older PWRs have burn-ups of between 40 000 to 50 000 MWD/THM corresponding to a Uranium enrichment of 3.5 to 4%. Higher burn-ups such as 60 000MWD/THM are achieved if the enrichment is increased to 5% which is the case in today's PWRs. HTRs with total ceramic fuel elements reach 100 000MWD/THM and more (Kugeler, et al., 1989).

The knowledge of the burn-up and the number of hours of full power operation allows for a simple estimation of the amount of fresh fuel which has to be inserted into a reactor per year and the amount of spent fuel which has to be removed from the core, this is more specific to reactors that have to be unloaded and refuelled (Kugeler, et al., 1989). In all PBRs reactors the downtime is dominated by maintenance and inspection. In a PBR which has online fuelling and no need for fuel reloading every 12 to 18 months, this allows it to operating more continuous hours per year and increases the

availability. Therefore, in the equation 4 below the “operating hours per year” value would increase for a PBR due to the higher availability. In the same equation 4 for a HTR the plant efficiency term would also increase as a HTR coupled to a steam cycle produces high quality steam (540˚C, 15MPa) which increases its efficiency to 40% whereas a PWR operates at 33%.

$$m^0{}_f = \frac{P^0{}_{el} \cdot T}{B \cdot \frac{\eta}{100}} \tag{4}$$

$$P^0{}_{el} = \text{Power (MW electric)}$$

$$T = \text{Operating hours per year}$$

$$\eta = \text{Plant efficiency (\%)}$$

$$B = \text{Burn} - \text{up}\ (\frac{\text{MWD}}{\text{THM}})$$

The yearly demand of natural uranium can be calculated from equation 5:

$$m^0{}_U = m^0{}_f \frac{e_f - e_t}{e_N - e_t}\ \zeta \tag{5}$$

$$m^0{}_f = \text{Amount Uranium in fresh fuel}\ (\frac{t}{\text{year}})$$

$$e_f = \text{Enrichment of fresh fuel}$$

$$e_t = \text{Enrichment of tails}$$

$$e_N = \text{Enrichment of natural Uranium}$$

$$\zeta = \text{Technical factor } (> 1)$$

The amount of natural Uranium and the necessary separative work required to produce 1kg or enriched Uranium is dependent on the degree of enrichment and the tail assay.

Table 4 shows this requirement with a fixed tails assay of 0.2 weight % U-235 (Kugeler, et al., 1989).

Table 4 – Requirement of natural uranium and separative work to produce 1 kg enriched uranium (tails assay: 0, 2 weight % U-235) (Kugeler, et al., 1989)

enrichment [weight %]	kg natural U per kg of product	kg separative work per kg product
0,711	1,000	0,000
1,00	1,566	0,380
2,0	3,523	2,194
2,5	4,501	3,229
3,0	5,479	4,306
3,5	6,458	5,414
4,0	7,436	6,544
10,0	19,178	20,863
20,0	38,748	45,747
90,0	175,734	227,341

The value function is given by equation 6:

$$V(e) = (1 - 2e).\ln(\frac{1-e}{e}) \quad (6)$$

Where e is the enrichment in weight fraction. The Separative Work Unit (SWU) associated with the specific amount of enriched Uranium is defined by equation 7 :

$$SWU = M_P.\ V(e_P) + M_T.\ V(e_T) - M_F.\ V(e_F) \quad (7)$$

With M_T being the mass of tails, M_F the mass of feed and M_P the mass of the product. The mass balance is shown in equation 8 :

$$M_T = M_F - M_P \tag{8}$$

Finally one gets the SWU in equation 9:

$$SWU = M_P . [V(e_P) - V(e_T)] - M_F . [V(e_F) - V(e_T)] \tag{9}$$

SWU has the unit mass (kg). The separative work necessary to provide a given amount of product increases with enrichment.

2.10 Costs of nuclear fuel

The fuel costs X_F (ct/kWh$_{el}$) for nuclear power plants consist of different variables is shown in equation 10: Specific to the HTMR-100, which is used in this thesis, the thermal efficiency of 40% due to a steam temperature and pressure of (540˚C, 15MPa), with 33 MW$_{el}$ being sent to the grid after the house loads and other loads are subtracted.

$$X_F = X_U + X_E + X_P = \frac{K_F}{B \cdot \frac{\eta}{100}} \tag{10}$$

$$X_U = \text{Cost share of natural Uranium } (\frac{ct}{kWh_{el}})$$

$$X_E = \text{Cost share of Uranium enrichment } (\frac{ct}{kWh_{el}})$$

$$X_P = \text{Share of manufacturing costs for the fuel elements } (\frac{ct}{kWh_{el}})$$

$$K_F = \text{Costs of the ready} - \text{to} - \text{use fuel } (\frac{ct}{t\ HM})$$

$$B = \text{Burn} - \text{up } (\frac{MWD}{tHM})$$

$$\eta = \text{Plant efficiency } (\%)$$

The investment for the initial core loading means the depreciation and payment of interest for the fuel used inside the core can either be related to the fuel cycle costs or as a capital investment. The following cost estimations will use the latter method for

the initial core loading, a capital investment and not a fuel cycle cost. To determine the cost shares of natural Uranium and as well as enrichment the exact enrichment of the fuel cycle has to be considered (Kugeler, et al., 1989). The costs of the ready to use fuel can be calculated according to equation 11 :

$$K_F = K_{Uranium} \cdot m + K_{Enrichment} \cdot a_s + K_{Production} \cdot z \qquad (11)$$

The meaning of the terms is shown below:

$$K_{Uranium} = \text{Cost of natural Uranium } \left(\frac{ct}{U_{nat}}\right)$$

$$m = \text{Quantity factor of enriched Uranium } \left(\frac{t\ U_{nat}}{t\ U_{enrich}}\right)$$

$$K_{Enrichment} = \text{Specific cost of enrichment } \left(\frac{ct}{t\ \text{spearative work}}\right)$$

$$a_s = \text{Separative} - \text{work} - \text{factor } \left(\frac{t\ \text{separation work}}{t\ U_{enrich}}\right)$$

$$K_{Production} = \text{Specific cost of production } \left(\frac{ct}{\text{Fuel element}}\right)$$

$$z = \text{Quantity of fuel elements } \left(\frac{\text{number of fuel elements}}{t\ U_{enrich}}\right)$$

2.11 Conclusion

Pebble fuel is expensive to manufacture. However, it does have its advantages in that high burn-ups can be achieved and that the reactor needs not to be shut down for fuelling due to the continuous loading scheme except for maintenance. Unfortunately, much higher enrichments are required in pebble fuel in order to achieve these higher burn-ups, compared to PWR fuel.

The fuel cost of Pebble Bed Reactors could potentially be reduced by optimizing the fuel mixtures, enrichments, Heavy Metal (HM) loadings to increase the cumulative heat energy produced over the lifetime of each fuel sphere and reduce the cost per fuel sphere. Increasing the burn-up and increasing the Heavy Metal loading per fuel sphere will obviously increase the cumulative heat energy produced per fuel sphere, which will mean that the reactor will utilize less fuel spheres. The optimum fuel composition is the one that generates the lowest fuel cost per joule of heat energy produced.

3 REACTOR CORE DESIGN AND NEUTRONIC MODEL DEVELOPMENT

3.1 General description

The HTMR100 reactor is a 100MW_{th} pebble bed high temperature gas reactor it has a cylindrical core and is based on an OTTO cycle. The helium flow direction is as follows, the helium enters at the bottom of the helium riser tubes and flows up alongside the core until it reaches the top of the reactor whereby it enters at the top of the pebble bed and flows down through the bed, collects at the bottom of the core and leaves through the co-axial duct. This cold gas entering the top of the OTTO core provides a flatter temperature profile in normal operations. An OTTO cycle was chosen for this reactor due to the simplicity of the fuel handling system and significant cost reductions associated with this simple system. The OTTO cycle has a higher power peaking factor and would have a higher fuel temperature in a loss of cooling accident known as a Depressurized Loss of Forced Cooling (DLOFC) accident. Therefore, switching from a MEDUL to an OTTO cycle results in a reduction of the core power of about 50%. Even so, the benefits of simplicity and lower plant cost might outweigh the cons of lower power output and thus the OTTO fuel cycle was chosen for the reactor design and neutronic modelling. See **Table 5** for the reactors parameters.

Table 5 – HTMR100 general description

	Nominal value/description	Unit
Thermal power	100	MW_{th}
Primary coolant	Helium	
Moderator	Graphite	
Core geometry	Cylindrical	
Core volume	28.1	m^3
Average power density	3.57	MW_{th}/m^3
Pebble bed diameter	260	cm
Pebble bed effective height	522.6	cm
Angle of defueling cone	30°	
Fuel circulation	1	
Core inlet temperature	250	°C
Core outlet temperature	750	°C
Coolant flow rate	39	kg/s
Primary coolant pressure	4	MPa
Core loading	~150000	pebbles/core
Fuel circulation rate	50 -250	pebbles/day
Nominal burn up	80-100	GWd/t

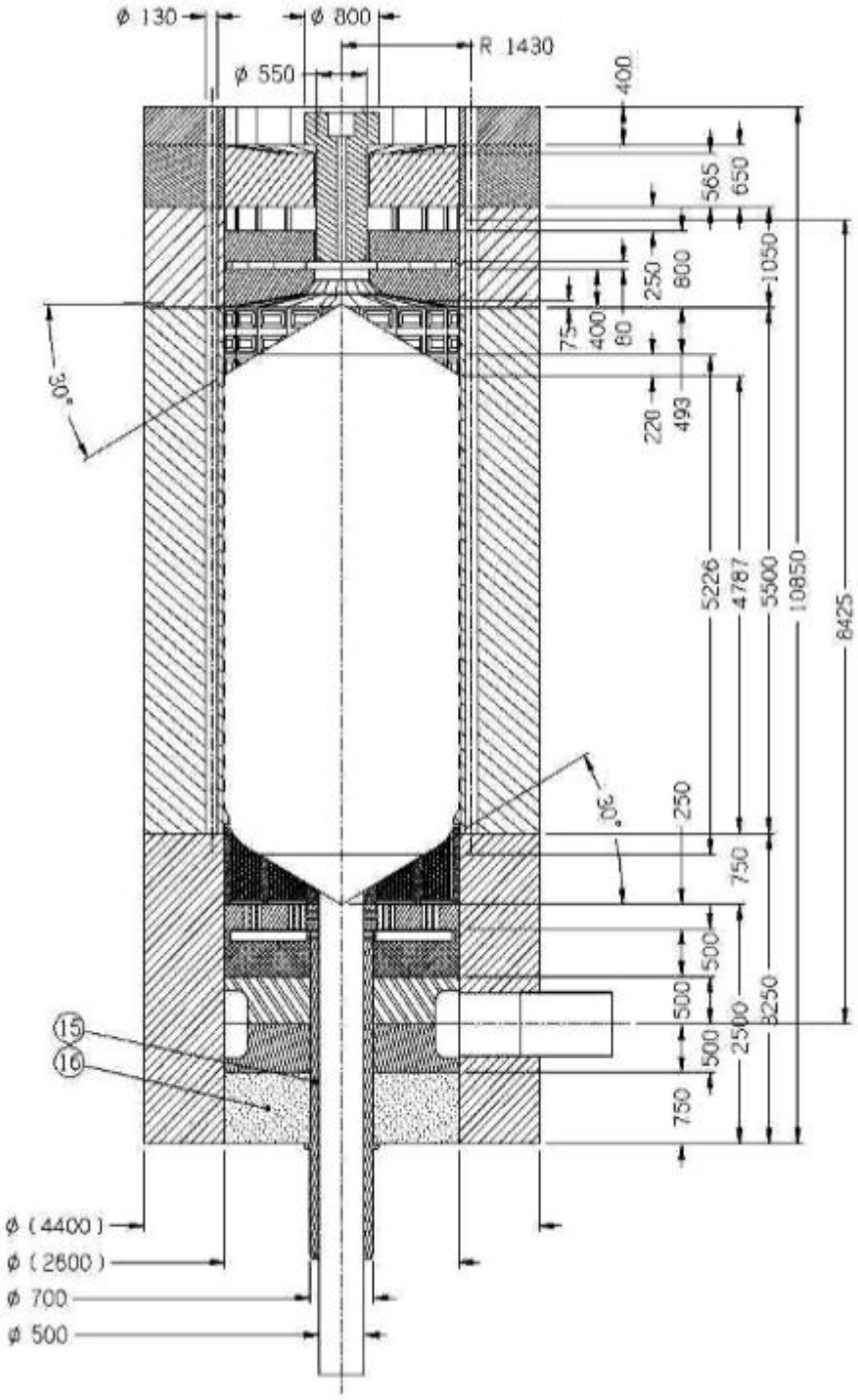

Figure 7 – HTMR100 geometrical layout

3.2 Neutronic model development

3.2.1 The VSOP suite of codes

VSOP is a computer code system for the comprehensive numerical simulation of the physics of thermal reactors. The application of the code implies processing of cross sections, the set-up of the reactor and of the fuel element, neutron spectrum evaluation, neutron diffusion calculation, fuel burn-up, fuel shuffling, reactor control, and thermal hydraulics of steady states and transients. The neutronics calculations can be performed in up to three dimensions. Thermal hydraulics is restricted to gas-cooled reactors in two spatial dimensions. Evaluation of fuel cycle costs over the reactor life time is made using the present worth method. The VSOP suite of codes can simulate start-up core conditions as well as equilibrium core conditions; this study will focus on equilibrium core conditions at steady state. The code uses quasi steady state approximations for transient calculations. **Figure 8** shows the VSOP code flow sheet for HTR core physic calculations.

The VSOP 99 system of codes is used to produce input models for the reactor geometry, fuel design, reactor physics characteristics analysis, fuel cycle layout and reactivity control simulation. Furthermore, the resonance absorption cross-section properties are modelled according to the Nordheim treatment for resolved and unresolved resonances. Furthermore, the code accounts for the neutron diffusion characteristics in void regions by taking into consideration the moderation effects of neutrons in the side reflectors as well as the control rod positions in the side reflectors. Convergence parameters are deployed to enable the achievement of steady state conditions. As a final step, the parameters are saved to provide restart conditions for in-depth follow-on studies, such as group-dependent flux evaluations, quasi steady-state transient simulations, such as DLOFC, PLOFC, temperature coefficient investigations, control rod characteristics, reactor kinetics parameters, etc.

The experimental facilities constructed and operated at NWU, such as the high-pressure test unit (HPTU) and the high temperature test unit (HTTU) are two experiments formed part of the HTTF experiments performed under the PBMR program in South Africa to benchmark the performance parameters of temperature

dependent thermal conductivity, pressure drop over the bed, etc., that are in use in VSOP. Data obtained under this program is extremely valuable as it adheres to NQA-1 quality standards.

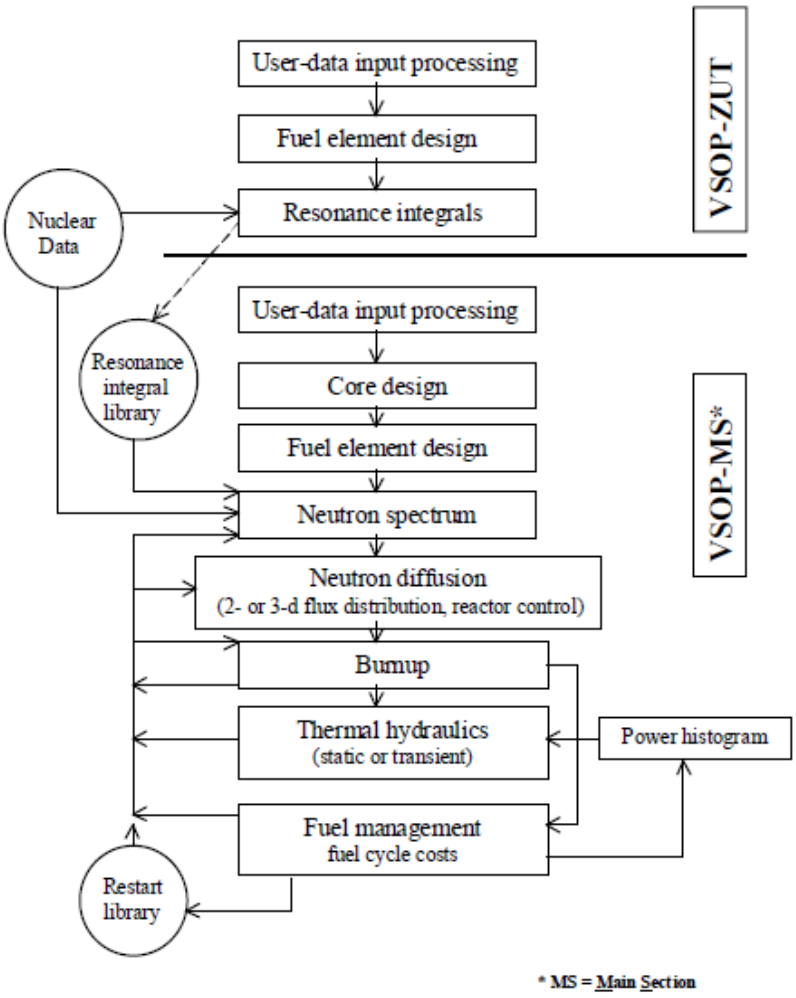

Figure 8 – VSOP code flow sheet for HTR core physic calculations

3.2.2 The HTMR100 VSOP model

The VSOP suite of codes is used to simulate a finite reactor core geometry for the HTMR100 cylindrical reactor core 2D model using the diffusion-based calculation method to simulate various fuel cycles and compare the neutronic results. The reactor core model is based on conventional pebble bed reactor with the cold helium gas entering the top of the reactor at 250˚C, making its way through the pebble bed where the gas picks up heat and exits the bottom of the reactor at 750˚C. The conventional material model for Thermix utilises a graphite reflector surrounded by carbon bricks, stagnant helium, a core barrel and a reactor pressure vessel as shown in **Figure 9**.

The core contains 16 equidistant core meshes and 4 meshes to represent the 30˚ angle of the bottom cone with pebble bed flow lines associated with this specific geometry.

No				1	2	3	4	5	6	7	8	9	10	11	12	13	14	15	16	17
								Reflector												
				Radial (Mesh 1)	(Mesh 2)	(Mesh 3)	Outer Core	Gap	Outer core to CR	CR	Graphite	Graphite	Gas Duct	Carbon Bricks	Radiative Gap Static He	Core Barrel	Radiative Gap Static He	RPV	Radiative Gap Static He	Fluid Region Model Boundary
			R Axis Mesh (Correct Location)	64.2	90.793	111.198	128.4	129.4	136.5	149.5	190.0	206.0	211.9	217.8	225.5	228.5	250.5	256.5	406.5	426.5
		Z Axis Mesh (Top Location)	Mesh Thickness (cm)	64.2	26.593	20.405	17.202	1	7.1	13	40.5	16	5.9	5.9	7.7	3	22	6	150	20
1	Fluid Region Model boundary	-454.3	-20.0	15	15	15	15	15	15	15	15	15	15	15	15	15	15	15	15	15
2	RPV	-434.3	-5.0	18	18	18	18	18	18	18	18	18	18	18	18	18	18	18	19	20
3	Radiation Gap (He)	-429.3	-150.0	21	21	21	21	21	21	21	21	21	21	21	21	17	7	18	19	20
4	Top Plate	-279.3	-20.0	23	23	23	23	23	23	23	23	23	23	23	23	17	7	18	19	20
5	Carbon Bricks	-259.3	-40.0	5	5	5	5	5	5	5	5	5	5	5	14	17	7	18	19	20
6	Top Reflector	-219.3	-42.5	22	22	22	22	22	22	22	22	22	22	5	14	17	7	18	19	20
7	Top Reflector	-176.8	-42.5	10	10	10	10	10	10	10	10	10	22	5	14	17	7	18	19	20
8	Top Reflector	-134.3	-42.5	9	9	9	9	2	2	32	3	4	3	5	14	17	7	18	19	20
9	Top Reflector	-91.8	-42.5	16	16	16	16	2	2	32	3	4	3	5	14	17	7	18	19	20
10	Void Cavity	0.0	-49.3	8	8	8	8	2	2	32	3	4	3	5	14	17	7	18	19	20
11	Core Equidistant Mesh	32.5	32.5	1	1	1	1	27	27	32	37	4	3	5	14	17	7	18	19	20
12	Core Equidistant Mesh	65.0	32.5	1	1	1	1	27	27	32	37	4	3	5	14	17	7	18	19	20
13	Core Equidistant Mesh	97.5	32.5	1	1	1	1	27	27	32	37	4	3	5	14	17	7	18	19	20
14	Core Equidistant Mesh	130.0	32.5	1	1	1	1	27	27	32	37	4	3	5	14	17	7	18	19	20
15	Core Equidistant Mesh	162.5	32.5	1	1	1	1	28	28	33	38	4	3	5	14	17	7	18	19	20
16	Core Equidistant Mesh	195.0	32.5	1	1	1	1	28	28	33	38	4	3	5	14	17	7	18	19	20
17	Core Equidistant Mesh	227.5	32.5	1	1	1	1	28	28	33	38	4	3	5	14	17	7	18	19	20
18	Core Equidistant Mesh	260.0	32.5	1	1	1	1	28	28	33	38	4	3	5	14	17	7	18	19	20
19	Core Equidistant Mesh	292.5	32.5	1	1	1	1	29	29	34	39	4	3	5	14	17	7	18	19	20
20	Core Equidistant Mesh	325.0	32.5	1	1	1	1	29	29	34	39	4	3	5	14	17	7	18	19	20
21	Core Equidistant Mesh	357.5	32.5	1	1	1	1	29	29	34	39	4	3	5	14	17	7	18	19	20
22	Core Equidistant Mesh	390.0	32.5	1	1	1	1	29	29	34	39	4	3	5	14	17	7	18	19	20
23	Core Equidistant Mesh	422.5	32.5	1	1	1	1	30	30	35	40	4	3	5	14	17	7	18	19	20
24	Core Equidistant Mesh	455.0	32.5	1	1	1	1	30	30	35	40	4	3	5	14	17	7	18	19	20
25	Core Equidistant Mesh	487.5	32.5	1	1	1	1	30	30	35	40	4	3	5	14	17	7	18	19	20
26	Core Equidistant Mesh	520.0	32.5	1	1	1	1	30	30	35	40	4	3	5	14	17	7	18	19	20
27	Cone Mesh 4	529.9	9.925	1	1	1	1	31	31	36	41	4	3	5	14	17	7	18	19	20
28	Cone Mesh 3	541.7	11.773	1	1	1	24	31	31	36	41	4	3	5	14	17	7	18	19	20
29	Cone Mesh 2	557.0	15.343	1	1	24	24	31	31	36	41	4	3	5	14	17	7	18	19	20
30	Cone Mesh 1	579.7	22.618	1	24	24	24	31	31	36	41	4	3	5	14	17	7	18	19	20
31	Bottom Reflector	632.76	53.100	24	24	24	24	31	31	36	41	4	3	5	14	17	7	18	19	20
32	Bottom Reflector	707.76	75.0	11	11	11	11	31	31	36	41	4	3	5	14	17	7	18	19	20
33	Bottom Reflector	757.76	50.0	6	6	6	6	25	25	25	25	4	26	5	14	17	7	18	19	20
34	Bottom Reflector	807.76	50.0	13	13	13	13	25	25	25	25	42	26	5	14	17	7	18	19	20
35	Bottom Reflector/ Carbon Bricks	882.76	75.0	5	5	43	5	5	5	5	5	5	5	5	14	17	7	18	19	20
36	RPV	885.26	2.5	18	18	44	18	18	18	18	18	18	18	18	18	18	18	18	19	20
37	Fluid Region Model boundary	905.26	20.0	12	12	12	12	12	12	12	12	12	12	12	12	12	12	12	12	12

Figure 9 – VSOP excel geometry model

3.2.3 VSOP code functionality.

The discussion of the sub-programs comprising the VSOP suite of codes is discussed in this section. This discussion will be based on the relevant calculational procedures involving the definition of the fuel constitution, geometrical setup and material composition for the VSOP simulations. The spherical fuel element flow patterns (pebble flow-lines) are needed and these are calculated based on the reactors geometry specific to its diameter. Flow line calculations are based on actual pebble bed reactors that were in operation or are in operation currently. This is based on the closest reactor core diameter. The HTMR100 uses adapted MEDUL-200 flow lines, however real flow-lines are determined experimentally and discretised in compliance with relevant numerical parameters but these approximations will not be far off. A calculational mesh relating to the fuel shuffling process is formed from the discretisation of the space left in between these so-called flow lines depending on among other factors the reactor to be modelled. Coupled neutronics and thermal-hydraulics are calculated in 2D in the Thermix VSOP calculations (Rutten, et al., 2009).

3.2.3.1 Fuel constitution and definition.

The basic fuel element design consists of fuel type, heavy metal loading, enrichment, nuclear material data and physical fuel element dimensions. There are eight types of fuels that VSOP can simulate, that being UO_2, UC, UC_2, ThO_2-UO_2, ThC-UC, ThC_2-UC_2, PuO_2 and ThO_2-PuO_2.

The pebble bed core approximates a near homogeneous mixture because of the distribution of coated particles in the graphite matrix this allows the neutrons to be well moderated within close distances from the initial neutron impact. This benefits the neutron economy and can thus exploit the U-235/Th-232 and U-233 fuel cycles due to the fact that the losses in neutrons are far less than other reactors (Kugeler, et al., 1989).

The HTR pebble bed has the flexibility to accommodate many types of fuel cycles. The fuel cycles that will be used in the simulations of the HTMR100 reactor core will be the LEU, ThLEU and ThHEU fuel cycles as these fuel cycles are the most likely to be realized. The ThHEU fuel cycle is a proliferation risk and is only investigated for the completeness of the thesis.

Table 6 – Fuel Sphere Description

Fuel pebble outer radius	**3**	**cm**	
Thickness fuel free zone	0.5	cm	
Fuel kernel diameter	500	micron	
Kernel coating material	C/C/SiC/C		
Layer thickness	95/40/35/40	µm	
Layer densities	1.05/1.90/35/40	g/cm^3	
Total HM content per equilibrium sphere	5 -16	g	
Fuel composition	8 – 15	wt%	Effective Enrichment
Fuel	LEU (8 wt%, 10 wt%, 15 wt% & 20 wt% U-235) ThLEU, (20 wt% U-235) ThHEU (93 wt% U-235)		

3.2.3.2 Resonance treatment

Prior to preforming the VSOP simulations the relevant resonance absorption cross sections must be generated in a subroutine called ZUT. This code uses the basic fuel element design data and prepares the resonance integral data which is later used by the main VSOP code. The resonance absorption cross sectional data at different temperatures is simulated at different temperatures stored in resint and later used in

the main VSOP run to preform different spectrum calculations. The infinitely diluted resonance integrals for the fertile isotopes Th-232 and U-238 are also calculated by resint (Rutten, et al., 2009).

3.2.3.3 Reactivity

The 2-D spatial flux distribution and multiplication factor K_{eff} is calculated with CITATION which is a subroutine of VSOP addresses neutron diffusion. The neutron diffusion equation used is:

$$-\bar{\nabla}D(\bar{r},E)\bar{\nabla}\Phi(\bar{r},E) + \left(\Sigma_a(\bar{r},E) + \Sigma_s(\bar{r},E)\right)\Phi = \int_{E'}\left(\Sigma_s(\bar{r},E'\rightarrow E) + \frac{\chi_E\left(\nu\Sigma_f(\bar{r},E)\right)}{k_{eff}}\right)\Phi(\bar{r},E)dE' \quad (12)$$

CITATION makes use of the THERMOS-library which contains 30 separate energy groups ranging from 10e-5 to 2.05 eV. Four neutron energy groups are used for the simulation of high temperature reactors, which is sufficient. These energy groups consist of one group that represents neutron energies in the thermal range 0 to 1.86 eV, two epithermal groups with neutron energies of 1.86 to 29 eV and 29 eV to 1.11 MeV respectively and one fast group with neutron energies between 1.11 to 10 MeV (Rutten, et al., 2009).

3.2.3.4 Burn-up

Burn-up calculations require the core power distribution, neutron flux and the multiplication factor which consists of mesh points for the energy groups in a discrete domain. Burn-up cycles are subdivided into course time intervals in which spectrum and diffusion calculations are done. In order for the normalization of neutron fluxes relative to core power distributions to be performed these course time intervals are divided into a number of finer time intervals. During each of these intervals the flux and power distribution, the weight of all heavy metals and the nuclide concentration of each region are calculated. There are 91 individual isotopes that can be simulated in these calculations per region. These isotopes include among others the chain from Th-232 to U-236 and then the chain from U-238 to Pu-242 (Rutten, et al., 2009).

3.2.3.5 Simulation procedure

The simulation procedure used to achieve the objects set out in the introduction of this report is divided into two parts. The first part of the procedure assesses the neutronic performance and provides data for each fuel cycle such as the conversion ratio, residence time, burn-up, neutron reproduction factor etc. The second part of the procedure utilizes the burn-up and residence time to calculate the uranium and thorium raw material requirements for each type of fuelling scheme as well as existing fuel sphere cost models from STL to assess the fuel sphere requirements of each fuel type the LUEC is calculated using the STL reactor cost model for a single reactor unit. These results will be compared on a neutronic as well as a cost basis to select the best fuel type possible (neutronically & cost wise) and to determine whether the thorium fuelling schemes are viable. A run was performed for each and every single fuel mixture. There are three fuel types LEU, ThLEU and ThHEU each with an effective enrichment of 8 wt%, 10 wt% and 15 wt% with heavy metal loadings of 5 g HM, 7 g HM, 10 g HM, 12 g HM and 16 g HM. This means that 15 runs were performed per fuel type, equating to 45 equilibrium runs in total as seen in **Table 7.** Each of these runs required resonance integral preparation resulting in 45 resint data files. Additional runs of LEU at 20 wt% were added for comparison which added an additional 5 runs.

Table 7 – VSOP equilibrium runs

LEU	**5 g HM**	**7 g HM**	**10 g HM**	**12 g HM**	**16 g HM**
8 wt%	X	X	X	X	X
10 wt%	X	X	X	X	X
15 wt%	X	X	X	X	X
20 wt%	X	X	X	X	X
ThLEU					
8 wt%	X	X	X	X	X
10 wt%	X	X	X	X	X
15 wt%	X	X	X	X	X
ThHEU					
8 wt%	X	X	X	X	X
10 wt%	X	X	X	X	X
15 wt%	X	X	X	X	X

1. **Neutronic performance.**

The simulation procedure used to determine the neutronic performance of each fuel cycle consists of two separate sequences that execute the relevant subroutines of the VSOP system of codes discussed above. These sequences will now be briefly discussed.

Sequence 1:

The first step in this sequence is to run the ZUT subroutine that uses an additional input file that contains information about the resonance absorption cross sections at different temperatures for the relevant fertile isotopes as well as the infinitely diluted fertile isotopes. This code then generates the “resint” which is needed by the VSOP code to perform the final calculations.

Sequence 2:

The VSOP code uses an input file setup by the user which describes the reactor core geometry and dimensions. In this file the materials of construction, void regions and pebble flow paths are provided. VSOP code is run to produce the final results of the equilibrium fuel cycle. These final results contain the relevant neutronic parameters, fuel cycle ore requirement as well as the fissile material required to achieve the necessary thermal power. This code uses all the prior data generated by the subroutines previously discussed as well as an additional input file describing among other specifications the number and thickness of the axial and radial meshes of the core as well as the layer and channel dimensions.

2. **Cost calculations**

The cost calculations are calculated from the residence time and burn-up achieved by each type of fuel mixture, this determines how many fuel spheres are consumed per day for each equilibrium core model. The uranium and thorium raw material requirements are then determined based on the heavy metal loading, effective enrichment and U-235 enrichment value. The uranium and thorium costs are then determined based on market prices on the 14th of August 2017. The uranium enrichment is determined by current market related data which is calculated from the “UxC Fuel Quantity & Cost Calculator”. The UxC uses the U_3O_8, conversion, UF6 and

SWU costs to calculate the Enriched Uranium Product (EUP) in $/kg which contains both the U-235 and U-238 fractions for various enrichments (UxC, n.d.). Thorium costs were obtained from Rhodia France for lab grade ThO_2 at 99.999% purity, this cost could become lower once thorium has a market value and is bought on an industrial scale. The costs are completely theoretically based and the fuel cost calculator does not take into account politics and availability of the enriched uranium, it also doesn't take into account the proliferation problems associated with HEU (20 wt% U-235 and above) or the amount of additional centrifuges that are needed for enrichments higher than 20 wt%, therefore ThHEU results are of interest, however they are not entirely reputable. All values up to 20 wt% are reputable and the main focus of this study is to assess LEU vs ThLEU as these are the only viable fuelling options in many countries where HEU is not allowed, HEU was just added for the completeness of the study. The remainder of the fuel sphere costs such as raw material, casting, coating, over-coating, pressing and machining costs are determined form the STL fuel cost models which take into account the amount of fuel spheres produced on a large scale in a fuel plant (250000FS/annum) as well as the heavy metal loadings, enrichments and burn-ups. Mass balances, utility, power requirements and staff salaries are just some of the costs taken into account in the STL fuel cost models. The fuel sphere price is then accurately based on the uranium and thorium raw material requirements and costs as well as the costs of the rest of the fuel sphere based on the STL models. The fuelling cycles can be accurately compared to determine which fuel cycle is the most cost effective based on a certain fuel. The LUEC is determined from the STL reactor cost model for a single unit, this provides the levilized costs for the capital investment, operation and maintenance, fresh fuel, spent fuel and decommissioning. The main focus is on the fresh fuel costs in US$/kWe and total costs in US$/kWh and US$/MWh.

4 RESULTS AND DISCUSSIONS

4.1 Neutronic simulations

This section presents and discusses the most important neutronic results for the various fuel types for the same reactor configuration. The LEU fuel option utilises various U-235 enrichments beginning at 8 wt%, 10 wt%, 15 wt% and 20 wt%. The ThLEU option utilises a U-235 enrichment of 20 wt% and ThHEU a U-235 enrichment of 93 wt%. **Table 8** further down shows the HM loading and effective enrichment for the three different fuel types with their associated fuel residence time, burn-ups and fuel consumption rate.

4.1.1 Burn-up and cumulative heat energy comparison

The most important factor which will lower the cost/kWh is the cumulative amount of heat energy produced per fuel sphere, this is the burn-up multiplied by the mass of heavy metal per fuel sphere. The reason why the detailed burn-up analysis is shown is to determine where the highest burn-ups are achieved and relate this to the optimum fuel costs which are directly linked to the cumulative amount of heat energy. The comparison below will discuss the influence of heavy metal loading and enrichment on burn-up. As can be seen in **Table 8** the general trend is as the enrichment increases so does the burn-up, however this is not the same general trend followed by the heavy metal loading. **Figure 10** , **Figure 11** and **Figure 12** show graphically where the highest burn-ups are achieved. The explanation for LEU fuel obtaining a higher burn-up at lower heavy metal loadings is that lower heavy metal loading means less fuel kernels per fuel sphere and thus larger volumes of graphite between fuel kernels. This means fewer collisions with fuel kernels during the process of moderation and thus more neutron moderation between successive collisions with fuel kernels. This increases the probability of neutrons slipping through the capture resonances of U-238, without being captured, i.e. it increases the resonance escape probability. This in turn increases k_{∞} of the fuel, which means that the fuel can burn deeper, i.e. down to lower enrichments, before it will drag k_{eff} down to below 1.0. Put differently, it is well-known that the standard Pebble Bed Reactor designs are under-moderated. Therefore anything that increases the moderation, such as less fuel kernels per fuel sphere, will increase k_{∞} and will thus increase the burn-up. It should however be noted that, due to the high cost of fuel spheres, the lowest fuel cost/kWh electricity produced, is more related to the cumulative amount of heat energy produced during the life of each fuel sphere, than to the burn-up. Therefore increasing the heavy metal loading above the value for the peak burn-up will likely result in higher cumulative energy per fuel sphere and thus lower fuel cost per kWh electrical energy produced.

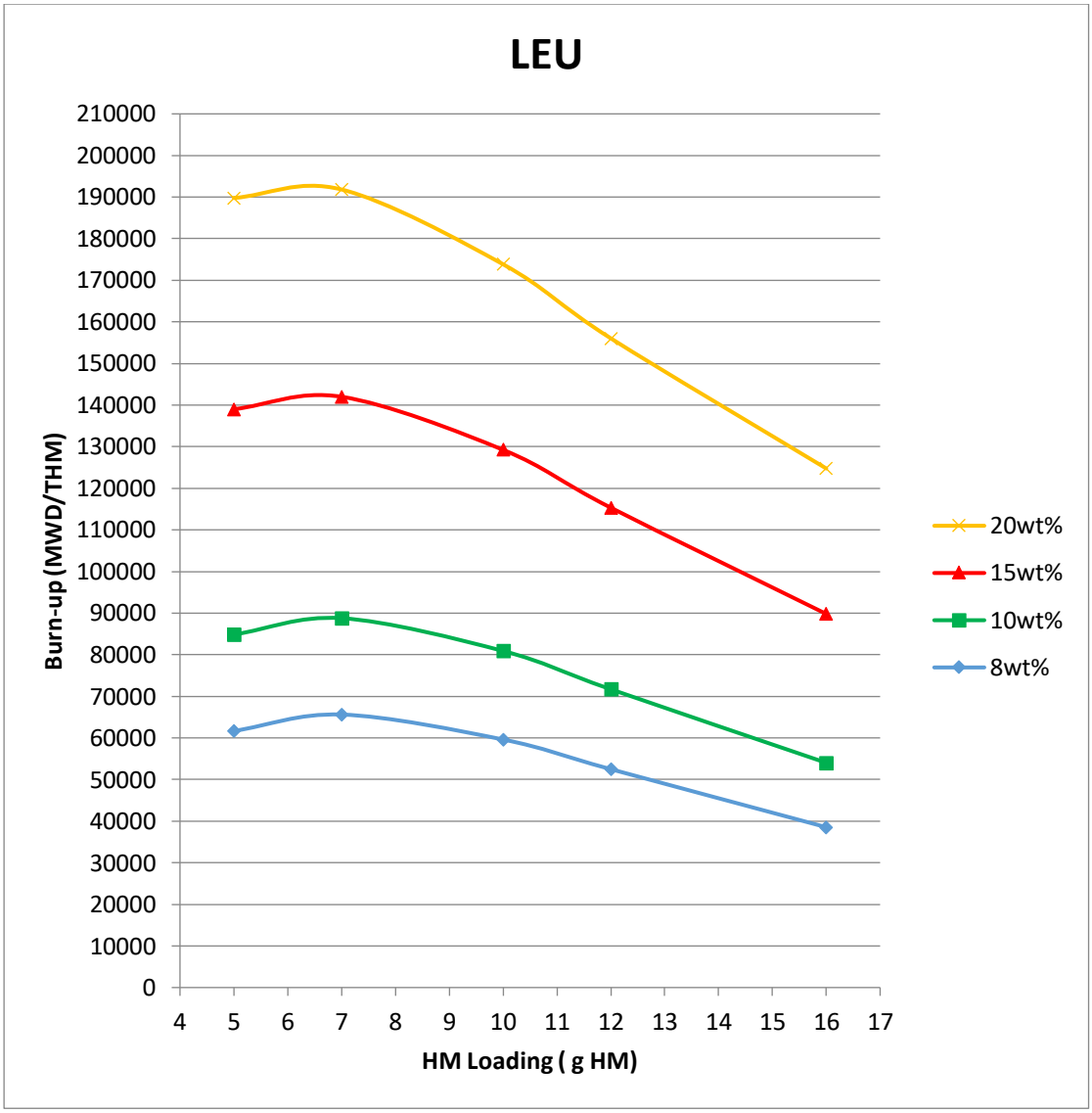

Figure 10 – Burn-up for various enrichments and heavy metal loadings for LEU fuel

The results for the highest burn-up on **Figure 10** lie at a 7 g HM loading for LEU fuel while the highest values for ThLEU **Figure 11** are at 10 g HM and ThHEU **Figure 12** lie at 12 g HM. These values show the optimum fuel to moderator ratio for the different fuels in terms of burn-up. A low heavy metal loading increases the distance between the fuel kernels, the neutron leakage is increased as there is not enough U-238 to capture neutrons or enough U-235 to absorb neutrons for fission. Higher leakage reduces k_{eff} and therefore reduces burn-up. However, as has been pointed out above, lower HM loading also lead to better moderation and thus to higher resonance escape probabilities, which increases k_{eff} and thus burn-up. These two effects thus oppose each other. The trend of maximum burn-up at a HM loading of 7 g per fuel sphere in **Figure 10** above suggests that when the HM loading is decreased below 7 g HM per

fuel sphere, increasing leakage dominates over increasing resonance escape probability and therefore burn-up decreases. When the HM loading is increased above 7 g HM per fuel sphere, decreasing resonance escape probability dominates over decreasing leakage and therefore burn-up decreases with increasing HM loading above 7 g HM per fuel sphere. **Figure 13** below shows that the core leakage is higher at lower heavy metal loadings and decreases as the heavy metal loading is increased.

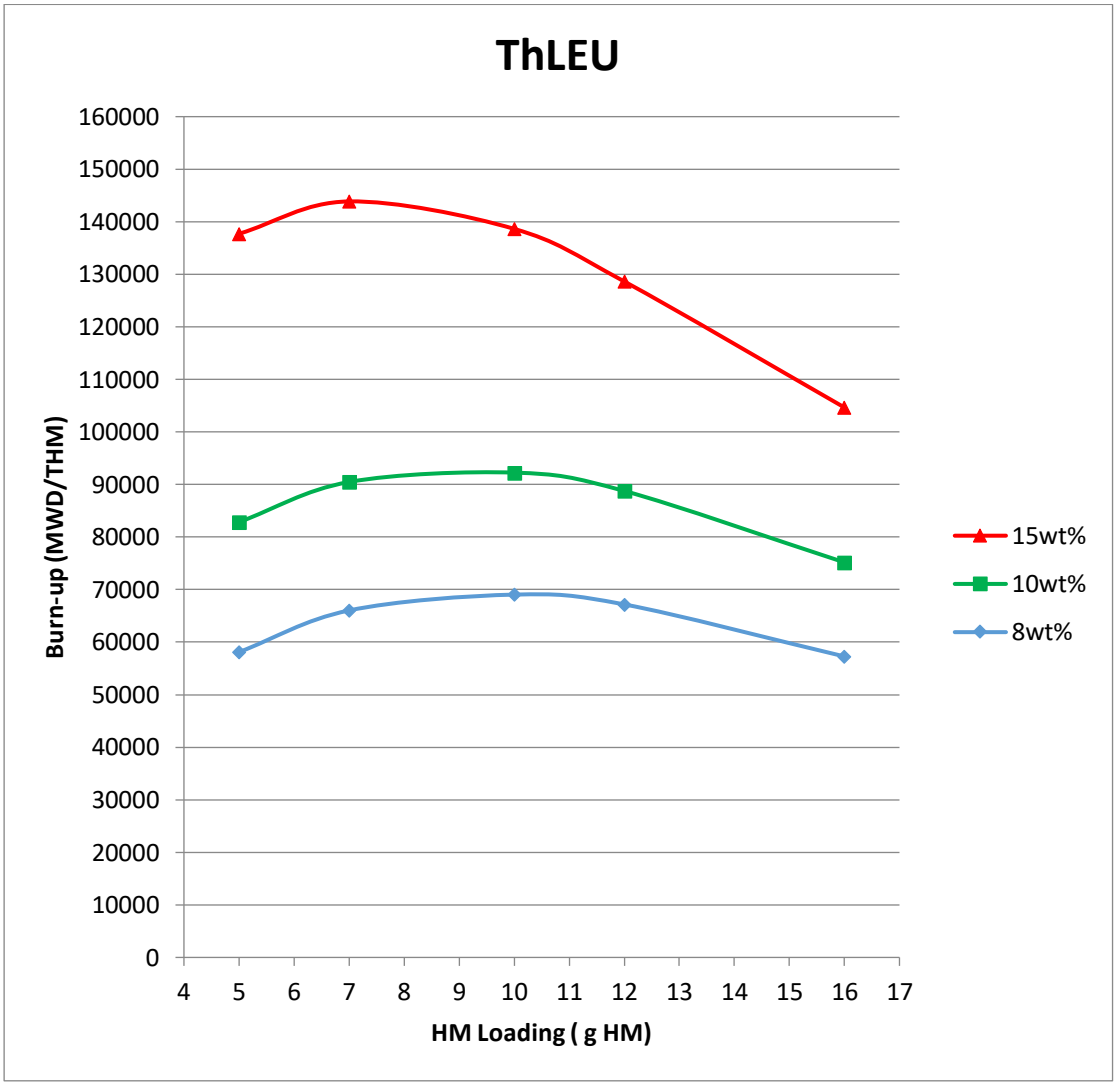

Figure 11 – Burn-up for various enrichments and heavy metal loadings for ThLEU fuel

As can be seen in **Figure 11**, the 15 wt% case tends to find its highest burn-up at 7 g heavy metal loading, compared to 10 g HM for the lower enrichments. The peak burn-up at 10 g HM per fuel sphere for the lower enriched Th mixtures can be explained as follows: the resonance integrals for Th-232 in the epithermal energy windows are about

4 times smaller than for U-238, which means that Th is four times less likely to capture epithermal neutrons than U-238. This means that the problem of decreasing resonance escape probability with increasing HM loading is much less pronounced for Th-based mixtures than for U-238 based mixtures and therefore the maximum burn-up will be attained at higher HM loadings for Th-based mixtures.

If you start with LEU (20 wt%) and start adding Th, the effective enrichment of the mixture decreases monotonously with increasing fractions of Th. This means that the 15% effective enrichment ThLEU fuel mixtures contains much less Th than those with the lower enrichments, which means that the 15% mixture will behave more like a U-238 based fuel, while the lower enrichments will behave more like Th-based fuels. This probably explains while, just like the pure LEU fuel mixtures the 15% ThLEU mixture has a maximum burn-up at 7 g HM per fuel sphere, while the lower enrichment ThLEU fuel mixture reach their maximum burn-up only at 10 g HM per fuel sphere.

By the same logic, the ThHEU fuel mixtures shown in **Figure 12** below contains almost no U-238 and therefore a higher fraction of Th-232. Therefore, they reach their maximum burn-ups at the even higher 12 g HM per fuel sphere.

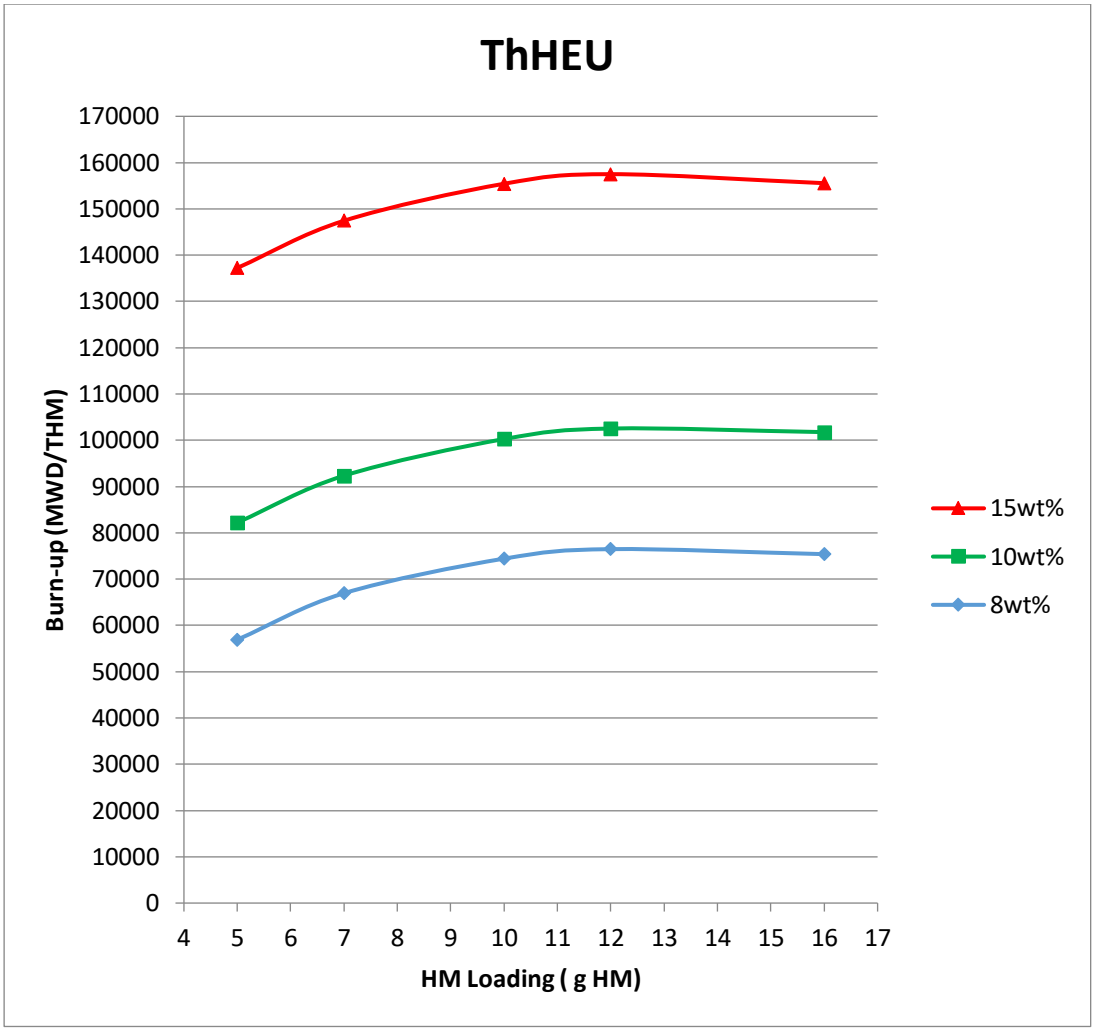

Figure 12 – Burn-up for various enrichments and heavy metal loadings for ThHEU fuel

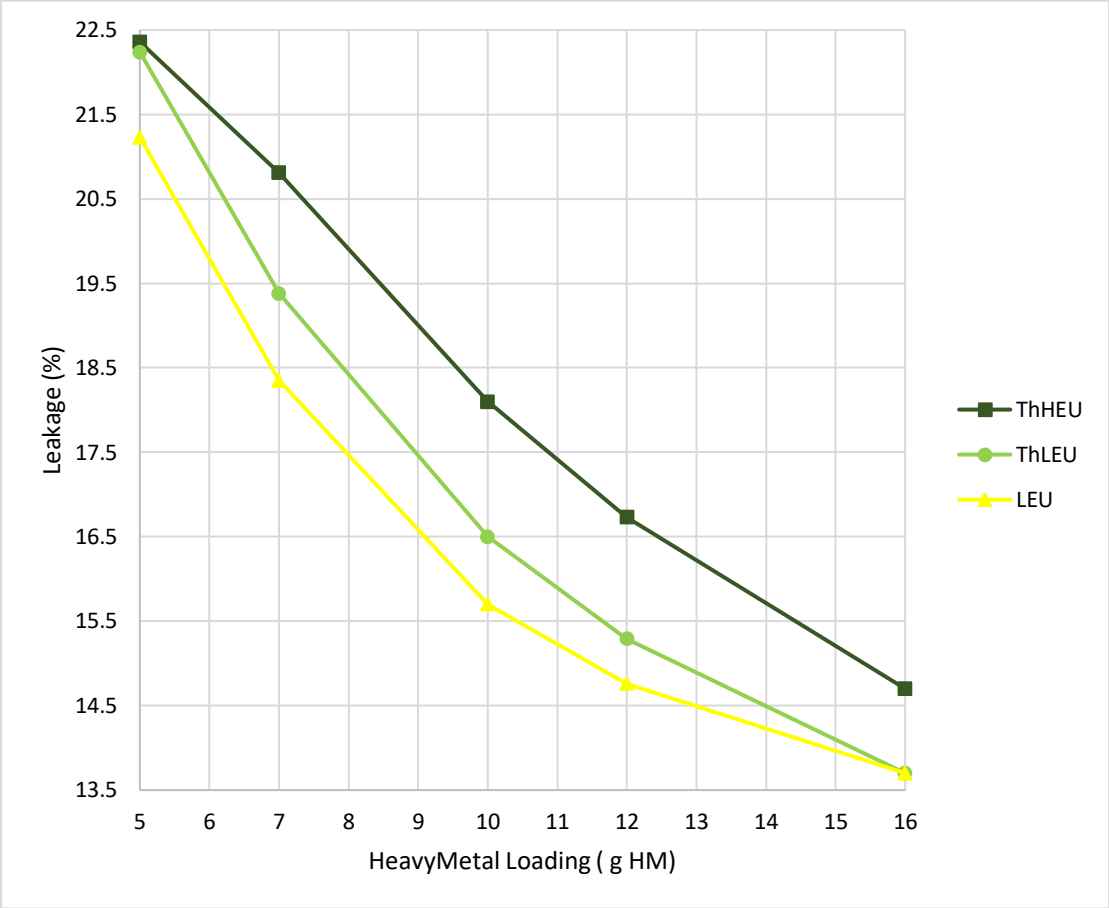

Figure 13 – Core Leakage at various HM loadings at 10 wt% enrichment

Figure 13 above shows that at lower heavy metal loadings the core leakage is higher such as with the 5 g HM per fuel sphere case the leakage percentage is much higher than for increased heavy metal loadings at 16 g HM per fuel sphere. The leakage rate is higher for the thorium-based fuels, this is due to Th-232 having a smaller capture cross section which is 4 times smaller than U-238 this leads to less captures and a higher K_{eff}. Replacing U-238 with Th-232 is only viable at high heavy metal loadings where there are enough thorium particles to make a substantial difference where the captures that do occur produce U-233. Th-232 that is replacing U-238 leads to less captures in the Th and thus leaves more neutrons available for causing fissions in the fissile fuel. This thorium is converted into U-233 which is the best thermal fuel in a HTR (Lung & Gremm, 1997).

The radar plot in **Figure 14** shown below displays the burn-up values discussed above in one graphical illustration, this shows how the burn-up patterns shift for the various fuels at different heavy metal loadings. The highest burn-up for LEU lies at a 7 g HM loading, ThLEU at 10 g HM and the ThHEU at 12 g HM as shown in the discussion above. A detailed discussion will be shown below which discusses the influence of heavy metal loading and enrichment on burn-up.

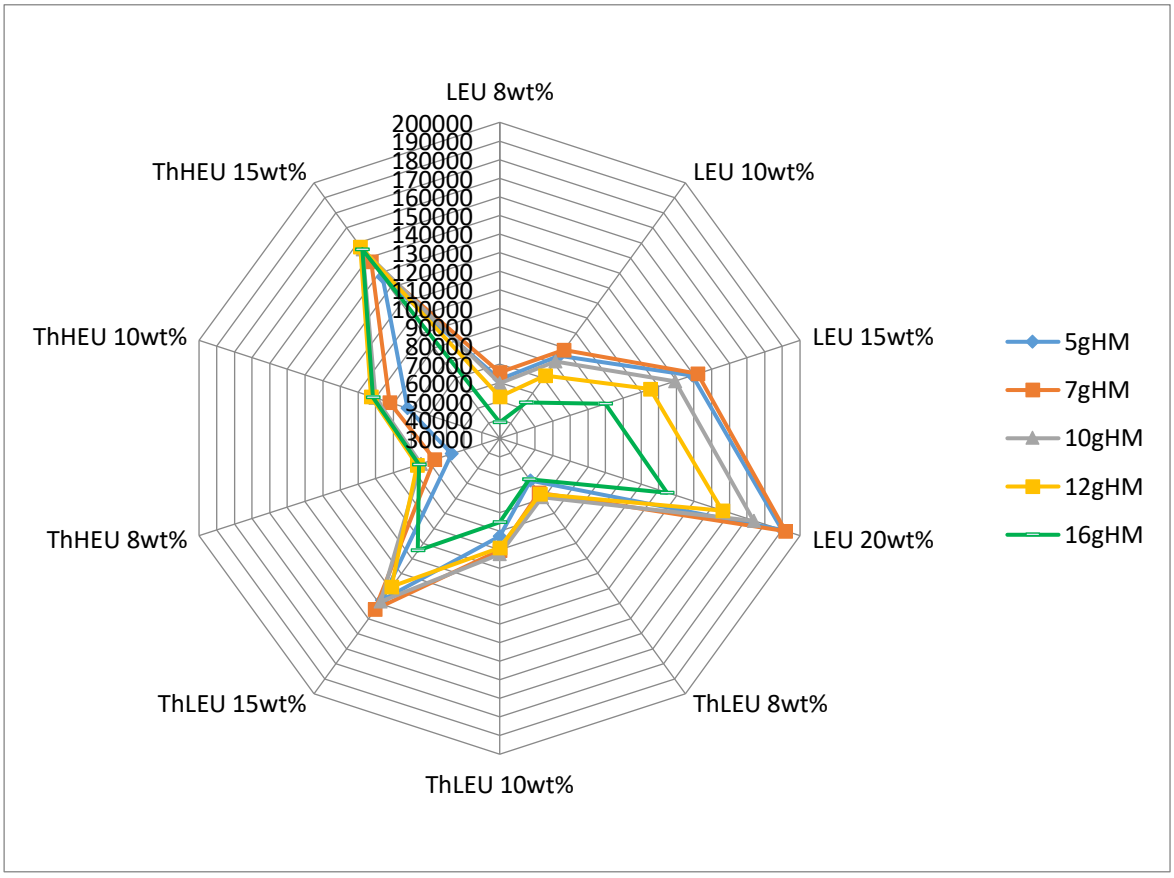

Figure 14 – Radar plot for the burn-up for various HM loadings and effective enrichments for LEU, ThLEU and ThHEU.

Figure 15 shows the burn-up versus HM loading for all the fuels at various enrichments in one graph. **Figure 16** shows the burn-up versus enrichments for all the various fuels at different HM loadings in one graph.

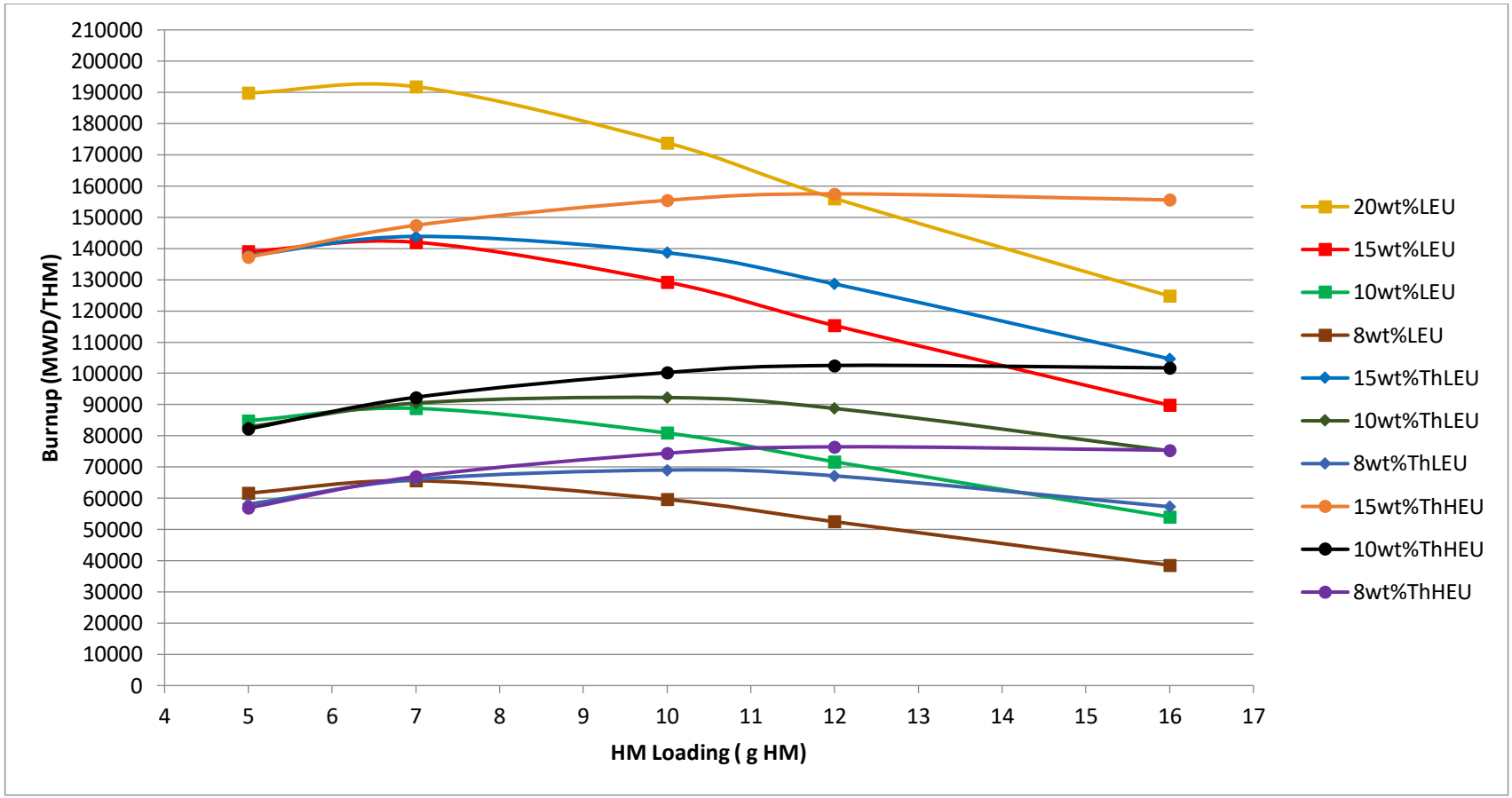

Figure 15 – Burn-up comparison for all the fuels at various HM loadings.

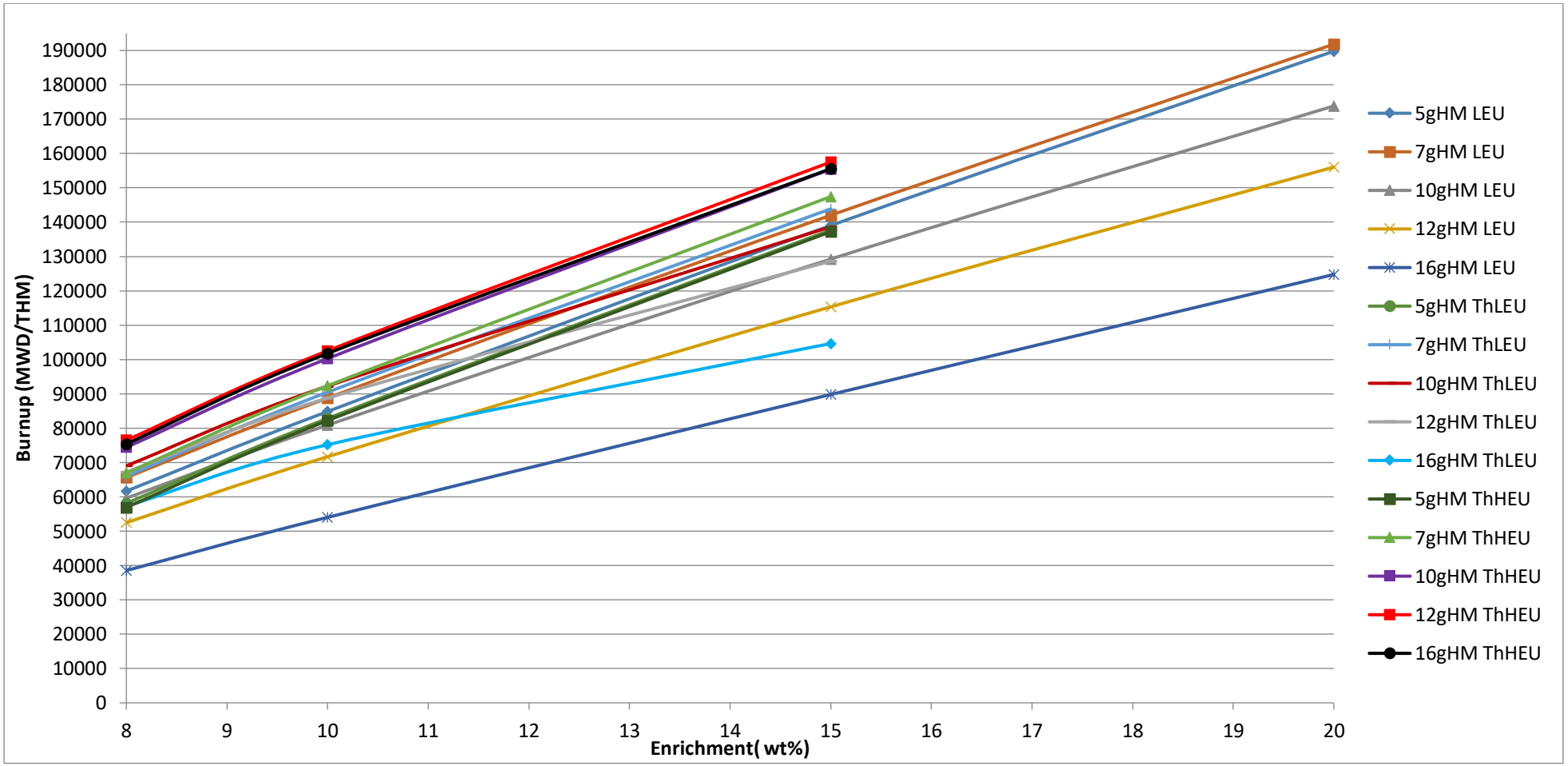

Figure 16 – Burn-up comparison for all the fuels at various enrichments

It is evident from **Figure 15** and **Figure 16** that the general trend seen is that as the enrichment increases so does the burn-up. However, it is also evident that the highest burnups are achieved for the fuels in their optimum fuel to moderation ratios, that being 7 g HM for LEU, 10 g HM for ThLEU and 12 g HM for ThHEU seen on **Figure 16**.

At low heavy metal loadings on **Figure 15** the burn-ups are relatively similar for all of the fuels. The thorium fuels only start to increase and outperform the LEU fuel at the higher heavy metal loadings (10 g HM upwards). The reason for this is that at lower heavy metal loadings the leakage factor is high due to the increased distance between the fuel kernels, as there is not enough U-238 and Th-232 to capture neutrons or enough U-235 to absorb neutrons for fission. Due to the increased moderation, more neutrons are moderated down to below the epithermal capture resonances without being captured in them, i.e. the resonance escape probability increases. The result is that neither U-238 nor Th-232 (which has an epithermal capture cross section 4 times smaller than that of U-238) are very effective at capturing neutrons. Therefore, the U-238 breeds little Pu-239 and the Th-232 breeds very little U-233. Therefore, most of the fissions come from the U-235 that was loaded in the fresh fuel, rather than from the small concentrations of Pu-239 or U-233 that was subsequently bred. Since for, equal HM loadings and equal effective enrichments, the LEU and ThLEU contains equal masses of U-235, it is unsurprising that they burn similarly and therefore produce very similar burn-ups at these low heavy metal loadings.

At higher heavy metal loadings, as shown in **Figure 15** the thorium based (ThLEU and ThHEU) fuels especially the ThHEU fuel outperforms LEU quite somewhat. This can be explained as follows: at higher HM loadings, the logic of the previous paragraph reverses as the moderation ratio decreases. Neutrons are thus less moderated between subsequent collisions with fuel kernels and therefore the resonance escape probability decreases, i.e. more captures result in U-238 breeding substantial amounts of Pu-239 and Th-232 breeding smaller, but still substantial amounts of U-233. Therefore, fissioning of U-235 becomes less dominant and the neutron economy of the LEU fuel thus substantially influenced by the neutron economy of the Pu-239 and that of the Th-LEU by a mixture of the neutron economies of the U-233 and Pu-239. U-233 is the best thermal fuel in an HTR (Lung & Gremm, 1997). U-233 has a much better neutron economy and thus also a much better conversion ratio than for Pu-239, which is bread from U-238. This explains why replacing U-238 with Th-232 results in

more fission neutrons produced in the U-233 than where only the Pu-239 is bred in the LEU. An improved neutron economy increases k_{eff} and thus increase the time that the fuel can stay in the reactor and thus the burn-up and cumulative heat energy are increased.

However, the fact the epithermal microscopic capture cross-sections of Th-232 is much smaller than that of U-238 and therefore the resonance integral for Th is about four times smaller than for U-238 is problematic. It means that if equal number densities of Th-232 and U-238 are loaded into a fuel sphere, the U-238 will breed about four times as much Pu-239, compared to the U-233 that will be bred by the Th-233. This means that the poor neutron economy of Pu-239 will dominate over the excellent neutron economy of U-233. Two obvious ways to counter this problem is to reduce the U-238 by increasing the enrichment from LEU to HEU or to increase the amount of Th in the fuel sphere by increasing the HM loading. Both strategies have been implemented in this study and both worked. As can be seen in the charts, the ThHEU outperformed the ThLEU. However, when the enrichment is increased above the 20 wt% of LEU, the nuclear weapons proliferation risk increases and therefore higher enrichments are prohibited by law in most countries and therefore it is not considered a viable strategy. Therefore, the most viable strategy for using Th in Pebble Bed Reactors is to increase the HM loading.

The reason to increase the heavy metal loading in a fuel sphere is to maximise the cumulative amount of heat energy per fuel sphere and also to reduce the fuel costs as a reactor using a higher heavy metal loading will consume less fuel spheres. These factors lead to ThLEU and ThHEU at (16 g HM and 8 wt%) outperforming LEU at (10 wt% at 16 g HM). The most impressive results are that at 16 g HM the ThHEU fuel (15 wt%) completely outperforms LEU fuel at 16 g HM (20 wt%) by around 30000 MWD/THM.

Table 8 and **Table 9** shows the fuel feed rate, this is linked to the fuel residence time and burn-up. The general trend is the higher the heavy metal loading and enrichment, the lower the amount of fuel spheres needed to keep the reactor critical. The obvious reason for this is that higher burn-up and higher HM loading by definition equates to higher total cumulative heat energy produced over the life of the fuel

sphere, which by definitions means that one has to add less fuel spheres in order to produce the days energy output.

Table 8 – Overall burn-up, fuel residence time and fuel sphere feed rate for runs up to 15 wt% effective enrichment

LEU	**Units**															
HEAVY METAL LOADING	g HM	5	5	5	7	7	7	10	10	10	12	12	12	16	16	16
FEED ENRICHMENT	wt%	8	10	15	8	10	15	8	10	15	8	10	15	8	10	15
AVG. FISSILE ENRICHMENT	%	4.5	4.85	5.78	4.53	5	6.34	5.2	5.95	7.9	5.68	6.61	8.97	6.47	7.66	10.62
AVG. FUEL RESIDENCE TIME	DAYS	470	647	1063	700	948	1518	908	1232	1970	958	1309	2108	938	1315	2186
AVG. BURN-UP	MWD/T	61675	84851	139016	65620	88782	142000	59615	80898	129242	52485	71686	115330	38540	54021	89802
PEBBLE FEED RATE	SPHERES/DAY	324	236	144	218	161	101	168	124	77	159	116	72	162	116	70
ThLEU																
HEAVY METAL LOADING	g HM	5	5	5	7	7	7	10	10	10	12	12	12	16	16	16
FEED ENRICHMENT	wt%	8	10	15	8	10	15	8	10	15	8	10	15	8	10	15
AVG. FISSILE ENRICHMENT	%	4.73	4.98	5.71	4.54	4.89	5.99	4.76	5.3	7.15	5.05	5.75	8.08	5.75	6.74	9.76
AVG. FUEL RESIDENCE TIME	DAYS	442	631	1052	704	965	1538	1051	1405	2114	1226	1621	2351	1392	1828	2547
AVG. BURN-UP	MWD/T	58108	82839	137713	66032	90475	143868	69044	92260	138642	67176	88771	128631	57272	75180	104656
PEBBLE FEED RATE	SPHERES/DAY	344	241	145	216	158	99	145	108	72	124	94	65	109	83	60

ThHEU																
HEAVY METAL LOADING	g HM	5	5	5	7	7	7	10	10	10	12	12	12	16	16	16
FEED ENRICHMENT	wt%	8	10	15	8	10	15	8	10	15	8	10	15	8	10	15
AVG. FISSILE ENRICHMENT	%	4.83	5.05	5.57	4.52	4.75	5.35	4.5	4.8	5.56	4.63	4.98	5.87	5.05	5.51	6.72
AVG. FUEL RESIDENCE TIME	DAYS	433	626	1048	713	985	1578	1132	1528	2375	1395	1873	2884	1833	2476	3793
AVG. BURN-UP	MWD/T	56922	82214	137237	66948	92348	147438	74426	100267	155432	76475	102537	157501	75392	101758	155552
PEBBLE FEED RATE	SPHERES/DAY	351	243	146	213	155	97	134	100	64	109	81	53	83	61	40

Table 9 – Overall burn-up, fuel residence time and fuel sphere feed rate for 20 wt% LEU

LEU	Units:					
HEAVY METAL LOADING	g HM	5	7	10	12	16
FEED ENRICHMENT	wt%	20	20	20	20	20
AVG. FISSILE ENRICHMENT	%	6.72	7.65	9.86	11.28	13.4
AVG. FUEL RESIDENCE TIME	DAYS	1452.9	2053	2652.2	2853.1	3038.4
AVG. BURN-UP	MWD/T	189780	191822	173837.5	156042.6	124758.4
PEBBLE FEED RATE	SPHERES/DAY	105	74	58	53	50

Table 10 and Table 11 show the power peaking maximum to average as well as the cumulative energy produced per fuel sphere. With regards to the peaking factors the ThLEU fuel has a slightly lower peaking factor compared to LEU, this is due to the peak flattening associated with adding thorium to a fuel sphere. The thorium shifts the axial power profile down from the concentrated power region at the top of the core and in this way flattens the axial power profiles. A detailed discussion will be done in the DLOFC section of the report where the axial power profiles are discussed for different fuels, HM loadings and enrichments. The main focus on these tables are the values for energy produced per fuel sphere MWD/FS, this is also shown graphically in **Figure 17** and **Figure 18** and discussed further down.

Table 10 – Cumulative energy produced per fuel sphere, maximum kW per fuel sphere & power peaking maximum

LEU																
HEAVY METAL LOADING	g HM	5	5	5	7	7	7	10	10	10	12	12	12	16	16	16
FEED ENRICHMENT	wt%	8	10	15	8	10	15	8	10	15	8	10	15	8	10	15
POWER PEAKING MAX./AVG.		2.29	2.55	3.05	2.31	2.52	2.95	2.17	2.38	2.74	2.07	2.24	2.73	2.06	2.3	2.75
MAX. POWER PER FUEL SPHERE	KW/FS	1.5	1.67	1.99	1.52	1.65	1.93	1.42	1.56	1.79	1.36	1.47	1.79	1.36	1.51	1.81
ENERGY PRODUCED PER FUEL SPHERE	MWD/FS	0.308	0.424	0.695	0.459	0.621	0.994	0.596	0.809	1.292	0.630	0.860	1.384	0.617	0.864	1.437
WATT PER FUEL SPHERE	W/FS	656	655	654	656	656	655	657	656	656	657	657	657	658	658	657
ThLEU																
HEAVY METAL LOADING	g HM	5	5	5	7	7	7	10	10	10	12	12	12	16	16	16
FEED ENRICHMENT	wt%	8	10	15	8	10	15	8	10	15	8	10	15	8	10	15
POWER PEAKING MAX./AVG.		2.17	2.49	3.08	2.24	2.5	3.06	2.16	2.38	2.82	2.06	2.27	2.74	1.89	2.15	2.69
MAX. POWER PER FUEL SPHERE	KW/FS	1.42	1.63	2.02	1.47	1.64	2	1.41	1.56	1.85	1.35	1.49	1.8	1.24	1.41	1.77

ENERGY PRODUCED PER FUEL SPHERE	MWD/FS	0.291	0.414	0.689	0.462	0.633	1.007	0.690	0.923	1.386	0.806	1.065	1.544	0.916	1.203	1.674
WATT PER FUEL SPHERE	W/FS	657	656	654	657	656	655	657	657	656	658	657	657	658	658	657
ThHEU																
HEAVY METAL LOADING	g HM	5	5	5	7	7	7	10	10	10	12	12	12	16	16	16
FEED ENRICHMENT	wt%	8	10	15	8	10	15	8	10	15	8	10	15	8	10	15
POWER PEAKING MAX./AVG.		2.13	2.45	3.36	2.22	2.52	3.53	2.21	2.51	3.46	2.16	2.45	3.32	1.97	2.28	3.11
MAX. POWER PER FUEL SPHERE	KW/FS	1.39	1.6	2.19	1.46	1.65	2.31	1.45	1.64	2.26	1.41	1.6	2.17	1.29	1.49	2.04
ENERGY PRODUCED PER FUEL SPHERE	MWD/FS	0.285	0.411	0.686	0.469	0.646	1.032	0.744	1.003	1.554	0.918	1.230	1.890	1.206	1.628	2.489
WATT PER FUEL SPHERE	W/FS	657	657	655	657	656	654	657	656	655	658	657	655	658	657	656

Table 11 – Cumulative energy produced per fuel sphere, maximum kW per fuel sphere & power peaking maximum for 20 wt% LEU

LEU	Units:					
HEAVY METAL LOADING	g HM	5	7	10	12	16
FEED ENRICHMENT	wt%	20	20	20	20	20
POWER PEAKING MAX./AVG.		3.65	3.47	3.26	3.26	3.31
MAX. POWER PER FUEL SPHERE	KW/FS	2.38	2.27	2.14	2.14	2.17
ENERGY PRODUCED PER FUEL SPHERE	MWD/FS	0.949	1.343	1.738	1.873	1.996
WATT PER FUEL SPHERE	W/FS	653	654	655	656	657

** The MWD/FS is calculated by taking the MWD/T dividing by 10^6 (g/Ton) and multiplying this by the g HM to obtain MWD/FS (cumulative energy).

**The W/FS is calculated from the MWD multiplied by 10^6 (W/MW) divided by the fuel residence time.

** The power peaking Max/Ave is calculated from the kW/FS multiplied with 10^3 (W/kW) divided by W/FS. This confirms what VSOP has calculated.

The plots for cumulative heat energy produced per fuel sphere, over the life of the fuel sphere, are shown in **Figure 17** , **Figure 18** below for all fuels, as a function of heavy metal loading and enrichment respectively. It can be seen from the figures that the cumulative energy produced over the lifecycle of the fuel spheres are higher for the thorium based fuel for the same effective enrichment when compared to the LEU fuels. **However, adding Th to a fuel sphere by definition always reduces its effective enrichment and increases its HM loading.** For instance taking 10 g 20 wt% LEU and adding 6 g of Th in order to produce a 16 g HM ThLEU fuel sphere will by definition reduce its effective enrichment from 20 wt% to 12.5 wt%. So, if one wants to determine the effect of adding Th, comparing “apples with apples” will require that one compares the performance of the 10 g 20 wt% LEU to the resulting 16 g 12.5 wt% ThLEU fuel sphere. As can be inferred from **Figure 18**, a 16 g 12.5 wt% ThLEU fuel sphere would produce a cumulative energy of only 1.44 MWD/FS, compared to 1.74 MWD/FS for the 10 g 20 wt% LEU fuel sphere from which it was formed. **Adding the Th thus reduces the cumulative energy by 17%**.

It can clearly be seen that the ThHEU at 15 wt% fuel outperforms the LEU fuel at 20 wt% in terms of cumulative heat energy production for 12 g HM to 16 g HM as shown in **Figure 17** , this was explained further in the burn-up discussion. It is to be noted that the burn-up is multiplied by the heavy metal loading which leads to higher heavy metal loadings having higher cumulative energies. In **Figure 18** it can be seen that the general trend for the same fuel has the highest cumulative heat energy for the highest heavy metal loading being 16 g HM and 5 g HM being the lowest.

Due to proliferation problems associated with HEU only LEU and ThLEU are shown in **Figure 19** and **Figure 20**.

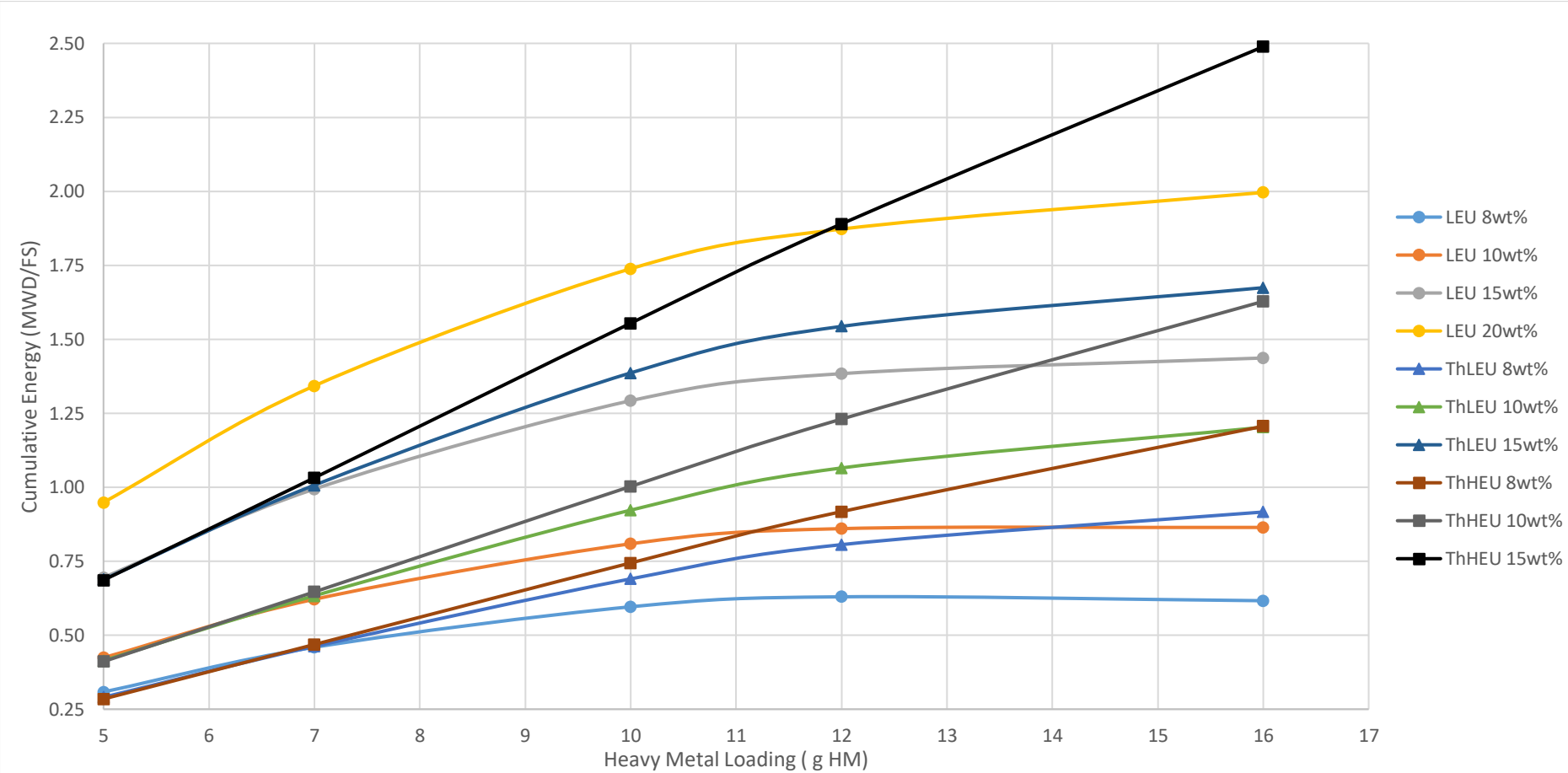

Figure 17 – Cumulative energy produced per fuel sphere for the various fuels, as a function of HM

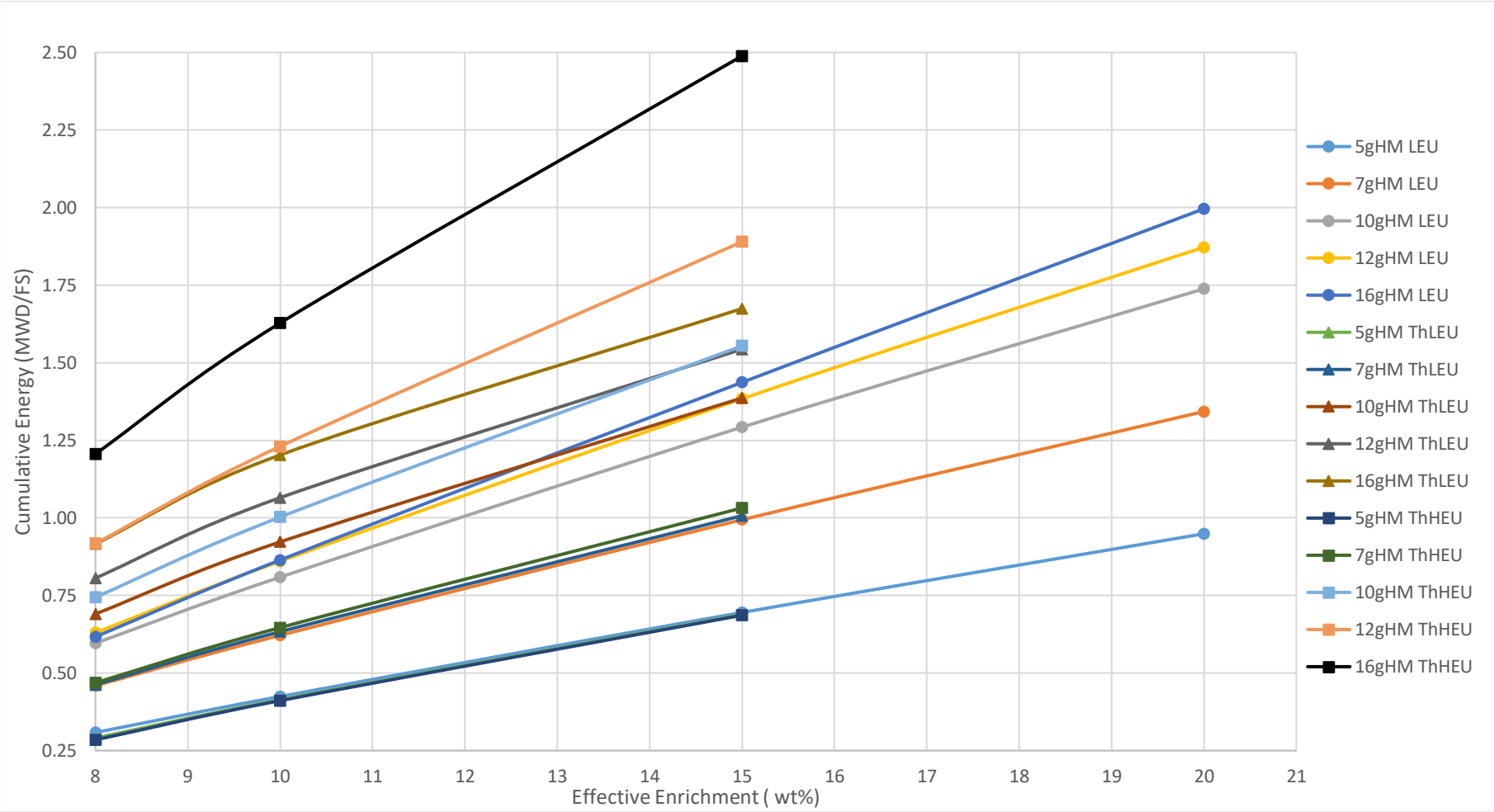

Figure 18 – Cumulative energy produced per fuel sphere for the various fuels based as a function of enrichment.

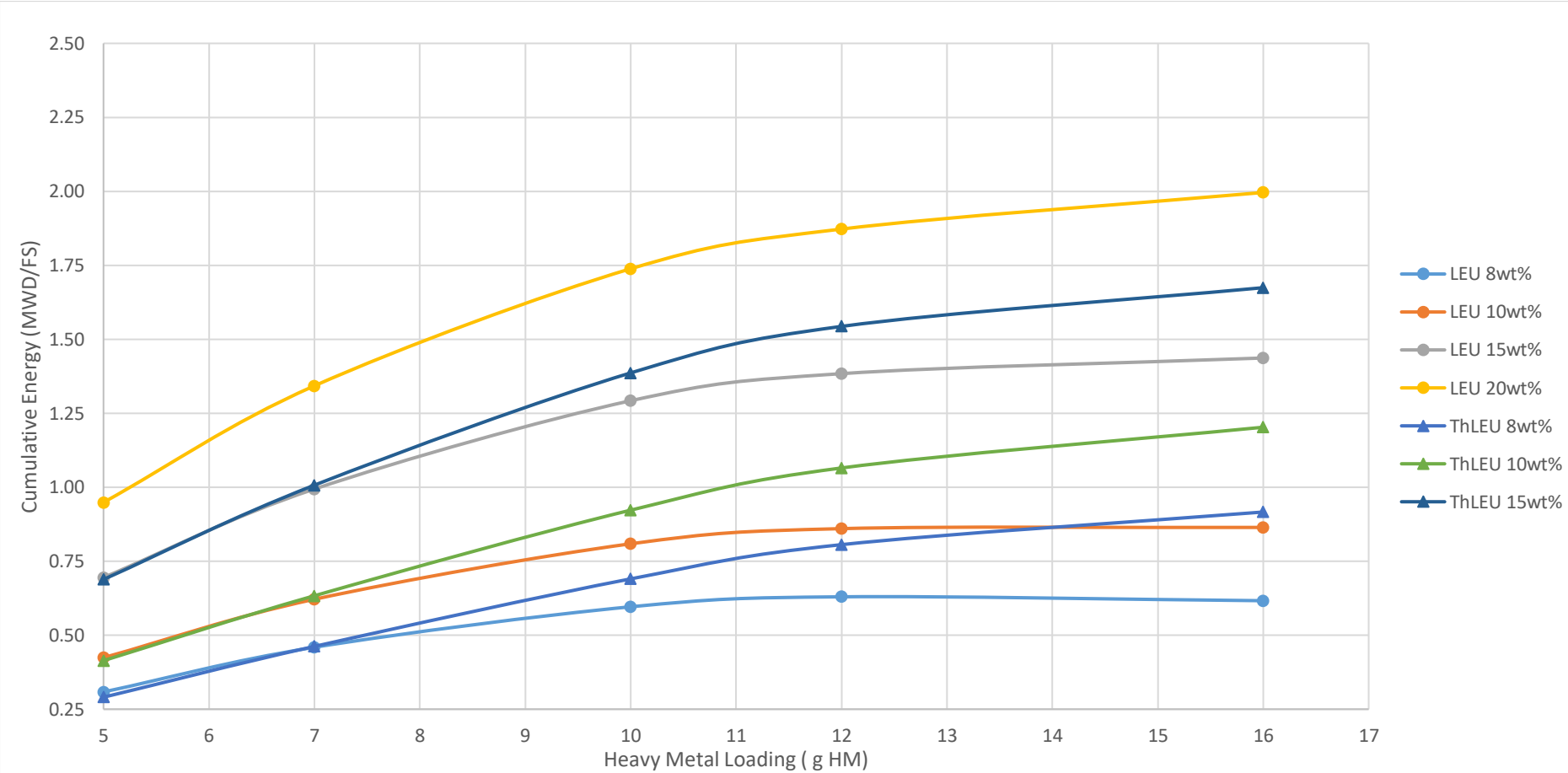

Figure 19 – Cumulative energy produced per fuel sphere for the LEU and ThLEU as a function of HM

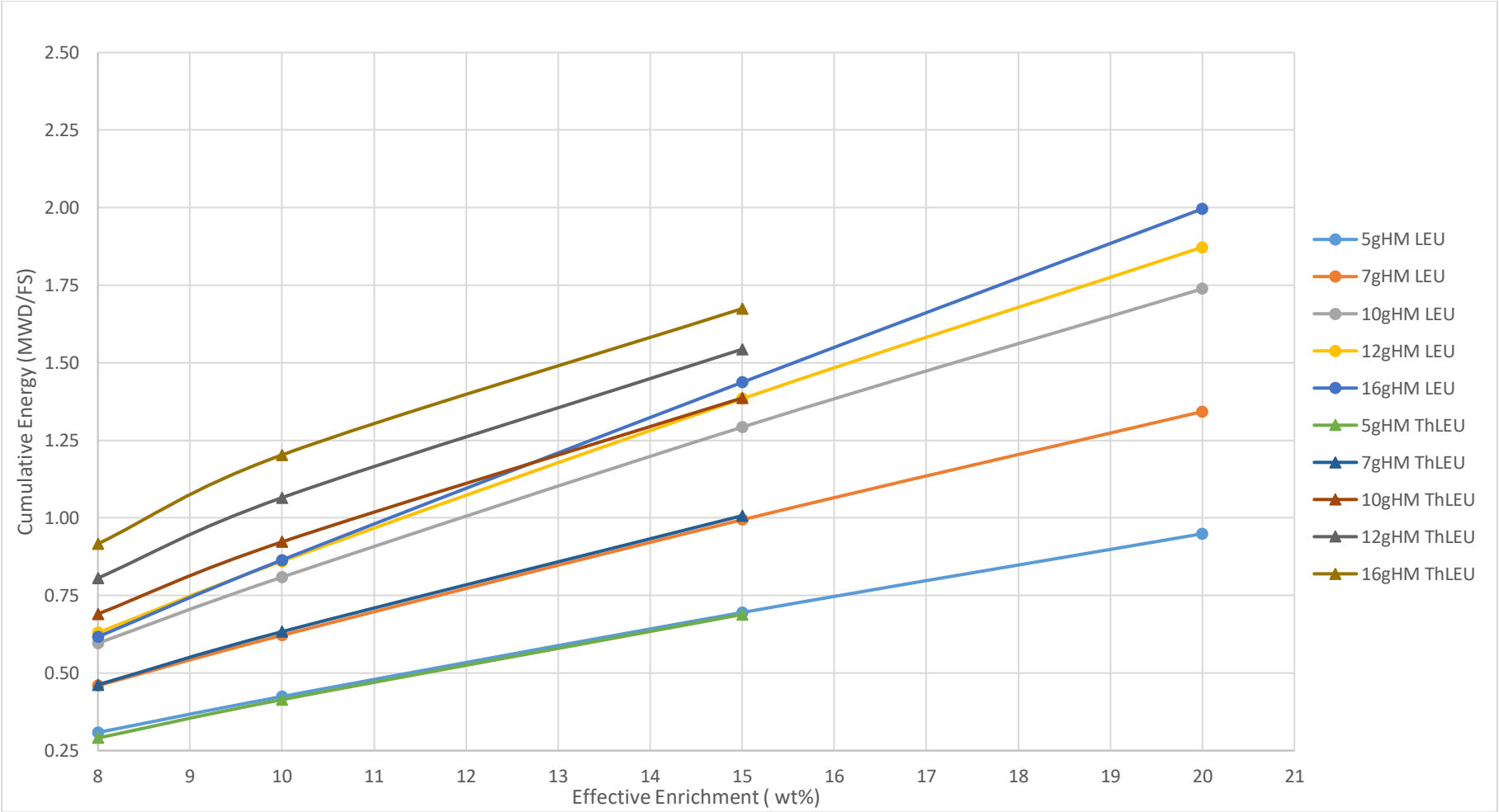

Figure 20 – Cumulative energy produced per fuel sphere for LEU and ThLEU based as a function of enrichment

Table 12 – Conversion ratio, source neutron/fissile absorption & capture/fission in fissile material

LEU																
HEAVY METAL LOADING	g HM	5	5	5	7	7	7	10	10	10	12	12	12	16	16	16
FEED ENRICHMENT	wt%	8	10	15	8	10	15	8	10	15	8	10	15	8	10	15
CONVERSION RATIO	CR	0.353	0.344	0.324	0.417	0.405	0.381	0.482	0.466	0.434	0.509	0.491	0.456	0.545	0.524	0.482
SOURCE NEUTR./FISSILE ABS.	ηε	1.985	1.982	1.978	1.969	1.966	1.959	1.951	1.945	1.933	1.942	1.934	1.919	1.929	1.917	1.894
CAPTURE/FISSION IN FISS.MAT.	α	0.28	0.28	0.279	0.303	0.304	0.305	0.324	0.328	0.333	0.331	0.337	0.345	0.336	0.346	0.36
ThLEU																
HEAVY METAL LOADING	g HM	5	5	5	7	7	7	10	10	10	12	12	12	16	16	16
FEED ENRICHMENT	wt%	8	10	15	8	10	15	8	10	15	8	10	15	8	10	15
CONVERSION RATIO	CR	0.353	0.337	0.314	0.414	0.395	0.369	0.476	0.455	0.423	0.506	0.483	0.447	0.549	0.523	0.478
SOURCE NEUTR./FISSILE ABS.	ηε	2.036	2.027	2	2.03	2.017	1.984	2.018	2.002	1.96	2.01	1.991	1.945	1.99	1.968	1.918

ThHEU																
HEAVY METAL LOADING	g HM	5	5	5	7	7	7	10	10	10	12	12	12	16	16	16
FEED ENRICHMENT	wt%	8	10	15	8	10	15	8	10	15	8	10	15	8	10	15
CONVERSION RATIO	CR	0.349	0.324	0.277	0.406	0.377	0.321	0.466	0.433	0.369	0.496	0.461	0.393	0.542	0.504	0.431
SOURCE NEUTR./FISSILE ABS.	ηε	2.069	2.071	2.065	2.074	2.073	2.063	2.075	2.072	2.056	2.072	2.068	2.049	2.061	2.055	2.032
CAPTURE/FISSION IN FISS.MAT.	α	0.177	0.174	0.171	0.176	0.174	0.174	0.178	0.177	0.181	0.181	0.182	0.188	0.19	0.193	0.203

The conversion ratios, source neutrons per fissile absorption and capture to fission ratios are briefly discussed but are not important drivers in terms increasing the cumulative energy or reducing the cost per kWh so not much attention is given to them. As can be seen in **Table 12** and **Table 13** the source neutrons per fissile absorption are higher for the thorium based fuels due to the fact that thorium produces U-233 which has the highest thermal and epithermal reproduction factor of all known fuels that is why these values are higher. (This is much higher for plutonium, provided that it is irradiated by fast neutrons.)

Table 13 – Conversion ratio, source neutron/fissile absorption & capture/fission in fissile material for 20 wt% LEU

LEU	Units:					
HEAVY METAL LOADING	g HM	5	7	10	12	16
FEED ENRICHMENT	wt%	20	20	20	20	20
CONVERSION RATIO	CR	0.304	0.357	0.405	0.423	0.444
SOURCE NEUTR./FISSILE ABS.	ηε	1.975	1.953	1.923	1.905	1.876
CAPTURE/FISSION IN FISS.MAT.	α	0.276	0.304	0.335	0.35	0.369

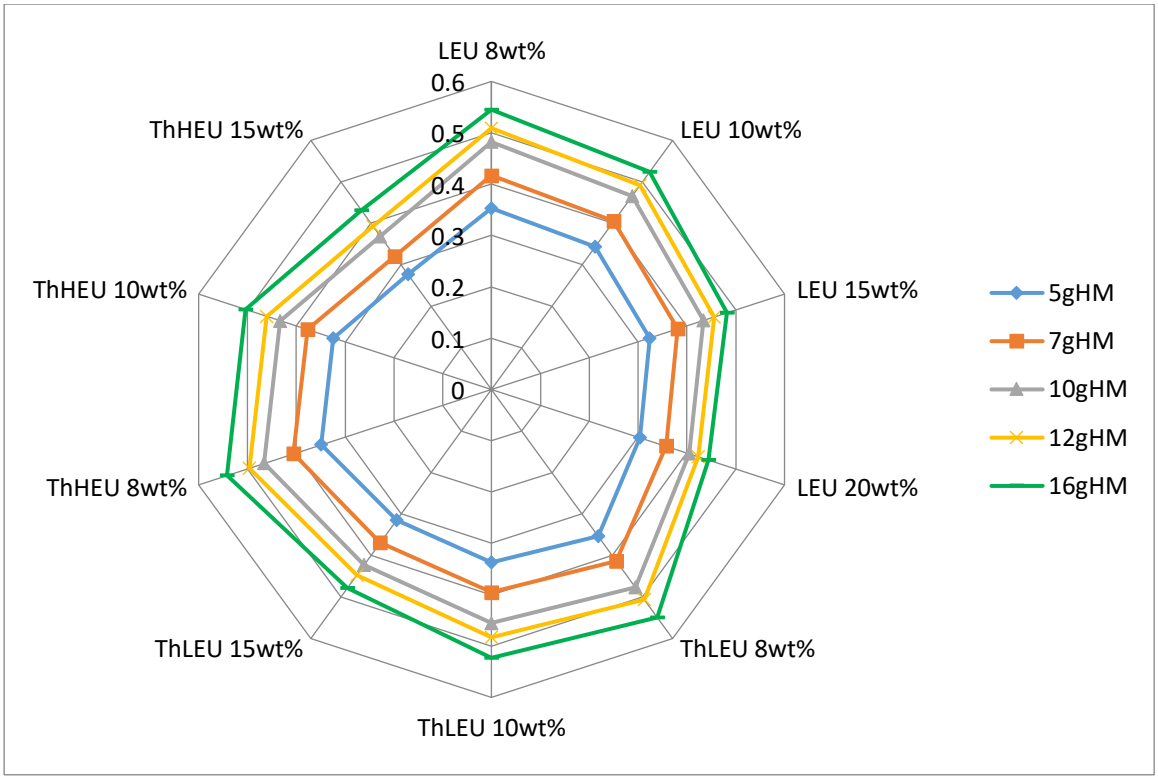

Figure 21 – Conversion ratio for various fuels

As can be seen in **Figure 21** the conversion ratio (CR) clearly increases for the increased heavy metal loading for all the cases. The conversion ratio has relatively little economic value and is, in these cases, inversely related to the enrichment and thus to the burn-up, which explains why increasing the conversion ratio does not reduce the fuel cost and therefore does not improve the profitability.

4.1.2 Detailed neutronic discussion for LEU, ThLEU and ThHEU for the same burn-up and HM loading.

The neutronic results will be focused on the same burn-up for a 10 g HM loading for all 3 fuel types. The reason for comparing the three fuels in terms of the same burn-up is to see how the neutronics is influenced.

In order to understand the neutronics it is important to understand how the 3 different fuels are broken down into their respective mass fraction as shown in **Table 14** .

Table 14 – Mass fractions of uranium and thorium in a 10 g HM, equal burn-up fuel sphere

		LEU	ThLEU	ThHEU
HEAVY METAL LOADING	g	10.00	10.00	10.00
EFFECTIVE ENRICHMENT	wt%	10.00	9.00	8.50
235U ENRICHMENT	%	10.00	20.00	93.00
235U MASS/ FS	g	1.00	0.90	0.85
238U MASS/ FS	g	9.00	3.60	0.06
232Th MASS/ FS	g	0.00	5.50	9.09
MASS U/ FS	g	10.00	4.50	0.91
Th/U RATIO		0.00	1.22	9.94
MASS UO2/ FS	g	11.35	5.11	1.04
MASS ThO2/ FS	g	0.00	6.26	10.34
MASS (ThU)O2/ FS	g	11.35	11.36	11.38
(Th,U)O2 / HM RATIO		1.135	1.136	1.138

As can be seen from **Table 14** the fractions of the U-235, U-238 and Th-232 vary for the 3 fuel types, LEU, ThLEU and ThHEU. The U-235 fissile mass fraction per fuel sphere varies for the 3 different fuel types for the same HM loading. This compares fuel spheres with different masses for the fissile fraction of U-235 and thus the results

will not be comparing the fuels on the same basis. LEU contains (1g U-235,10 wt%), ThLEU (0.9g U-235, 9 wt%) and ThHEU (0.85g U-235, 8.5 wt%). However, the neutronic effects can now be discussed based on the same burn-up and HM loading.

Table 15 – Global neutronic data for 10 g HM, equal burn-up fuel sphere

	Units:	LEU	ThLEU	ThHEU
HEAVY METAL LOADING	g HM	10	10	10
FEED ENRICHMENT	wt%	10	9	8.5
AVG. FISSILE ENRICHMENT	%	5.95	5.02	4.58
AVG. FUEL RESIDENCE TIME	DAYS	1232.3	1234.1	1236.4
AVG. BURN-UP	MWD/T	80898	81065	81236.5
PEBBLE FEED RATE	SPHERES/DAY	123.61	123.36	123.10
KEFF		1.0000	1.0000	1.0000
FISSIONS/ENERGY	E+10 (FISS/WS)	3.07	3.073	3.103
POWER PEAKING MAX./AVG.		2.38	2.29	2.3
MAX. POWER PER FUEL SPHERE	KW/FS	1.56	1.5	1.51
CONVERSION RATIO	CR	0.466	0.465	0.457
SOURCE NEUTR./FISSILE ABS.	ηε	1.945	2.01	2.075
CAPTURE/FISSION IN FISS.MAT.	α	0.328	0.249	0.177
FAST DOSIS SPENT FUEL ELEM.	E+21/CM2	2.89	2.87	2.84

As can be seen in **Table 15** above the average burn-up is roughly equal with the same average fuel residence time for the 3 fuels. Something to be taken into consideration is that LEU has an advantage due to the fact that the mass fraction of U-235 is higher and thus the feed enrichment 10 wt% and average fissile enrichment is higher for the same burn-up when compared to the other fuels, that is why LEU has a higher power peaking value and thus a higher kW per fuel sphere. As thorium is added the neutron reproduction rate, highest fission yield per neutron absorbed and thus the source

neutron per fissile absorption increases for the thorium based fuels as U-233 is created. LEU being (1.945), ThLEU (2.01) and ThHEU (2.075).

The captures per fission in the fissile material as captures-to-fissions only occur in the fissile isotopes of U-235 Pu-239, Pu-241 and U-233. It is highest for LEU due to a higher mass of U-235, followed by ThLEU and ThHEU due to lower U-235 masses and low production of U-233 due to low Th HM loadings. Thorium is only viable at higher HM loadings.

Table 16 – Neutron losses in heavy metals for 10 g HM, equal burn-up fuel sphere

		LEU	ThLEU	ThHEU
NEUTRONS LOST IN HEAVY METALS ESP.	%			
NEUTRON LOSSES IN HEAVY METALS	%	76.48	74.33	72.07
ESP. IN FISSILE ISOTOPES	%	51.4	49.74	48.2
ESP. IN TH-232	%		12.02	21.81
ESP. IN PA-233	%		0.25	0.47
ESP. IN U -233	%		6.02	12.26
ESP. IN U -234	%	0.15	0.26	0.41
ESP. IN U -235	%	32.53	34.12	35.64
ESP. IN U -236	%	0.51	0.55	0.6
ESP. IN U -237	%			
ESP. IN U -238	%	19.86	8.96	0.22
ESP. IN NP-237	%	0.14	0.17	0.21
ESP. IN NP-239	%	0.03	0.01	
ESP. IN PU-238	%	0.02	0.04	0.06
ESP. IN PU-239	%	16.19	7.92	0.25
ESP. IN PU-240	%	4.18	2.22	0.07
ESP. IN PU-241	%	2.68	1.68	0.06
ESP. IN PU-242	%	0.1	0.05	
ESP. IN AM-241	%	0.05	0.03	
ESP. IN AM-242M	%			
ESP. IN AM-243	%	0.02	0.01	
IN FISSION PRODUCTS	%	6.2	6.92	7.45
ESP. IN XE-135	%	1.89	2.05	2.15
CORE-LEAKAGE	%	15.7	16.58	17.77

Table 16 shows the higher fraction of neutrons lost in Th-232 in the ThHEU fuel leads to greater U-233 yields. More neutrons are lost in Xe-135 for the thorium-based fuels.

Table 17 shows the fractional neutrons produced by the three fuels. As can be seen the fraction of neutrons produced by U-233 for the ThHEU is far higher than the other fuels. This ThHEU fuel also discharges more U-233 seen in Table 18.

Table 17 – Fractional neutrons produced by 10 g HM, equal burn-up fuel sphere

		LEU	ThLEU	ThHEU
FRACTIONAL NEUTRONS PRODUCED BY	%			
TH - 232	%		0.05	0.09
U - 233	%		13.43	27.44
U -234	%			
U -235	%	64.76	68.48	71.85
U -236	%	0.02	0.02	0.03
U -238	%	0.44	0.18	
NP - 238	%			
PU - 238	%			
PU-239	%	29.03	14.22	0.45
PU-240	%	0.01		
PU-241	%	5.71	3.57	0.12
AM-242M	%	0.02	0.01	

Table 18 also shows that the plutonium discharge from the ThHEU fuel is significantly less than that from the other fuel cycles and therefore limits the risks regarding proliferation associated with Pu-239. The ThLEU fuel also produces less Pu-239 compared to the LEU fuel.

Table 18 – Fuel supply and discharge of 10 g HM, equal burn-up fuel

		LEU		ThLEU		ThHEU	
FUEL SUPPLY - DISCHARGE		Supply	Discharge	Supply	Discharge	Supply	Discharge
TH-232	KG/GWD(TH)			6.698	6.3894	11.0965	10.5448
U -233	KG/GWD(TH)			0.0000	0.1477	0.0000	0.2294
U -234	KG/GWD(TH)	0.0121	0.0081	0.0112	0.0211	0.0116	0.0337
U -235	KG/GWD(TH)	1.2344	0.3791	1.1102	0.2294	1.0551	0.1523
U -236	KG/GWD(TH)	0.0000	0.1446	0.0000	0.1428	0.0000	0.1429
U -238	KG/GWD(TH)	11.0975	10.5663	4.4864	4.2504	0.1069	0.1013
NP-237	KG/GWD(TH)	0.0000	0.0097	0.0000	0.0096	0.0000	0.0096
PU-238	KG/GWD(TH)	0.0000	0.0036	0.0000	0.0037	0.0000	0.0037
PU-239	KG/GWD(TH)	0.0000	0.0947	0.0000	0.0265	0.0000	0.0008
PU-240	KG/GWD(TH)	0.0000	0.0520	0.0000	0.0204	0.0000	0.0006
PU-241	KG/GWD(TH)	0.0000	0.0347	0.0000	0.0122	0.0000	0.0003
PU-242	KG/GWD(TH)	0.0000	0.0178	0.0000	0.0113	0.0000	0.0004
AM-241	KG/GWD(TH)	0.0000	0.0043	0.0000	0.0014	0.0000	
AM-242M	KG/GWD(TH)						
AM-243	KG/GWD(TH)	0.0000	0.0022	0.0000	0.001	0.0000	
CM-244	KG/GWD(TH)	0.0000	0.0005	0.0000	0.0003	0.0000	

Table 18 shows that less U-235 is discharged for the thorium based fuels, meaning that the thorium fuels utilise it better, less U-235 is also needed as U-233 is formed.

4.1.3 LEU 20 wt% compared to ThLEU 10 wt% effective enrichment as well as a ThHEU 10 wt% effective enrichment.

The neutronic results discussed below will focus on a 10 g HM loading for the U-235 content being enriched to 20 wt%. This would be comparing the mass of (1g) of U-235 for the ThLEU and ThHEU cases but will however be comparing (2g) of U-235 for the LEU case.

In order to understand the neutronics it is important to understand how the 3 different fuels are broken down into their respective mass fraction as shown in **Table 19**.

Table 19 – Mass fractions of 20 wt% LEU, ThLEU 10 wt% effective & ThHEU 10 wt% effective.

		LEU	ThLEU	ThHEU
HEAVY METAL LOADING	g	10.00	10.00	10.00
EFFECTIVE ENRICHMENT	wt%	20.00	10.00	10.00
235U ENRICHMENT	%	20.00	20.00	93.00
235U MASS/ FS	g	2.00	1.00	1.00
238U MASS/ FS	g	8.00	4.00	0.08
232Th MASS/ FS	g	0.00	5.00	8.92
MASS U/ FS	g	10.00	5.00	1.08
Th/U RATIO		0.00	1.00	8.30
MASS UO2/ FS	g	11.35	5.67	1.22
MASS ThO2/ FS	g	0.00	5.69	10.16
MASS (ThU)O2/FS	g	11.35	11.36	11.38
(Th,U)O2 / HM RATIO		1.135	1.136	1.138

As can be seen from **Table 19** the mass fraction of U-235 is higher for the LEU case, this should lead to improved results such as higher burn-ups and increased residence times. Adding Thorium decreases the enrichment in the following cases and LEU should outperform the thorium based fuels.

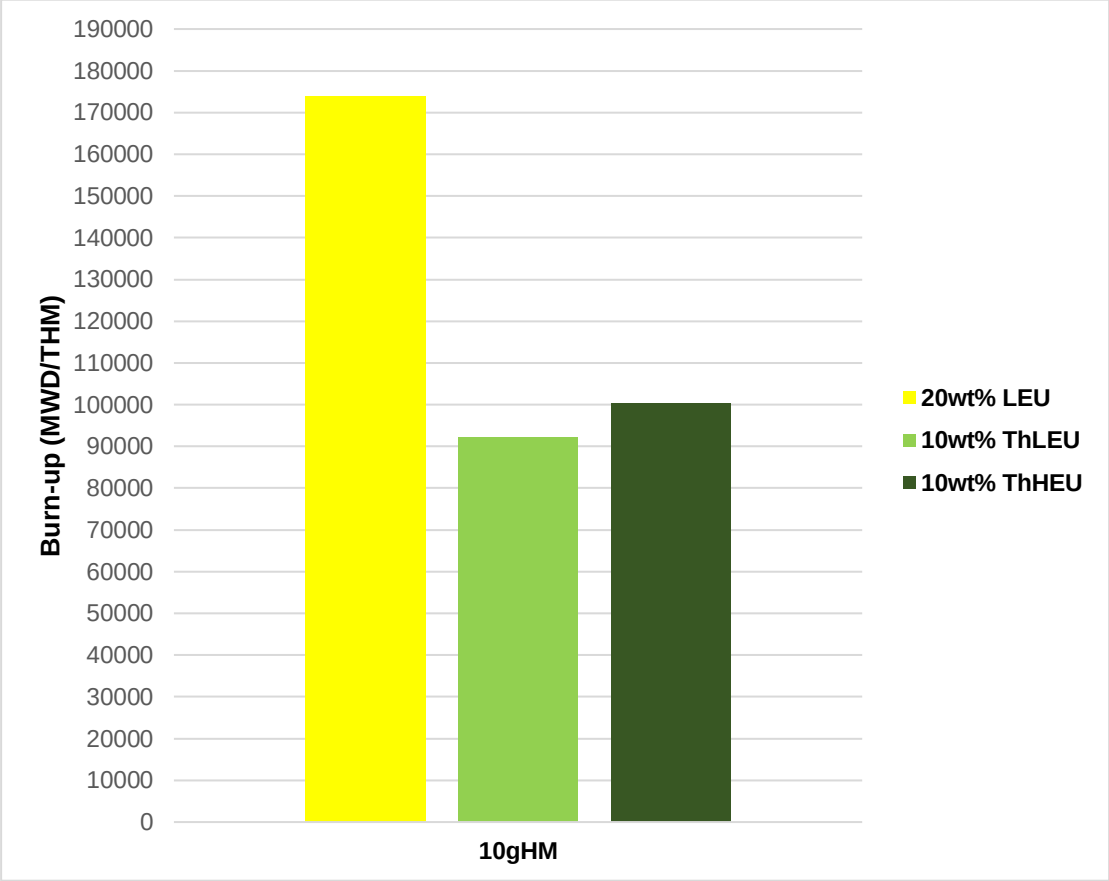

Figure 22 – Burn-up comparison for 10 g HM at various enrichments for LEU, ThLEU & ThHEU

Figure 22 compares a 10 g HM loading for the 3 fuels shown above. The LEU would outperform the thorium-based fuels with regards to burn-up and extended residence times due to the fact that this fuel contains more U-235 (2g) compared to the thorium fuels containing (1g) each. Due to the high burn-ups, the extremely long residence time and high fluence would be seen by the 20wt% LEU fuel due to the high enrichment. The dpa (displacement per atom) would be high and the fuel would fail due to irradiation damage.

Table 20 – Global neutronic data for 10 g HM for 20 wt% LEU, ThLEU 10 wt% effective & ThHEU 10 wt% effective.

	Units:	LEU	ThLEU	ThHEU
HEAVY METAL LOADING	g HM	10	10	10
FEED ENRICHMENT	wt%	20	10	10
AVG. FISSILE ENRICHMENT	%	9.68	5.3	4.8
AVG. FUEL RESIDENCE TIME	DAYS	2652.2	1405.1	1527.5
AVG. BURN-UP	MWD/T	173837	92259.7	100267.2
PEBBLE FEED RATE	SPHERES/DAY	58	108	100
KEFF		1.0000	0.9999	1.0000
FISSIONS/ENERGY	E+10 (FISS/WS)	3.045	3.07	3.103
POWER PEAKING MAX/AVG.		3.26	2.38	2.51
MAX POWER PER FUEL SPHERE	KW/ FS	2.14	1.56	1.64
CONVERSION RATIO	CR	0.405	0.455	0.433
SOURCE NEUTR./FISSILE ABS.	ηε	1.923	2.002	2.072
CAPTURE/FISSION IN FISS.MAT.	α	0.335	0.257	0.177
FAST DOSIS SPENT FUEL ELEM.	E+21/CM2	6.12	3.27	3.49

The global data in Table 20 shows that the residence time increases as the enrichment is increased, or as more U-235 is added to a fuel sphere. This is why LEU outperforms the other fuels as the U-235 content is higher, (2g) U-235 compared to (1g) U-235 for the thorium cases. This in turn increases the burn-up and the amount of energy that can be extracted from a fuel sphere. These factors decrease the amount of fuel spheres that need to be supplied to the reactor daily.

U-233 has a reproduction factor of 2.29 compared to 2.05 for U-235 and 1.8 for Pu-239. This can be seen by the source neutron per fissile absorption shown in **Table 20** with LEU being (1.923), ThLEU (2.002) and ThHEU (2.072). This shows that the U-233 formed in the thorium fuels still produces more neutrons per collision.

Table 21 – Neutron losses in heavy metals for 20 wt% LEU, ThLEU 10 wt% effective & ThHEU 10 wt% effective.

		LEU	ThLEU	ThHEU
NEUTRON LOSSES IN HEAVY METALS	%	75.27	74.24	71.21
ESP. IN FISSILE ISOTOPES	%	52	49.95	48.27
ESP. IN TH-232	%		10.52	20.51
ESP. IN PA-233	%		0.22	0.47
ESP. IN U -233	%		5.49	12.54
ESP. IN U -234	%	0.22	0.27	0.47
ESP. IN U -235	%	34.35	33.84	35.34
ESP. IN U -236	%	1.11	0.62	0.73
ESP. IN U -237	%			
ESP. IN U -238	%	16.55	9.75	0.26
ESP. IN NP-237	%	0.44	0.21	0.3
ESP. IN NP-239	%	0.02	0.02	
ESP. IN PU-238	%	0.11	0.05	0.1
ESP. IN PU-239	%	14.41	8.69	0.31
ESP. IN PU-240	%	4.46	2.51	0.09
ESP. IN PU-241	%	3.24	1.93	0.07
ESP. IN PU-242	%	0.16	0.06	
ESP. IN AM-241	%	0.12	0.04	
ESP. IN AM-242M	%	0.01		
ESP. IN AM-243	%	0.06	0.02	
IN FISSION PRODUCTS	%	8.01	7.23	8.2
ESP. IN XE-135	%	1.63	2.02	2.14
CORE-LEAKAGE	%	15.7	16.54	18.08

Table 21 shows the higher fraction of neutrons lost in the thorium fuels. More neutrons are lost in Xe-135 for the thorium based fuels.

Table 22 shows the fractional neutrons produced by fissions in the three fissile fuels. It can be seen that Pu-239 plays more of a significant role in the LEU fuel.

Table 22 – Fractional neutrons produced by 10 g HM for 20 wt% LEU, ThLEU 10 wt% effective & ThHEU 10 wt% effective.

		LEU	ThLEU	ThHEU
FRACTIONAL NEUTRONS PRODUCED BY	%			
TH - 232	%		0.05	0.09
U - 233	%		12.24	28.06
U -234	%			
U -235	%	66.86	67.74	71.07
U -236	%	0.05	0.03	0.03
U -238	%	0.38	0.2	
NP - 238	%			0.01
PU - 238	%	0.02		0.01
PU-239	%	25.72	15.6	0.56
PU-240	%	0.02		
PU-241	%	6.89	4.11	0.16
AM-242M	%	0.04	0.01	

Table 23also shows that the plutonium discharge from the ThHEU fuel is significantly less than that from the other fuel cycles and therefore limits the risks regarding proliferation associated with Pu-239.

Table 23 – Fuel supply and discharge of 10 g HM for 20 wt% LEU, ThLEU 10 wt% effective & ThHEU 10 wt% effective.

		LEU		ThLEU		ThHEU	
FUEL SUPPLY - DISCHARGE		Supply	Discharge	Supply	Discharge	Supply	Discharge
TH-232	KG/GWD(TH)			5.3426	5.0719	8.8145	8.2956
U -233	KG/GWD(TH)			0.0000	0.1238	0.0000	0.1896
U -234	KG/GWD(TH)	0.0116	0.0063	0.0109	0.0194	0.0111	0.0326
U -235	KG/GWD(TH)	1.147	0.2489	1.0824	0.2077	1.0045	0.1113
U -236	KG/GWD(TH)	0.0000	0.1534	0.0000	0.1418	0.0000	0.1400
U -238	KG/GWD(TH)	4.5761	4.1353	4.3737	4.1167	0.1018	0.0953
NP-237	KG/GWD(TH)	0.0000	0.0171	0.0000	0.0104	0.0000	0.0107
PU-238	KG/GWD(TH)	0.0000	0.0103	0.0000	0.0044	0.0000	0.0049
PU-239	KG/GWD(TH)	0.0000	0.0564	0.0000	0.0271	0.0000	0.0009
PU-240	KG/GWD(TH)	0.0000	0.0274	0.0000	0.0205	0.0000	0.0007
PU-241	KG/GWD(TH)	0.0000	0.024	0.0000	0.0127	0.0000	0.0004
PU-242	KG/GWD(TH)	0.0000	0.0204	0.0000	0.0129	0.0000	0.0005
AM-241	KG/GWD(TH)	0.0000	0.0055	0.0000	0.0016	0.0000	
AM-242M	KG/GWD(TH)						
AM-243	KG/GWD(TH)	0.0000	0.0029	0.0000	0.0013	0.0000	
CM-244	KG/GWD(TH)	0.0000	0.0012	0.0000	0.0004	0.0000	

4.1.4 Comparing cases for fuels which can be realised, LEU 20 wt%, 10 g HM compared to ThLEU 16.66 wt% effective enrichment 12 g HM.

The neutronic results discussed below will focus on high burn-up cases which can be realised; this is why ThHEU will not be discussed. A 10 g HM loading 20 wt% LEU fuel (2g) of U-235 will be compared to a ThLEU fuel at 12 g HM and 16.66 wt% (2g) U-235. This will be done in order to determine what the effects are of adding thorium to a 20 wt% LEU fuel sphere. Adding 2g of thorium increases the HM loading and decreases the enrichment.

In order to understand the neutronics it is important to understand how the different fuels are broken down into their respective mass fractions as shown in **Table 24**.

Table 24 – Mass fractions of LEU 20 wt%, 10 g HM compared to ThLEU 16.66 wt% effective enrichment 12 g HM.

		LEU	ThLEU
HEAVY METAL LOADING	g	10.00	12.00
EFFECTIVE ENRICHMENT	wt%	20.00	16.66
235U ENRICHMENT	%	20.00	20.00
235U MASS/ FS	g	2.00	2.00
238U MASS/ FS	g	8.00	8.00
232Th MASS/ FS	g	0.00	2.00
MASS U/ FS	g	10.00	10.00
Th/U RATIO		0.00	0.20
MASS UO2/ FS	g	11.35	11.34
MASS ThO2/ FS	g	0.00	2.28
MASS (ThU)O2/ FS	g	11.35	13.62
(Th,U)O2 / HM RATIO		1.135	1.135

As can be seen from **Table 24** the total mass of U-235 is the same for both cases. Adding thorium decreases the enrichment and increases the HM content.

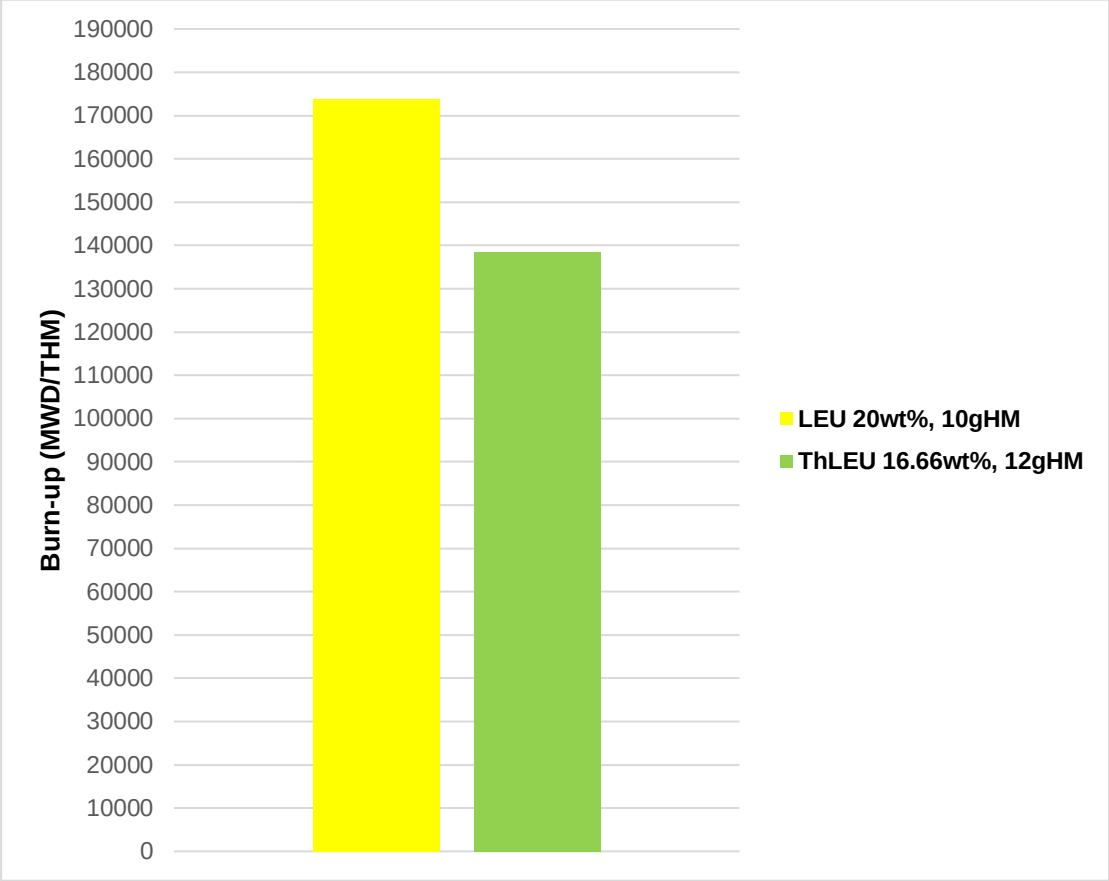

Figure 23 – Burn-up comparison for LEU 20 wt%, 10 g HM compared to ThLEU 16.66 wt% effective enrichment 12 g HM.

Figure 23 compares the 2 fuels shown above. The LEU would outperform the thorium-based fuel with regards to burn-up and extended residence times due to the fact that the thorium reduces the effective enrichment while creating a higher HM content. Both fuels are compared on the same U-235 mass being (2g). Due to the high burn-ups, extremely long residence time and high fluence would be seen by the 20wt% LEU fuel, due to the high enrichment. The dpa (displacement per atom) would be high and the fuel would fail due to irradiation damage.

Table 25 – Global neutronic data for LEU 20 wt%, 10 g HM compared to ThLEU 16.66 wt% effective enrichment 12 g HM.

	Units:	LEU	ThLEU
HEAVY METAL LOADING	g HM	10	12
FEED ENRICHMENT	wt%	20	16.66
AVG. FISSILE ENRICHMENT	%	9.68	9.04
AVG. FUEL RESIDENCE TIME	DAYS	2652.2	2350.8
AVG. BURN-UP	MWD/T	173837	138453
PEBBLE FEED RATE	SPHERES/DAY	58	60
KEFF		1.0000	1.0000
FISSIONS/ENERGY	E+10 (FISS/WS)	3.045	3.052
POWER PEAKING MAX/AVG.		3.26	2.92
MAX POWER PER FUEL SPHERE	KW/ FS	2.14	1.92
CONVERSION RATIO	CR	0.405	0.439
SOURCE NEUTR./FISSILE ABS.	ηε	1.923	1.931
CAPTURE/FISSION IN FISS.MAT.	α	0.335	0.326
FAST DOSIS SPENT FUEL ELEM.	E+21/CM2	6.12	5.83

The global data in **Table 25** shows that the residence time and burn-up are higher for the LEU fuel not being mixed with Thorium. LEU outperforms ThLEU even though the U-235 (2g) is the same for both cases the effective/overall enrichment is lower when thorium is added to uranium.

The capture-to-fission (in the fissile material) is higher in the case which has a higher U-235 content that being the 20 wt% feed enrichment in the LEU fuel compared to the 16.66 wt% in the thorium based fuel. The U-233 is also a fissile fuel, however small amounts are created.

Table 26 – Neutron losses in heavy metals for LEU 20 wt%, 10 g HM compared to ThLEU 16.66 wt% effective enrichment 12 g HM.

		LEU	ThLEU
NEUTRON LOSSES IN HEAVY METALS	%	75.27	76.6
ESP. IN FISSILE ISOTOPES	%	52	51.77
ESP. IN TH-232	%		3.13
ESP. IN PA-233	%		0.06
ESP. IN U -233	%		1.59
ESP. IN U -234	%	0.22	0.25
ESP. IN U -235	%	34.35	34.24
ESP. IN U -236	%	1.11	1.03
ESP. IN U -237	%		
ESP. IN U -238	%	16.55	15.57
ESP. IN NP-237	%	0.44	0.38
ESP. IN NP-239	%	0.02	0.02
ESP. IN PU-238	%	0.11	0.08
ESP. IN PU-239	%	14.41	13.18
ESP. IN PU-240	%	4.46	4
ESP. IN PU-241	%	3.24	2.76
ESP. IN PU-242	%	0.16	0.12
ESP. IN AM-241	%	0.12	0.1
ESP. IN AM-242M	%	0.01	0.01
ESP. IN AM-243	%	0.06	0.04
IN FISSION PRODUCTS	%	8.01	7.41
ESP. IN XE-135	%	1.63	1.55
CORE-LEAKAGE	%	15.7	14.98

Table 26 shows the higher fraction of neutrons lost in the ThLEU fuel. More neutrons are lost in Xe-135 for LEU fuel.

The **Table 27** shows that the majority of the fissions originate from U-235 and Pu-239 showing that thorium is just a spectator in small quantities/ low HM loadings such as this case. The thorium mass should be increased and should replace the U-238 to have any real effect of obtaining a contribution from U-233.

Table 27 – Fractional neutrons produced by LEU 20 wt%, 10 g HM compared to ThLEU 16.66 wt% effective enrichment 12 g HM.

		LEU	ThLEU
FRACTIONAL NEUTRONS PRODUCED BY	%		
TH - 232	%		0.02
U - 233	%		3.5
U -234	%		
U -235	%	66.86	66.57
U -236	%	0.05	0.05
U -238	%	0.38	0.38
NP - 238	%		
PU - 238	%	0.02	0.01
PU-239	%	25.72	23.52
PU-240	%	0.02	0.01
PU-241	%	6.89	5.87
AM-242M	%	0.04	0.04

Table 28 – Fuel supply and discharge of LEU 20 wt%, 10 g HM compared to ThLEU 16.66 wt% effective enrichment 12 g HM.

		LEU		ThLEU	
FUEL SUPPLY - DISCHARGE		Supply	Discharge	Supply	Discharge
TH-232	KG/GWD(TH)			1.1805	1.0992
U -233	KG/GWD(TH)			0.0000	0.0385
U -234	KG/GWD(TH)	0.0116	0.0063	0.012	0.0107
U -235	KG/GWD(TH)	1.147	0.2489	1.1929	0.2997
U -236	KG/GWD(TH)	0.0000	0.1534	0.0000	0.1556
U -238	KG/GWD(TH)	4.5761	4.1353	4.8204	4.4063
NP-237	KG/GWD(TH)	0.0000	0.0171	0.0000	0.0167
PU-238	KG/GWD(TH)	0.0000	0.0103	0.0000	0.0093
PU-239	KG/GWD(TH)	0.0000	0.0564	0.0000	0.0623
PU-240	KG/GWD(TH)	0.0000	0.0274	0.0000	0.027
PU-241	KG/GWD(TH)	0.0000	0.024	0.0000	0.0251
PU-242	KG/GWD(TH)	0.0000	0.0204	0.0000	0.0178
AM-241	KG/GWD(TH)	0.0000	0.0055	0.0000	0.0054
AM-242M	KG/GWD(TH)			0.0000	
AM-243	KG/GWD(TH)	0.0000	0.0029	0.0000	0.0023
CM-244	KG/GWD(TH)	0.0000	0.0012	0.0000	0.0008

This data clearly demonstrates the dilemma of Th-based fuels:

Of the fertile fuels in the fresh 12 g 16.66 wt% ThLEU mixture, Th comprises a substantial 20%, while the remaining 80% is U-238. When it comes to neutrons lost (i.e. absorbed) in these two fertile fuels, Th contributes 16.7%, which is still substantial. In pebble fuel fissioning of the fertile fuels comprises a very small fraction of fissions and therefore it can be neglected. It can thus be assumed that the overwhelming fraction of these absorptions will result in radiative capture, which will respectively

breed U-233 and Pu-239. It can thus be assumed that approximately 16.7% of the breeding from these two isotopes will result in U-233.

When it comes to neutrons lost in U-233 and Pu-239, only 10.8% is lost in U-233. This can be explained by the fact that the microscopic fission cross section of U-233 is only about half that of Pu-239. This means that even if U-233 were to be present in the fuel at equal concentrations to Pu-239, fissions from Pu-239 would still dominate.

Although absorption for radiative capture is substantial, especially for Pu-239, the majority of these absorptions still end up in fissions. This means that the fraction of fissions from U-233, with its excellent neutron economy, is much smaller than from Pu-239, with its poor neutron economy in thermal and epithermal neutron spectra. Added to this is the fact that the overwhelming majority of fissions still come from U-235. The outcome of all these matters is that the improvement in neutron economy that was achieved from breeding U-233 from the added Th-232 is very small. This can be seen in the facts that changing from the 10g 20 wt% LEU to the 12 g 16.66% ThLEU improved the conversion ratio only negligibly from 40.5% to 43.9% and the ratio of source fission neutrons born to absorptions in the fissile fuel isotopes only from 1.923 to 1.931. On the down side, the addition of Th decreased the enrichment and therefore the burn-up by 20.3% and the cumulative energy per fuel sphere by 4.4%.

The dilemma is that in order to improve the neutron economy further, one would have to add even more Th, which will decrease enrichment and therefore the burn-up and cumulative energy even further.

4.1.5 Comparing cases for fuels which can be realised, LEU 10 wt%, 7 g HM compared to ThLEU 10 wt% effective enrichment 10 g HM.

The neutronic results discussed below will focus on high burn-up cases which can be realised; this is why ThHEU will not be discussed. A 7 g HM loading 10 wt% LEU fuel (0.7g) of U-235 will be compared to a ThLEU fuel at 10 g HM and 10 wt% (1g) U-235. This will be done in order to determine how the optimum fuel to moderator cases compare to one another in terms of neutronics.

In order to understand the neutronics it is important to understand how the different fuels are broken down into their respective mass fraction as shown in **Table 29**.

Table 29 – Mass fractions of LEU 10 wt%, 7 g HM compared to ThLEU 10 wt% effective enrichment 10 g HM.

		LEU	ThLEU
HEAVY METAL LOADING	g	7.00	10.00
EFFECTIVE ENRICHMENT	wt%	10.00	10.00
235U ENRICHMENT	%	10.00	20.00
235U MASS/FS	g	0.70	1.00
238U MASS/FS	g	6.30	4.00
232Th MASS/FS	g	0.00	5.00
MASS U/FS	g	7.00	5.00
Th/U RATIO		0.00	1.00
MASS UO2/FS	g	7.94	5.67
MASS ThO2/FS	g	0.00	5.69
MASS (ThU)O2/FS	g	7.94	11.36
(Th,U)O2 / HM RATIO		1.135	1.136

As can be seen from **Table 29** the mass fraction of U-235 is higher for the ThLEU fuel so this fuel should outperform the LEU fuel.

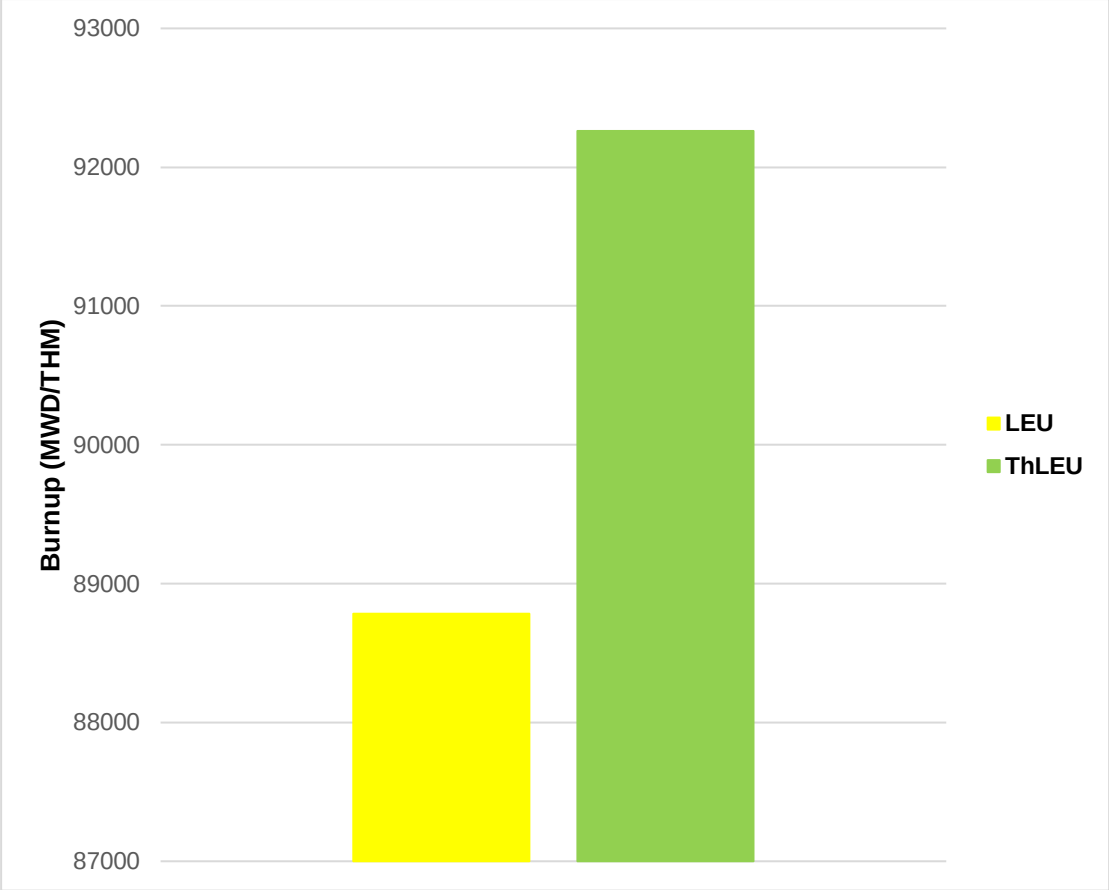

Figure 24 – Burn-up comparison for LEU 10 wt%, 7 g HM compared to ThLEU 10 wt% effective enrichment 10 g HM.

Figure 24 compares the 2 fuels shown above. The ThLEU fuel outperforms the LEU fuel, this is due to the higher effective enrichment due to the higher mass of U-235.

Table 30 – Global neutronic data for LEU 10 wt%, 7 g HM compared to ThLEU 10 wt% effective enrichment 10 g HM.

	Units:	LEU	ThLEU
HEAVY METAL LOADING	g HM	7	10
FEED ENRICHMENT	wt%	10	10
AVG. FISSILE ENRICHMENT	%	5	5.3
AVG. FUEL RESIDENCE TIME	DAYS	947.9	1405.1
AVG. BURNUP	MWD/T	88782.3	92259.7
PEBBLE FEED RATE	SPHERES/DAY	161	108
KEFF		0.9999	0.9999
FISSIONS/ENERGY	E+10 (FISS/WS)	3.046	3.07
POWER PEAKING MAX./AVG.		2.52	2.38
MAX. POWER PER BALL	KW/BALL	1.65	1.56
CONVERSION RATIO	CR	0.405	0.455
SOURCE NEUTR./FISSILE ABS.	ηε	1.966	2.002
CAPTURE/FISSION IN FISS.MAT.	α	0.304	0.257
FAST DOSIS SPENT FUEL ELEM.	E+21/CM2	2.23	3.27

The global data in **Table 30** shows that the residence time and burn-up are higher for the ThLEU fuel due to the higher U-235 mass.

Table 31 – Neutron losses in heavy metals for 10 wt%LEU 7 g HM and 10 wt%ThLEU at 10 g HM

		LEU	ThLEU
NEUTRONS LOST IN HEAVY METALS ESP.	%		
NEUTRON LOSSES IN HEAVY METALS	%	72.39	74.24
ESP. IN FISSILE ISOTOPES	%	50.86	49.95
ESP. IN TH-232	%		10.52
ESP. IN PA-233	%		0.22
ESP. IN U -233	%		5.49
ESP. IN U -234	%	0.14	0.27
ESP. IN U -235	%	33.34	33.84
ESP. IN U -236	%	0.43	0.62
ESP. IN U -237	%		
ESP. IN U -238	%	16.81	9.75
ESP. IN NP-237	%	0.12	0.21
ESP. IN NP-239	%	0.03	0.02
ESP. IN PU-238	%	0.03	0.05
ESP. IN PU-239	%	14.71	8.69
ESP. IN PU-240	%	3.8	2.51
ESP. IN PU-241	%	2.81	1.93
ESP. IN PU-242	%	0.1	0.06
ESP. IN AM-241	%	0.04	0.04
ESP. IN AM-242M	%		
ESP. IN AM-243	%	0.02	0.02
IN FISSION PRODUCTS	%	6.8	7.23
ESP. IN XE-135	%	2.18	2.02
CORE-LEAKAGE	%	18.35	16.54

Table 31 shows the LEU fuel has a higher core leakage, this is due to the lower HM loading.

Table 32 shows that the majority of the fissions originate from U-235 and Pu-239 in the LEU fuel whereas the ThLEU fuel is a mixture of this as well as fissions coming from U-233.

Table 32 – Fractional neutrons produced by 10 wt%LEU 7 g HM and 10 wt%ThLEU at 10 g HM

		LEU	ThLEU
FRACTIONAL NEUTRONS PRODUCED BY	%		
TH - 232	%		0.05
U - 233	%		12.24
U -234	%		
U -235	%	67.21	67.74
U -236	%	0.02	0.03
U -238	%	0.31	0.2
NP - 238	%		
PU - 238	%		
PU-239	%	26.44	15.6
PU-240	%		
PU-241	%	5.98	4.11
AM-242M	%	0.01	0.01

Table 33 – Fuel supply and discharge of 10 wt%LEU 7 g HM and 10 wt%ThLEU at 10 g HM

		LEU		ThLEU	
FUEL SUPPLY - DISCHARGE		Supply	Discharge	Supply	Discharge
TH-232	KG/GWD(TH)			5.3426	5.0719
U -233	KG/GWD(TH)			0.0000	0.1238
U -234	KG/GWD(TH)	0.011	0.0073	0.0109	0.0194
U -235	KG/GWD(TH)	1.1234	0.2502	1.0824	0.2077
U -236	KG/GWD(TH)	0.0000	0.1406	0.0000	0.1418
U -238	KG/GWD(TH)	10.0994	9.6517	4.3737	4.1167
NP-237	KG/GWD(TH)	0.0000	0.008	0.0000	0.0104
PU-238	KG/GWD(TH)	0.0000	0.0028	0.0000	0.0044
PU-239	KG/GWD(TH)	0.0000	0.0532	0.0000	0.0271
PU-240	KG/GWD(TH)	0.0000	0.0467	0.0000	0.0205
PU-241	KG/GWD(TH)	0.0000	0.0232	0.0000	0.0127
PU-242	KG/GWD(TH)	0.0000	0.0187	0.0000	0.0129
AM-241	KG/GWD(TH)	0.0000	0.0024	0.0000	0.0016
AM-242M	KG/GWD(TH)				
AM-243	KG/GWD(TH)	0.0000	0.0021	0.0000	0.0013
CM-244	KG/GWD(TH)	0.0000	0.0005	0.0000	0.0004

4.2 DLOFC Fuel Temperatures

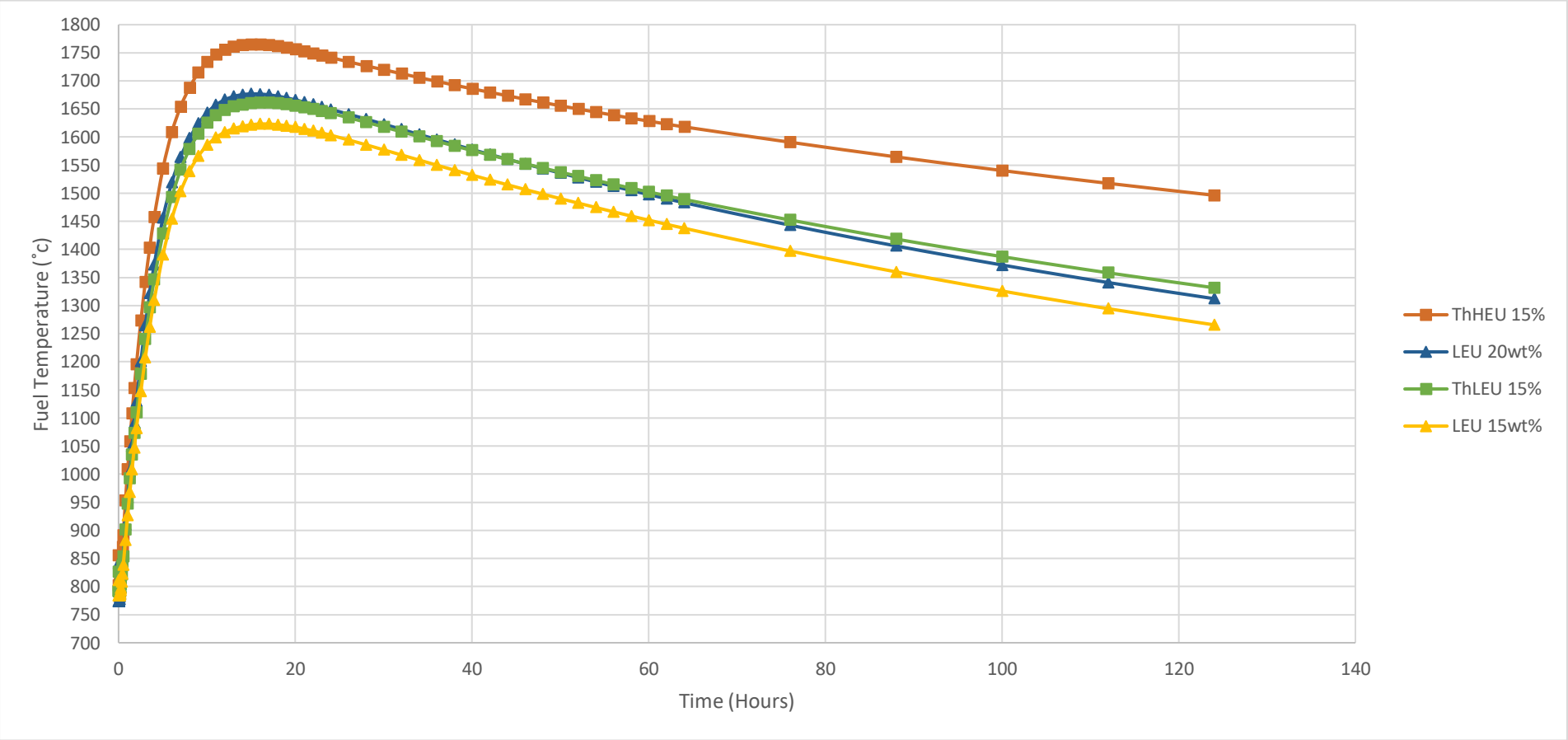

Figure 25 – DLOFC fuel temperatures of LEU, ThLEU at 15 wt% and including 20 wt% LEU for 10 g HM.

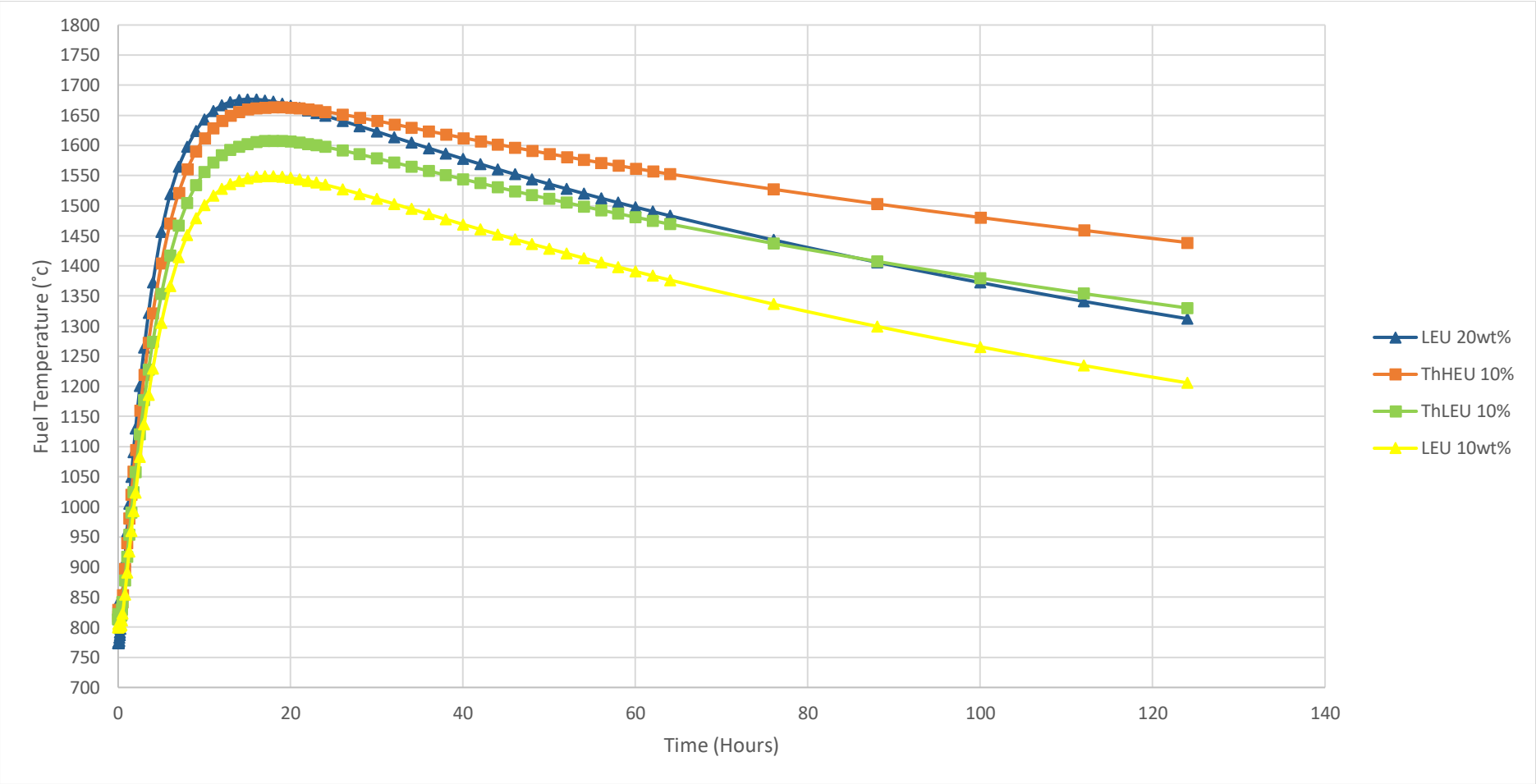

Figure 26 – DLOFC fuel temperatures of LEU, ThLEU at 10 wt% and including 20 wt% LEU for 10 g HM.

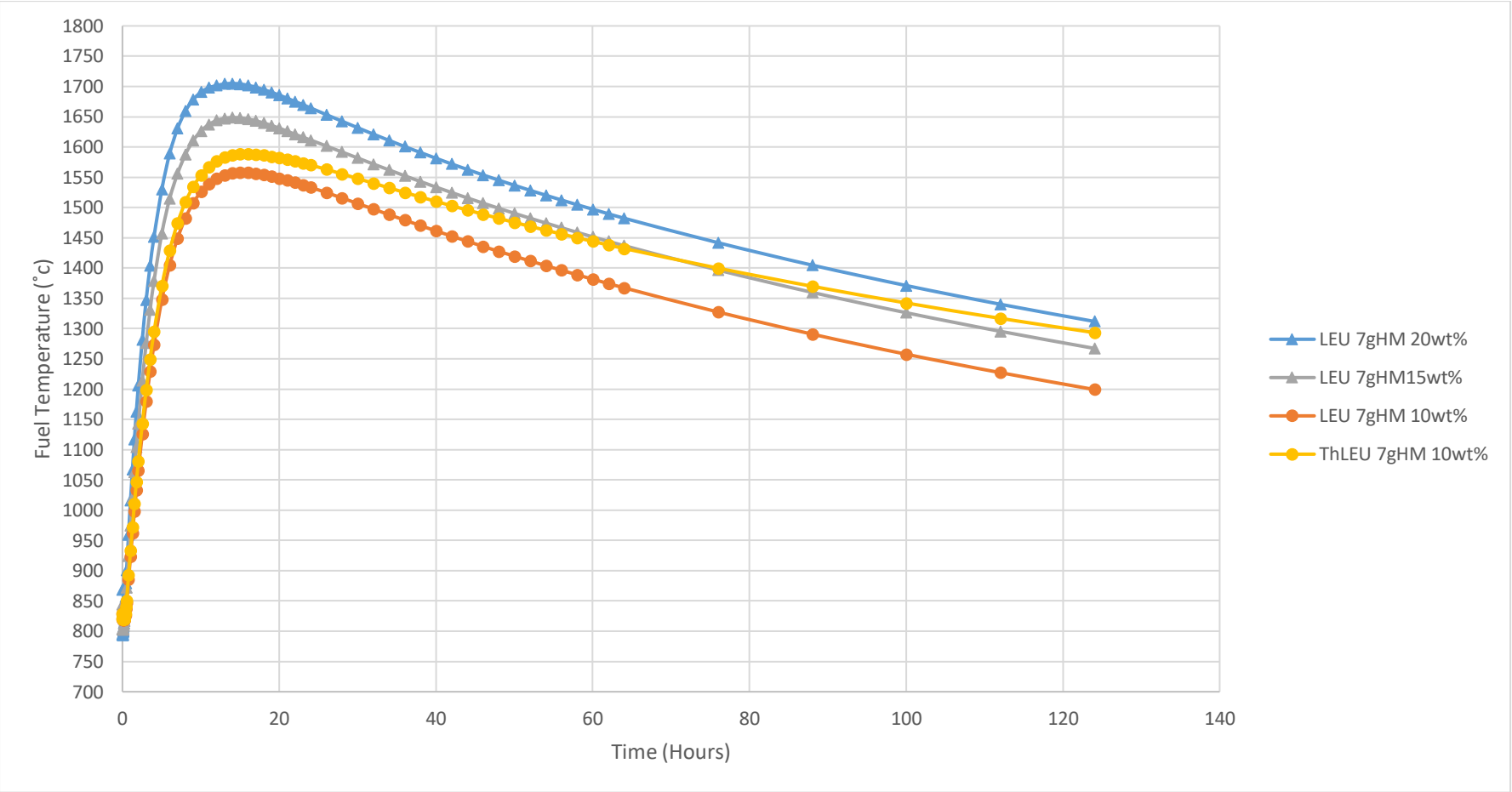

Figure 27 – DLOFC fuel temperatures of LEU, ThLEU at 10 wt% and including 15 wt% & 20 wt% LEU for 7 g HM.

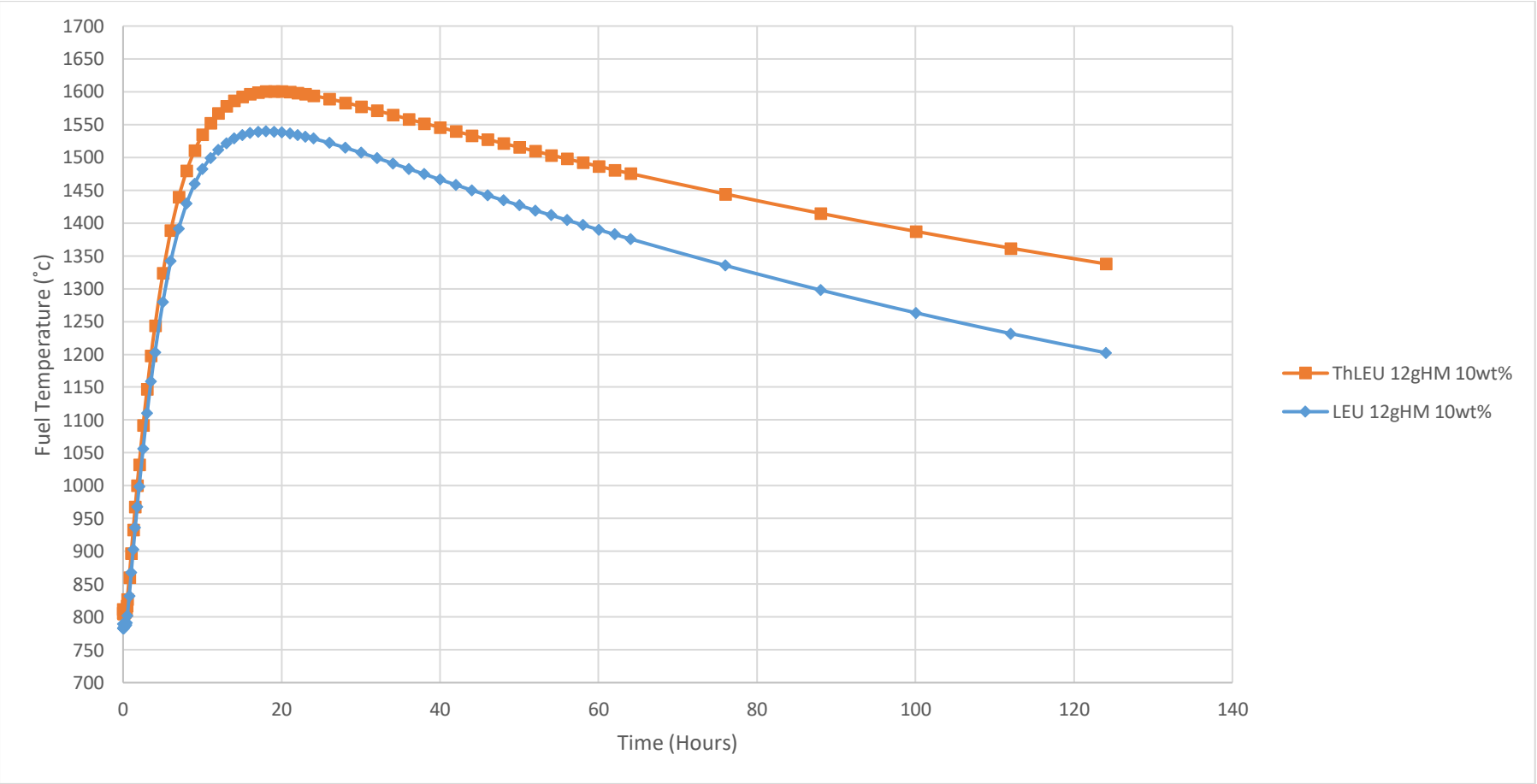

Figure 28 – DLOFC fuel temperatures of LEU, ThLEU at 10 wt% for 12 g HM.

As can be seen with the DLOFC temperatures the 20 wt%, 10 g HM case is used as a reference. The main aim of the DLOFC runs is to analyse the fuel when a loss of coolant accident occurs and see whether the fuel remains below its operating limits (1600˚C) for a certain time. This ensures that no gaseous metallic fission products diffuse through the SiC layer. A few cases were simulated at higher enrichments (15 wt% effective) and normal operating enrichments (10 wt% effective). It can be seen from **Figure 25** that the all the higher enrichments 20 wt% LEU, 15 wt% ThLEU and 15 wt% ThHEU all fail the DLOFC requirements to remain below 1600˚C. In **Figure 26** the LEU 20 wt% and ThHEU 10 wt% cases fail the DLOFC requirements; however, both the LEU 10 wt% and ThLEU 10 wt% cases pass the DLOFC requirements and can be used as fuels in this reactor. These cases are only simulated for a 10 g HM loading.

In order for the reactor to be inherently safe both in a water ingress accident and a DLOFC event runs were performed at 7 g HM for both LEU and ThLEU, these results are shown in **Figure 27**. Both the LEU and ThLEU fuels conform to the DLOFC requirements at 10 wt% enrichment, both being under 1600˚C. The LEU cases at 15 wt% and 20 wt% for 7 g HM exceed the 1600˚C limit and do not qualify.

Higher HM loadings 12 g HM do not exceed the DLOFC limits however they will exceed the water ingress maximum HM loading limits, these DLOFC runs of this are shown in **Figure 28**. The main findings are that at higher enrichments for all the fuels 15 wt% and up to 20 wt% the DLOFC fuel temperatures are too high this leads to the conclusion that high enrichments lead to higher fuel temperatures in an accident scenario where the coolant is lost. The enrichments should stay at around 10 wt% and lower.

The thorium runs produce higher DLOFC temperatures due to the formation of protactinium. The production of Pa-233 is an intermediate isotope during breeding of U-233. Pa-233 has a half-life of 27 days and when it transmutates into U-233 there will be a reactivity surge due to the delayed neutron production (Lung & Gremm, 1997). In comparison to uranium decay to Np-239 with a half-life of 2.3 days which means the reactivity surge will occur shortly after reactor shutdown. This longer half-life also

results in the build-up of much higher concentrations of Pa-233, which plays a significant role in the decay heat production in the case of a DLOFC accident.

This delayed effect causes the peak DLOFC temperatures to be higher for the thorium based fuels, especially the thorium fuels which contain more thorium (ThHEU will have a higher DLOFC fuel temperature when compared to ThLEU). The gradient of the thorium DLOFC curves is less steep when compared to the uranium curves, this is due to the longer half-life associated with Pa-233 production thus extending the times it takes the reactor to cool down.

The DLOFC cases that passed the DLOFC requirements of 1600˚are shown in **Figure 29** which are the lower enrichments at any HM loading. The enrichments over 10 wt% lead to values exceeding 1600˚C, therefore this reactor has to operate at lower enrichments to be inherently safe.

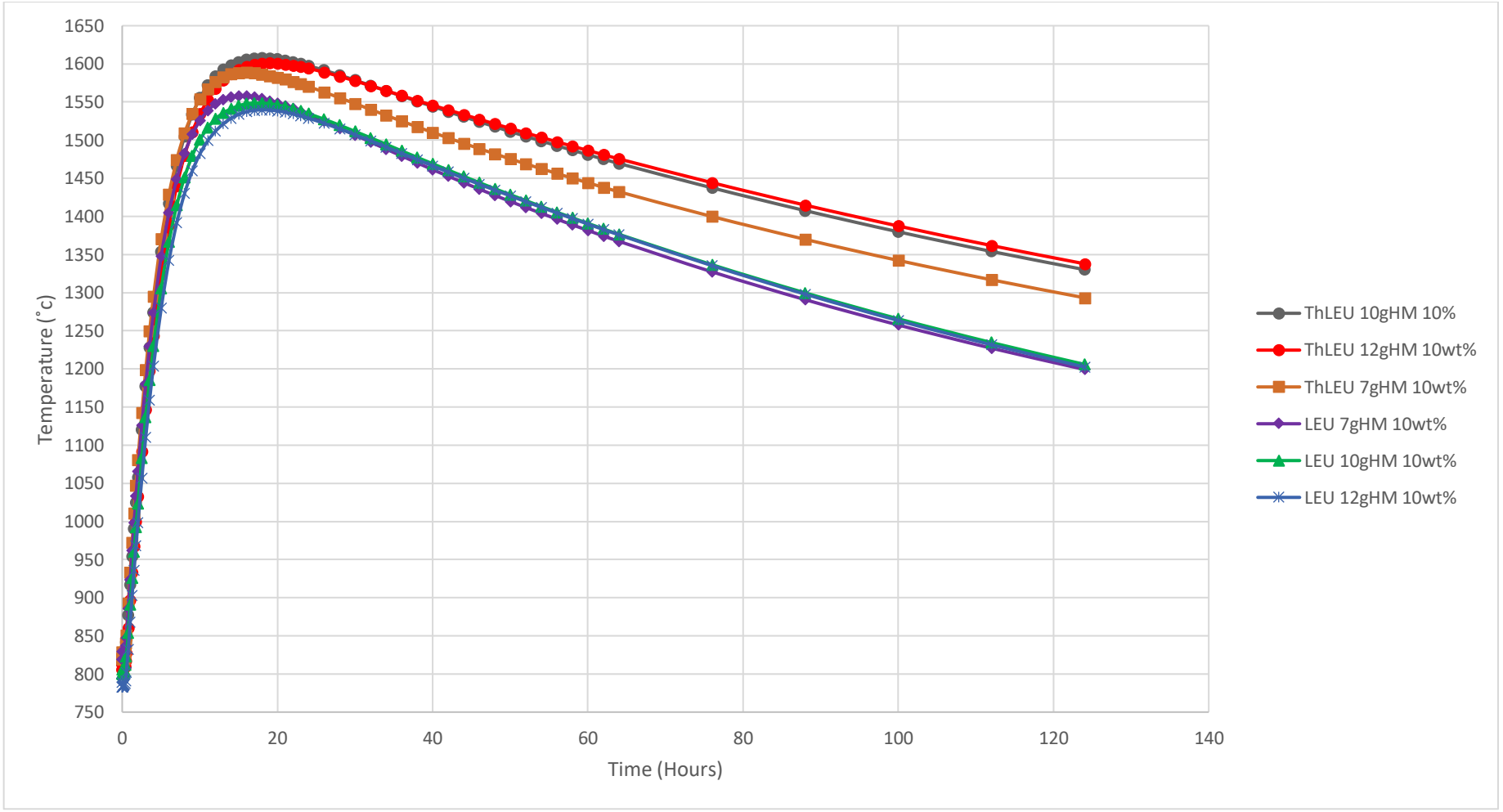

Figure 29 – DLOFC fuel temperatures of LEU & ThLEU under 1600˚C.

Table 34 – Maximum DLOFC fuel temperatures in decreasing order

Fuel Type	Max DLOFC Fuel Temperature (˚C)
ThHEU 10 g HM 15 wt%	1765.0
LEU 10 g HM 20 wt%	1676.7
ThHEU 10 g HM 10 wt%	1663.5
ThLEU 10 g HM 15 wt%	1661.1
LEU 10 g HM 15 wt%	1623.2
ThLEU 10 g HM 10 wt%	1607.6
ThLEU 12 g HM 10 wt%	1600.8
ThLEU 7 g HM 10 wt%	1588.7
LEU 7 g HM 10 wt%	1558.0
LEU 10 g HM 10 wt%	1548.6
LEU 12 g HM 10 wt%	1539.6

Table 35 –DLOFC fuel temperatures as a function of enrichment

Fuel Type	Max DLOFC Fuel Temperature (˚C)
LEU 10 g HM 20 wt%	1676.7
LEU 10 g HM 15 wt%	1623.2
LEU 10 g HM 10 wt%	1548.6
ThLEU 10 g HM 15 wt%	1661.1
ThLEU 10 g HM 10 wt%	1607.6
ThHEU 10 g HM 15 wt%	1765.0
ThHEU 10 g HM 10 wt%	1663.5

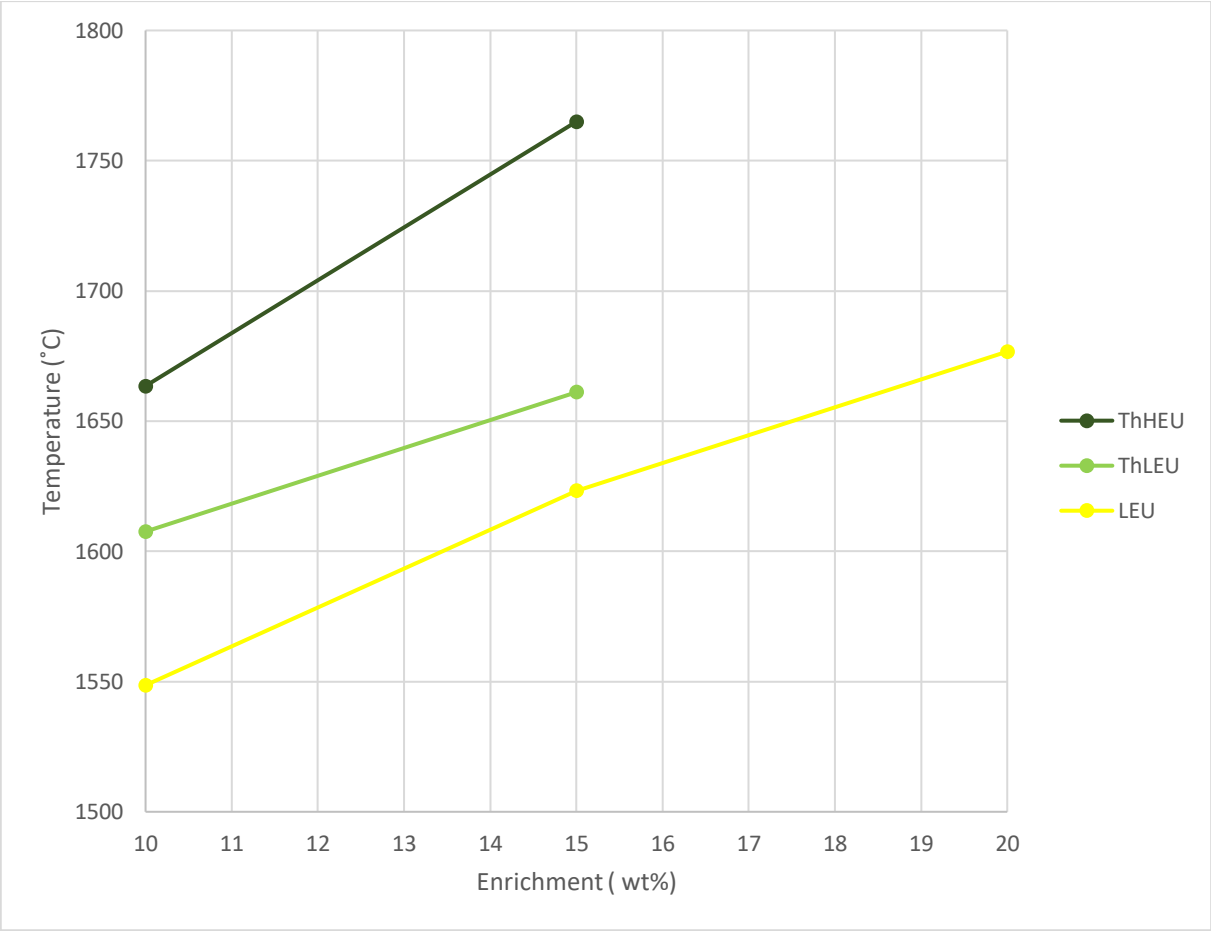

Figure 30 – DLOFC fuel temperatures as a function of enrichment for 10 g HM loading

Table 36 –DLOFC fuel temperatures as a function of HM loading

Fuel Type	Max DLOFC Fuel Temperature (˚C)
LEU 7 g HM 10 wt%	1558
LEU 10 g HM 10 wt%	1548.6
LEU 12 g HM 10 wt%	1539.6
ThLEU 7 g HM 10 wt%	1588.7
ThLEU 10 g HM 10 wt%	1607.6
ThLEU 12 g HM 10 wt%	1600.8

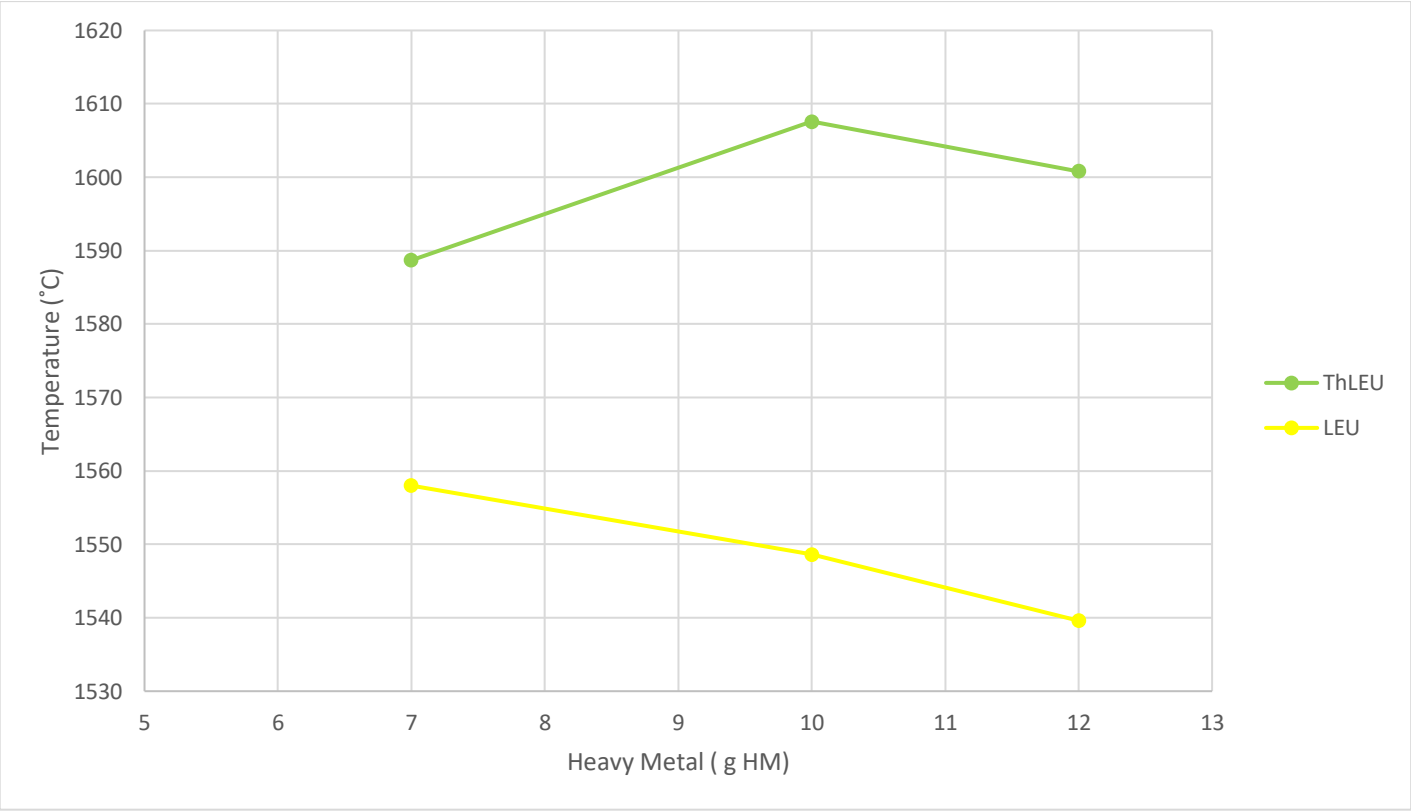

Figure 31 – DLOFC fuel temperatures as a function of heavy metal loading for 10 wt% enrichment

Table 34 , **Table 35** and **Table 36** show the general trends which have come out of this DLOFC study are that as the enrichment increases the DLOFC fuel temperatures increase and as thorium is added the DLOFC temperatures increase. See **Figure 30** to compare LEU, ThLEU and ThHEU fuel. It can clearly be seen that ThHEU has the highest fuel temperatures followed by ThLEU and finally the lowest fuel temperature being LEU. This is again due to the thorium-based fuels having increased thorium contents and thus more production of Pa-233 which has a much longer half-life than the corresponding Np-239 in the U-238 transmutation chain. This means that the decay heat generated from the decay of Pa-233 to U-233 will last much longer into a DLOFC accident than for the corresponding decay of Np-239 to Pu-239. This results in increases maximum fuel temperatures for Th-based fuels during DLOFC accidents. ThHEU will have the largest production of Pa-233 and thus have an even higher DLOFC fuel temperature.

As the heavy metal loading increases the DLOFC fuel temperatures decrease, however the decreased value at 7 g HM ThLEU shown in **Figure 31** is due to the ThLEU behaving more like LEU fuel at lower heavy metal loadings due to the fact that there is just not enough thorium in the fuel sphere. The low amount of thorium leads to less Pa-233 production and thus a lower DLOFC temperature when compared to the ThLEU cases at 10 g HM and 12 g HM, they tend to follow the trend of a higher HM loading a lower fuel temperature in a DLOFC.

In order to investigate the reason for the decreasing maximum DLOFC temperatures with increasing HM loading, the axial power density profiles were also investigated. **Figure 32** , **Figure 33** and **Figure 34** are the relative axial power profiles, a discussion will be done to determine what influence the relative axial power profiles have on the DLOFC fuel temperatures for the various fuels at different HM loadings and enrichments.

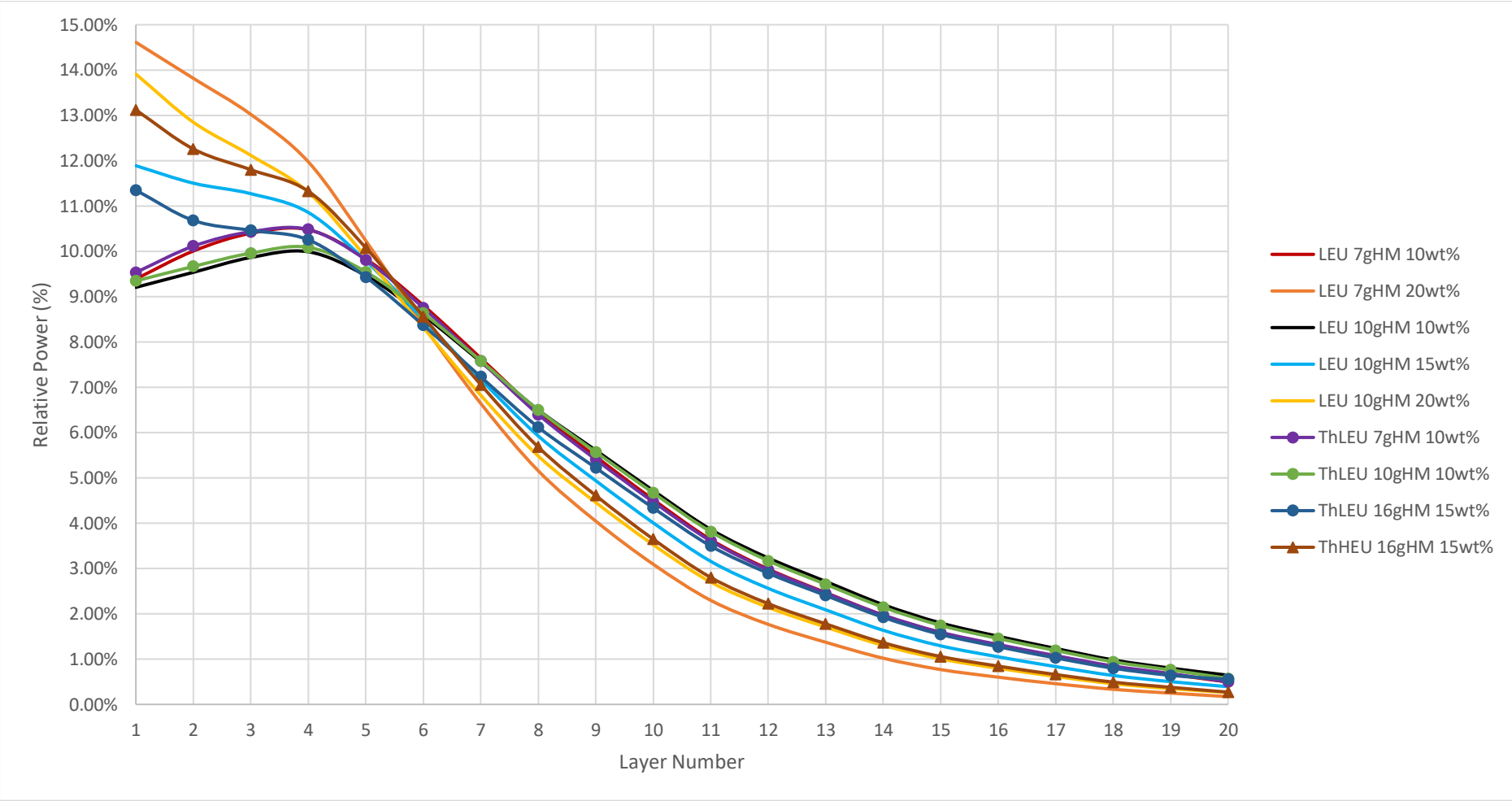

Figure 32 – Axial power profiles for various fuels at different HM loadings and enrichments

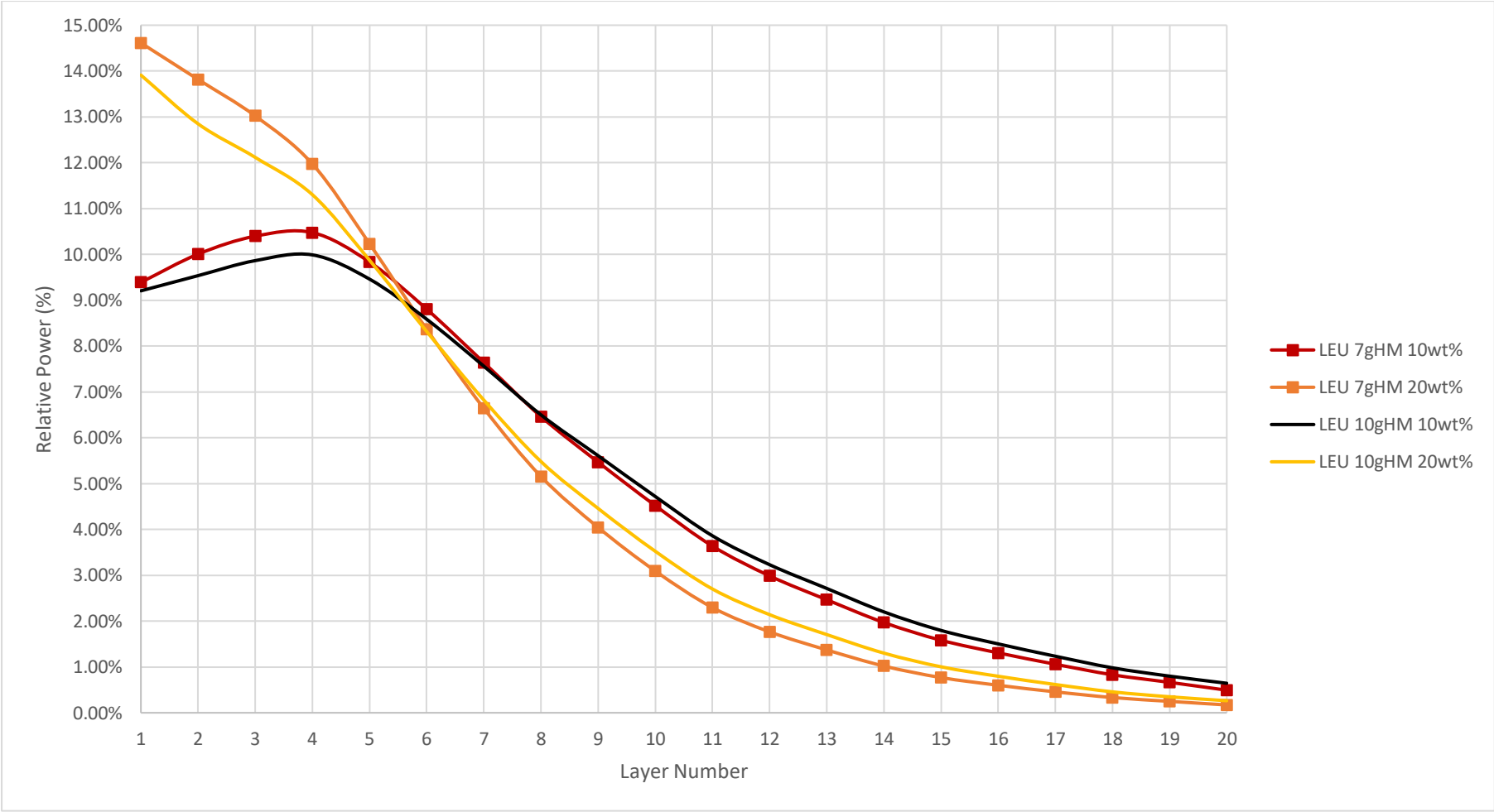

Figure 33 – Axial power profiles for LEU fuels at different HM loadings and enrichments

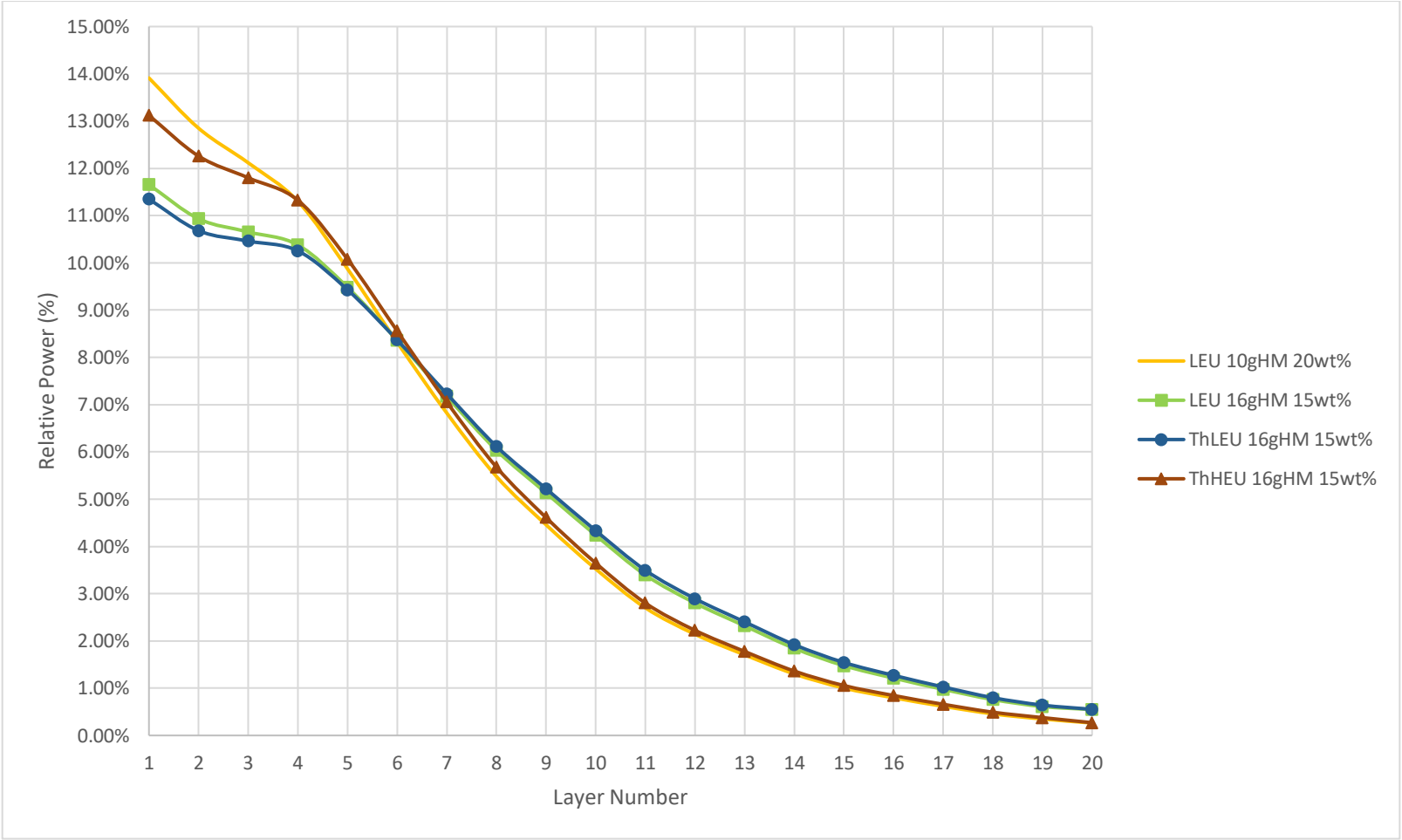

Figure 34 – Axial power profiles for LEU, ThLEU and ThHEU

The relative axial power profiles are shown above are shown to determine how they affect the DLOFC fuel temperatures for various enrichments, HM loadings and different fuels. In **Figure 33** increased enrichment concentrates the power to the top of the core and also increases the maximum relative power at the top due to the power profile being moved up. Increasing enrichment from 10 wt% to 20 wt% for LEU at both 7 g HM and 10 g HM increase the relative power towards the top of the core as seen in the figure. This overloads and concentrates the power at the top of the core, there is therefore more probability that a hotspot can occur at the top of the core due to the increased power and therefore also increased DLOFC fuel temperatures. Increasing the enrichment increases the power per fuel sphere at the top of the core and decreases it towards the bottom as the entire core is only still 100MW. This increased enrichment however allows the fuel to burn to a lower value as can be seen in **Figure 33**. It begins at a higher relative power but also ends at a lower relative power. In a DLOFC accident the power is concentrated at the top of the core where there is a smaller area for heat dissipation, if the enrichment is high the fuel will get extremely hot and exceed the maximum DLOFC fuel temperature.

Increasing the HM loading as seen in **Figure 33** reduces the relative power at the top of the core and shifts the peak downwards. It can be seen in the figure that increasing the HM loading indeed does shift the power down and reduces the maximum. Higher HM loadings burn slower and last longer, they also increase the power level lower down in the core. The higher the HM loading the flatter the profile which reduces the chances for hotspots as it spreads the power out over a larger area and in a DLOFC accident the fuel temperatures will be lower.

In **Figure 34** thorium-based fuels are compared to LEU fuel. It can be seen that thorium does in fact lower the peak and flatten the relative power profiles thus reducing the chances of a hotspot at the top of the core however; the thorium DLOFC fuel temperatures discussed in the previous section are still hotter than their uranium counterparts for the same enrichments and HM loadings, due to Pa-233 formation as previously discussed. Therefore even though thorium does flatten the relative axial power profiles which usually lowers the DLOFC fuel temperature the production of Pa-233 with its long half-life increases the thorium-based fuel temperatures in a DLOFC accident more than the uranium fuels.

4.3 Fuel costs (Steenkampskraal Thorium Limited, 2017)

The cost calculations are calculated from the residence time and burn-up achieved by each type of fuel mixture, this determines how many fuel spheres are consumed per day for each equilibrium core model. The uranium and thorium raw material requirements are then calculated based on the heavy metal loading, effective enrichment and U-235 enrichment value. The uranium and thorium costs are then determined based on current market prices. The uranium enrichment is determined by current market related data which is calculated from the "UxC Fuel Quantity & Cost Calculator" on the 14th of August 2017. The UxC uses the U_3O_8, conversion, UF6 and SWU costs to calculate the Enriched Uranium Product (EUP) in $/kg which contains both the U-235 and U-238 fractions for various enrichments (UxC, n.d.). The costs are completely theoretically based and the fuel cost calculator does not take into account politics and availability of the enriched uranium, it also doesn't take into account the proliferation problems associated with HEU (20 wt% U-235 and above) or the number of additional centrifuges that are needed for enrichments higher than 20 wt%, therefore ThHEU results are of interest, however they are not entirely reputable. All values up to 20 wt% are reputable and the main focus of this study is to assess LEU vs ThLEU as these are the only viable fuelling options in many countries where HEU is not allowed, HEU was just added for the completeness of the study. The remaining fuel sphere costs such as raw material, casting, coating, over-coating, pressing and machining costs are determined form the STL fuel cost models which take into account the amount of fuel spheres produced on a large-scale fuel plant model producing 250000 fuel sphere per year, the heavy metal loadings, enrichments and burn-ups, mass balances, utility, power requirements and staff salaries are just some of the costs taken into account in the STL fuel cost models. The fuel sphere price is then accurately based on the uranium and thorium raw material requirements as well as their costs. The remaining costs of the fuel spheres are based on the STL fuel plant cost models. The fuelling cycles can be accurately compared to determine which fuel is the most cost effective based on the same effective enrichment and heavy metal loading . The LUEC is determined from the STL reactor cost model for a single unit, this provides the Levilised costs for the capital investment, operation and maintenance, fresh fuel, spent fuel and decommissioning. The main focus is on the fresh fuel costs in US$/kWe and total costs in US$/kWh and US$/MWh.

4.3.1 Fuel sphere costs

The following uranium and thorium costs are in oxide form UO_2 and ThO_2. The uranium prices shown are for enriched uranium which were obtained by using market values and the "UxC Fuel Quantity and Cost Calculator" (UxC, n.d.). These prices are updated every 2 weeks and are based on the 14th of August 2017. The thorium price was obtained from Rhodia France with a cost of $150.00/kg for nuclear grade ThO2 99.999% purity. This value is for lab scale applications and a further cost reduction would occur for large industrial scale thorium oxide once there is a market for it. **Table 37** shows the current market prices. As stated above the costs are completely theoretically based and the fuel cost calculator does not take into account politics and availability of the enriched uranium, it also doesn't take into account the proliferation problems associated with HEU (20 wt% U-235 and above). All values up to 20 wt% are reputable and the main focus of this study is to assess LEU vs ThLEU.

Table 37 – Uranium and Thorium prices

93% U-235	**21053.04**	**$/kgU**
20% U-235	4296.72	$/kgU
15% U-235	3169.67	$/kgU
10% U-235	2049.35	$/kgU
8% U-235	1604.55	$/kgU
Th-232	150	$/kgTh

Figure 35 below shows an almost linear relationship between EUP in $/Kg U vs U-235. These are the costs obtained from the fuel cost models. The linear relationship which is shown lasted up to 20wt % enrichment for which LEU based fuel, upon which the "UxC Fuel Quantity and Cost Calculator" (UxC, n.d.). However, these calculated costs might not necessarily accurately represent real world prices: The fact that no commercial fuel enrichment company develops fuel enriched to over 20wt%, unless it is for military applications which are only viable in certain nuclear weapons countries, due to the associated nuclear weapons proliferation problems. Therefore it was not

possible to obtain real word prices for LEU which is enriched as high as the vicinity of 20 wt%.

The HEU fuel prices calculated in this study are not reported in the conclusions as this is not reputable, nor has it been verified. The “UxC Fuel Quantity and Cost Calculator” for enrichments over 20 wt% are theoretical and are based on current market prices, however these are not to be referenced as real costs. Any enrichment far below 20wt% is reputable and can be used as a reference. The ThHEU fuel has been analysed neutronically to determine the cumulative heat energy and use this as a comparison to the LEU and ThLEU fuels.

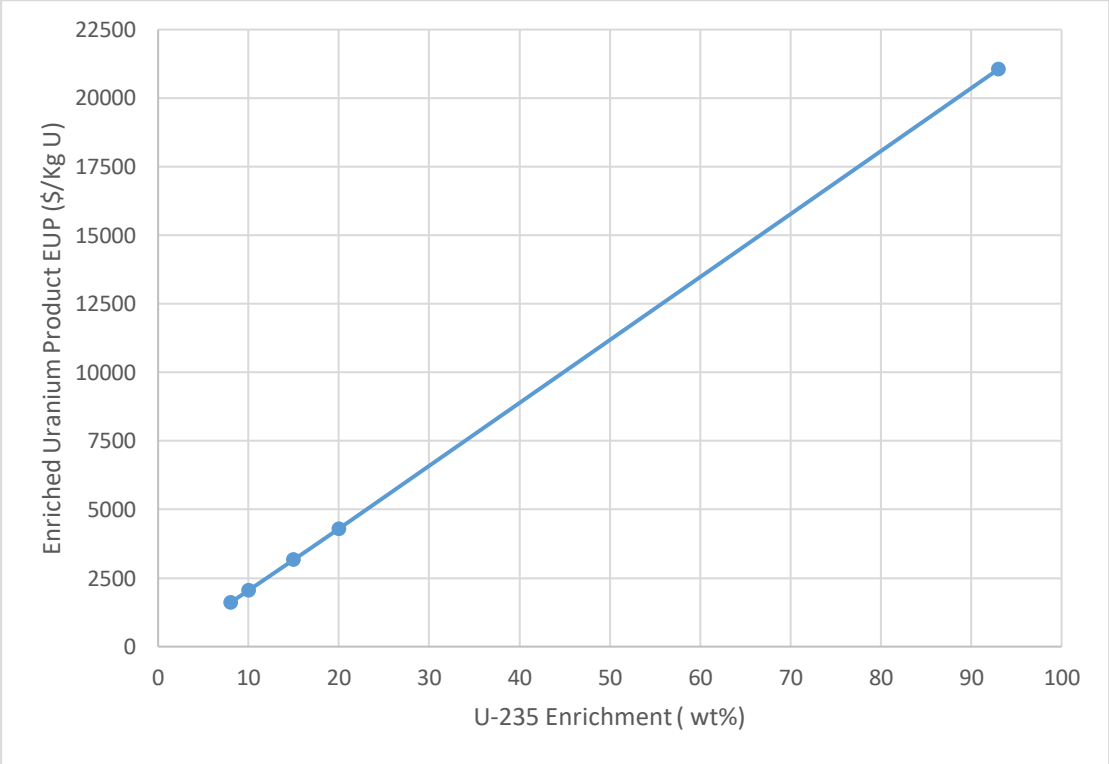

Figure 35 – Enriched Uranium Product Price vs U-235 Enrichment

4.3.2 LEU fuel sphere costs

The following costs shown are for LEU fuel with a heavy metal loading of 10 g HM/fuel sphere and a 10 wt% enrichment.

Table 38 – Fuel sphere costs (OPEX & CAPEX), 10 g HM, 10 wt% LEU, 250000 FS/annum (Steenkampskraal Thorium Limited, 2017)

Cost Component	Kernel	Coated Particle	Matrix Graphite	Fuel Sphere
OPEX				
Direct raw materials and consumables	$23.21	$7.99	$5.43	$1.96
Overhead raw materials and consumables	$2.50	$2.50	$2.50	$2.50
Maint & Spares process equipment	$0.97	$3.21	$0.49	$1.17
Maint & Spares E,R,QC	$0.63	$0.63	$0.63	$0.63
Direct Staff	$1.98	$1.10	$0.66	$2.64
Overhead Staff	$4.37	$4.37	$4.37	$4.37
Other Overheads	$0.74	$0.74	$0.74	$0.74
Plant upgrades	$0.72	$0.72	$0.72	$0.72
Decommissioning	$0.49	$0.49	$0.49	$0.49
OPEX Total	$35.61	$21.76	$16.04	$15.23
OPEX Cumulative	$35.61	$57.37	$73.40	$88.64
CAPEX	6.69%	13.75%	3.41%	8.11%
Direct Process Equipment	$3.92	$8.06	$2.00	$4.75
Overhead Equipment	$9.97	$9.97	$9.97	$9.97
CAPEX Total	$13.89	$18.03	$11.97	$14.72
CAPEX Cumulative	$13.89	$31.92	$43.89	$58.62
Total (CAPEX +OPEX)	**$49.50**	**$39.79**	**$28.01**	**$29.96**
Total Cumulative	$49.50	$89.29	$117.30	$147.26

Table 38 shows the cost breakdown of the different stages of fuel manufacture with the kernel costs being $23.21. The kernel costs consist of two parts, the uranium costs $ 20.616 and the kernel manufacturing costs $ 2.59 which equate to $23.21. This shows that the uranium fraction within the entire fuel sphere cost is 14%, however the total OPEX and CAPEX costs of the kernels are $49.50 which is 33.6% of the total fuel sphere cost. The coated particle costs are $39.79 which is 27%, matrix graphite costs are $28.01 being 19% and the fuel sphere costs are $29.96 being 20.34% of the total cost. The overall cost of a fuel sphere of 10 g HM, 10 wt% is $147.26/fuel sphere.

Figure 36 , **Figure 37** and **Figure 38** show the OPEX, CAPEX and Overall costs broken down into their respective fractions.

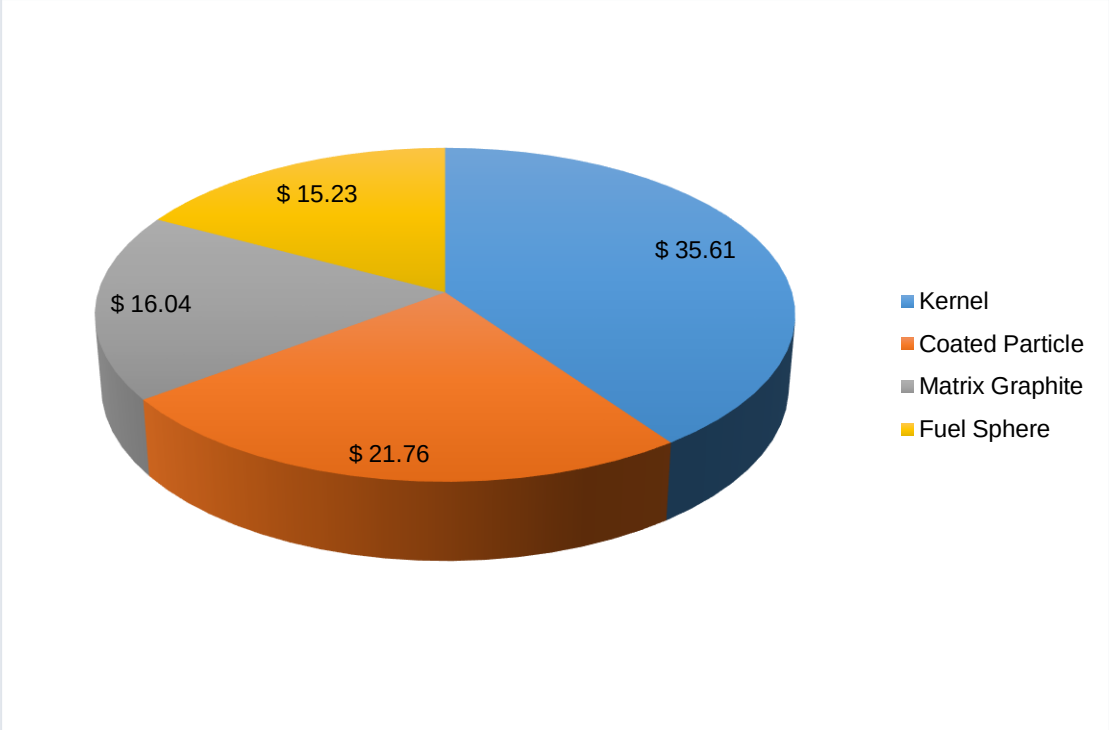

Figure 36 – Fuel sphere OPEX costs for LEU 10 g HM, 10 wt% enrichment, 250000 FS/annum

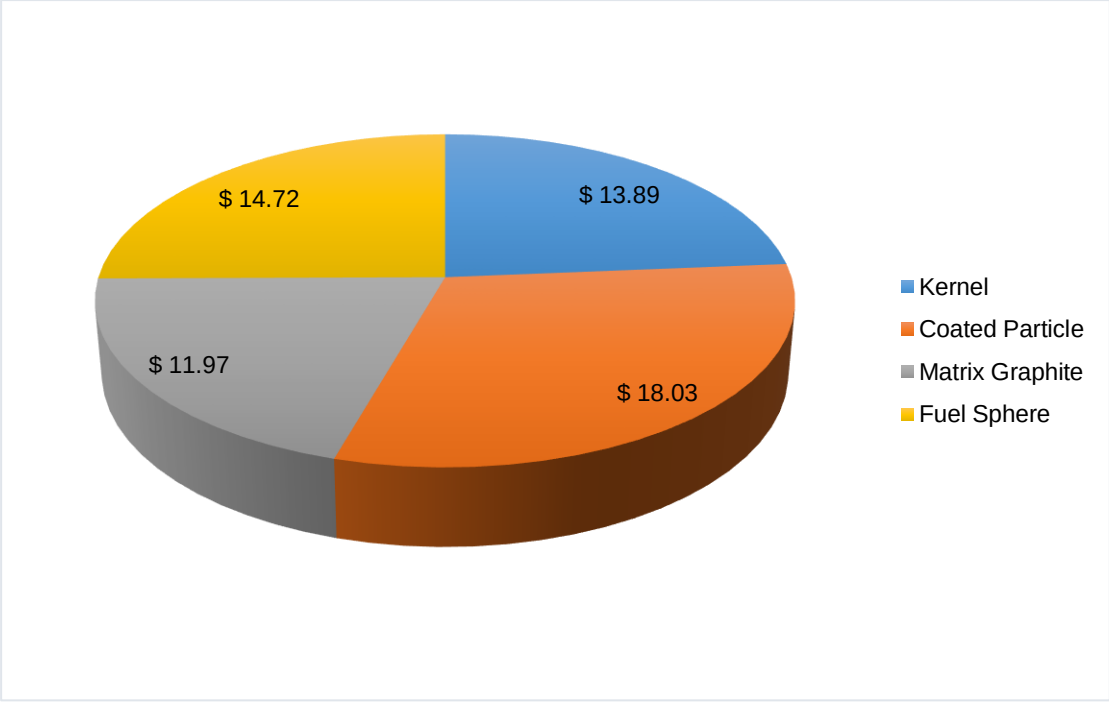

Figure 37 – Fuel sphere CAPEX costs for LEU 10 g HM, 10 wt% enrichment, 250000 FS/annum

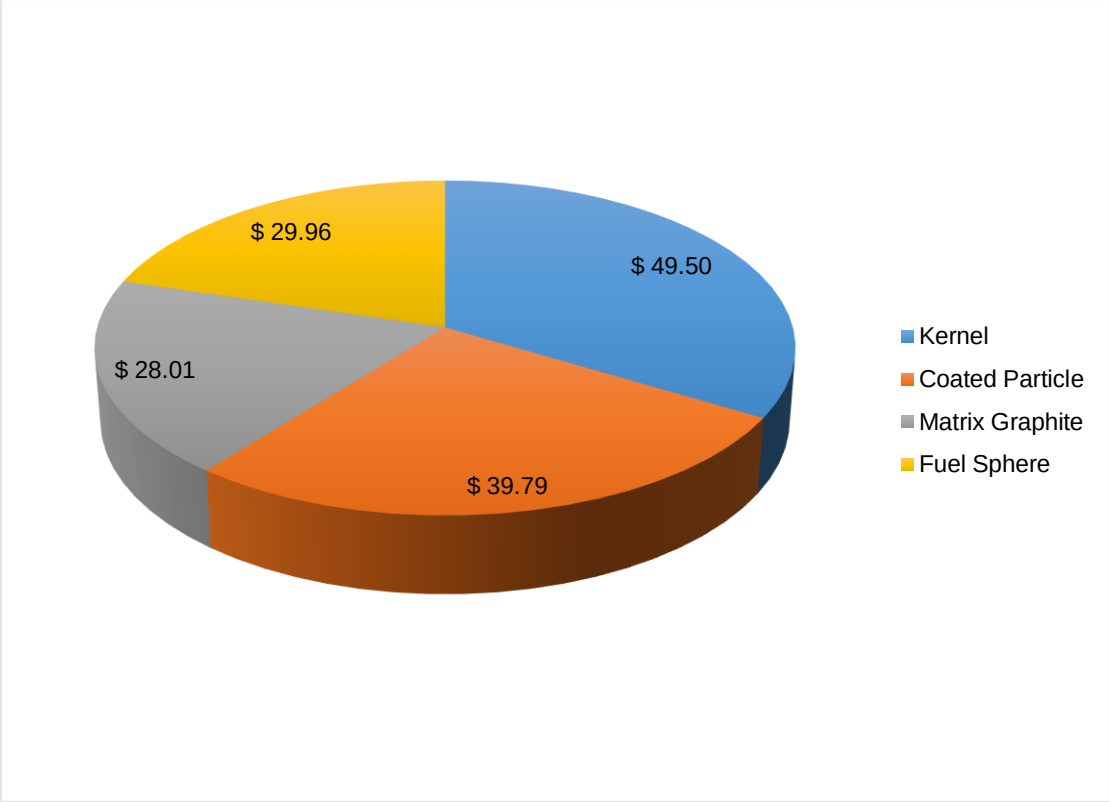

Figure 38 – Fuel sphere OPEX and CAPEX costs for LEU 10 g HM, 10 wt% enrichment, 250000 FS/annum

4.3.3 ThLEU fuel sphere costs

The following costs shown are for ThLEU fuel with a heavy metal loading of 10 g HM per fuel sphere and a 10 wt% enrichment.

Table 39 – Fuel sphere costs (OPEX & CAPEX), 10 g HM, 10 wt% ThLEU, 250000 FS/annum (Steenkampskraal Thorium Limited, 2017)

Cost Component	Kernel	Coated Particle	Matrix Graphite	Fuel Sphere
OPEX				
Direct raw materials and consumables	$24.96	$7.99	$5.42	$1.96
Overhead raw materials and consumables	$2.50	$2.50	$2.50	$2.50
Maint & Spares process equipment	$0.97	$3.21	$0.49	$1.17
Maint & Spares E,R,QC	$0.63	$0.63	$0.63	$0.63
Direct Staff	$1.98	$1.10	$0.66	$2.64
Overhead Staff	$4.37	$4.37	$4.37	$4.37
Other Overheads	$0.74	$0.74	$0.74	$0.74
Plant upgrades	$0.72	$0.72	$0.72	$0.72
Decommissioning	$0.49	$0.49	$0.49	$0.49
OPEX Total	$37.36	$21.76	$16.03	$15.23
OPEX Cumulative	$37.36	$59.12	$75.14	$90.38
CAPEX	6.69%	13.75%	3.41%	8.11%
Direct Process Equipment	$3.93	$8.08	$2.01	$4.76
Overhead Equipment	$9.99	$9.99	$9.99	$9.99
CAPEX Total	$13.92	$18.08	$12.00	$14.76
CAPEX Cumulative	$13.92	$32.00	$44.00	$58.75
Total (CAPEX +OPEX)	**$51.28**	**$39.83**	**$28.03**	**$29.99**
Total Cumulative	$51.28	$91.12	$119.14	$149.13

Table 39 shows the cost breakdown of the different stages of fuel manufacture with the kernel costs being $24.96. The kernel costs consist of three parts, the uranium costs $ 21.612, thorium costs of $0.7545 and the kernel manufacturing costs $ 2.59 which equate to $24.96. This shows that the uranium fraction within the entire fuel sphere cost is 14.5% and thorium fraction 0.5%, however the total OPEX and CAPEX costs of the kernel is $51.28 which is 34.4% of the total fuel sphere cost. The coated particle costs are $39.83 which is 26.71%, matrix graphite costs are$28.03 being 18.79% and the fuel sphere costs $29.99 being 20.11% of the total cost. The overall cost of a fuel sphere of 10 g HM, 10 wt% is $149.13/fuel sphere. **Figure 39** , **Figure 40** and **Figure 41** show the OPEX, CAPEX and Overall costs broken down into their respective fractions.

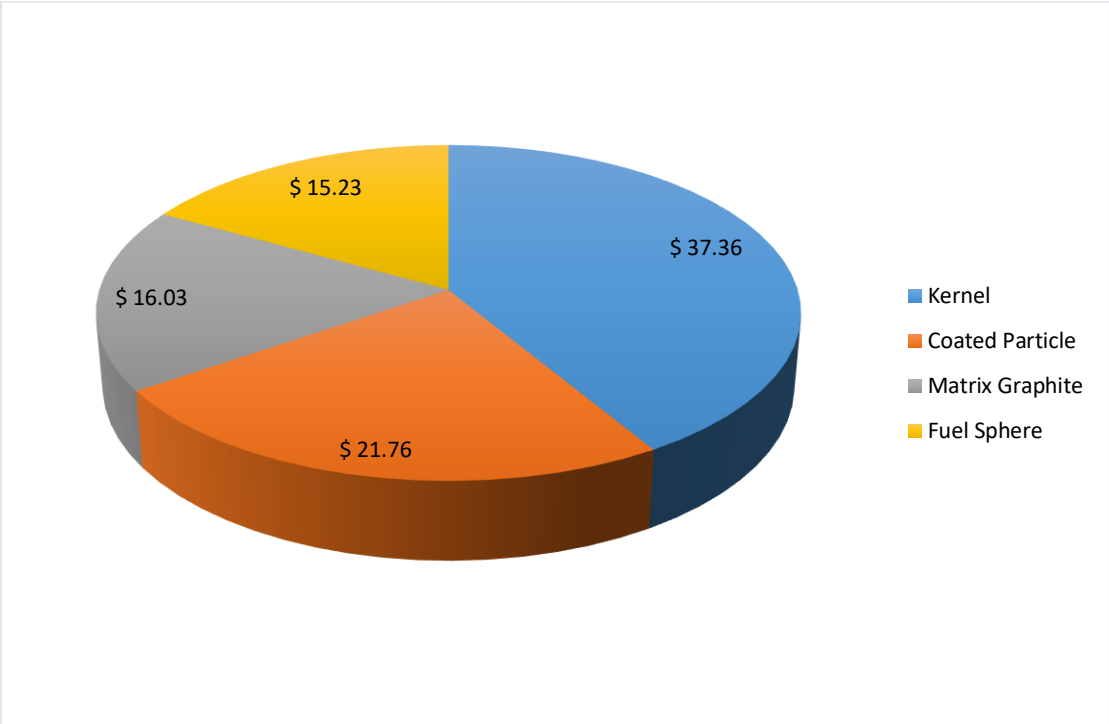

Figure 39 – Fuel sphere OPEX costs for ThLEU 10 g HM, 10 wt% enrichment, 250000 FS/annum

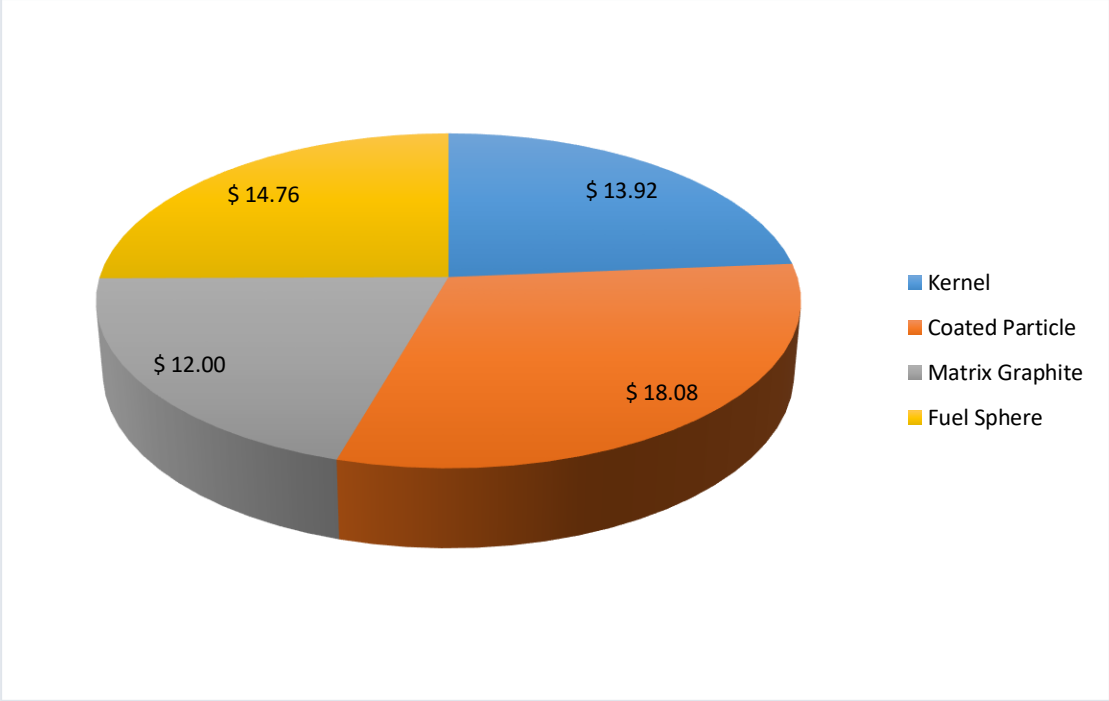

Figure 40 – Fuel sphere CAPEX costs for ThLEU 10 g HM, 10 wt% enrichment, 250000 FS/annum

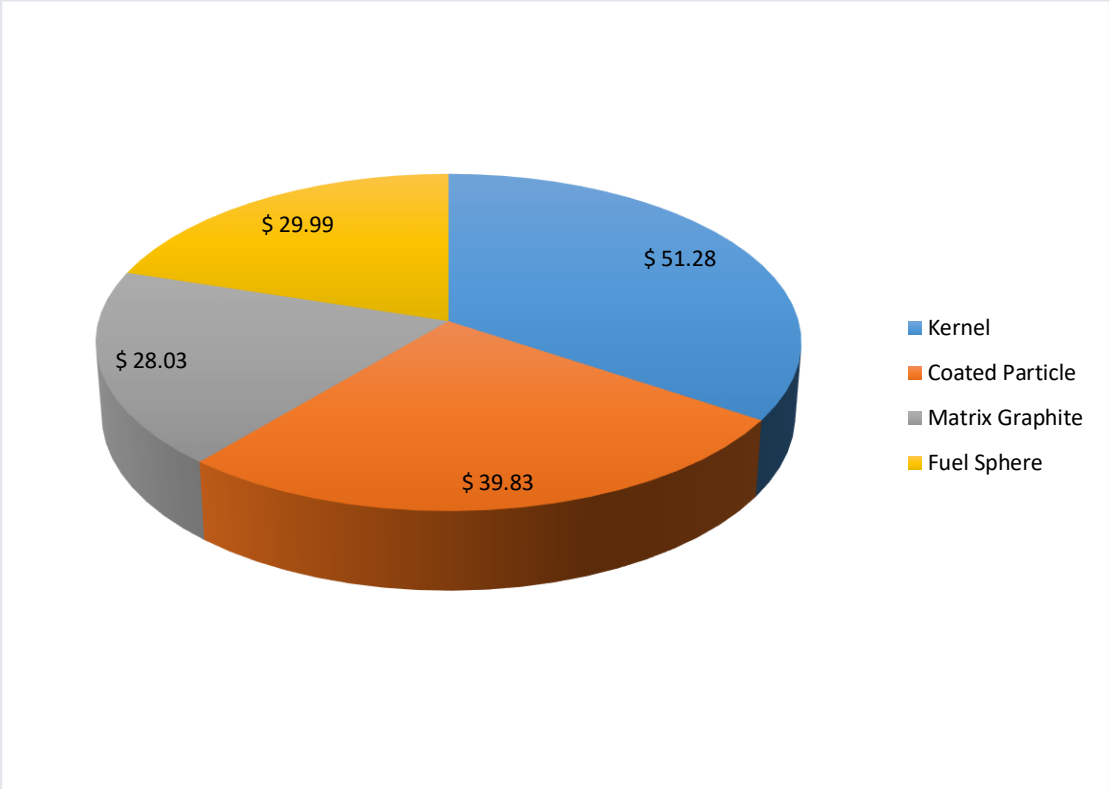

Figure 41 – Fuel sphere OPEX and CAPEX costs for ThLEU 10 g HM, 10 wt% enrichment, 250000 FS/annum

4.3.4 ThHEU fuel sphere costs

The following costs shown are for ThHEU fuel with a heavy metal loading of 10 g HM/fuel sphere and a 10 wt% enrichment. As stated above the costs are completely theoretically based and the fuel cost calculator does not take into account politics and availability of the enriched uranium, it also doesn't take into account the proliferation problems associated with HEU (20 wt% U-235 and above). All values up to 20 wt% are reputable and the main focus of this study is to assess LEU vs ThLEU.

Table 40 – Fuel sphere costs (OPEX & CAPEX), 10 g HM, 10 wt% ThHEU, 250000 FS/annum (Steenkampskraal Thorium Limited, 2017)

Cost Component	Kernel	Coated Particle	Matrix Graphite	Fuel Sphere
OPEX				
Direct raw materials and consumables	$26.71	$7.99	$5.42	$1.96
Overhead raw materials and consumables	$2.50	$2.50	$2.50	$2.50
Maint & Spares process equipment	$0.97	$3.21	$0.49	$1.17
Maint & Spares E,R,QC	$0.63	$0.63	$0.63	$0.63
Direct Staff	$1.98	$1.10	$0.66	$2.64
Overhead Staff	$4.37	$4.37	$4.37	$4.37
Other Overheads	$0.74	$0.74	$0.74	$0.74
Plant upgrades	$0.72	$0.72	$0.72	$0.72
Decommissioning	$0.49	$0.49	$0.49	$0.49
OPEX Total	$39.11	$21.76	$16.03	$15.23
OPEX Cumulative	$39.11	$60.87	$76.90	$92.13
CAPEX	6.69%	13.75%	3.41%	8.11%
Direct Process Equipment	$3.94	$8.10	$2.01	$4.78
Overhead Equipment	$10.02	$10.02	$10.02	$10.02
CAPEX Total	$13.95	$18.12	$12.03	$14.79
CAPEX Cumulative	$13.95	$32.07	$44.10	$58.89
Total (CAPEX +OPEX)	**$53.07**	**$39.88**	**$28.05**	**$30.03**
Total Cumulative	$53.07	$92.94	$121.00	$151.02

Table 40 shows the cost breakdown of the different stages of fuel manufacture with the kernel costs being $26.71. The kernel costs consist of three parts, the uranium costs $22.77, thorium costs of $1.35 and the kernel manufacturing costs $2.59 which equate to $26.71. This shows that the uranium fraction within the entire fuel sphere cost is 15.08% and thorium fraction 0.9%, however the total OPEX and CAPEX costs of the kernel is $53.07 which is 35.14% of the total fuel sphere cost. The coated particle costs are $39.88 which is 26.40%, matrix graphite costs are $28.05 being 18.58% and the fuel sphere costs are $30.03 being 19.88 % of the total cost. The overall cost of a fuel sphere of 10 g HM, 10 wt% is $151.02/fuel sphere. **Figure 42**, **Figure 43** and **Figure 44** show the OPEX, CAPEX and Overall costs broken down into their respective fractions.

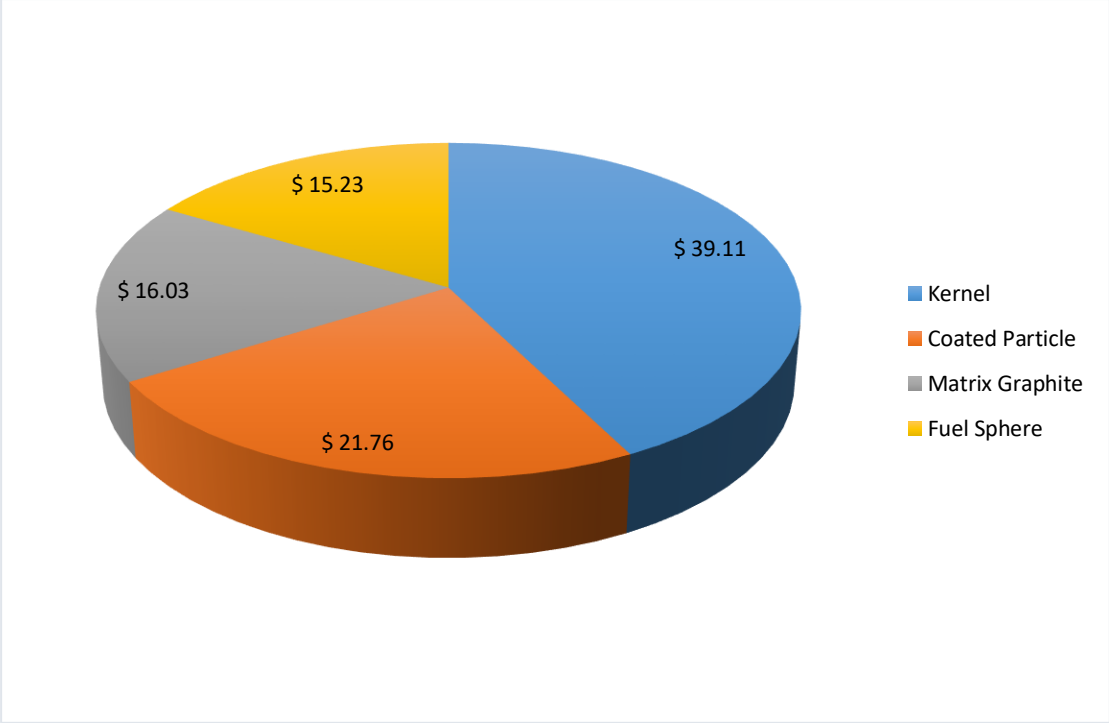

Figure 42 – Fuel sphere OPEX costs for ThHEU 10 g HM, 10 wt% enrichment, 250000 FS/annum

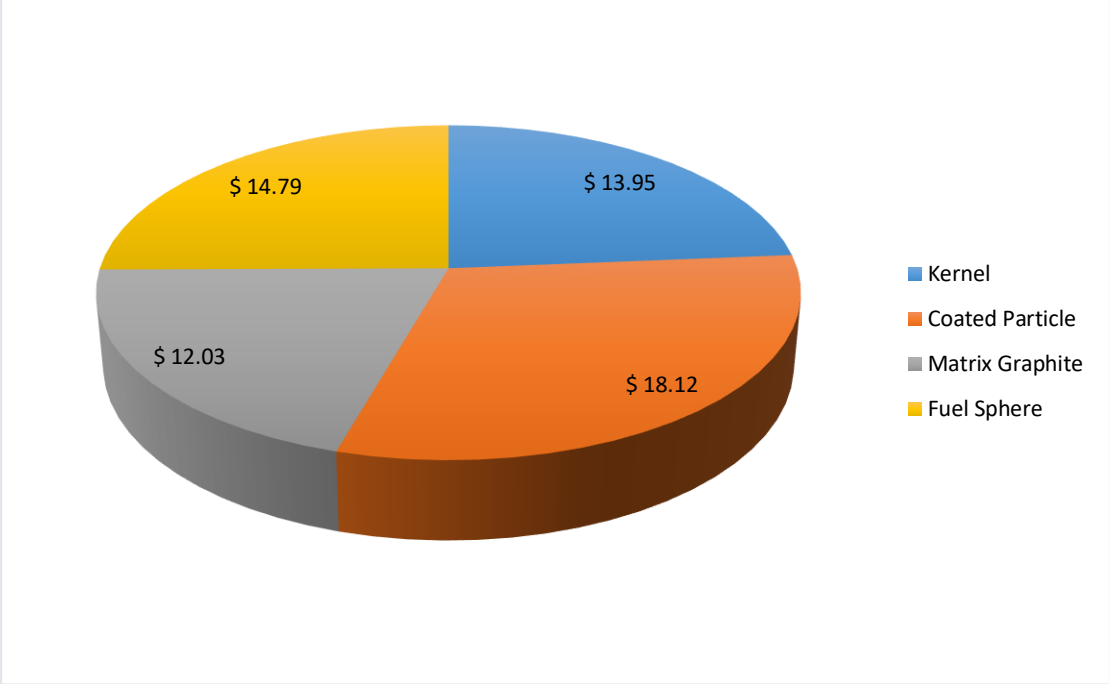

Figure 43 – Fuel sphere CAPEX costs for ThHEU 10 g HM, 10 wt% enrichment, 250000 FS/annum

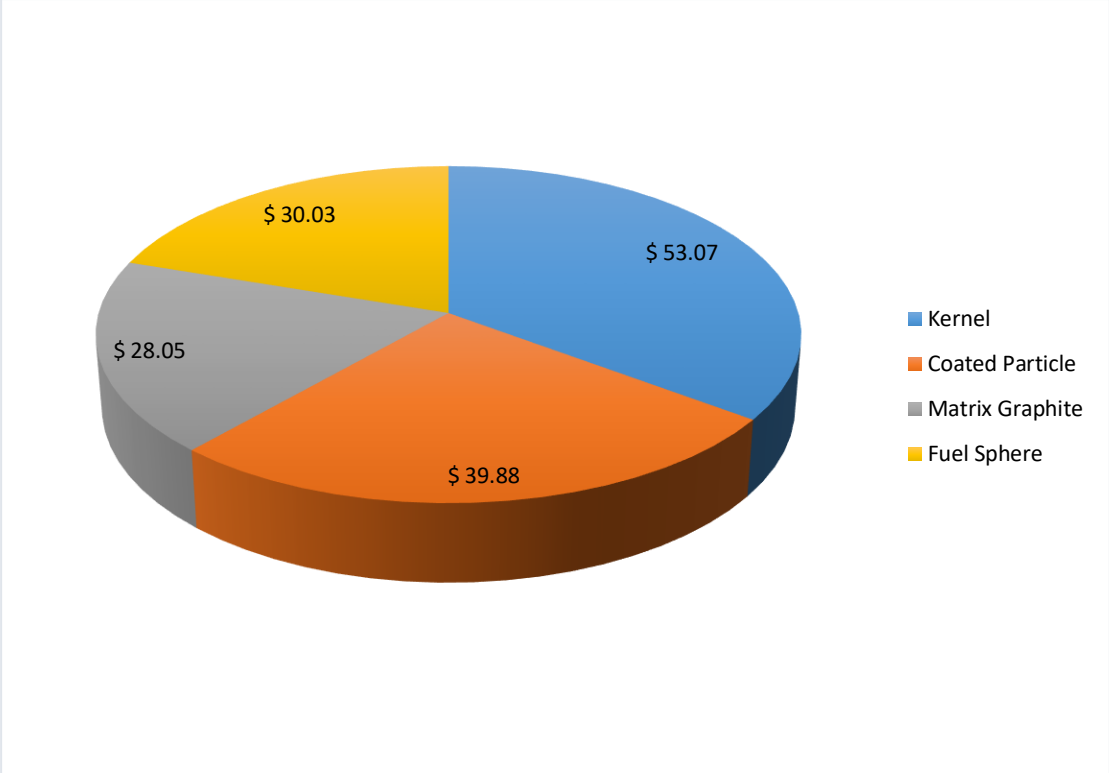

Figure 44 – Fuel sphere OPEX and CAPEX costs for ThHEU 10 g HM, 10 wt% enrichment, 250000 FS/annum

4.3.5 Fuel sphere cost breakdown

The following costs shown are for the 3 different fuels, a breakdown is given for the individual fuel sphere costs and the representative fractions of uranium and thorium within each fuel sphere.

Table 41 – Fuel sphere costs for LEU, 250000 FS/annum fuel plant

HEAVY METAL LOADING	**g**	**5**	**5**	**5**	**7**	**7**	**7**	**10**	**10**	**10**	**12**	**12**	**12**	**16**	**16**	**16**
EFFECTIVE ENRICHMENT	wt%	8	10	15	8	10	15	8	10	15	8	10	15	8	10	15
COST U	$/ FS	8.0708	10.3080	15.9430	11.2990	14.4310	22.3210	16.1420	20.6160	31.8870	19.3700	24.7400	38.2640	25.8270	32.9860	51.0190
FUEL SPHERE COST	$/ FS	126.99	129.40	135.48	131.23	134.61	143.12	142.43	147.26	159.41	147.49	153.28	167.87	161.63	169.35	188.79
NUMBER FUEL SPHERE	FS /DAY	324	236	144	218	161	101	168	124	77	159	116	72	162	116	70

Table 42 – Fuel sphere costs for ThLEU, 250000 FS/annum fuel plant

HEAVY METAL LOADING	**g**	**5**	**5**	**5**	**7**	**7**	**7**	**10**	**10**	**10**	**12**	**12**	**12**	**16**	**16**	**16**
EFFECTIVE ENRICHMENT	wt%	8	10	15	8	10	15	8	10	15	8	10	15	8	10	15
COST U	$/ FS	8.6449	10.8060	16.2090	12.1030	15.1290	22.6930	17.2900	21.6120	32.4180	20.7480	25.9350	38.9020	27.6640	34.5800	51.8700
COST Th	$/ FS	0.4527	0.3772	0.1886	0.6338	0.5281	0.2641	0.9054	0.7545	0.3772	1.0865	0.9054	0.4527	1.4486	1.2072	0.6036
COST U&Th	$/ FS	9.0976	11.1832	16.3976	12.7368	15.6571	22.9571	18.1954	22.3665	32.7952	21.8345	26.8404	39.3547	29.1126	35.7872	52.4736
FUEL SPHERE COST	$/ FS	128.08	130.33	135.95	132.76	135.91	143.78	144.63	149.13	160.38	150.33	155.73	169.22	165.38	172.58	190.57
NUMBER FUEL SPHERE	FS /DAY	344	241	145	216	158	99	145	108	72	124	94	65	109	83	60

Table 43 – Fuel sphere costs for ThHEU, 250000 FS/annum fuel plant

HEAVY METAL LOADING	**g**	**5**	**5**	**5**	**7**	**7**	**7**	**10**	**10**	**10**	**12**	**12**	**12**	**16**	**16**	**16**
EFFECTIVE ENRICHMENT	wt%	8	10	15	8	10	15	8	10	15	8	10	15	8	10	15
COST U	$/ FS	9.1093	11.3867	17.0800	12.7531	15.9413	23.9120	18.2186	22.7733	34.1600	21.8624	27.3280	40.9919	29.1498	36.4373	54.6559
COST Th	$/ FS	0.6896	0.6734	0.6328	0.9654	0.9427	0.8859	1.3792	1.3467	1.2656	1.6550	1.6161	1.5187	2.2067	2.1548	2.0250
COST U&Th	$/ FS	9.7989	12.0600	17.7128	13.7185	16.8840	24.7979	19.5978	24.1200	35.4256	23.5174	28.9440	42.5107	31.3565	38.5920	56.6809
FUEL SPHERE COST	$/ FS	128.83	131.27	137.37	133.82	137.23	145.77	146.15	151.02	163.21	152.14	157.99	172.62	167.80	175.61	195.11
NUMBER FUEL SPHERE	FS /DAY	351	243	146	213	155	97	134	100	64	109	81	53	83	61	40

Table 44 – Summation of fuel sphere costs, 250000 FS/annum fuel plant

HEAVY METAL LOADING	g	5	5	5	7	7	7	10	10	10	12	12	12	16	16	16
EFFECTIVE ENRICHMENT	wt%	8	10	15	8	10	15	8	10	15	8	10	15	8	10	15
LEU	$/ FS	126.94	129.34	135.38	131.16	134.52	142.98	142.33	147.13	159.22	147.38	153.14	167.64	161.47	169.15	188.49
ThLEU	$/ FS	128.08	130.33	135.95	132.76	135.91	143.78	144.63	149.13	160.38	150.33	155.73	169.22	165.38	172.58	190.57
ThHEU	$/ FS	128.83	131.27	137.37	133.82	137.23	145.77	146.15	151.02	163.21	152.14	157.99	172.62	167.8	175.61	195.11

Table 45 – Summation of fuel sphere costs, 250000 FS/annum fuel plant for 20 wt% LEU

HEAVY METAL LOADING	g	5	7	10	12	16
ENRICHMENT	wt%	20	20	20	20	20
COST U/FUEL SPHERE	$/ FS	21.6	30.3	43.2	51.9	69.2
FUEL SPHERE COST	$/ FS	141.59	151.67	171.63	182.54	208.35
NUMBER FUEL SPHERE	FS/DAY	105	74	57	53	50

Table 41 , **Table 42** ,**Table 43** and **Table 45** show the total cost of uranium and thorium per fuel sphere as well as the cost of an individual fuel sphere based on the effective enrichment and heavy metal loading for the various fuels. The uranium and thorium cost is shown as individual costs but are included in the fuel sphere costs shown in the table. The tables also show the fuel sphere feed rate and the total fuel costs. **Table 44** shows the individual fuel sphere costs for various heavy metal loadings and enrichments. The individual fuel spheres are cheaper when the heavy metal loading and enrichment are lower; however the reactor requires more fuel spheres when these are lower. Thus as more heavy metal and enrichment is loaded into a fuel sphere the fuel feed rate to the reactor is lower and the burn-up higher. The cost of the enriched uranium in a fuel sphere is small compared to the cost of manufacturing the whole fuel sphere, including the fuel kernels, particle coatings and pressing the graphite sphere. This means that in terms of reducing total fuel cost/kWh of electricity produced, it is more important to reduce the total number of fuel spheres consumed per hour than to reduce the total cost of the uranium that is consumed per hour. Therefore the main driving factor in the reduction of total fuel costs is increasing the cumulative amount of heat energy produced over the life of the fuel sphere, which is defined as the burn-up multiplied by the amount of heavy metal per fuel sphere, as opposed to increasing the burn-up. It has been shown in the previous chapters that increasing the heavy metal loading above the value for the maximum burn-up resulted in higher cumulative energy per fuel sphere and, by the logic above, in lower total fuel cost per kWh electrical energy produced. The overall cost or total fuel sphere cost per day is reduced as seen in the figures. This is the general trend observed in tables and figures. It is not to say that the higher the heavy metal loading the lower the fuel sphere cost, there is an optimum which will be shown in the levelised cost study which follows.

4.3.6 Levelised Costs

The levelised costs are now discussed which take everything into account to determine the $US/kWe for a single 100MWth unit. The levilized costs account for the capital costs, operation and maintenance costs, fresh fuel costs, spent fuel costs and the decommissioning costs to determine the Levilized Unit Electric Costs LUEC. The results are reported in terms of (US$/kWh) as well as (US$/MWh). The focus will be on the fresh fuel costs (US$/kWe) and the remaining costs will assume to remain constant. All values are based on current market prices and exchange rates. **Table 46** and **Table 47** show the reactor properties and output costs.

Table 46 – Reactor properties

Thermal Output	100	MWth
Thermal Efficiency	40%	
Total Electricity to grid	33	MWe
House load	3	MWe
Electricity Utilization Factor	90%	
Electricity Availability Factor	95%	
Load Factor	95%	

The fuel sphere costs are inputted based on the STL fuel cost models into the STL reactor costing model. The LUEC are based on the following equation 13:

$$LUEC = \frac{\sum_{t=1}^{n}\left[\frac{I_t + O\&M_t + D\&D + F_t + R}{(1+r)^t}\right]}{\sum_{t=1}^{n}\left[\frac{E_t}{(1+r)^t}\right]} \quad (13)$$

This formula takes into account all the capital, operation and maintenance, fresh fuel, spent fuel and decommissioning costs to give an overall cost. The following acronyms refer to:

It	Investment expenditures in year t
O&M	Operation & Maintenance expenditures in year t
D&D	Decontamination & Decommissioning
Ft	Fuel expenditures in year t
R	Royalty fee per reactor
Et	Electricity generation in year t
r	Discount rate
n	Life of system

Table 47 – Output Costs for LEU fuel at 10 g HM, 10 wt%

Burn up	**80 898**	**MWD/THM**
HM (Heavy Metal)	10	g
Fuel Spheres per day	124	per day
Fuel Spheres per annum	45119	per year
Fuel Sphere Cost	$147.26	
Fresh Fuel cost per annum	$6 644 156.84	per year
Levelized Fresh Fuel Cost	**0.0233**	**US$/kWe**
	Single-Units	1st NPP First Of A Kind (FOAK)
Th-100 NPP units		1
Electricity price (US$/kWh)		0.17
MWe		33
Electricity production (kWe)		285 305 520
Pre-Construction Cost		$100 000 000
Direct Cost		$132 785 308
Indirect Cost		$44 064 057
Contingency		$33 196 327
Total Capital Investment Cost		$310 045 692
Levelized Capital Cost (US$/kWe)		0.063
O&M		$7 577 021
Levelized O&M Cost (US$/kWe)		0.0266
Fresh Fuel Cost		$6 644 157
Levelized Fresh Fuel Cost (US$/kWe)		0.0233
Spent fuel (interim storage)		$2 030 334
Levelized Spent fuel cost (US$/kWe)		0.0071
Decommissioning sinking fund per year		$3 319 633
Levelized Decommissiong cost (US$/kWe)		0.0116
LUEC (US$/kWh)		**0.132**
LUEC (US$/MWh)		**132**

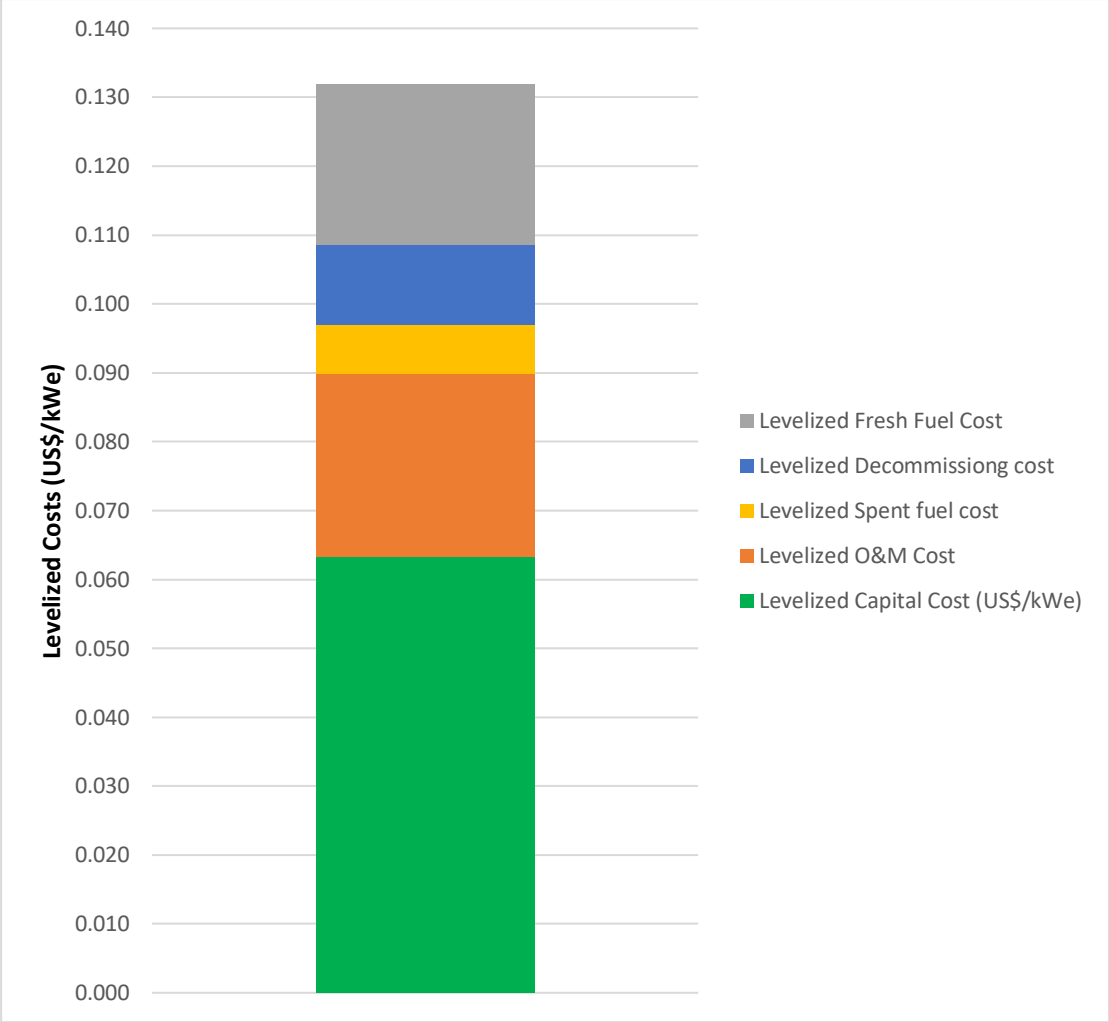

Figure 45 – Overall fuel sphere costs for LEU 10 g HM, 10 wt%

The area shown in **Figure 45** at the top of the figure (levilized fresh fuel) will be the only costs that will change for the various enrichments and loadings due to the burn-up changing which affects the fresh fuel costs. The total levilized costs can be reduced by increasing the amount of reactors at a given site, only a single reactor unit is shown 0.132 $/kWh (132 $/MWh). If the number of reactors onsite were increased to 4 the LUEC would decrease to 0.089 $/kWh (89 $/MWh) which would make the small modular pebble bed 100MW reactor a much more feasible and cost competitive option.

Table 48 – LUEC costs LEU fuel up to 15 wt%

LEU	Units:															
HEAVY METAL LOADING	g HM	5	5	5	7	7	7	10	10	10	12	12	12	16	16	16
EFFECTIVE ENRICHMENT	wt%	8	10	15	8	10	15	8	10	15	8	10	15	8	10	15
AVG. FUEL RESIDENCE TIME	DAYS	470	647	1063	700	948	1518	908	1232	1970	958	1309	2108	938	1315	2186
AVG. BURN-UP	MWD/T	61675	84851	139016	65620	88782	142000	59615	80898	129242	52485	71686	115330	38540	54021	89802
PEBBLE FEED RATE	SPHERES/DAY	324	236	144	218	161	101	168	124	77	159	116	72	162	116	70
FUEL SPHERE COST	$/ FS	127.0	129.4	135.5	131.2	134.6	143.1	142.4	147.3	159.4	147.5	153.3	167.9	161.6	169.4	188.8
LEVILIZED FRESH FUEL COST	US$/kWe	0.053	0.039	0.025	0.037	0.028	0.018	0.031	0.023	0.016	0.030	0.023	0.016	0.034	0.025	0.017
LUEC (US$/kWh)	US$/kWh	0.173	0.154	0.135	0.151	0.138	0.126	0.142	0.132	0.122	0.141	0.131	0.121	0.144	0.133	0.122
LUEC (US$/MWh)	US$/MWh	173	154	135	151	138	126	142	132	122	141	131	121	144	133	122

Table 49 – LUEC costs LEU fuel 20 wt%

HEAVY METAL LOADING	g HM	**5**	**7**	**10**	**12**	**16**
FEED ENRICHMENT	wt%	20	20	20	20	20
AVG. FUEL RESIDENCE TIME	DAYS	1453	2053	2652	2853	3038
AVG. BURN-UP	MWD/T	189780	191822	173838	156043	124758
PEBBLE FEED RATE	SPHERES/DAY	105	74	58	53	50
FUEL SPHERE COST	$/FS	141.6	151.7	171.6	182.5	208.4
LEVILIZED FRESH FUEL COST	US$/kWe	0.019	0.014	0.013	0.012	0.013
LUEC (US$/kWh)	(US$/kWh)	0.127	0.120	0.117	0.117	0.118
LUEC (US$/MWh)	(US$/MWh)	127	120	117	117	118

Table 50 – LUEC costs ThLEU fuel up to 15 wt% effective enrichment

ThLEU	Units:															
HEAVY METAL LOADING	g	5	5	5	7	7	7	10	10	10	12	12	12	16	16	16
EFFECTIVE ENRICHMENT	wt%	8	10	15	8	10	15	8	10	15	8	10	15	8	10	15
235U ENRICHMENT	%	20	20	20	20	20	20	20	20	20	20	20	20	20	20	20
AVG. FUEL RESIDENCE TIME	DAYS	442	631	1052	704	965	1538	1051	1405	2114	1226	1621	2351	1392	1828	2547
AVG. BURN-UP	MWD/T	58108	82839	137713	66032	90475	143868	69044	92260	138642	67176	88771	128631	57272	75180	104656
PEBBLE FEED RATE	SPHERES/DAY	344	241	145	216	158	99	145	108	72	124	94	65	109	83	60
FUEL SPHERE COST	$/ FS	128.1	130.3	136.0	132.8	135.9	143.8	144.6	149.1	160.4	150.3	155.7	169.2	165.4	172.6	190.6
LEVILIZED FRESH FUEL COST	US$/kWe	0.056	0.040	0.025	0.037	0.027	0.018	0.027	0.021	0.015	0.024	0.019	0.014	0.023	0.018	0.015
LUEC (US$/kWh)	US$/kWh	0.178	0.156	0.135	0.151	0.138	0.126	0.137	0.128	0.120	0.133	0.126	0.119	0.131	0.125	0.120
LUEC (US$/MWh)	US$/MWh	178	156	135	151	138	126	137	128	120	133	126	119	131	125	120

Table 51 – LUEC costs ThHEU fuel up to 15 wt% effective enrichment

ThHEU	Units:															
HEAVY METAL LOADING	g	5	5	5	7	7	7	10	10	10	12	12	12	16	16	16
EFFECTIVE ENRICHMENT	wt%	8	10	15	8	10	15	8	10	15	8	10	15	8	10	15
235U ENRICHMENT	%	93	93	93	93	93	93	93	93	93	93	93	93	93	93	93
AVG. FUEL RESIDENCE TIME	DAYS	433	626	1048	713	985	1578	1132	1528	2375	1395	1873	2884	1833	2476	3793
AVG. BURN-UP	MWD/T	56922	82214	137237	66948	92348	147438	74426	100267	155432	76475	102537	157501	75392	101758	155552
PEBBLE FEED RATE	SPHERES/DAY	351	243	146	213	155	97	134	100	64	109	81	53	83	61	40
FUEL SPHERE COST	$/ FS	128.8	131.3	137.4	133.8	137.2	145.8	146.2	151.0	163.2	152.1	158.0	172.6	167.8	175.6	195.1
LEVILIZED FRESH FUEL COST	US$/kWe	0.058	0.041	0.026	0.037	0.027	0.018	0.025	0.019	0.023	0.021	0.016	0.012	0.018	0.014	0.010
LUEC (US$/kWh)	US$/kWh	0.180	0.156	0.136	0.150	0.138	0.125	0.134	0.127	0.119	0.129	0.123	0.116	0.124	0.119	0.114
LUEC (US$/MWh)	US$/MWh	180	156	136	150	138	125	134	127	119	129	123	116	124	119	114

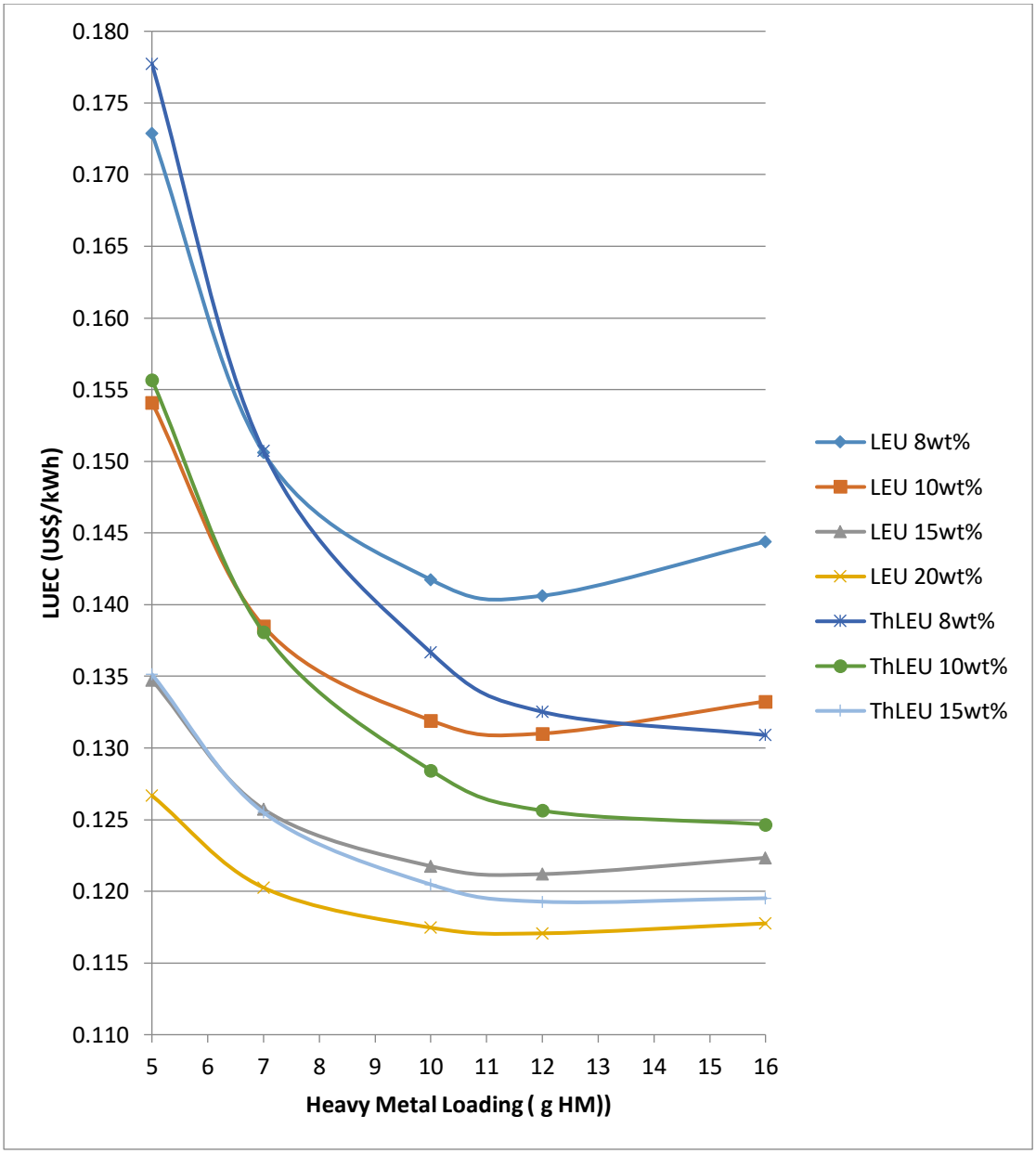

Figure 46 – Levilized unit energy costs per kWh of electrical energy produced as a function of HM loading, for various enrichments.

The results in **Figure 46** show that as the HM loading and enrichment is increased the cumulative heat energy increases and the LUEC decreases. ThHEU will not be discussed due to the proliferation problems associated with it. LEU at 20 wt% and 12 g HM is the lowest at 12 g HM followed by 10 g HM and 12 g HM. ThLEU at 15 wt% and 12 g HM is lower than LEU at 15 wt% for all HM loadings.

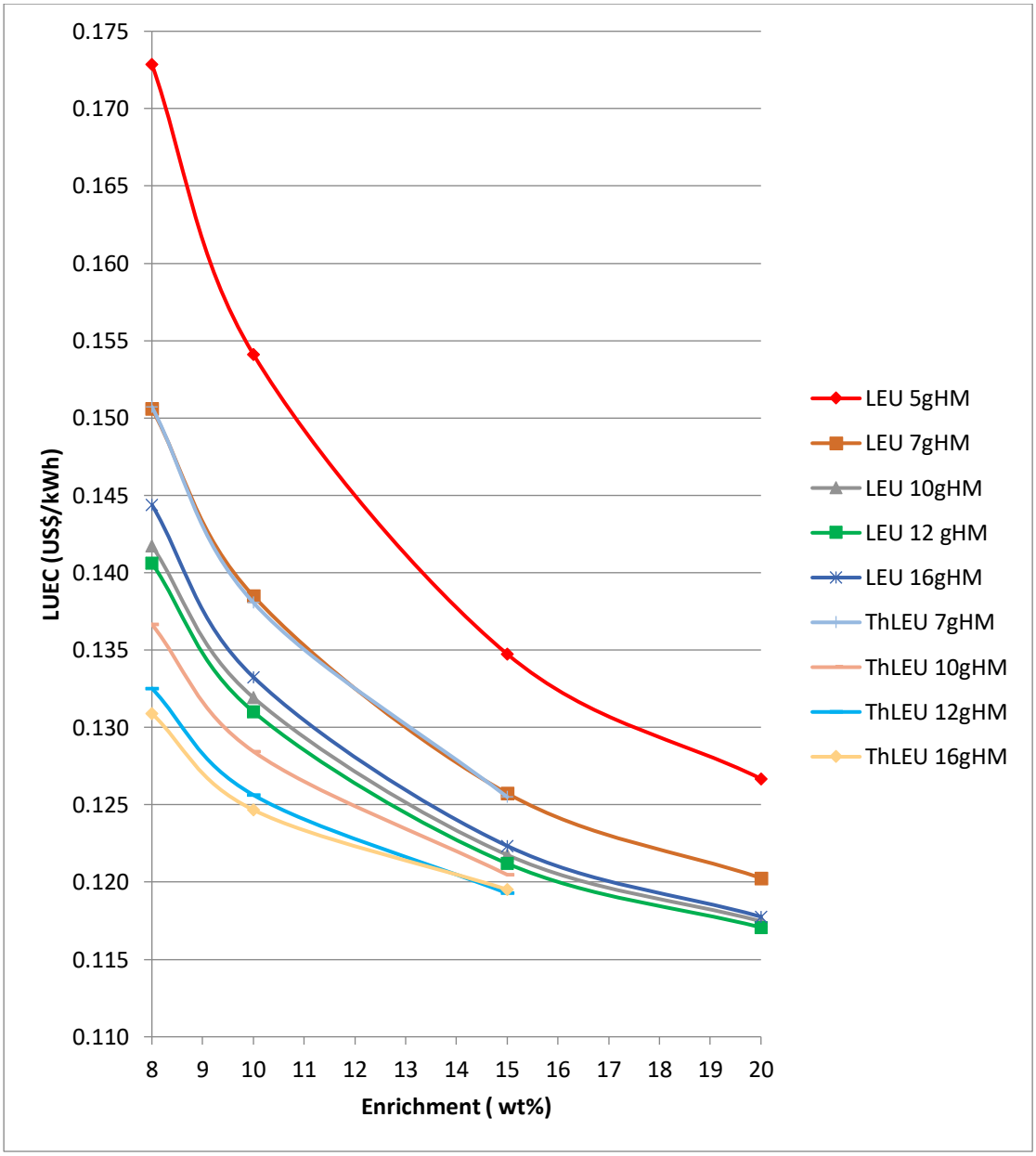

Figure 47 – Levelised unit energy costs per kWh of electrical energy as a function of enrichment, for various HM loadings.

Figure 47 is a confirmation of the above statements that as the enrichment is increased the cumulative heat energy increases and the LUEC decreases.

Reducing the total fuel cost per kWh of electrical energy produced is more related to increasing the cumulative amount of heat energy produced during the life of each fuel sphere, than to increasing the burn-up. Therefore, increasing the heavy metal loading

above the value for the maximum burn-up will likely result in lower fuel cost per kWh electrical energy produced.

As can be seen from **Figure 46** and **Figure 47** LEU at 20 wt% for 12 g HM would provide the lowest LUEC at (LUEC = 117 US$/MWh) closely followed by LEU at 10 g HM (LUEC 117 US$/MWh) and LEU at 16 g HM (LUEC 118 US$/MWh).

In **Figure 46** at lower enrichments such as 15 wt% ThLEU would have the lowest LUEC at 12 g HM (LUEC = 119 US$/MWh) followed by ThLEU at 16 g HM (LUEC = 120 US$/MWh) and ThLEU at 10 g HM (LUEC = 120 US$/MWh). LEU at 15 wt% would have a minimum at 12 g HM (LUEC = 121 US$/MWh).

In **Figure 46** it can be seen that at 10 wt% enrichment it can be seen that at higher enrichments ThLEU has a lower LUEC compare to LEU at the same enrichment. ThLEU being lowest at 16 g HM (LUEC = 125 US$/MWh) followed by 12 g HM (LUEC = 126 US$/MWh) while LEU at 12 g HM is lowest (LUEC = 131 US$/MWh).

The general trend which is observed is that as the enrichment and HM increase the cumulative amount of heat energy increases and the LUEC decreases however, there is a point at where increasing the HM loading to a greater extent actually lowers the LUEC and there is an optimum for each fuel type. It can also be seen that generally 12 g HM actually provides a lower LUEC than compared to 16 g HM for each fuel.

Another observation is that the maximum burn-up discussed at the beginning of the results and discussion chapter does not account for the lowest LUEC. The cumulative amount of heat energy is the driving factor to a lower LUEC and thus increasing the HM loading and enrichment will provide a lower LUEC up to a certain HM loading. These higher enrichments and heavy metal loadings increase the cumulative amount of heat energy per kWh which reduces the fuel costs.

Thorium based fuels only start performing at higher HM loadings. Replacing U-238 with Th-232 is only viable at high heavy metal loadings where there are enough thorium

particles to make a substantial difference where the captures that do occur produce U-233. Th-232 which is replacing U-238 leads to less captures in the Th and thus leaves more neutrons available for causing fissions in the fissile fuel. This thorium is converted into U-233 which is the best thermal fuel in a HTR (Lung & Gremm, 1997). Increasing the HM loading and enrichment does in fact increase the cumulative heat energy produced and does lower the LUEC.

4.4 Verification & Validation

In this section there will be a comparison between the work Prof Eben Mulder completed for STL vs the work I have completed here for my thesis for the same reactor geometry and configuration. Prof Mulder uses the VSOP-A suite of codes while I use VSOP 99/11. The VSOP-A set of data has been independently derived by a separate system of design codes (DATA2, ZUT, BIRGIT, FIRZIT, TOTMOS-A, etc.) this approach verifies the data produced by VSOP 99/11. The results are similar and the V&V is successful. Prof Mulder used the following input parameters which are the same as my models as seen in **Table 52** and **Table 53**.

Table 52 – HTMR100 general description Prof Eben Mulder model

	Nominal value/description	Unit
Thermal power	100	MW_{th}
Primary coolant	Helium	
Moderator	Graphite	
Core geometry	Cylindrical	
Core volume	27.6	m^3
Average power density	3.62	MW_{th}/m^3
Pebble bed diameter	260	cm
Pebble bed effective height	552	cm

Table 53 – HTMR100 general description STL model

	Nominal value/description	Unit
Thermal power	100	MW_{th}
Primary coolant	Helium	
Moderator	Graphite	
Core geometry	Cylindrical	
Core volume	28.1	m^3
Average power density	3.57	MW_{th}/m^3
Pebble bed diameter	260	cm
Pebble bed effective height	522.6	cm

The core heights, volume and power density are slightly different; however, the burn-up should be similar for the various fuels. The STL models use 10 wt% enrichment whereas Prof Mulder uses 10.82 wt% for LEU and 10.76 wt% for ThLEU. It is unnecessary to do precise models because of the differences in graphite impurities and volume differences.

Table 54 – HTMR100 neutronic output Prof Eben Mulder model for 12 g HM

Cycle		Th/U20%	LEU
Enrichment of feed fuel	w%	10.76	10.82
Fuel residence time	Years	3.8	3.8
Target burn-up	MWd/Kg HM	77.5	77.4
Conversion ratio		0.519	0.487
U_3O_8 requirement	Kg/GWd_{th}	359	357
Loading → unloading:			
Fissile: U-233	Kg/GWd_{th}	0 – 0.14	-
U-235	Kg/GWd_{th}	1.39 – 0.50	1.40 – 0.52
Pu-239 + Pu-241	Kg/GWd_{th}	0 – 0.11	0 – 0.17
Fertile: Th-232	Kg/GWd_{th}	5.90 – 5.65	-
U-238	Kg/GWd_{th}	5.62 – 5.25	11.51 – 10.95
Pu-240	Kg/GWd_{th}	0 – 0.03	0 – 0.05
Additionally Pu-242	Kg/GWd_{th}	0 – 0.01	0 – 0.02
Fractional neutron absorption :			
Fissile: U-233	%	3.7	-
U-235	%	34.4	33.3
Pu-239 + Pu-241	%	12.9	18.5
Fertile: Th-232	%	9.4	-
U-238	%	14.0	20.9
Pu-240	%	3.1	4.5
Additionally Pu-242	%	0.1	0.1
In-situ utilization of bred nuclides:			
U-233	%	40.2	-
Pu-239 + Pu241	%	75.6	73.4

Table 55 – HTMR100 neutronic output STL models 12 g HM

LEU	Units	
HEAVY METAL LOADING	g HM	12
FEED ENRICHMENT	wt%	10
AVG. FISSILE ENRICHMENT	%	6.61
AVG. FUEL RESIDENCE TIME	DAYS	1309
AVG. BURN-UP	MWD/T	71686
PEBBLE FEED RATE	SPHERES/DAY	116
ThLEU		
HEAVY METAL LOADING	g HM	12
FEED ENRICHMENT	wt%	10
AVG. FISSILE ENRICHMENT	%	5.75
AVG. FUEL RESIDENCE TIME	DAYS	1621
AVG. BURN-UP	MWD/T	88771
PEBBLE FEED RATE	SPHERES/DAY	94

As will be shown below the HM loading is the same for both cases 12 g HM and comparing a 10 wt% enrichment for LEU as well as ThLEU (Th/U20%) the burn-ups are relatively similar for both models when compared to Prof Mulders model shown in Table 54 and **Table 55** . The VSOP-A and VSOP results will not be the exact same due to different concentrations of impurities within the graphite as well as a slightly different core height, volume and power density as well as the nuclear data libraries. The LEU model for VSOP-A provides a burn-up of 77400 MWD/T (residence time 3.8 years) while VSOP99/11 has a value of 71686 MWD/T for a residence time of 3.6 years. The ThLEU model in VSOP-A has a burn-up of 77500 MWD/T (residence time 3.8 years) while VSOP99/11 has a burn-up of 88771 MWD/T with a residence time of 4.44 years. Prof Mulder used a slightly higher uranium enrichment 10.86 wt% as opposed to 10 wt% used in the VSOP 99/11 models. This is why his burn-up results are slightly higher, however still comparable. The LEU case is enough evidence to support the theory that the two models are similar. The conversion ratio of the LEU fuel

is also similar 0.487 for VSOP-A and 0.491 for the VSOP 99/11 model as seen in Table 54 and **Table 56**.

Table 56 – HTMR100 STL model, Conversion ratio, source neutron/fissile absorption & capture/fission in fissile material

LEU		
HEAVY METAL LOADING	g HM	12
FEED ENRICHMENT	wt%	10
CONVERSION RATIO	CR	0.491
SOURCE NEUTR./FISSILE ABS.	ηε	1.934
CAPTURE/FISSION IN FISS.MAT.	α	0.337
ThLEU		
HEAVY METAL LOADING	g HM	12
FEED ENRICHMENT	wt%	10
CONVERSION RATIO	CR	0.483
SOURCE NEUTR./FISSILE ABS.	ηε	1.991

The fraction of neurons absorbed in the LEU models for VSOP-A are 33.3% in U-235 and 20.9% in U-238 as seen in **Table 54**. VSOP99/11 has values of 33.09% in U-235 and 21.4% in U-238 that can be seen in **Table 57** . Pu-239 & Pu-241 are 20.9% in VSOP-A while in VSOP99/11 they are 18.61. In VSOP-A for the ThLEU case seen in **Table 54** 3.7% U-233 is absorbed while in VSOP99/11 seen in **Table 58** this is 5.58% with U-235 34.4% and 14% in U-238 in VSOP-A and 33.59 and 10.49% in U-238 in VSOP99/11. For ThLEU the Pu-239 & Pu-241 are 12.9% in VSOP-A while in VSOP99/11 they are 11.06. These values are within range.

Table 57 – Neutron losses in heavy metals for LEU STL model

HEAVY METAL LOADING	g HM	12
FEED ENRICHMENT	wt%	10
NEUTRON LOSSES IN HEAVY METALS	%	78.23
ESP. IN FISSILE ISOTOPES	%	51.7
ESP. IN TH-232	%	
ESP. IN PA-233	%	
ESP. IN U -233	%	
ESP. IN U -234	%	0.16
ESP. IN U -235	%	33.09
ESP. IN U -236	%	0.53
ESP. IN U -237	%	
ESP. IN U -238	%	21.40
ESP. IN NP-237	%	0.13
ESP. IN NP-239	%	0.03
ESP. IN PU-238	%	0.02
ESP. IN PU-239	%	16.29
ESP. IN PU-240	%	4.09
ESP. IN PU-241	%	2.32
ESP. IN PU-242	%	0.08
ESP. IN AM-241	%	0.06
ESP. IN AM-242M		
ESP. IN AM-243	%	0.02
IN FISSION PRODUCTS	%	5.68
ESP. IN XE-135	%	1.71
CORE-LEAKAGE	%	14.76

Table 58 – Neutron losses in heavy metals for ThLEU STL model

HEAVY METAL LOADING	g HM	12
FEED ENRICHMENT	wt%	10
NEUTRON LOSSES IN HEAVY METALS	%	76.14
ESP. IN FISSILE ISOTOPES	%	50.22
ESP. IN TH-232	%	11.19
ESP. IN PA-233	%	0.21
ESP. IN U -233	%	5.58
ESP. IN U -234	%	0.28
ESP. IN U -235	%	33.59
ESP. IN U -236	%	0.68
ESP. IN U -237	%	
ESP. IN U -238	%	10.49
ESP. IN NP-237	%	0.22
ESP. IN NP-239	%	0.01
ESP. IN PU-238	%	0.05
ESP. IN PU-239	%	9.13
ESP. IN PU-240	%	2.64
ESP. IN PU-241	%	1.93
ESP. IN PU-242	%	0.06
ESP. IN AM-241	%	0.04
ESP. IN AM-242M		
ESP. IN AM-243	%	0.02
IN FISSION PRODUCTS	%	6.93
ESP. IN XE-135	%	1.86
CORE-LEAKAGE	%	15.29

The VSOP-A LEU in Table 54 model has a U-235 supply of 1.4 Kg/GWd and a U-238 of 11.51 Kg/GWd while VSOP99/11shown in Table 59 has a U-235 supply of 1.4 Kg/GWd and a U-238 of 12.53 Kg/GWd. The ThLEU model in VSOP-A in Table 54 has

a U-233 discharge of 0.14 Kg/GWd and a U-235 supply of 1.39 Kg/GWd and a U-238 of 5.62. VSOP99/11 in **Table 60** has a U-233 discharge of 0.1388 Kg/GWd and a U-235 supply of 1.12 Kg/GWd and a U-238 of 4.54. All these values are in range and the VSOP-A and VSOP99/11 models produce similar results thus verifying and validating the results which I ran.

Table 59 – Supply/Discharge LEU STL model

		Supply	Discharge
TH-232	Kg/GWd		
U -233	Kg/GWd		
U -234	Kg/GWd	0.0137	0.0095
U -235	Kg/GWd	1.3939	0.5241
U -236	Kg/GWd	0.0000	0.1528
U -238	Kg/GWd	12.531	11.9586
NP-237	Kg/GWd	0.0000	0.0104
PU-238	Kg/GWd	0.0000	0.0036
PU-239	Kg/GWd	0.0000	0.1324
PU-240	Kg/GWd	0.0000	0.0557
PU-241	Kg/GWd	0.0000	0.0411
PU-242	Kg/GWd	0.0000	0.0154
AM-241	Kg/GWd	0.0000	0.0053
AM-242M	Kg/GWd		
AM-243	Kg/GWd	0.0000	0.0019
CM-244	Kg/GWd	0.0000	0.0004

Table 60 – Supply/Discharge ThLEU STL model

		Supply	Discharge
TH-232	Kg/GWd	5.556	5.2677
U -233	Kg/GWd	0	0.1388
U -234	Kg/GWd	0.0114	0.0203
U -235	Kg/GWd	1.1256	0.2563
U -236	Kg/GWd	0.0000	0.1444
U -238	Kg/GWd	4.5484	4.2712
NP-237	Kg/GWd	0.0000	0.0116
PU-238	Kg/GWd	0.0000	0.005
PU-239	Kg/GWd	0.0000	0.0351
PU-240	Kg/GWd	0.0000	0.0215
PU-241	Kg/GWd	0.0000	0.0156
PU-242	Kg/GWd	0.0000	0.0129
AM-241	Kg/GWd	0.0000	0.0021
AM-242M	Kg/GWd		
AM-243	Kg/GWd	0.0000	0.0013
CM-244	Kg/GWd	0.0000	0.0004

5 SUMMARY, CONCLUSIONS AND RECOMMENDATIONS

5.1 Thorium

Due to HEU being a proliferation risk, ThHEU fuel can be ruled out. It does, however, outperform LEU fuels in terms of the highest cumulative energy per fuel sphere and the lowest LUEC. Therefore, LEU at 20 wt% and high HM loadings (12 g HM) is the best fuel to use in this 100MW_{th} OTTO cycle reactor which would provide the highest cumulative energy per fuel sphere and the lowest LUEC by just the analysis of the burn-up, cumulative heat energy and LUEC results. The safety aspects have not been taken into consideration.

Adding thorium to LEU at 20wt% always reduces the enrichment. It means that if equal number densities of Th-232 and U-238 are loaded into a fuel sphere, the U-238 will breed about four times as much Pu-239, compared to the U-233 that will be bred by the Th-233. This means that the poor neutron economy of Pu-239 will dominate over the excellent neutron economy of U-233. Two obvious ways to counter this problem is to reduce the U-238 by increasing the enrichment from LEU to HEU or to increase the amount of Th in the fuel sphere by increasing the HM loading. Both strategies have been implemented in this study and both worked. ThHEU outperformed the ThLEU. However, when the enrichment is increased above the 20 wt% of LEU, the nuclear weapons proliferation risk increases and therefore as higher enrichments are prohibited by law in most countries, it is not considered a viable strategy. The most viable strategy for using Th in Pebble Bed Reactors is to increase the HM loading.

5.2 Maximum burn-up

The trend of maximum burn-up at a HM loading of 7 g per fuel sphere for LEU suggests that when the HM loading is decreased below 7 g HM per fuel sphere, increasing leakage dominates over increasing resonance escape probability and therefore burn-up decreases. When the HM loading is increased above 7 g HM per fuel sphere, decreasing resonance escape probability dominates over decreasing leakage and therefore burn-up decreases with increasing HM loading above 7 g HM per fuel sphere.

The peak burn-up at 10 g HM per fuel sphere for the ThLEU mixtures can be explained as follows; the resonance integrals for Th-232 in the epithermal energy windows are about 4 times smaller than for U-238, which means that Th is by a factor four weaker capturer of epithermal neutrons than U-238. This means that the problem of decreasing resonance escape probability with increasing HM loading is much less pronounced for Th-based mixtures than for U-238 based mixtures and therefore the maximum burn-up will be attained at higher HM loadings for Th-based mixtures.

If one starts with LEU (20 wt%) and starts adding Th, the effective enrichment of the mixture decreases monotonously with increasing fractions of Th. This means that the 15% effective enrichment ThLEU fuel mixtures contains much less Th than those with the lower enrichments, which means that the 15% mixture will behave more like a U-238 based fuel, while the lower enrichments will behave more like Th-based fuels. This explains while, just like the pure LEU fuel mixtures the 15% ThLEU mixture has a maximum burn-up at 7 g HM per fuel sphere, while the lower enrichment ThLEU fuel mixture reach their maximum burn-up only at 10 g HM per fuel sphere.

By the same logic, the ThHEU fuel mixtures contain almost no U-238 and therefore a higher fraction of Th-232. Therefore they reach their maximum burn-ups at the even higher 12 g HM per fuel sphere.

5.3 Individual fuel sphere costs

The individual fuel spheres are cheaper when the heavy metal loading and enrichments are lower; however, the reactor requires more fuel spheres when these values are lower. Thus, as more heavy metal and enrichment is loaded into a fuel sphere the fuel pebble feed rate required by the reactor is lower and the burn-up higher. The main driving factor in the reduction of costs is the cumulative amount of heat energy which is obtained from the burn-up multiplied by the amount of heavy metal per fuel sphere; therefore, due to the high cost of fuel spheres, the lowest fuel cost per kWh electricity produced, is more related to the cumulative amount of heat energy produced during the life of each fuel sphere, than to the burn-up. Therefore, increasing the heavy metal loading above the value for the peak burn-up results in higher cumulative energy per fuel sphere and thus lower fuel cost per kWh electrical energy produced. The general trend observed is the higher the enrichment and heavy

metal loading the higher the cumulative heat energy and the lower the LUEC will be. The uranium and thorium costs per fuel sphere are low when compared to the actual processes and manufacturing of a fuel sphere and thus the main costs have to do with all aspects associated with manufacturing a fuel sphere thus if the cumulative heat energy can be increased by adding more heavy metal and increasing the enrichment within a fuel sphere the cost/kWh can be reduced and thereby making the fuel cheaper.

5.4 LUEC

As discussed in the LUEC previously the LEU at 20 wt% for 12 g HM would provide the lowest LUEC at (LUEC = 117 US$/MWh) closely followed by LEU at 10 g HM (LUEC = 117 US$/MWh) and LEU at 16 g HM (LUEC = 118 US$/MWh) (Steenkampskraal Thorium Limited, 2017).

Lower enrichments such as 15 wt% ThLEU would have the lowest LUEC at 12 g HM (LUEC = 119 US$/MWh) followed by ThLEU at 16 g HM (LUEC = 120 US$/MWh) and ThLEU at 10 g HM (LUEC = 120 US$/MWh). LEU at 15 wt% would have a minimum at 12 g HM (LUEC = 121 US$/MWh) (Steenkampskraal Thorium Limited, 2017).

At 10 wt% enrichment it can be seen that at higher enrichments ThLEU has a lower LUEC compared to LEU at the same enrichment. ThLEU being lowest at 16 g HM (LUEC = 125 US$/MWh) followed by 12 g HM (LUEC = 126 US$/MWh) while LEU at 12 g HM is lowest (LUEC = 131 US$/MWh) (Steenkampskraal Thorium Limited, 2017).

The general trend which is observed is that as the enrichment and HM increase the cumulative amount of heat energy increases and the LUEC decreases; however, there is a point at where increasing the HM loading to a greater extent actually increases the LUEC and there is an optimum for each fuel type. It can also be seen that generally 12 g HM actually provides a lower LUEC than compared to 16 g HM for each fuel.

Another observation is that the maximum burn-up discussed at the beginning of the results and discussion chapter does not account for the lowest LUEC. The cumulative amount of heat energy is the driving factor to a lower LUEC and thus increasing the

HM loading and enrichment will provide a lower LUEC up to a certain HM loading. These higher enrichments and heavy metal loadings increase the cumulative amount of heat energy per kWh which reduces the fuel costs.

5.5 DLOFC

The main aim of the DLOFC runs is to analyse the fuel when a loss of coolant accident occurs and see whether the fuel remains below its operating limitation of 1600˚C for a certain period of time. This ensures that no gaseous metallic fission products diffuse through the SiC layer. Fuels with enrichments higher than 10 wt% surpass the Maximum DLOFC temperature limitation of 1600 ˚C. ThHEU fuel at 10wt% also fails the DLOFC temperature limitations due to the formation of larger amounts of Pa-233 being formed which is summed up below. LEU and ThLEU of 10 wt% enrichment and lower remain below the maximum DLOFC temperature limitation for all HM loadings, that being LEU at 7 g HM, 10 g HM and 12g HM.

The general trends which have been deduced from this DLOFC study are that as the enrichment increases the DLOFC fuel temperatures increase. The increased enrichment in the fuel concentrates the power to the top of the core and also increases the maximum relative power at the top due to the power profile being moved up. This overloads and concentrates the power at the top of the core, there is therefore more probability that a hotspot can occur at the top of the core due to the increased power and therefore also increased DLOFC fuel temperatures.

Thorium based fuels also increase the DLOFC fuel temperatures. ThHEU has the highest fuel temperatures followed by ThLEU and finally the lowest fuel temperature being LEU. This is again due to the thorium-based fuels having increased thorium contents and thus more production of Pa-233 which has a longer half-life and increases the maximum fuel temperatures. ThHEU will have the largest production of Pa-233 and thus have the highest DLOFC fuel temperature, ThLEU will be second with LEU having the lowest fuel temperature as Np-239 formed from U-238 has a short half-life.

Another trend observed is as the heavy metal loading increases the DLOFC fuel temperatures decreases. Increasing the HM loading reduces the relative power at the top of the core and shifts the peak downwards. Higher HM loadings burn slower and last longer, they also increase the power level lower down in the core. The higher the HM loading the flatter the profile which reduces the chances for hotspots as it spreads the power out over a larger area and in a DLOFC accident the fuel temperatures will

be lower. Thorium also shifts the power profiles down by reducing the relative power at the top of the core, however the Pa-233 formation outweighs the axial power reduction and the thorium-based fuels still have higher DLOFC fuel temperatures.

5.6 Water-Ingress

The heavy metal loading also needs to be kept at a lower limit due to problems associated with potential water-ingress problems with a steam generator tube rupture. Limiting the mass of heavy metal per fuel sphere (inherent safety) will also limit the reactivity increase when water ingresses into the reactor core. A lower HM loading reduces the volume fraction of the coated fuel particles and thus increases the average distance between fuel kernels. Neutrons thus, on average, traverse longer path lengths of graphite between collisions with fuel kernels. The probability of getting moderated before being captured in the resonances of U-238, i.e. the resonance escape probability, thus increases. Since fewer neutrons are now captured in the fuel, reducing these captures even further, by improving the moderation by means of water ingress, will thus cause a smaller increase in k_{eff}. The safest HM loading to use when using a LEU fuel cycle would be a 7 g HM loading. According to (Lohnert G.H., 1992) for any amount of water/steam that ingresses into the reactor core a 7 g HM loading or lower would be sufficiently low enough (under moderated) that the effects from water ingress such as reactivity increase and decrease in control rod worth will not lead to a spike in reactivity which may run away if all safety systems were to fail. So, the only fuels to qualify would be 7 g HM LEU or lower for inherent safe operation of this $100MW_{th}$ reactor core, 5 g HM would be best however the cumulative heat energy produced by this fuel is low and the fuel pebble feed rate is extremely high to the reactor as many pebbles are needed daily to keep the reactor critical. The 5 g HM fuel has a low burn-up and cumulative energy and thus the 7 g HM (6.3g U-238) is suggested for the 100MW reactor for LEU based fuel. The only cases that would be able to provide a decent burn-up/ cumulative heat energy at a low fuel consumption rate is LEU at 7 g HM 10 wt% (LUEC = 138.49 US$/MWh)

Thorium based fuels such as ThLEU can be inherently safe at a higher HM loading in a water ingress scenario due to the fact the resonance integrals for Th-232 in the epithermal energy windows are about 4 times smaller than for U-238, which means that Th is a factor four weaker capturer of epithermal neutrons than U-238 thus adding Th reduces these captures even further and thus a higher HM loading can be allowed

for these fuels which wouldn't increase k_{eff} excessively. Thorium fuels also need to be used at higher HM loadings in order to effectively be used due to the fact that Th-232 in the epithermal energy is around 4 times smaller than for U-238.

If the inherent water ingress value is safest for a 7 g HM LEU case which contains (6.3g U-238) then the ThLEU fuel which provides the same U-238 equivalent mass taking into consideration of thorium being 4 times smaller (6.3g – ¼ x 6.3g = 4.8g U-238) would be a ThLEU at a HM loading of 12 g HM (1.2g U-235, 4.8g U-238 and 6g Th). Anything under this would also be inherently safe too.

5.7 Final conservative summary

The main driving factor in the reduction of costs is the cumulative amount of heat energy which generally relates to the lowest LUEC. The general trend seen is the higher the enrichment and HM loading the higher the cumulative heat energy and the lower the LUEC. There is an optimum when it comes to the LUEC as increasing the HM loading continuously eventually raises the LUEC.

ThHEU is not a potential fuel due to the fact that HEU has proliferation problems associated with it. LEU and ThLEU are the only fuels which can be used in this 100MWth OTTO reactor. LEU at 20 wt% and 12 g HM would have the highest cumulative energy per fuel sphere and the lowest total LUEC however this reactors requirement is inherently safety, therefore conservative DLOFC and water-ingress limitations are placed on this $100MW_{th}$ reactor. Therefore there are only a select few fuels which qualify for inherent safety.

All LEU and ThLEU fuels at 10wt% and below remain below the DLOFC temperature limitation. The fuels which surpass the conservative water-ingress requirements are LEU at 7 g HM and lower and ThLEU at 12gHM or lower.

Therefore the two fuels which qualify the DLOFC and water ingress requirements which provide the lowest LUEC and highest cumulative amount of heat energy are LEU at 7 g HM and 10 wt% which has a LUEC of (138.49 US$/MWh) and a burn-up of

88782 MWD/THM which uses 161 fuel spheres per day and ThLEU at 10 wt% 12 g HM (LUEC = 126 US$/MWh) and a burn-up of 88771 MWD/THM at 94 fuel spheres per day. I would therefore recommend the ThLEU fuel to a utility for this 100MW_{th} reactor (Steenkampskraal Thorium Limited, 2017).

If there is no possibility of water ingress (such as a direct cycle) higher HM loadings should rather be used. The fuel sphere costs can be reduced if the fuel sphere plants throughput could be increased from 250 000 fuel spheres/annum (147.26$/FS, 10 wt% 10 g HM LEU) to 800 000 fuel spheres/annum (91.05 $/FS 10 wt% 10 g HM LEU), however a larger fleet of reactors would be needed for such a large fuel plant. The cost in terms of $/kWh or $/MWh can be reduced if the fuel sphere costs are reduced as well as if there are more reactors on the same site, this greatly reduces costs from 132 $/MWh (1 unit) to 89 $/MWh (4 units) and thus a pebble bed reactor option is feasible and cost competitive (all around the world) with other forms of energy (Steenkampskraal Thorium Limited, 2017).

5.8 Conclusion

Pebble Bed Reactor (PBR) fuel is expensive and if the fuel costs per unit of electrical energy produce ($/kWh) can be reduced it would make the pebble bed reactor a more feasible option. The two components of the cost of producing the fuel spheres are the cost of producing the coated fuel particles, which includes of the cost of the fuel kernels which contain the enriched nuclear fuel (for instance Low Enriched Uranium (LEU)) and the cost of the coating layers around these fuel kernels, and the cost of the producing the graphite spheres in which these fuel kernels are imbedded. The cost of the coatings and the graphite spheres dominate over the cost of the nuclear fuel. Therefore, the attempt to reduce total fuel costs should not focus primarily on reducing the cost of the nuclear fuel, but rather on reducing the costs of the fuel manufacture. In practice this means that the number of fuel spheres used to produce a unit of electrical energy should be reduced. Therefore, the cumulative amount of heat energy produced over the life of the fuel sphere should be increased. By definition this can be achieved by increasing the burn-up of the nuclear fuel and by increasing the heavy metal (HM) loading per fuel sphere.

This was attempted by varying the enrichment and HM loading for LEU and for a mixture of thorium (Th) and LEU (ThLEU), as well as a mixture of Th and Highly Enriched Uranium (HEU), in a small 100 MW_{th} Pebble Bed Reactor with a cylindrical

core and a Once Through Then Out (OTTO) fuelling cycle. The neutron physics and thermo-hydraulic performance of this core were simulated using the VSOP 99/11 suite of codes. The aim with the addition of Th was to improve the neutron economy as the U-233 which is bred from the Th-232 is the fissile nuclear fuel with the best neutron economy in thermal nuclear reactors. The HEU-based fuels showed the best performance. However, since the use of HEU is illegal in most countries, due to its high nuclear weapons proliferation risk, the performance of the HEU fuels were excluded from this summary.

As was expected, the results showed that the burn-up of the nuclear fuel increased sharply and monotonously with increasing enrichment. Therefore, the LEU with the highest allowable enrichment, namely 20 wt%, produced the highest burn-up and therefore the highest cumulative energy per fuel sphere and therefore the lowest total fuel cost per unit of electrical energy produced.

Adding Th to LEU fuel sphere in order to obtain a ThLEU fuel sphere by definition reduces the enrichment of the mixture and increases the HM loading. This decrease in enrichment decreased the burn-up substantially and therefore the ThLEU fuel spheres always produced lower cumulative energies than the pure 20 wt% fuel spheres from which they were formed.

From the very low HM loading of 5 g HM/ fuel sphere, the burnup first increased with increasing HM loading until it peaked at 7 g HM for LEU and at 10 g HM for ThLEU, where after it decreased with increasing HM loading. The reason for the poor burn-up at very low HM loadings was excessive neutron leakage from the core. The reason for decreasing burnups at very high HM loadings was that the decreasing distance between fuel kernels resulted in under moderation, which is known to reduce burn-up.

Since, for a given burn-up, cumulative energy per fuel sphere is directly proportional to HM loading, increasing the HM loading above the values of maximum burn-up resulted in increased cumulative energies, where after it peaked and declined as increasing HM loading sharply reduced the burn-up by increasing the problem of under moderation. The maximum cumulative energy was achieved at 16 g HM loading for LEU and at 16 g HM loading for ThLEU, however the lowest Levilised Unit Energy Costs (LUEC) were achieved at 12 g HM for LEU and 12 g HM for ThLEU. The general trend which is observed is that as the enrichment and HM increase the cumulative amount of heat energy increases and the LUEC decreases; however there is a point

at where increasing the HM loading to a greater extent actually increases the LUEC and there is an optimum for each fuel type. It can also be seen that generally 12 g HM actually provides a lower LUEC than compared to 16 g HM for each fuel.

The lowest total fuel costs were achieved for the following fuel compositions for a single FOAK reactor on site, not a multi-pack (many reactors on one site):

LEU at 20 wt% for 12 g HM would provide the lowest LUEC at (LUEC = 117 US$/MWh) closely followed by LEU at 10 g HM (LUEC = 117 US$/MWh) and LEU at 16 g HM (LUEC = 118 US$/MWh).

Lower enrichments such as 15 wt% ThLEU would have the lowest LUEC at 12 g HM (LUEC = 119 US$/MWh) followed by ThLEU at 16 g HM (LUEC = 120 US$/MWh) and ThLEU at 10 g HM (LUEC = 120 US$/MWh). LEU at 15 wt% would have a minimum at 12 g HM (LUEC = 121 US$/MWh).

At 10 wt% enrichment it can be seen that at higher enrichments ThLEU has a lower LUEC compare to LEU at the same enrichment. ThLEU being lowest at 16 g HM (LUEC = 125 US$/MWh) followed by 12 g HM (LUEC = 126 US$/MWh) while LEU at 12 g HM is lowest (LUEC = 131 US$/MWh).

Increasing the enrichment unfortunately substantially increased the maximum fuel temperature during Depressurised Loss Of Forced Coolant (DLOFC) accidents. The reason was that increasing enrichment increased the sharpness in the peaks, near the top of the fuel core, in the axial profiles of the power density. This increased power hotspot near the top of the core also resulted in a hotspot in the decay heat and thus in the maximum temperature profiles during the DLOFC accidents. This increase in DLOFC temperatures with increasing enrichment means that there is a limit to the extent that increasing enrichments can be used to reduce fuel costs.

On the other hand, increasing the HM loading slightly reduced the maximum DLOFC temperatures. The reason was that increasing HM loading reduced the sharpness of the axial power density peaks and thus, by the logic explained above, reduced the maximum DLOFC temperatures slightly.

Although it was not investigated in this study, it is well-known that increasing HM loading increases the risk of the reactivity and thus the power increasing dangerously during a water ingress accident. This means that although increasing HM loading in many cases decreased the total fuel cost and decreased the maximum DLOFC temperature slightly, there is a limit to which this technique can be utilized safely. Near the optimum point, a large increase in HM loading also often produced only a small decrease in fuel cost and DLOFC temperature. In such cases it is recommended that the lower HM loading be selected, as this will probably produce a relatively large reduction in the risk regarding water ingress at the price of only a small increase in fuel cost. The addition of thorium did in fact increase the maximum DLOFC fuel temperature however the ThLEU fuels at lower enrichments did not exceed the maximum limit.

The fuels which would be suitable for this reactor are LEU at 10wt% at 12 g HM (LUEC 131 US$/MWh) which would provide a low LUEC for that fuel and surpass the DLOFC temperature requirement however a lower HM should be used such as 7 g HM loading due to problems associated with water-ingress, therefore LEU at 10wt% and 7 g HM should be used (LUEC = 138.49 US$/MWh). ThLEU that would be suggested is 10wt% and 12 g HM as ThLEU can be inherently safe at a higher HM loading in a water ingress scenario (LUEC = 126 US$/MWh). I would suggest the ThLEU fuel to a utility. These LUEC would also decrease if there were more reactor units on a single site. A single reactor unit per site was analysed. These reactor and fuel cost models are applicable worldwide.

5.9 Recommendations

I would recommend that a study should be done with regards to reducing the fuel plant production costs and looking at new technologies; however a fuel expert will be needed as a consultant to a student doing a study on this. Reducing the complexity of the fuel production processes by investigating new or continuous technologies will greatly reduce the fuel sphere costs. A detailed study should also be done on water ingress effects based on variety of fuels at different HM loadings and enrichments.

6 REFERENCES

1. Anantharaman, K., Shivakumar, V. & Saha, D., 2008. Utalisation of thorium in reactors. *Journal of Nuclear Materials,* Volume 383, pp. 119-121.
2. BP, 2015. *BP Stasistical Review of World Energy,* s.l.: s.n.
3. Goldberg, S. & Rosner, R., 2011. *Nuclear Reactors:Generation to Generation,* s.l.: American Academy of Arts and Sciences..
4. International Atomic Energy Agency, 2000. *Thorium based fuel options for generation of electricity: developments in the 1990's,* s.l.: IAEA-TECDOC-1155.
5. International Atomic Energy Agency, 2000. *Thorium fuel cycle - Potential benefits and challanges,* s.l.: IAEA-TECDOC-1450.
6. International Atomic Energy Agency, 2010. *High Temperature Reactor Fuels and Materials,* s.l.: IAEA-TECDOC-1645.
7. International Atomic Energy Agency, 2015. *Preformance Analysis Review of Thorium Triso Coated Particles During Manufacture, Irradiation and Accident Condition Heating Tests,* s.l.: IAEA-TECDOC-1716.
8. International Energy Agency, 2011. *World Energy Outlook,* s.l.: OECD/IEA.
9. International Energy Agency, 2015. *CO2 Emissions from Fuel Combustion, IEA Statistics Highlights,* s.l.: OECD/IEA.
10. Jordan, B., Eggert, R., Dixon, B. & Carlsen, B., 2014. 'Thorium: Does Crystal Abundance Lead to Economic Availability?'. *Colorado School of Mines, Division of Economics and Business.*
11. Kazimi, M. et al., 1999. On the use of thorium in light water reactors. Issue Department of Nuclear Engineering Cambridge.
12. Kruger, J., 2014. *Nuclear Engineering II, NUCI 883 Lecture Notes: School of Mechanical and Nuclear Engineering. University of the North West.* s.l.:s.n.
13. Kugeler, K., Alkan, Z. & Poppe, N., n.d. *High Temperature Reactor Technology (Vol. 1).* s.l.:s.n.

14. Lamarsh, J. & Baratta, A., 2001. *Introduction to Nuclear Engineering.* New Jersey:Prentice-Hall: s.n.

15. Lior, N., 2009. Sustainable Energy Development:The present (2009) situation and possible paths to the future. *Energy,* pp. 3976-3994.

16. Lohnert G.H., 1992. The consequences of water ingress into the primary circuit of an HTR-Modul - From the design basis accident to hypothetical postulates. *Nuclear Engineering and Design,* 134(North Holland), pp. 159-176.

17. Lung, M. & Gremm, O., 1997. Perspectives of the thorium fuel cycle. *Nuclear Engineering and Design,* Volume 180, pp. 133-146.

18. Mcdowell, B. et al., 2011. High Temperature Gas Reactors:Assessment of Applicable Codes and Standards. Issue October.

19. McWilliams, A. J., 2015. *High Temperature Gas-cooled Reactor (HTGR) Graphite Pebble Fuel: Review of Technologies for Reprocessing,* s.l.: s.n.

20. Rutten, H., Haas, K. & Pohl, C., 2009. *Computer Code System V.S.O.P (99/11) Update 2011 of V.S.O.P(99)-Version 2009 Code Manual.* institute of Energy and Climate Research ed. s.l.:Julich Forschungszentrum.

21. Serfontein, D., 2014. Optimisation of deep burn incineration of reactor waste plutonium in a PBMR DPP-400 core.

22. Shippingport Atomic Power Station, n.d. *Photographs Written Historical and Descriptive Data, Historic American Engineering Record Shippingport Atomic Power Station,* s.l.: s.n.

23. Sokolov, F., Fukuda, K. & Nawada, H., 2005. Thorium fuel cycle - Potential benefits and challanges. Issue International Atomic Energy Agency.

24. Steenkampskraal Thorium Limited, 2017. *Fuel & Full Fuel Plant Cost Model - UO2(MASTER),* s.l.: STL.

25. Steenkampskraal Thorium Limited, 2017. *Fuel & Full Fuel Plant Cost Model - UO2_ThO2 (MASTER)_ThHEU,* s.l.: STL.

26. Steenkampskraal Thorium Limited, 2017. *Fuel & Full Fuel Plant Cost Model - UO2_ThO2 (MASTER)_ThLEU,* s.l.: STL.

27. Tanaka, T. et al., 1991. Present status of the High Temperature Test Reactor (HTTR). *Nuclear Engineering and Design,* 132(Japan Atomic Energy. Research Institute), pp. 85-93.

28. UxC, n.d. *UxC Fuel Quantity & Cost Calculator.* [Online] Available at: https://www.uxc.com/p/tools/FuelCalculator.aspx

29. Weisser, D., 2006. *A guide to life-cycle greenhouse gas (GHG) emissions from electric supply technologies,* s.l.: IAEA.

30. Wu, Z. & Zhong, D., 2002. The design features of the HTR-10. *Nuclear Engineering and Design,* Volume 218, pp. 25-32.

31. Zhang, Z. et al., 2004. Design of the Chinese Modular High Temperature Gas-cooled Reactor HTR-PM. Volume 2nd International topical meeting on High Temperature Reactor Technology.

7 APPENDICES

7.1 Appendix A

Table 61 – Mass of various heavy metals per fuel sphere for LEU, ThLEU & ThHEU

LEU																	
HEAVY METAL LOADING	g	5.0	5.0	5.0	7.0	7.0	7.0	10.0	10.0	10.0	12.0	12.0	12.0	16.0	16.0	16.0
EFFECTIVE ENRICHMENT	wt%	8.0	10.0	15.0	8.0	10.0	15.0	8.0	10.0	15.0	8.0	10.0	15.0	8.0	10.0	15.0
235U ENRICHMENT	%	8.0	10.0	15.0	8.0	10.0	15.0	8.0	10.0	15.0	8.0	10.0	15.0	8.0	10.0	15.0
235U MASS/FS	g	0.4	0.5	0.8	0.6	0.7	1.1	0.8	1.0	1.5	1.0	1.2	1.8	1.3	1.6	2.4
238U MASS/FS	g	4.6	4.5	4.3	6.4	6.3	6.0	9.2	9.0	8.5	11.0	10.8	10.2	14.7	14.4	13.6
232Th MASS/FS	g	0.0	0.0	0.0	0.0	0.0	0.0	0.0	0.0	0.0	0.0	0.0	0.0	0.0	0.0	0.0
MASS U/FS	g	5.0	5.0	5.0	7.0	7.0	7.0	10.0	10.0	10.0	12.0	12.0	12.0	16.0	16.0	16.0
Th/U RATIO		0.0	0.0	0.0	0.0	0.0	0.0	0.0	0.0	0.0	0.0	0.0	0.0	0.0	0.0	0.0
MASS UO2/FS	g	5.7	5.7	5.7	7.9	7.9	7.9	11.3	11.3	11.3	13.6	13.6	13.6	18.2	18.2	18.2
MASS ThO2/FS	g	0.0	0.0	0.0	0.0	0.0	0.0	0.0	0.0	0.0	0.0	0.0	0.0	0.0	0.0	0.0
MASS (ThU)O2/FS	g	5.7	5.7	5.7	7.9	7.9	7.9	11.3	11.3	11.3	13.6	13.6	13.6	18.2	18.2	18.2
(Th,U)O2 / HM RATIO		1.1	1.1	1.1	1.1	1.1	1.1	1.1	1.1	1.1	1.1	1.1	1.1	1.1	1.1	1.1
ThLEU																	
HEAVY METAL LOADING	g	5.0	5.0	5.0	7.0	7.0	7.0	10.0	10.0	10.0	12.0	12.0	12.0	16.0	16.0	16.0
EFFECTIVE ENRICHMENT	wt%	8.0	10.0	15.0	8.0	10.0	15.0	8.0	10.0	15.0	8.0	10.0	15.0	8.0	10.0	15.0
235U ENRICHMENT	%	20.0	20.0	20.0	20.0	20.0	20.0	20.0	20.0	20.0	20.0	20.0	20.0	20.0	20.0	20.0
235U MASS/FS	g	0.4	0.5	0.8	0.6	0.7	1.1	0.8	1.0	1.5	1.0	1.2	1.8	1.3	1.6	2.4
238U MASS/FS	g	1.6	2.0	3.0	2.2	2.8	4.2	3.2	4.0	6.0	3.8	4.8	7.2	5.1	6.4	9.6
232Th MASS/FS	g	3.0	2.5	1.3	4.2	3.5	1.8	6.0	5.0	2.5	7.2	6.0	3.0	9.6	8.0	4.0
MASS U/FS	g	2.0	2.5	3.8	2.8	3.5	5.3	4.0	5.0	7.5	4.8	6.0	9.0	6.4	8.0	12.0
Th/U RATIO		1.5	1.0	0.3	1.5	1.0	0.3	1.5	1.0	0.3	1.5	1.0	0.3	1.5	1.0	0.3
MASS UO2/FS	g	2.3	2.8	4.3	3.2	4.0	6.0	4.5	5.7	8.5	5.4	6.8	10.2	7.3	9.1	13.6
MASS ThO2/FS	g	3.4	2.8	1.4	4.8	4.0	2.0	6.8	5.7	2.8	8.2	6.8	3.4	10.9	9.1	4.6
MASS (ThU)O2/FS	g	5.7	5.7	5.7	8.0	8.0	7.9	11.4	11.4	11.4	13.6	13.6	13.6	18.2	18.2	18.2
(Th,U)O2 / HM RATIO		1.1	1.1	1.1	1.1	1.1	1.1	1.1	1.1	1.1	1.1	1.1	1.1	1.1	1.1	1.1
ThHEU																	
HEAVY METAL LOADING	g	5.0	5.0	5.0	7.0	7.0	7.0	10.0	10.0	10.0	12.0	12.0	12.0	16.0	16.0	16.0
EFFECTIVE ENRICHMENT	wt%	8.0	10.0	15.0	8.0	10.0	15.0	8.0	10.0	15.0	8.0	10.0	15.0	8.0	10.0	15.0
235U ENRICHMENT	%	93.0	93.0	93.0	93.0	93.0	93.0	93.0	93.0	93.0	93.0	93.0	93.0	93.0	93.0	93.0
235U MASS/FS	g	0.4	0.5	0.8	0.6	0.7	1.1	0.8	1.0	1.5	1.0	1.2	1.8	1.3	1.6	2.4
238U MASS/FS	g	0.0	0.0	0.1	0.0	0.1	0.1	0.1	0.1	0.1	0.1	0.1	0.1	0.1	0.1	0.2
232Th MASS/FS	g	4.6	4.5	4.2	6.4	6.2	5.9	9.1	8.9	8.4	11.0	10.7	10.1	14.6	14.3	13.4
MASS U/FS	g	0.4	0.5	0.8	0.6	0.8	1.1	0.9	1.1	1.6	1.0	1.3	1.9	1.4	1.7	2.6
Th/U RATIO		10.6	8.3	5.2	10.6	8.3	5.2	10.6	8.3	5.2	10.6	8.3	5.2	10.6	8.3	5.2
MASS UO2/FS	g	0.5	0.6	0.9	0.7	0.9	1.3	1.0	1.2	1.8	1.2	1.5	2.2	1.6	2.0	2.9
MASS ThO2/FS	g	5.2	5.1	4.8	7.3	7.1	6.7	10.4	10.2	9.5	12.5	12.2	11.5	16.6	16.2	15.3
MASS (ThU)O2/FS	g	5.7	5.7	5.7	8.0	8.0	8.0	11.4	11.4	11.4	13.7	13.7	13.7	18.2	18.2	18.2
(Th,U)O2 / HM RATIO		1.1	1.1	1.1	1.1	1.1	1.1	1.1	1.1	1.1	1.1	1.1	1.1	1.1	1.1	1.1

7.2 Appendix B

Table 62 – Overall Global neutronic Data for LEU Fuel up to 15 wt%

	Units:	LEU	LEU	LEU	LEU	LEU	LEU	LEU	LEU	LEU	LEU	LEU	LEU	LEU	LEU	LEU
HEAVY METAL LOADING	g HM	5	5	5	7	7	7	10	10	10	12	12	12	16	16	16
FEED ENRICHMENT	wt%	8	10	15	8	10	15	8	10	15	8	10	15	8	10	15
AVG. FISSILE ENRICHMENT	%	4.5	4.85	5.78	4.53	5	6.34	5.2	5.95	7.9	5.68	6.61	8.97	6.47	7.66	10.62
AVG. FUEL RESIDENCE TIME	DAYS	470	647	1063	700	948	1518	908	1232	1970	958	1309	2108	938	1315	2186
	MWD/T	61675	84851	139016	65620	88782	142000	59615	80898	129242	52485	71686	115330	38540	54021	89802
PEBBLE FEED RATE	SPHERES/DAY	324	236	144	218	161	101	168	124	77	159	116	72	162	116	70
KILOWATT HOUR/FUEL SPHERE	kWh/FS	7401	10182	16682	11024	14915	23856	14308	19416	31018	15116	20646	33215	14799	20744	34484
KILOWATT/FUEL SPHERE	kW/FS	308	424	695	459	621	994	596	809	1292	630	860	1384	617	864	1437
FISSIONS/ENERGY	E+10 (FISS/WS)	3.05	3.05	3.05	3.05	3.05	3.05	3.04	3.07	3.04	3.05	3.04	3.04	3.05	3.05	3.05
POWER PEAKING MAX./AVG.		2.29	2.55	3.05	2.31	2.52	2.95	2.17	2.38	2.74	2.07	2.24	2.73	2.06	2.30	2.75
MAX. POWER PER FUEL SPHERE	KW/ FS	1.50	1.67	1.99	1.52	1.65	1.93	1.42	1.56	1.79	1.36	1.47	1.79	1.36	1.51	1.81
CONVERSION RATIO	CR	0.35	0.34	0.32	0.42	0.41	0.38	0.48	0.47	0.43	0.51	0.49	0.46	0.55	0.52	0.48
SOURCE NEUTR./FISSILE ABS.	ηε	1.99	1.98	1.98	1.97	1.97	1.96	1.95	1.95	1.93	1.94	1.93	1.92	1.93	1.92	1.89
CAPTURE/FISSION IN FISS.MAT.	α	0.28	0.28	0.28	0.30	0.30	0.31	0.32	0.33	0.33	0.33	0.34	0.35	0.34	0.35	0.36
FAST DOSIS SPENT FUEL ELEM.	E+21/CM2	1.11	1.52	2.47	1.65	2.23	3.54	2.14	2.89	4.58	2.25	3.06	4.88	2.17	3.03	4.99

Table 63 – Overall Global neutronic Data for LEU Fuel at 20 wt%

	Units:	LEU	LEU	LEU	LEU	LEU
HEAVY METAL LOADING	g HM	5	7	10	12	16
FEED ENRICHMENT	wt%	20	20	20	20	20
AVG. FISSILE ENRICHMENT	%	6.72	7.65	9.86	11.28	13.4
AVG. FUEL RESIDENCE TIME	DAYS	1452.9	2053	2652.2	2853.1	3038.4
AVG. BURNUP	MWD/T	189780.2	191822	173837.5	156042.6	124758.4
PEBBLE FEED RATE	SPHERES/DAY	105	74	58	53	50
KEFF		0.9999	0.9999	1.0000	1.0000	0.9999
FISSIONS/ENERGY	E+10 (FISS/WS)	3.053	3.048	3.045	3.046	3.05
POWER PEAKING MAX./AVG.		3.65	3.47	3.26	3.26	3.31
MAX. POWER PER BALL	KW/BALL	2.38	2.27	2.14	2.14	2.17
CONVERSION RATIO	CR	0.304	0.357	0.405	0.423	0.444
SOURCE NEUTR./FISSILE ABS.	ηε	1.975	1.953	1.923	1.905	1.876
CAPTURE/FISSION IN FISS.MAT.	α	0.276	0.304	0.335	0.35	0.369
FAST DOSIS SPENT FUEL ELEM.	E+21/CM2	3.34	4.74	6.12	6.54	6.88

Table 64 – Overall Global neutronic Data for ThLEU Fuel

	Units:	ThLEU	ThLEU	ThLEU	ThLEU	ThLEU	ThLEU	ThLEU	ThLEU	ThLEU	ThLEU	ThLEU	ThLEU	ThLEU	ThLEU	ThLEU
HEAVY METAL LOADING	g HM	5	5	5	7	7	7	10	10	10	12	12	12	16	16	16
FEED ENRICHMENT	wt%	8	10	15	8	10	15	8	10	15	8	10	15	8	10	15
AVG. FISSILE ENRICHMENT	%	4.73	4.98	5.71	4.54	4.89	5.99	4.76	5.3	7.15	5.05	5.75	8.08	5.75	6.74	9.76
AVG. FUEL RESIDENCE TIME	DAYS	442	631	1052	704	965	1538	1051	1405	2114	1226	1621	2351	1392	1828	2547
AVG. BURN-UP	MWD/T	58108	82839	137713	66032	90475	143868	69044	92260	138642	67176	88771	128631	57272	75180	104656
PEBBLE FEED RATE	SPHERES/DAY	344	241	145	216	158	99	145	108	72	124	94	65	109	83	60
KILOWATT HOUR/FUEL SPHERE	kWh/ FS	6973	9941	16526	11093	15200	24170	16571	22142	33274	19347	25566	37046	21992	28869	40188
KILOWATT/FUEL SPHERE	kW/ FS	291	414	689	462	633	1007	690	923	1386	806	1065	1544	916	1203	1674
FISSIONS/ENERGY	E+10 (FISS/WS)	3.08	3.075	3.064	3.078	3.072	3.059	3.076	3.07	3.055	3.076	3.069	3.055	3.075	3.069	3.057
POWER PEAKING MAX./AVG.		2.17	2.49	3.08	2.24	2.5	3.06	2.16	2.38	2.82	2.06	2.23	2.74	1.89	2.15	2.69
MAX. POWER PER FUEL SPHERE	KW/ FS	1.42	1.63	2.02	1.47	1.64	2	1.41	1.56	1.85	1.35	1.46	1.8	1.24	1.41	1.77
CONVERSION RATIO	CR	0.353	0.337	0.314	0.414	0.395	0.369	0.476	0.455	0.423	0.506	0.483	0.447	0.549	0.523	0.478
SOURCE NEUTR./FISSILE ABS.	$\eta\varepsilon$	2.036	2.027	2.000	2.03	2.017	1.984	2.018	2.002	1.96	2.01	1.991	1.945	1.99	1.968	1.918
CAPTURE/FISSION IN FISS.MAT.	α	0.215	0.225	0.250	0.226	0.239	0.272	0.24	0.257	0.299	0.249	0.268	0.312	0.264	0.285	0.332
FAST DOSIS SPENT FUEL ELEM.	E+21/CM2	1.03	1.46	2.43	1.64	2.24	3.56	2.44	3.27	4.9	2.85	3.76	5.43	3.22	4.22	5.83

Table 65 – Overall Global neutronic Data for ThHEU Fuel

	Units:	ThHEU	ThHEU	ThHEU	ThHEU	ThHEU	ThHEU	ThHEU	ThHEU	ThHEU	ThHEU	ThHEU	ThHEU	ThHEU	ThHEU	ThHEU
HEAVY METAL LOADING	g HM	5	5	5	7	7	7	10	10	10	12	12	12	16	16	16
FEED ENRICHMENT	wt%	8	10	15	8	10	15	8	10	15	8	10	15	8	10	15
AVG. FISSILE ENRICHMENT	%	4.83	5.05	5.57	4.52	4.75	5.35	4.5	4.8	5.56	4.63	4.98	5.87	5.05	5.51	6.72
AVG. FUEL RESIDENCE TIME	DAYS	433	626	1048	713	985	1578	1132	1528	2375	1395	1873	2884	1833	2476	3793
AVG. BURN-UP	MWD/T	56922	82214	137237	66948	92348	147438	74426	100267	155432	76475	102537	157501	75392	101758	155552
PEBBLE FEED RATE	SPHERES/DAY	351	243	146	213	155	97	134	100	64	109	81	53	83	61	40
KILOWATT HOUR/FUEL SPHERE	kWh/ FS	6831	9866	16468	11247	15514	24770	17862	24064	37304	22025	29531	45360	28950	39075	59732
KILOWATT/FUEL SPHERE	kW/ FS	285	411	686	469	646	1032	744	1003	1554	918	1230	1890	1206	1628	2489
FISSIONS/ENERGY	E+10 (FISS/WS)	3.096	3.097	3.097	3.1	3.1	3.1	3.103	3.103	3.102	3.104	3.105	3.103	3.106	3.106	3.104
POWER PEAKING MAX./AVG.		2.13	2.45	3.36	2.22	2.52	3.53	2.21	2.51	3.46	2.16	2.45	3.32	1.97	2.28	3.11
MAX. POWER PER FUEL SPHERE	KW/ FS	1.39	1.6	2.19	1.46	1.65	2.31	1.45	1.64	2.26	1.41	1.6	2.17	1.29	1.49	2.04
CONVERSION RATIO	CR	0.349	0.324	0.277	0.406	0.377	0.321	0.466	0.433	0.369	0.496	0.461	0.393	0.542	0.504	0.431
SOURCE NEUTR./FISSILE ABS.	ηε	2.069	2.071	2.065	2.074	2.073	2.063	2.075	2.072	2.056	2.072	2.068	2.049	2.061	2.055	2.032
CAPTURE/FISSION IN FISS.MAT.	α	0.177	0.174	0.171	0.176	0.174	0.174	0.178	0.177	0.181	0.181	0.182	0.188	0.19	0.193	0.203
FAST DOSIS SPENT FUEL ELEM.	E+21/CM2	0.99	1.43	2.36	1.64	2.25	3.55	2.6	3.49	5.35	3.2	4.28	6.51	4.21	5.66	8.56

Table 66 – Neutron losses in heavy metals for LEU up to 15 wt%

HEAVY METAL LOADING	g HM	5	5	5	7	7	7	10	10	10	12	12	12	16	16	16
FEED ENRICHMENT	wt%	8	10	15	8	10	15	8	10	15	8	10	15	8	10	15
NEUTRON LOSSES IN HEAVY METALS	%	68.7	68.48	68.02	72.7	72.39	72	76.8	76.5	75.86	78.57	78.23	77.58	80.95	80.6	79.87
ESP. IN FISSILE ISOTOPES	%	50.39	50.44	50.55	50.79	50.86	51.1	51.3	51.4	51.72	51.5	51.7	52.12	51.84	52.2	52.8
ESP. IN TH-232	%															
ESP. IN PA-233	%															
ESP. IN U -233	%															
ESP. IN U -234	%	0.12	0.14	0.17	0.12	0.14	0.17	0.13	0.15	0.19	0.14	0.16	0.2	0.16	0.18	0.23
ESP. IN U -235	%	35.73	35.5	35.76	33.46	33.34	33.8	32.6	32.5	33.26	33.16	33.09	33.92	35.22	35.1	36.02
ESP. IN U -236	%	0.25	0.33	0.54	0.32	0.43	0.69	0.38	0.51	0.82	0.39	0.53	0.86	0.37	0.52	0.87
ESP. IN U -237	%			0.01												
ESP. IN U -238	%	15.13	14.29	12.91	17.78	16.81	15.33	21	19.9	18.00	22.64	21.40	19.37	25.30	23.87	21.50
ESP. IN NP-237	%	0.05	0.09	0.19	0.07	0.12	0.25	0.08	0.14	0.28	0.08	0.13	0.27	0.06	0.11	0.24
ESP. IN NP-239	%	0.04	0.03	0.03	0.03	0.03	0.03	0.03	0.03	0.02	0.03	0.03	0.02	0.03	0.02	0.02
ESP. IN PU-238	%		0.02	0.06	0.01	0.03	0.07	0.01	0.02	0.06		0.02	0.05		0.01	0.03
ESP. IN PU-239	%	12.83	12.65	11.96	14.99	14.71	14	16.4	16.2	15.33	16.44	16.29	15.46	15.4	15.5	14.82
ESP. IN PU-240	%	2.67	3.04	3.38	3.45	3.8	4.1	3.8	4.18	4.48	3.69	4.09	4.42	3.12	3..59	4
ESP. IN PU-241	%	1.82	2.29	2.83	2.35	2.81	3.29	2.23	2.68	3.13	1.9	2.32	2.74	1.22	1.57	1.96
ESP. IN PU-242	%	0.03	0.06	0.12	0.06	0.1	0.17	0.06	0.1	0.14	0.05	0.08	0.12	0.03	0.05	0.07
ESP. IN AM-241	%	0.01	0.02	0.03	0.02	0.04	0.06	0.03	0.05	0.09	0.03	0.06	0.1	0.03	0.05	0.09
ESP. IN AM-242M										0.01			0.01			
ESP. IN AM-243	%			0.03		0.02	0.05	0.01	0.02	0.04		0.02	0.03			0.02
IN FISSION PRODUCTS	%	5.92	6.67	8.04	6.08	6.8	8.01	5.59	6.2	7.25	5.13	5.68	6.62	4.27	4.73	5.54
ESP. IN XE-135	%	2.35	2.34	2.3	2.21	2.18	2.1	1.96	1.89	1.75	1.8	1.71	1.53	1.53	1.42	1.2
CORE-LEAKAGE	%	21.39	21.31	21.1	18.41	18.35	18.1	15.7	15.7	15.66	14.74	14.76	14.8	13.57	13.7	13.82

Table 67 – Neutron losses in heavy metals for LEU at 20 wt%

NEUTRONS LOST IN HEAVY METALS ESP.		LEU	LEU	LEU	LEU	LEU
NEUTRON LOSSES IN HEAVY METALS	%	67.55	71.44	75.27	76.94	79.16
ESP. IN FISSILE ISOTOPES	%	50.65	51.21	52	52.48	53.29
ESP. IN TH-232	%					
ESP. IN PA-233	%					
ESP. IN U -233	%					
ESP. IN U -234	%	0.19	0.2	0.22	0.23	0.26
ESP. IN U -235	%	36.42	34.66	34.35	35.1	37.24
ESP. IN U -236	%	0.73	0.93	1.11	1.17	1.22
ESP. IN U -237	%	0.01				
ESP. IN U -238	%	11.86	14.10	16.55	17.78	19.63
ESP. IN NP-237	%	0.31	0.4	0.44	0.43	0.4
ESP. IN NP-239	%	0.03	0.03	0.02	0.02	0.02
ESP. IN PU-238	%	0.11	0.13	0.11	0.09	0.06
ESP. IN PU-239	%	11.24	13.13	14.41	14.53	13.96
ESP. IN PU-240	%	3.43	4.1	4.46	4.41	4.04
ESP. IN PU-241	%	2.99	3.42	3.24	2.85	2.1
ESP. IN PU-242	%	0.14	0.19	0.16	0.13	0.08
ESP. IN AM-241	%	0.04	0.07	0.12	0.13	0.13
ESP. IN AM-242M				0.01	0.02	0.01
ESP. IN AM-243	%	0.04	0.06	0.06	0.04	0.02
IN FISSION PRODUCTS	%	9.04	8.91	8.01	7.32	6.19
ESP. IN XE-135	%	2.27	2.03	1.63	1.4	1.05
CORE-LEAKAGE	%	20.99	18.04	15.7	14.9	14

Table 68 – Neutron losses in heavy metals for ThLEU

HEAVY METAL LOADING	g HM	5	5	5	7	7	7	10	10	10	12	12	12	16	16	16
FEED ENRICHMENT	wt%	8	10	15	8	10	15	8	10	15	8	10	15	8	10	15
NEUTRON LOSSES IN HEAVY METALS	%	67.38	66.99	66.94	70.8	70.47	70.6	74.5	74.2	74.55	76.39	76.14	76.41	79.31	79.1	79.05
ESP. IN FISSILE ISOTOPES	%	49.12	49.34	50	49.26	49.57	50.4	49.6	50	51.01	49.76	50.22	51.41	50.26	50.8	52.13
ESP. IN TH-232	%	10.65	8.23	3.52	12.11	9.32	3.98	13.7	10.5	4.53	14.49	11.19	4.86	15.95	12.4	5.48
ESP. IN PA-233	%	0.26	0.21	0.1	0.28	0.23	0.1	0.27	0.22	0.1	0.26	0.21	0.09	0.24	0.19	0.09
ESP. IN U -233	%	4.06	3.87	2.03	5.45	4.84	2.35	6.43	5.49	2.51	6.62	5.58	2.5	6.33	5.33	2.38
ESP. IN U -234	%	0.18	0.2	0.21	0.21	0.23	0.23	0.25	0.27	0.25	0.26	0.28	0.26	0.27	0.28	0.28
ESP. IN U -235	%	39.37	38.04	36.86	36.62	35.59	34.8	34.6	33.8	33.7	34.22	33.59	33.92	35.01	34.5	35.52
ESP. IN U -236	%	0.26	0.36	0.56	0.36	0.48	0.72	0.48	0.62	0.9	0.53	0.68	0.96	0.57	0.73	1.01
ESP. IN U -237	%			0.01												
ESP. IN U -238	%	5.77	6.92	9.55	6.91	8.27	11.37	8.15	9.75	13.37	8.78	10.49	14.38	9.75	11.64	15.92
ESP. IN NP-237	%	0.05	0.1	0.2	0.09	0.15	0.28	0.14	0.21	0.35	0.15	0.22	0.35	0.14	0.21	0.33
ESP. IN NP-239	%	0.01	0.02	0.02	0.01	0.02	0.02	0.01	0.02	0.02	0.01	0.01	0.02	0.01	0.01	0.02
ESP. IN PU-238	%		0.02	0.07	0.02	0.04	0.09	0.03	0.05	0.09	0.03	0.05	0.08	0.02	0.04	0.05
ESP. IN PU-239	%	4.95	6.22	8.93	6.07	7.5	10.6	7.1	8.69	11.98	7.49	9.13	12.34	7.7	9.32	12.19
ESP. IN PU-240	%	1.05	1.55	2.57	1.5	2.06	3.2	1.91	2.51	3.67	2.03	2.64	3.74	2.03	2.61	3.54
ESP. IN PU-241	%	0.74	1.21	2.19	1.12	1.64	2.68	1.39	1.93	2.83	1.42	1.93	2.65	1.22	1.62	2.04
ESP. IN PU-242	%	0.01	0.02	0.07	0.02	0.04	0.11	0.03	0.06	0.13	0.04	0.06	0.11	0.03	0.05	0.07
ESP. IN AM-241	%			0.02	0.01	0.02	0.04	0.02	0.04	0.07	0.03	0.04	0.09	0.03	0.05	0.1
ESP. IN AM-242M										0.01			0.01			0.01
ESP. IN AM-243	%			0.02			0.03		0.02	0.04		0.02	0.04		0.01	0.02
IN FISSION PRODUCTS	%	5.9	6.79	8.21	6.42	7.25	8.43	6.53	7.23	7.96	6.33	6.93	7.41	5.59	6.04	6.28
ESP. IN XE-135	%	2.38	2.36	2.32	2.27	2.24	2.16	2.08	2.02	1.84	1.94	1.86	1.63	1.65	1.54	1.27
CORE-LEAKAGE	%	22.25	22.24	21.78	19.44	19.38	18.8	16.6	16.5	16.1	15.33	15.29	15.05	13.64	13.7	13.83

Table 69 – Neutron losses in heavy metals for ThHEU

HEAVY METAL LOADING	g HM	5	5	5	7	7	7	10	10	10	12	12	12	16	16	16
FEED ENRICHMENT	wt%	8	10	15	8	10	15	8	10	15	8	10	15	8	10	15
NEUTRON LOSSES IN HEAVY METALS	%	66.37	65.3	63.53	69.24	68.09	66.2	72.4	71.2	69.34	74.08	72.87	71.02	76.82	75.6	73.8
ESP. IN FISSILE ISOTOPES	%	48.33	48.3	48.43	48.21	48.23	48.5	48.2	48.3	48.64	48.26	48.36	48.8	48.52	48.7	49.22
ESP. IN TH-232	%	16.88	15.55	13	19.5	17.95	15	22.3	20.5	17.2	23.69	21.83	18.34	25.94	23.9	20.22
ESP. IN PA-233	%	0.41	0.41	0.39	0.46	0.45	0.42	0.47	0.47	0.43	0.46	0.46	0.42	0.43	0.42	0.38
ESP. IN U -233	%	6.59	7.68	8.09	9.44	10.2	10.1	12	12.5	11.96	13.07	13.51	12.77	14.03	14.5	13.7
ESP. IN U -234	%	0.22	0.27	0.37	0.29	0.36	0.47	0.38	0.47	0.58	0.43	0.52	0.64	0.48	0.59	0.72
ESP. IN U -235	%	41.58	40.39	39.95	38.56	37.73	37.9	35.9	35.3	36	34.88	34.42	35.29	34.16	33.7	34.74
ESP. IN U -236	%	0.27	0.38	0.62	0.4	0.54	0.84	0.55	0.73	1.12	0.64	0.84	1.27	0.76	1.01	1.52
ESP. IN U -237	%			0.02		0.01	0.02			0.01			0.01			
ESP. IN U -238	%	0.15	0.18	0.25	0.18	0.22	0.31	0.21	0.26	0.36	0.23	0.28	0.39	0.26	0.31	0.43
ESP. IN NP-237	%	0.06	0.11	0.25	0.11	0.19	0.39	0.18	0.3	0.57	0.22	0.35	0.66	0.27	0.43	0.79
ESP. IN NP-238	%						0.01			0.01			0.01			
ESP. IN NP-239	%															
ESP. IN PU-238	%	0.01	0.03	0.09	0.03	0.06	0.16	0.05	0.1	0.23	0.06	0.11	0.26	0.07	0.13	0.28
ESP. IN PU-239	%	0.14	0.18	0.32	0.18	0.24	0.42	0.23	0.31	0.54	0.25	0.34	0.58	0.27	0.37	0.62
ESP. IN PU-240	%	0.02	0.05	0.09	0.04	0.07	0.12	0.06	0.09	0.16	0.07	0.1	0.18	0.08	0.11	0.2
ESP. IN PU-241	%		0.04	0.08	0.03	0.05	0.11	0.05	0.07	0.14	0.06	0.08	0.15	0.06	0.09	0.16
ESP. IN PU-242	%															
ESP. IN AM-241	%															
ESP. IN AM-242M																
ESP. IN AM-243	%															
IN FISSION PRODUCTS	%	5.92	6.94	8.72	6.66	7.7	9.46	7.16	8.2	9.9	7.25	8.28	9.92	7.03	8.05	9.57
ESP. IN XE-135	%	2.39	2.39	2.38	2.3	2.29	2.28	2.15	2.14	2.1	2.04	2.02	1.97	1.81	1.77	1.67
CORE-LEAKAGE	%	22.94	22.36	24.03	20.38	20.81	21.5	17.7	18.1	18.71	16.32	16.73	17.35	14.36	14.7	15.36

Table 70 – Neutron Produced by LEU up to 15 wt%

HEAVY METAL LOADING	g HM	5	5	5	7	7	7	10	10	10	12	12	12	16	16	16
FEED ENRICHMENT	wt%	8	10	15	8	10	15	8	10	15	8	10	15	8	10	15
TH - 232	%															
U - 233	%															
U -235	%	72.75	72.1	72.23	67.68	67.21	67.59	65.28	64.76	65.4	65.89	65.31	65.96	69.11	68.27	68.7
U -236	%	0.01	0.01	0.02	0.01	0.02	0.03	0.02	0.02	0.04	0.02	0.02	0.04	0.02	0.03	0.04
U -238	%	0.23	0.22	0.21	0.32	0.31	0.29	0.45	0.44	0.41	0.54	0.53	0.49	0.72	0.7	0.65
NP - 238	%			0.01												
PU - 238	%															
PU-239	%	23.12	22.77	21.48	26.97	26.44	25.03	29.46	29.03	27.41	29.47	29.15	27.59	27.54	27.63	26.37
PU-240	%						0.01	0.01	0.01	0.01	0.01	0.01	0.02	0.01	0.01	0.02
PU-241	%	3.87	4.87	6.01	4.99	5.98	7	4.75	5.71	6.67	4.05	4.94	5.84	2.59	3.34	4.18
AM-242M	%			0.01		0.01	0.02	0.01	0.02	0.03	0.01	0.02	0.03		0.01	0.02

Table 71 – Neutron Produced by LEU at 20 wt%

FRACTIONAL NEUTRONS PRODUCED BY	%	LEU	LEU	LEU	LEU	LEU
TH - 232	%					
U - 233	%					
U -235	%	73.21	68.84	66.86	67.43	69.98
U -236	%	0.03	0.04	0.05	0.06	0.06
U -238	%	0.19	0.27	0.38	0.45	0.6
NP - 238	%	0.02	0.01			
PU - 238	%	0.01	0.02	0.02	0.02	0.01
PU-239	%	20.16	23.5	25.72	25.89	24.79
PU-240	%		0.01	0.02	0.02	0.02
PU-241	%	6.35	7.27	6.89	6.07	4.48
AM-242M	%	0.01	0.03	0.04	0.04	0.04

Table 72 – Neutron Produced by ThLEU

HEAVY METAL LOADING	g HM	5	5	5	7	7	7	10	10	10	12	12	12	16	16	16
FEED ENRICHMENT	wt%	8	10	15	8	10	15	8	10	15	8	10	15	8	10	15
TH - 232	%	0.03	0.02	0.01	0.04	0.03	0.02	0.06	0.05	0.02	0.07	0.06	0.03	0.09	0.08	0.04
U - 233	%	9.14	8.71	4.55	12.24	10.85	5.25	14.36	12.24	5.56	14.76	12.41	5.51	14.02	11.78	5.21
U -235	%	80.24	77.37	74.53	74.28	71.94	69.76	69.65	67.74	66.57	68.45	66.77	66.31	69.2	67.64	68.1
U -236	%	0.01	0.01	0.02	0.02	0.02	0.03	0.02	0.03	0.04	0.02	0.03	0.05	0.03	0.04	0.05
U -238	%	0.08	0.1	0.15	0.11	0.14	0.2	0.16	0.2	0.29	0.19	0.24	0.35	0.25	0.31	0.46
NP - 238	%			0.01			0.01									
PU - 238	%						0.01			0.01			0.01			0.01
PU-239	%	8.92	11.2	16.03	10.92	13.48	18.97	12.76	15.6	21.42	13.45	16.35	22.04	13.78	16.65	21.71
PU-240	%									0.01			0.01			0.01
PU-241	%	1.56	2.57	4.66	2.37	3.5	5.71	2.96	4.11	6.02	3.03	4.1	5.63	2.59	3.45	4.35
AM-242M	%						0.02		0.01	0.03		0.02	0.03	0.01	0.02	0.03

Table 73 – Neutron Produced by ThHEU

HEAVY METAL LOADING	g HM	5	5	5	7	7	7	10	10	10	12	12	12	16	16	16
FEED ENRICHMENT	wt%	8	10	15	8	10	15	8	10	15	8	10	15	8	10	15
TH - 232	%	0.05	0.04	0.04	0.06	0.06	0.06	0.09	0.09	0.08	0.11	0.1	0.1	0.14	0.14	0.13
U - 233	%	14.83	17.28	18.18	21.19	22.89	22.57	26.95	28.06	26.7	29.21	30.15	28.44	31.22	32.26	30.34
U -234	%												0.01		0.01	0.01
U -235	%	84.82	82.24	80.99	78.32	76.45	76.3	72.4	71.07	71.84	70.06	68.87	69.96	67.96	66.65	67.93
U -236	%	0.01	0.02	0.03	0.02	0.02	0.04	0.02	0.03	0.05	0.03	0.04	0.06	0.03	0.05	0.07
U -238	%															0.01
NP - 238	%			0.02		0.01	0.02		0.01	0.02		0.01	0.02			0.02
PU - 238	%						0.02		0.01	0.03		0.01	0.03		0.02	0.04
PU-239	%	0.24	0.33	0.57	0.32	0.44	0.75	0.41	0.56	0.96	0.45	0.62	1.04	0.49	0.67	1.1
PU-240	%															
PU-241	%	0.04	0.08	0.16	0.07	0.12	0.23	0.1	0.16	0.3	0.12	0.18	0.32	0.13	0.19	0.34
AM-242M	%															

Table 74 – Fuel Supply and Discharge for LEU up to 15 wt%

HEAVY METAL LOADING	gHM	5		5		5		7		7		7		10		10		10		12		12		12		16		16		16	
FEED ENRICHMENT	wt%	8		10		15		8		10		15		8		10		15		8		10		15		8		10		15	
	KG/GWD(TH)	Supply	Discharge	Supply	Discharge	Supply	Discharge	Supply	Discharge	Supply	Discharge	Supply	Discharge	Supply	Discharge	Supply	Discharge	Supply	Discharge	Supply	Discharge	Supply	Discharge	Supply	Discharge	Supply	Discharge	Supply	Discharge	Supply	Discharge
TH-232	KG/GWD(TH)																														
U -233	KG/GWD(TH)																														
U -234	KG/GWD(TH)	0.0121	0.009	0.0115	0.008	0.0107	0.0064	0.0114	0.0081	0.011	0.0073	0.0105	0.0061	0.0125	0.0091	0.0121	0.0081	0.0116	0.0068	0.0142	0.0106	0.0137	0.0095	0.013	0.0079	0.0194	0.0153	0.0182	0.0134	0.0167	0.011
U -235	KG/GWD(TH)	1.2943	0.3633	1.1748	0.2507	1.0736	0.1455	1.2169	0.34	1.1234	0.2502	1.0521	0.1693	1.3407	0.4827	1.2344	0.3791	1.158	0.2858	1.5236	0.6518	1.3939	0.5241	1.2987	0.4093	2.0759	1.1533	1.8509	0.931	1.6693	0.7276
U -236	KG/GWD(TH)	0.0000	0.1479	0.0000	0.1464	0.0000	0.1461	0.0000	0.1416	0.0000	0.1406	0.0000	0.1417	0.0000	0.1446	0.0000	0.1446	0.0000	0.1484	0.0000	0.152	0.0000	0.1528	0.0000	0.1588	0.0000	0.1716	0.0000	0.1741	0.0000	0.1839
U -238	KG/GWD(TH)	14.8716	14.4713	10.5618	10.1837	6.0726	5.7317	13.9824	13.5087	10.0994	9.6517	5.9513	5.5437	15.4056	14.8441	11.0975	10.5663	6.5501	6.0695	17.5065	16.9013	12.531	11.9586	7.346	6.8288	23.8534	23.1792	16.6398	16.0032	9.4426	8.8698
NP-237	KG/GWD(TH)	0.0000	0.005	0.0000	0.0062	0.0000	0.0087	0.0000	0.0064	0.0000	0.008	0.0000	0.011	0.0000	0.0077	0.0000	0.0097	0.0000	0.0138	0.0000	0.0082	0.0000	0.0104	0.0000	0.0151	0.0000	0.0083	0.0000	0.0109	0.0000	0.0164
PU-238	KG/GWD(TH)	0.0000	0.0011	0.0000	0.0019	0.0000	0.0037	0.0000	0.0018	0.0000	0.0028	0.0000	0.0054	0.0000	0.0022	0.0000	0.0036	0.0000	0.007	0.0000	0.0022	0.0000	0.0036	0.0000	0.0073	0.0000	0.0017	0.0000	0.0031	0.0000	0.0068
PU-239	KG/GWD(TH)	0.0000	0.0583	0.0000	0.0412	0.0000	0.0241	0.0000	0.0713	0.0000	0.0532	0.0000	0.0354	0.0000	0.1187	0.0000	0.0947	0.0000	0.0691	0.0000	0.1611	0.0000	0.1324	0.0000	0.1013	0.0000	0.2575	0.0000	0.2179	0.0000	0.1713
PU-240	KG/GWD(TH)	0.0000	0.0574	0.0000	0.0459	0.0000	0.0301	0.0000	0.0586	0.0000	0.0467	0.0000	0.0315	0.0000	0.0642	0.0000	0.052	0.0000	0.0358	0.0000	0.0678	0.0000	0.0557	0.0000	0.0391	0.0000	0.0729	0.0000	0.0614	0.0000	0.0445
PU-241	KG/GWD(TH)	0.0000	0.0208	0.0000	0.0179	0.0000	0.0124	0.0000	0.0268	0.0000	0.0232	0.0000	0.0174	0.0000	0.0375	0.0000	0.0347	0.0000	0.0286	0.0000	0.0427	0.0000	0.0411	0.0000	0.0357	0.0000	0.0458	0.0000	0.0471	0.0000	0.0435
PU-242	KG/GWD(TH)	0.0000	0.0128	0.0000	0.0157	0.0000	0.0182	0.0000	0.0162	0.0000	0.0187	0.0000	0.0205	0.0000	0.0153	0.0000	0.0178	0.0000	0.0202	0.0000	0.0131	0.0000	0.0154	0.0000	0.0179	0.0000	0.0085	0.0000	0.0107	0.0000	0.0132
AM-241	KG/GWD(TH)	0.0000	0.0015	0.0000	0.0015	0.0000	0.0014	0.0000	0.0023	0.0000	0.0024	0.0000	0.0025	0.0000	0.0038	0.0000	0.0043	0.0000	0.005	0.0000	0.0045	0.0000	0.0053	0.0000	0.0067	0.0000	0.0048	0.0000	0.0062	0.0000	0.0088
AM-242M	KG/GWD(TH)																							0.0000	0.0001	0.0000		0.0000		0.0000	0.0001
AM-243	KG/GWD(TH)	0.0000	0.0008	0.0000	0.0013	0.0000	0.0024	0.0000	0.0014	0.0000	0.0021	0.0000	0.0033	0.0000	0.0015	0.0000	0.0022	0.0000	0.0028	0.0000	0.0012	0.0000	0.0019	0.0000	0.0023	0.0000	0.0007	0.0000	0.0011	0.0000	0.0014
CM-244	KG/GWD(TH)	0.0000	0.0001	0.0000	0.0002	0.0000	0.0006	0.0000	0.0002	0.0000	0.0005	0.0000	0.0011	0.0000	0.0003	0.0000	0.0005	0.0000	0.0009	0.0000	0.0002	0.0000	0.0004	0.0000	0.0007	0.0000		0.0000	0.0002	0.0000	0.0004

Table 75 – Fuel Supply and Discharge for LEU at 20 wt%

FUEL SUPPLY - DISCHARGE		LEU		LEU		LEU		LEU		LEU	
	KG/GWD(TH)	Supply	Discharge	Supply	Discharge	Supply	Discharge	Supply	Discharge	Supply	Discharge
TH-232	KG/GWD(TH)										
U -233	KG/GWD(TH)										
U -234	KG/GWD(TH)	0.0106	0.0057	0.0105	0.0055	0.0116	0.0063	0.0129	0.0073	0.0162	0.0098
U -235	KG/GWD(TH)	1.0469	0.105	1.0372	0.1349	1.147	0.2489	1.2789	0.3614	1.6013	0.6301
U -236	KG/GWD(TH)	0.0000	0.1473	0.0000	0.1442	0.0000	0.1534	0.0000	0.1654	0.0000	0.1929
U -238	KG/GWD(TH)	4.1767	3.8643	4.1383	3.7642	4.5761	4.1353	5.1026	4.629	6.3886	5.8667
NP-237	KG/GWD(TH)	0.0000	0.0105	0.0000	0.0135	0.0000	0.0171	0.0000	0.0189	0.0000	0.0211
PU-238	KG/GWD(TH)	0.0000	0.0054	0.0000	0.0078	0.0000	0.0103	0.0000	0.011	0.0000	0.0107
PU-239	KG/GWD(TH)	0.0000	0.017	0.0000	0.0267	0.0000	0.0564	0.0000	0.0848	0.0000	0.147
PU-240	KG/GWD(TH)	0.0000	0.022	0.0000	0.0235	0.0000	0.0274	0.0000	0.0302	0.0000	0.0348
PU-241	KG/GWD(TH)	0.0000	0.0091	0.0000	0.0135	0.0000	0.024	0.0000	0.0306	0.0000	0.0381
PU-242	KG/GWD(TH)	0.0000	0.0188	0.0000	0.0209	0.0000	0.0204	0.0000	0.0184	0.0000	0.014
AM-241	KG/GWD(TH)	0.0000	0.0013	0.0000	0.0025	0.0000	0.0055	0.0000	0.0077	0.0000	0.0106
AM-242M	KG/GWD(TH)							0.0000	0.0001	0.0000	0.0002
AM-243	KG/GWD(TH)	0.0000	0.0026	0.0000	0.0034	0.0000	0.0029	0.0000	0.0024	0.0000	0.0015
CM-244	KG/GWD(TH)	0.0000	0.0009	0.0000	0.0014	0.0000	0.0012	0.0000	0.0009	0.0000	0.0005

Table 76 – Fuel Supply and Discharge for ThLEU

HEAVY METAL LOADING	gHM	5		5		5		7		7		7		10		10		10		12		12		12		16		16		16	
FEED ENRICHMENT	wt%	8		10		15		8		10		15		8		10		15		8		10		15		8		10		15	
	KG/GWD(TH)	Supply	Discharge	Supply	Discharge	Supply	Discharge	Supply	Discharge	Supply	Discharge	Supply	Discharge	Supply	Discharge	Supply	Discharge	Supply	Discharge	Supply	Discharge	Supply	Discharge	Supply	Discharge	Supply	Discharge	Supply	Discharge	Supply	Discharge
TH-232	KG/GWD(TH)	10.2054	9.9348	5.9453	5.7357	1.7743	1.6842	8.9798	8.6708	5.4438	5.2051	1.6996	1.5971	8.592	8.2419	5.3426	5.0719	1.7665	1.6493	8.8346	8.4626	5.556	5.2677	1.9056	1.7797	10.3703	9.9607	6.5667	6.2474	2.3449	2.203
U -233	KG/GWD(TH)	0.0000	0.1610	0	0.1055	0	0.0356	0	0.1629	0	0.1089	0	0.0393	0	0.1782	0	0.1238	0	0.0498	0	0.1951	0	0.1388	0	0.0588	0	0.2408	0	0.1768	0	0.078
U -234	KG/GWD(TH)	0.0139	0.0198	0.0122	0.017	0.0109	0.0108	0.0122	0.0211	0.0111	0.018	0.0104	0.011	0.0117	0.0229	0.0109	0.0194	0.0108	0.0118	0.0121	0.0239	0.0114	0.0203	0.0117	0.0127	0.0141	0.0258	0.0134	0.0222	0.0144	0.015
U -235	KG/GWD(TH)	1.3783	0.37	1.2045	0.2283	1.0784	0.1291	1.2128	0.2716	1.1029	0.1864	1.033	0.1322	1.1604	0.268	1.0824	0.2077	1.0736	0.1971	1.1932	0.31	1.1256	0.2563	1.1582	0.275	1.4006	0.4967	1.3304	0.4364	1.4252	0.5012
U -236	KG/GWD(TH)	0.0000	0.1596	0.0000	0.1538	0.0000	0.1486	0.0000	0.1499	0.0000	0.1453	0.0000	0.1426	0.0000	0.1449	0.0000	0.1418	0.0000	0.1444	0.0000	0.1463	0.0000	0.1444	0.0000	0.1515	0.0000	0.1579	0.0000	0.1583	0.0000	0.1729
U -238	KG/GWD(TH)	5.5697	5.4196	4.8671	4.6864	4.3577	4.1073	4.9009	4.7202	4.4566	4.2396	4.1741	3.8739	4.6892	4.475	4.3737	4.1167	4.3383	3.9836	4.8216	4.5904	4.5484	4.2712	4.6801	4.2982	5.6597	5.4029	5.3758	5.0683	5.7589	5.3364
NP-237	KG/GWD(TH)	0.0000	0.0051	0.0000	0.0064	0.0000	0.0087	0.0000	0.0068	0.0000	0.0082	0.0000	0.011	0.0000	0.0087	0.0000	0.0104	0.0000	0.014	0.0000	0.0097	0.0000	0.0116	0.0000	0.0155	0.0000	0.0109	0.0000	0.0133	0.0000	0.0176
PU-238	KG/GWD(TH)	0.0000	0.0011	0.0000	0.0019	0.0000	0.0037	0.0000	0.0019	0.0000	0.003	0.0000	0.0054	0.0000	0.0029	0.0000	0.0044	0.0000	0.0076	0.0000	0.0034	0.0000	0.005	0.0000	0.0084	0.0000	0.0035	0.0000	0.0053	0.0000	0.0085
PU-239	KG/GWD(TH)	0.0000	0.0205	0.0000	0.0176	0.0000	0.0162	0.0000	0.0212	0.0000	0.0197	0.0000	0.0212	0.0000	0.0266	0.0000	0.0271	0.0000	0.0367	0.0000	0.0328	0.0000	0.0351	0.0000	0.053	0.0000	0.0521	0.0000	0.0592	0.0000	0.096
PU-240	KG/GWD(TH)	0.0000	0.0212	0.0000	0.0208	0.0000	0.021	0.0000	0.0205	0.0000	0.0202	0.0000	0.0213	0.0000	0.0204	0.0000	0.0205	0.0000	0.0233	0.0000	0.021	0.0000	0.0215	0.0000	0.0253	0.0000	0.0236	0.0000	0.0246	0.0000	0.0296
PU-241	KG/GWD(TH)	0.0000	0.0077	0.0000	0.0081	0.0000	0.0084	0.0000	0.0092	0.0000	0.0095	0.0000	0.0108	0.0000	0.0118	0.0000	0.0127	0.0000	0.0171	0.0000	0.0139	0.0000	0.0156	0.0000	0.0223	0.0000	0.0185	0.0000	0.0218	0.0000	0.0307
PU-242	KG/GWD(TH)	0.0000	0.0052	0.0000	0.0083	0.0000	0.0145	0.0000	0.0077	0.0000	0.0111	0.0000	0.0174	0.0000	0.0095	0.0000	0.0129	0.0000	0.0182	0.0000	0.0098	0.0000	0.0129	0.0000	0.0172	0.0000	0.0085	0.0000	0.0111	0.0000	0.0137
AM-241	KG/GWD(TH)	0.0000	0.0005	0.0000	0.0007	0.0000	0.0009	0.0000	0.0008	0.0000	0.001	0.0000	0.0015	0.0000	0.0012	0.0000	0.0016	0.0000	0.0031	0.0000	0.0015	0.0000	0.0021	0.0000	0.0044	0.0000	0.0022	0.0000	0.0033	0.0000	0.0067
AM-242M	KG/GWD(TH)	0.0000																						0.0000		0.0000		0.0000		0.0000	0.0001
AM-243	KG/GWD(TH)	0.0000	0.0002	0.0000	0.0005	0.0000	0.0015	0.0000	0.0005	0.0000	0.0009	0.0000	0.0021	0.0000	0.0007	0.0000	0.0013	0.0000	0.0023	0.0000	0.0008	0.0000	0.0013	0.0000	0.0021	0.0000	0.0006	0.0000	0.001	0.0000	0.0014
CM-244	KG/GWD(TH)	0.0000		0.0000		0.0000	0.0004	0.0000		0.0000	0.0002	0.0000	0.0007	0.0000	0.0002	0.0000	0.0004	0.0000	0.0009	0.0000	0.0002	0.0000	0.0004	0.0000	0.0008	0.0000	0.0001	0.0000	0.0003	0.0000	0.0004

Table 77 – Fuel Supply and Discharge for ThHEU

HEAVY METAL LOADING	gHM	5		5		5		7		7		7		10		10		10		12		12		12		16		16		16	
FEED ENRICHMENT	wt%	8		10		15		8		10		15		8		10		15		8		10		15		8		10		15	
	KG/GWD(TH)	Supply	Discharge	Supply	Discharge	Supply	Discharge	Supply	Discharge	Supply	Discharge	Supply	Discharge	Supply	Discharge	Supply	Discharge	Supply	Discharge	Supply	Discharge	Supply	Discharge	Supply	Discharge	Supply	Discharge	Supply	Discharge	Supply	Discharge
TH-232	KG/GWD(TH)	15.9448	15.5201	10.7526	10.3612	6.0158	5.689	13.552	13.0598	9.5688	9.116	5.5974	5.2194	12.1912	11.6275	8.8145	8.2956	5.3122	4.8779	11.8675	11.2673	8.6225	8.0696	5.2457	4.7818	12.0458	11.3876	8.6961	8.0885	5.3188	4.8065
U -233	KG/GWD(TH)	0.0000	0.2489	0	0.1877	0	0.1135	0	0.2427	0	0.184	0	0.1135	0	0.2471	0	0.1896	0	0.121	0	0.257	0	0.1988	0	0.1297	0	0.2908	0	0.2278	0	0.1546
U -234	KG/GWD(TH)	0.0156	0.0266	0.0135	0.0259	0.0121	0.0233	0.0133	0.03	0.012	0.0291	0.0112	0.0257	0.0119	0.034	0.0111	0.0326	0.0107	0.0284	0.0116	0.0359	0.0108	0.0344	0.0105	0.0299	0.0118	0.0388	0.0109	0.0372	0.0107	0.0327
U -235	KG/GWD(TH)	1.4182	0.364	1.2253	0.2031	1.0969	0.0907	1.2053	0.2276	1.0904	0.136	1.0206	0.0679	1.0843	0.1747	1.0045	0.1113	0.9686	0.0639	1.0555	0.1714	0.9826	0.1128	0.9565	0.07	1.0714	0.2056	0.991	0.1403	0.9698	0.097
U -236	KG/GWD(TH)	0.0000	0.1665	0.0000	0.1602	0.0000	0.1555	0.0000	0.1545	0.0000	0.1493	0.0000	0.1462	0.0000	0.1445	0.0000	0.14	0.0000	0.1385	0.0000	0.1415	0.0000	0.1371	0.0000	0.1364	0.0000	0.1423	0.0000	0.1375	0.0000	0.1378
U -238	KG/GWD(TH)	0.1437	0.14	0.1242	0.1197	0.1111	0.105	0.1221	0.1177	0.1105	0.1051	0.1034	0.0959	0.1099	0.1045	0.1018	0.0953	0.0981	0.0892	0.107	0.1011	0.0996	0.0926	0.0969	0.0871	0.1086	0.102	0.1004	0.0926	0.0983	0.0873
NP-237	KG/GWD(TH)	0.0000	0.0052	0.0000	0.0066	0.0000	0.0088	0.0000	0.007	0.0000	0.0085	0.0000	0.0108	0.0000	0.0091	0.0000	0.0107	0.0000	0.0133	0.0000	0.0103	0.0000	0.0119	0.0000	0.0149	0.0000	0.0122	0.0000	0.0142	0.0000	0.0178
PU-238	KG/GWD(TH)	0.0000	0.0011	0.0000	0.002	0.0000	0.0038	0.0000	0.0021	0.0000	0.0032	0.0000	0.0056	0.0000	0.0033	0.0000	0.0049	0.0000	0.008	0.0000	0.0041	0.0000	0.0059	0.0000	0.0096	0.0000	0.0051	0.0000	0.0075	0.0000	0.0124
PU-239	KG/GWD(TH)	0.0000	0.0006	0.0000	0.0006	0.0000	0.0007	0.0000	0.0007	0.0000	0.0007	0.0000	0.001	0.0000	0.0008	0.0000	0.0009	0.0000	0.0013	0.0000	0.0009	0.0000	0.0011	0.0000	0.0015	0.0000	0.0012	0.0000	0.0014	0.0000	0.002
PU-240	KG/GWD(TH)	0.0000	0.0006	0.0000	0.0006	0.0000	0.0008	0.0000	0.0006	0.0000	0.0007	0.0000	0.0009	0.0000	0.0006	0.0000	0.0007	0.0000	0.001	0.0000	0.0006	0.0000	0.0007	0.0000	0.001	0.0000	0.0006	0.0000	0.0007	0.0000	0.001
PU-241	KG/GWD(TH)	0.0000	0.0002	0.0000	0.0002	0.0000	0.0003	0.0000	0.0002	0.0000	0.0003	0.0000	0.0004	0.0000	0.0003	0.0000	0.0004	0.0000	0.0005	0.0000	0.0004	0.0000	0.0004	0.0000	0.0006	0.0000	0.0004	0.0000	0.0005	0.0000	0.0007
PU-242	KG/GWD(TH)	0.0000	0.0001	0.0000	0.0002	0.0000	0.0005	0.0000	0.0002	0.0000	0.0004	0.0000	0.0007	0.0000	0.0003	0.0000	0.0005	0.0000	0.0009	0.0000	0.0004	0.0000	0.0005	0.0000	0.0009	0.0000	0.0004	0.0000	0.0006	0.0000	0.001
AM-241	KG/GWD(TH)	0.0000		0.0000		0.0000		0.0000		0.0000		0.0000		0.0000		0.0000		0.0000		0.0000		0.0000		0.0000	0.0001	0.0000		0.0000		0.0000	0.0002
AM-242M	KG/GWD(TH)	0.0000																						0.0000		0.0000		0.0000		0.0000	
AM-243	KG/GWD(TH)	0.0000		0.0000		0.0000		0.0000		0.0000		0.0000		0.0000		0.0000		0.0000	0.0001	0.0000		0.0000		0.0000	0.0001	0.0000		0.0000		0.0000	0.0001
CM-244	KG/GWD(TH)	0.0000		0.0000		0.0000		0.0000		0.0000		0.0000		0.0000		0.0000		0.0000		0.0000		0.0000		0.0000		0.0000		0.0000		0.0000	